# International Symposium and School of Young Scientists
# INTERFACIAL PHENOMENA AND HEAT TRANSFER

## BOOK OF ABSTRACTS

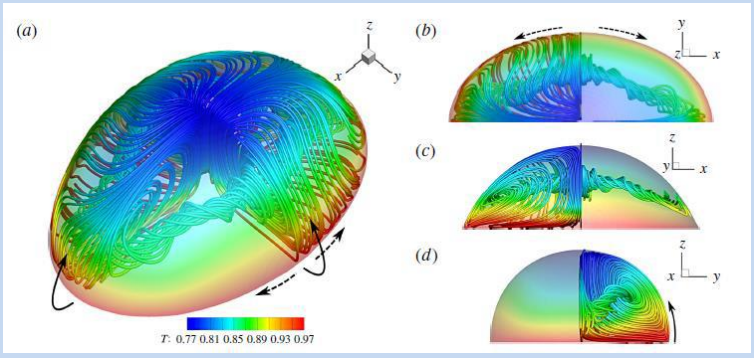


**Matar**

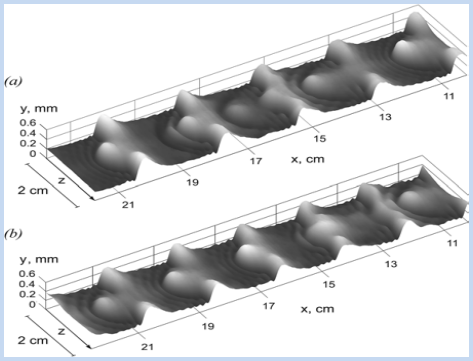


**Alekseenko et al.**

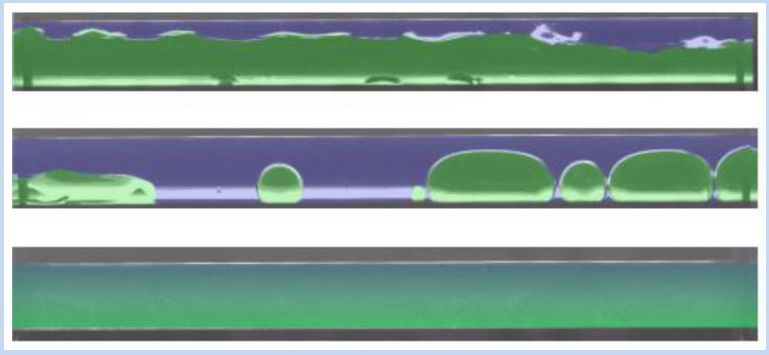

**Ohta**

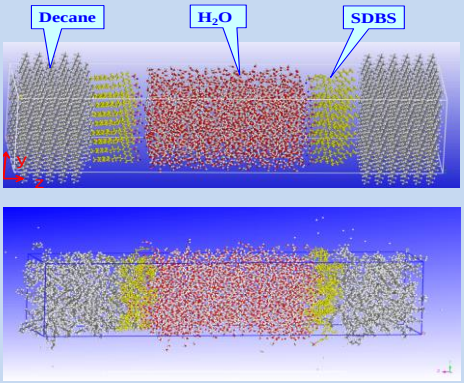


**Bai et al.**

Editors: Vladimir S. Ajaev
Sergey V. Alekseenko
Elena F. Bykovskaya
Oleg A. Kabov
Haruhiko Ohta
Dmitry V. Zaitsev

**Kutateladze Institute of Thermophysics SB RAS,**
**Novosibirsk, Russia, March 2-4, 2016**

IPHT 2016 Novosibirsk

# BOOK OF ABSTRACTS

## International Symposium and School of Young Scientists
## INTERFACIAL PHENOMENA AND HEAT TRANSFER

### Symposium Chairs:


**Vladimir S. Ajaev**
Southern Methodist University, Department of Mathematics, Dallas TX, USA

**Sergey V. Alekseenko**
Kutateladze Institute of Thermophysics, SB RAS, Novosibirsk, Russia

**Oleg A. Kabov**
Kutateladze Institute of Thermophysics, SB RAS, Novosibirsk, Russia

**Haruhiko Ohta**
Kyushu University, Dept. of Aeronautics and Astronautics, Fukuoka, Japan


### Symposium Organizers:

- Kutateladze Institute of Thermophysics, SB RAS, Novosibirsk, Russia
- Kyushu University, Nishi-ku, Fukuoka, Japan
- Southern Methodist University, Dallas, TX, USA
- Begell House, Inc., Danbury, CT, USA

### Sponsor


**Russian Science Foundation,** Project N 15-19-30038 "Interfacial phenomena in complex micro scale two-phase flows"


### Scientific Secretaries

Elena F. Bykovskaya, Dmitry V. Zaitsev,
Kutateladze Institute of Thermophysics, SB RAS

**Kutateladze Institute of Thermophysics SB RAS,**
**Novosibirsk, Russia, March 2-4, 2016**

**Website:** http://www.itp.nsc.ru/htl/symposium-16/

## Symposium Objective

The symposium is intended to provide a platform for researchers to exchange information and identify research needs in the interdisciplinary, rapidly developing research area of interfacial phenomena encompassing several disciplines including chemical engineering, mechanical engineering, applied mathematics, physics, and chemistry.

## Topics for the presentations include

- Pool boiling: CHF, dry spot spreading, boiling crises, contact line effects
- Flow boiling, shear-driven films: CHF, nano and microstructured surfaces, wave structure, dry spots
- Wetting, superhydrophobic surfaces, droplet evaporation, complex fluids
- Thermocapillary flows: instability, evaporation, gas flow, and gravity effects
- Flows in microchannels and minichannels: drag reduction, two-phase flow patterns, wettability effects
- Interfacial and phase change phenomena

## Scientific Committee

- Vladimir S. Ajaev, SMU, USA
- Sergey V. Alekseenko, IT, Russia
- Alidad Amirfazli, UA, Canada
- Hitoshi Asano, KoU, Japan
- Avram Bar-Cohen, UM, USA
- Bo-Feng Bai, XJU, China
- Luis Antonio Davalos-Orozco, UNAM, Mexico
- David Brutin, IUSTI, France
- Catherine Colin, IMFT, France
- Evgeny A. Chinnov, IT, Russia
- Andrey G. Fedorov, GIT, USA
- Irina Graur, IUSTI, France
- Olga N. Goncharova, ASU, Russia
- Hang Guo, BUT, China
- Oleg A. Kabov, IT, Russia
- Thodoris Karapantsios, AUT, Greece
- Osamu Kawanami, UH, Japan
- Sameer Khandekar, IIT, India
- Paolo Di Marco, UNIPI , Italy
- Dmitriy Markovich, IT, Russia
- Haruhiko Ohta, KU, Japan
- Yoav Peles, UCF, USA
- Huihe Qiu, HKUST, Hong Kong
- Amir Riaz, UM, USA
- Peter Stephan, TUD, Germany
- Lounes Tadrist, IUSTI, France
- Koji Takahashi, KU, Japan
- John R. Thome, EPFL, Switzerland
- Amos Ullmann, TAU, Israel
- Jian-Fu Zhao, IM, China

# Interfacial Phenomena and Heat Transfer

**Editor-in-Chief: Oleg A. Kabov**

The journal "Interfacial Phenomena and Heat Transfer" publishes original research articles and reviews covering the topics discussed in the abstracts collected in the present volume. The Editors and Editorial Board Members of the journal are the initiators and organizers of the IPHT Symposium and School of Young Scientists. A special issue of the journal will be published following the conference. Papers for this issue will be subject to the regular review procedure of the journal. Begell House is pleased to provide attendees to the Conference full access to the articles published in this journal. All published articles (Volume 1, 2013, Volume 2, 2014 and Volume 3, 2015) and forthcoming articles can be accessed through the journal website http://www.dl.begellhouse.com/journals/728e68e739b67efe.html

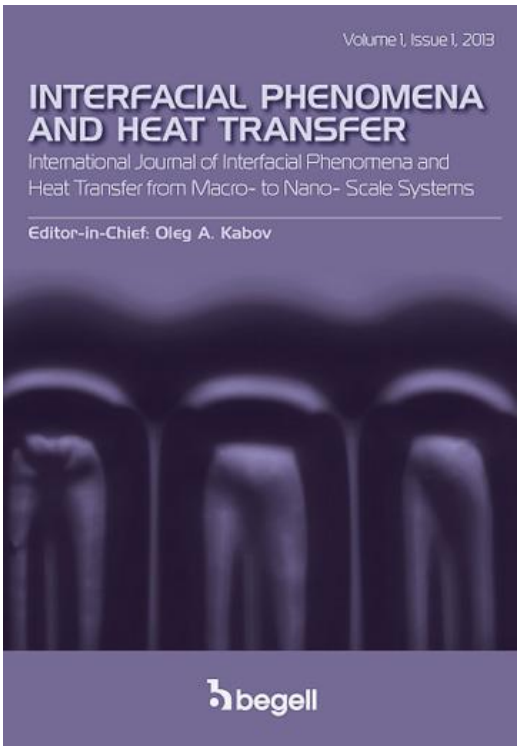


## Announcement

Begell House Publishers Inc. and the Editors of Interfacial Phenomena and Heat Transfer journal are pleased to announce the establishment of the Interfacial Phenomena and Heat Transfer Award to honor outstanding achievements in research areas covered by the journal in the form of original and transformative research, leadership in the scientific community, and profound contributions to education. The winner will be determined by an international committee of distinguished scientists representing different research areas and different countries. Nominations can be submitted by the members of the Editorial Board of IPHT and the members of the Scientific Committee of the IPHT Symposium.

# Welcome

On behalf of the Organizing Committee, it is our pleasure to welcome all participants of the International Symposium and School of Young Scientists "Interfacial Phenomena and Heat Transfer" to Novosibirsk. The third largest city in Russia, often referred to as "the capital of Siberia", Novosibirsk is home to a number of research centers and institutes, including the Kutateladze Institute of Thermophysics. The long tradition of research in both fluid mechanics and heat transfer makes this institute a natural venue for the symposium, the first of its kind. A wide range of topics in the rapidly developing and highly interdisciplinary field of interfacial phenomena and heat transfer are covered, including boiling, shear-driven films, droplet evaporation, contact line phenomena, thermocapillary flows, and two-phase flows in microchannels and minichannels. The conference is made possible by financial support from the Russian Science Foundation. A special issue of the journal "Interfacial Phenomena and Heat Transfer" will be published following the conference. Papers for this issue will be subject to the regular review procedure of the journal. The Organizing Committee wishes all participants a pleasant stay in Novosibirsk and a productive conference.

Symposium Chairs

For more information about the Symposium please visit the website
http://www.itp.nsc.ru/htl/symposium-16/

# CONTENTS

**Oral presentations and posters:**



## 3. WETTING, SUPERHYDROPHOBIC SURFACES, DROPLET EVAPORATION, COMPLEX FLUIDS

**Lectures:**



**Oral presentations and posters:**

## 5. FLOWS IN MICROCHANNELS AND MINICHANNELS: DRAG REDUCTION, TWO-PHASE FLOW PATTERNS, WETTABILITY EFFECTS

**Lectures:**



**Oral presentations and posters:**

# Electrostatic effects in the apparent contact line region under a vapor bubble

Christiaan Ketelaar[1] and Vladimir Ajaev[1,2,3]

[1]Southern Methodist University, Department of Mathematics
Dallas, TX 75275, USA
[2]National Research Tomsk Polytechnic University, Tomsk 634050, Russia
[3]Kutateladze Institute of Thermophysics SB RAS, Lavrentyev Ave., 1, Novosibirsk, 630090, Russia
ajaev@smu.edu

Studies of heat transfer near apparent contact lines are important for a number of applications such as pool boiling, micro heat pipes, microfluidic actuation, and many others. Present work is motivated by a configuration of a vapor bubble on a heated substrate, as sketched in Fig. 1. It is well known that the part of the substrate that appears dry on macroscale is often covered by a micro- or nanoscale adsorbed film. Thus, what appears to be a line of contact between the bubble surface and the substrate is in fact a transition region between the curved bubble surface and the flat film, as schematically shown in the figure. Numerous theoretical and experimental studies of this configuration are reviewed in Wayner (1999) and Ajaev and Homsy (2006).

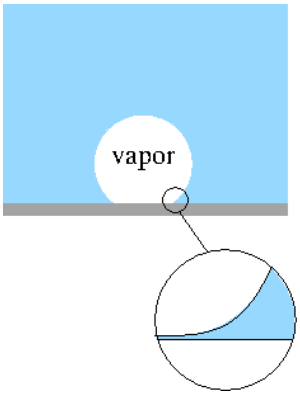


**Figure 1**. A sketch of a small isolated vapor bubble of radius $R_0$ formed on a heated substrate; the enlarged view of the apparent contact line region is shown.

Despite significant progress in understanding heat transfer near apparent contact lines, the issue of electrostatic interactions between interfaces in this context received very little attention. Such interactions stem from the presence of electric charges both in the liquid, in the form of ions, and at interfaces. Liquid is assumed to be an aqueous solution, so electrical double layers of characteristic thickness $\lambda_D$ are formed at interfaces. In the present study, the electric field in the liquid is determined from the solution of the classical Poisson-Boltzmann equation,

$$\psi_{yy} = \kappa^2 \sinh\psi \qquad (1)$$

The electric potential here is scaled by $k_B T_s / e$, where $k_B$ is the Boltzmann constant, $e$ is the elementary charge, $T_s$ is the saturation temperature. Equation (1) is solved numerically with the conditions of constant scaled substrate potential $\psi_0$ and liquid-vapor interface charge density $q$.

The vertical coordinate $y$ above is nondimensionalized by the characteristic thickness $d$ of the liquid film in the apparent contact line region. Standard lubrication approximation (Oron et al. 1997, Craster and Matar, 2009) is used for the viscous flow, with the assumptions of small capillary number and small ratio $d/R_0$. The film thickness (scaled by $d$) is then determined by the evolution equation,

$$h_t + J + \frac{1}{3}\left[h^3\left(h_{xx} + \kappa^2 Q\cosh\tilde{\psi} + \frac{\alpha}{h^3}\right)_x\right]_x - \frac{1}{2}\kappa Q q\left[h^2\tilde{\psi}_h h_x\right]_x = 0 \qquad (2)$$

Here the scaled evaporative flux is given by

$$J = \frac{\delta\left(\frac{1}{2}\kappa^2 Q q^2 - h_{xx} - \kappa^2 Q\cosh\tilde{\psi} - \frac{\alpha}{h^3}\right) + T_0}{K + h} \qquad (3)$$

We use the standard definitions of the parameters $K, \delta$ which appear in the nondimensional form of the so-called non-equilibrium condition at the interface, discussed e.g. in Ajaev and Homsy (2006), $\alpha$ is the scaled Hamaker constant, $T_0$ is the nondimensional superheat, and $\tilde{\psi}$ is the electric potential at the liquid-vapor interface. In contrast to many previous studies, our formulation incorporates the electrostatic contribution to stresses in the fluid not only in the interfacial normal stress, but also in the shear stress balance. Equation (2) with the expression for flux given by (3) has been solved numerically using a finite-difference approach for both steady and expanding/contracting bubbles.

Changes in the steady interface shape in the apparent contact line region are best visualized by plotting the curvature as a function of coordinate. Such plots are shown in Fig. 2, with the result for negligible electrostatic effects also plotted for comparison. Let us first discuss the latter, corresponding to the black solid line in Fig. 2. This profile has a single point of maximum with curvature equal to 28.8 in our nondimensional units. To the left of the point of maximum, there is a sharp drop in the curvature caused by the increasingly dominant London-van der Waals forces as the region of flat ultra-thin film is approached. To the right of the maximum, the curvature gradient is negative, providing the capillary pressure gradient which drives the flow of liquid into the transition region (from right to left). This flow compensates for the evaporative mass loss in the transition region.

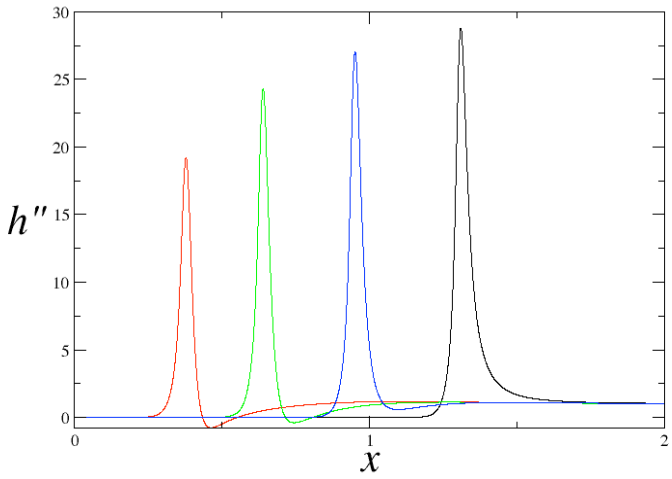


**Figure 2:** Interfacial curvature in the lubrication-type approximation as a function of local coordinate for negligible electrostatic effects (black line) and three different values of substrate potential: $\psi_0 = -3$ (blue line), $\psi_0 = -4$ (green line), and $\psi_0 = -5$ (red line).

Fig. 2 also shows three curvature profiles obtained when the electrostatic effects are included into the model. For each of them, there is still a point of maximum, but the maximum curvature value is lower than for *Q=0*, down to 19.2 at the highest absolute value of the substrate potential used in the simulation. The sharp drop to the left of the point of maximum happens on a length scale similar to the case of negligible electrostatic effects, suggesting that it is mostly due to the London-van der Waals forces. However, to the right of the maximum, the curvature is no longer a monotonic function of the spatial coordinate. In fact, there is a point of minimum at which the curvature can be negative for sufficiently low substrate potentials, so that the interface becomes concave down. Since the flow of liquid into the transition region still has to be maintained to conserve mass, there is clearly a range of values of thickness where the electrostatic effects take over from the capillary pressure gradient as the main driving force behind this flow. In that range, the capillary pressure gradient is negative and thus is acting against the flow into the region where most evaporation takes place.

Overall, the transition region where the curvature departs significantly from the two constant values corresponding to the two endpoints of the interval is clearly wider for *Q=0.1* than for the case of *Q=0*; its width increases with the increase in the magnitude of the solid surface potential.

For heat transfer applications, the key quantity of interest is the evaporative flux. Fig. 3 shows typical scaled local evaporative flux profiles for negligible electrostatic effects (black dashed line) and for *Q=0.1* (blue line). For both curves, there is a single point of maximum, but the actual value of the maximum flux is lower for the case when the electrostatic effects are considered. However, the evaporative flux profile is also wider for *Q=0.1*, which is consistent with the observations of similar trend in the discussion of interface curvature profiles above and can be explained as follows. The highest values of the local evaporative flux are expected when the film is sufficiently thin so that the thermal resistance is small but thick enough to avoid strong suppression of evaporation by the disjoining pressure. This intermediate film thickness region becomes wider when the electrostatic effects are included in the model. Thus, the flux profiles are also wider for *Q=0.1*.

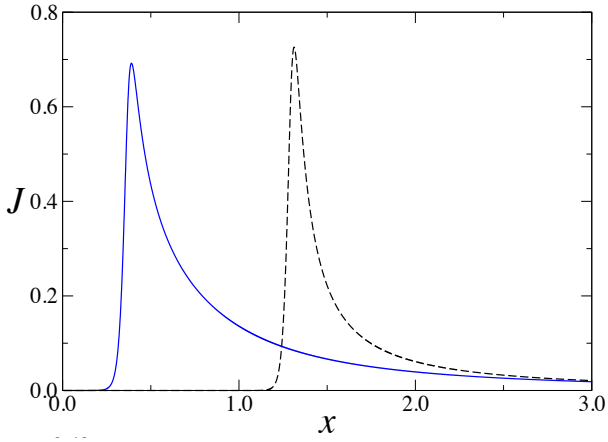


**Figure 3:** Local scaled evaporative flux for *Q=0* and *Q=0.1*.

Integration of local evaporative flux profiles leads to a value of the total amount of evaporation from the contact line region. We found this value to be increasing as the substrate potential is increased. Thus, electrostatic interactions lead to increase of the amount of evaporation near the contact line, an important conclusion for practical applications.

The work is supported by the Ministry of Education and Science of Russia (project identifier RFMEFI61315X0038).

**References**

Wayner P. C., Intermolecular forces in phase-change heat transfer: 1998 Kern award review, AIChE J., Vol. 45, pp. 2055-2068 (1999)

Ajaev V.S., Homsy G. M. Modeling shapes and dynamics of confined bubbles, Annu. Rev. Fluid Mech., Vol. 38, pp.277-307 (2006)

Oron A., Bankoff S.G., Davis S.H. Long-scale evolution of thin liquid films, Rev. Mod. Phys., Vol. 69, pp. 931-980 (1997)

Craster R.V., Matar O.K. Dynamics and stability of thin liquid films, Rev. Mod. Phys., Vol. 81, pp. 1131-1198 (2009)

# Boling Heat Transfer to Immiscible Mixtures for High-performance Cooling of Semiconductors

Haruhiko Ohta

Kyushu University, Dept. Aeronautics and Astronautics
744 Motooka, Nishi-ku, Fukuoka 813-0044, Japan
ohta@aero.kyushu-u.ac.jp

## 1. Introduction

Heat transfer characteristics during nucleate boiling of miscible non-azeotropic mixtures are widely investigated, and the heat transfer deterioration is unavoidable owing to the existence of mass diffusion resistance caused by the preferential evaporation of more-volatile component. Only thermocapillary force due to the concentration gradient along the surface of thin liquid film underneath bubbles was expected to improve the heat transfer characteristics. According to the detailed experiments by the group of the present author, a new knowledge that the heat transfer enhancement also occurs at low concentration of alcohol aqueous mixtures. The result creates additional interest from a scientific point of view, while it has no engineering value because of its small rate of the enhancement. On the other hand, the present author noticed that the boiling heat transfer to immiscible mixtures has superior performance when they are applied to the coolants. However, there is very limited number of existing studies on the boiling of immiscible mixtures for the purpose of cooling.

## 2. Requirements from cooling systems

Recently, a number of studies are directed to the cooling of semiconductor chips with high heat generation density larger than 100W/cm$^2$, while our target is power electronics with a size of e.g. 150mm×150mm with heat fluxes larger than 200W/cm$^2$ assuming future demands. Requirements are summarized as follows: i) Increase of critical heat flux (CHF), ii) Reduction of surface temperature not to exceed the temperature limitation of semiconductors taking account of the thermal resistance between the semiconductors and the surface of cooling jacket, iii) Operation at the pressure higher than the atmospheric without increasing liquid temperature in order to prevent the mixing of air which seriously deteriorates the heat transfer during the condensation. iv) Stability of surface temperature transition, i.e. the prevention of excessive overshoot of surface temperature, just before the boiling initiation, which is required for the cooling of e.g. automobile inverters inevitably accompanied by a large variation of thermal load. According to the investigations by the group of the present author, immiscible mixtures have a potential to satisfy all of the above requirements under the appropriate operating conditions including the configuration around the heating surface (Kita et al. (2014), Ohta et al. (2015)).

## 3. Immiscible mixtures

Because the summation of the partial vapor pressures of both components becomes the total pressure, subcooling is always given to both liquids as shown in Fig.1. Smaller and larger degrees of subcooling are imposed to the more-volatile and less-volatile liquid in a self-sustaining way since the both liquids are compressed by the lower and higher vapor pressures of less-volatile and more-volatile components, respectively. As an ideal combination, we consider the use of more-volatile liquid with larger density (FC72) and less-volatile one with smaller density (water) in pool boiling as shown in Fig.2. The equilibrium temperature is 51.6°C at the total pressure of 0.1MPa, where the degrees of subcooling for FC72 and water are 4.3K and 48.4K, respectively. Boiling is initiated from the more-volatile liquid with small overshoot of surface temperature. Because CHF for FC72 of a stratified thin layer with small subcooling is smaller than that for pure FC72 under the same total pressure, and the temperature jump occurs by further increase of heat flux. The temperature jump is not large to results in the catastrophic temperature excursion, but it remains in a certain range. The phenomenon is referred to as "Intermediate heat flux burnout" by the present author. The mixing of both liquids occurs by two mechanisms, i.e. the penetration of FC72 rising bubbles accompanied by the liquid of FC72 across the liquid-liquid interface acted as a barrier, and/or by Taylor instability. At higher heat flux, the heat transfer to water by convection or nucleate boiling is enhanced by the generation of FC72 bubbles resulting in the reduction of surface temperature compared to that of pure water under the same pressure. This is regarded as the substantial heat transfer enhancement because the surface temperature during nucleate boiling is not largely changed by the liquid subcooling. Since water is highly subcooled, by the high vapor pressure of FC72, the value of CHF is expected to be increased drastically.

## 4. Pool boiling experiments

Pool boiling experiments were performed using a horizontal flat and smooth heating surface of 40mm in diameter facing upwards. For FC72/Water, The value of CHF increases up to 300W/cm$^2$ at 0.1MPa as shown in Fig.3. It is note worthy that the small amount of FC72 to water increases the CHF of water drastically without employing the heating surface with macro or microstructures on it. The reduction of surface temperature from that of water is observed at high heat fluxes. The generation of FC72 bubbles enhances the heat transfer to water by the agitation of thermal boundary layers or by the increased turbulence during the convention and by the promotion of evaporation from the thin liquid layers squeezed by the FC72 bubbles during nucleate boiling. The jump of surface temperature at moderate heat flux is classified to two categories; one

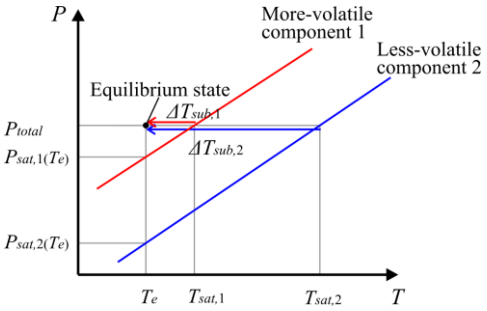


**Figure 1:** Subcooling of component liquids.

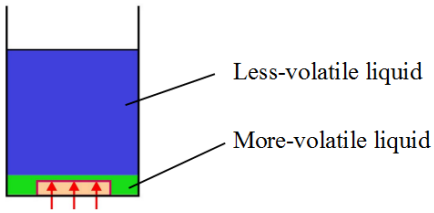


**Figure 2:** Pool boiling system investigated.

is abrupt increase of surface temperature at a certain heat flux, the other is gradual increase of surface temperature with increasing heat flux keeping the steady-state at each heat flux. The difference is explained by the process in the mixing of component liquids, and the former case occurs by Taylor instability while the latter by the penetration of FC72 bubbles across the liquid-liquid interface. It is at least clear from the past experiments that both the increase of CHF and the reduction of surface temperature are simultaneously possible even at the same composition by the small addition of more-volatile liquid with larger density to the bulk of less-volatile liquid with smaller density.

## 5. Flow boiling experiments

The experiments were performed by using a stainless steel tube of 7mm in inner diameter and 300mm in length oriented horizontally. The thermocouples are located on the bottom and the top of tubes at three different locations of upstream, midstream and downstream to evaluate the local heat transfer performances. FC72/Water is used as a test fluid again. Because of the inertia by the liquid flow, the distribution of both liquids changes with both flow rates. The investigation was started from the classification of flow patterns consisted of both liquids under unheated conditions where examples are shown in Fig.4. The flow patterns of unheated conditions have significant importance because the bubbles of FC72 remains in the liquid phase of FC72 owing to the existence of liquid-liquid interface as a barrier for the bubble penetration to the water flow. In the experiments, only the fluid temperature at the exit of the heated tube is measured. To evaluate the local heat transfer coefficients at the position of thermocouples, the temperature distribution of fluid composed of both liquid and FC72 vapor along the tube axis is needed. A parameter which represents the heat transferred to FC72 to the total is introduced and the measured exit fluid temperatures are well reproduced within an error of 1K by the heat balance equations, where the values of the parameter is given by only a function of inlet volumetric flow rates and is independent of heat flux. The result is consistent with the flow patterns where the locations of FC72 bubbles are limited in its liquid phase and the ratio of areas for both liquids contacting to the inner tube wall is almost unchanged regardless the change of heat flux.

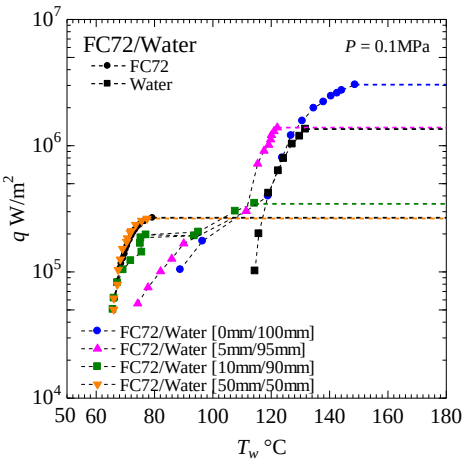


**Figure 3:** An example of results from pool boiling experiment.

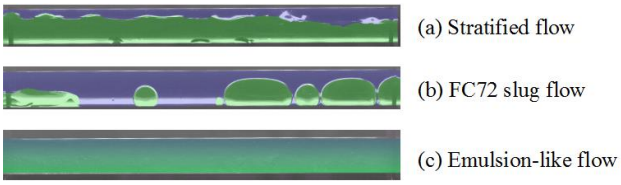


**Figure 4:** Flow patterns unheated conditions.

It is clear from the experiments that the addition of small amount of FC72 to water flow enhances the forced convection of water by the generation of FC72 bubbles. In this case, the flow pattern before heating is emulsion-like flow where fine droplets of FC72 are dispersed in the bulk flow of water. However, the rate of the enhancement is quite insensitive to the flow rate ratios. Especially in emulsion-like flow, the distribution of FC72 fine droplets are quite uniform compared to other flow patterns, and similar enhancement is expected in the systems with different orientations and in different gravity or acceleration fields.

## 6. Summary

Through the pool and flow boiling experiments, it was clarified that immiscible mixtures as working fluids have superior heat transfer characteristics not expected so far by the use of pure component fluids or miscible non-azeotropic mixtures. It is emphasized that the drastic increase of CHF value is possible in pool boiling without introducing the complicated structures of surfaces. The stratification of liquids due to the density difference can be eliminated in flow boiling system with dispersed fine droplets of more-volatile liquids and the enhancement of heat transfer is expected in cooling systems with different configurations.

The present author express the appreciation for the support by Grant-in-Aid for Challenging Exploratory Research 25630067.

## References

Kita, 5 S., Ohnishi, S., Fukuyama, Y. and Ohta, H., Improvement of Nucleate Boiling heat Transfer Characteristics by Using Immiscible Mixtures, Proc. 15th Int. Heat Transfer Conf., Kyoto, Japan, IHTC1-8941 (2014).

Ohta H., Iwata K., Yamamoto D. and Shinmoto Y., Superior Heat Transfer Characteristics in Boiling of Immiscible Mixtures, 26th Int. Symp. Transport Phenomena, ISTP-26, Leoben, Austria, USB, 8 pages (2015).

# Slowed-down boiling crisis: experiments and modeling

Vadim Nikolayev

Service de Physique de l'Etat Condensé, CEA, CNRS, Université Paris-Saclay, CEA Saclay, 91191 Gif-sur-Yvette Cedex, France
vadim.nikolayev@cea.fr

Nucleate boiling is characterized by extremely high heat transfer rates and for this reason is widely used. However, there is a limit called boiling crisis (BC), which corresponds to a transition from nucleate to film boiling where the heater is covered by a continuous vapor film that drastically reduces the heat transfer. The transition occurs when the heater heat flux exceeds a threshold called critical heat flux (CHF). Despite decades of research, the physical mechanisms that trigger the boiling crisis are still not understood mainly because its detailed observation is very difficult under usual conditions where the boiling is violent and BC lasts about 1 ms.

In this lecture, I review both experimental and theoretical work on BC carried out in our group. The experiments have been conducted in a close vicinity of the liquid-vapor critical point where the thermal diffusivity is very small so that boiling is slowed down: in our experiments BC lasts up to 10s. In addition, CHF becomes very small, which is convenient for experiments. However, the surface tension decreases too. It is thus necessary to carry out the experiments under reduced gravity conditions to preserve conventional bubble geometry (to avoid the flattening of the bubble interfaces by gravity).

We compare here several near-critical saturated pool boiling experiments performed by us and low gravity conventional boiling experiments. First, we discuss experiments carried out with the DECLIC apparatus with the $SF_6$ fluid at 46°C (Lecoutre et al. 2014) onboard the International Space Station. Next, we describe two experiments conducted in ground-based magnetic gravity compensation installations at Grenoble. In all cases the most interesting observations are those of the dry areas under the bubbles on a heater. They are performed "from below", through the transparent heater made of the transparent ITO film.

Although magnetic gravity compensation experiments provide much more versatility (a possibility of changing in situ the view angle, the fluid pressure, the gravity level etc.), experiments are possible only with one cryogenic fluid (H2 at 33K). They also impose a spatial variation of effective gravity that leads to a particular phase distribution in the fluid cell. The DECLIC experiments are complementary since they are incomparably more precise and show thus much more details of BC.

Two regimes of dry spot growth are identified: separate dry spot growth observed far from the boiling crisis and chain dry spots' coalescence regime (avalanches of coalescences) immediately before causing the dryout of the heater. A transition between two this regimes is observed too.

We show that the triggering phenomenon of BC is related to the dry spot spreading; the relevant mechanism is microscopic and should act in the vicinity of the triple vapor-liquid-heater contact line. Just before the boiling crisis, the apparent contact angle is close to 90°. This observation conforms to the proposed theoretically CHF criterion (90° apparent receding contact angle at the moment of bubble departure, Janeček & Nikolayev 2014). The chain coalescences occur because the dry areas under the bubbles spread so fast that the contact lines have no time to relax between subsequent bubble coalescences (Nikolayev et al. 2015). While in the circular regime, the probability distribution of the dry spot sizes is Gaussian, chain dry spots' coalescence regime leads to the power law probability distribution (Charignon et al. 2015). The dry spot contours show some features of self-similar scale-free geometrical objects (fractals). Such observations place the boiling crisis in a context of the phenomena exhibiting criticality, where such a behavior is usual.

In the second part of communication we present results of theoretical and numerical modeling of the boiling crisis. It is assumed to be triggered by spreading of dry spots under individual bubbles that occurs due to the apparent contact angle growth, when the apparent contact angle attains 90°. Such a mechanism is studied via numerical simulation of the single bubble growth. The apparent contact angle is obtained from the hydrodynamic modeling of the vicinity of the triple contact line (microregion). The microregion model is based on the lubrication approach extended to treat the high interface slopes. The microregion model is compared to previous experimental and numerical data obtained for moderate superheating of the heater. The macroregion is modeled within a simplified 2D quasistationary approach that neglects the fluid motion. The critical heat flux (CHF) of BC obtained from such a formulation is calculated as a function of gravity level and the heater wetting properties. The results agree qualitatively with other existing experimental data.

## References

Charignon, T., Lloveras, P., Chatain, D., Truskinovsky, L., Vives, E., Beysens, D. & Nikolayev, V. S. Criticality in the slowed-down boiling crisis at zero gravity, Phys. Rev. E, 2015 vol. 91, 053007.

Lecoutre, C., Garrabos, Y., Beysens, D., Nikolayev, V. & Hahn, I. Boiling phenomena in near-critical $SF_6$ observed in weightlessness, Acta Astronaut., 2014 vol. 100, 22 – 29.

Janeček, V. & Nikolayev, V. S. Triggering the boiling crisis: a study of the dry spot spreading mechanism, Interfacial Phenomena and Heat Transfer, 2014 vol. 2 (4), 363 – 383.

Nikolayev, V., Garrabos, Y., Lecoutre, C., Charignon, T., Hitz, D., Chatain, D., Guillaument, R., Marre, S. & Beysens, D. Boiling Crisis Dynamics: Low Gravity Experiments at High Pressure, Microgravity Sci. Technol., 2015 vol. 27 (4), 253 – 260.

# Thermocapillary breakdown of a horizontal spot-heated liquid layer

Yuriy Lyulin[1], Serafim Spesivtsev[1,2], Igor Marchuk[1,3], Oleg Kabov[1,2], Jean-Claude Legros[1]

[1] Institute of Thermophysics, 1, Lavrentiev Ave., 630090, Novosibirsk, Russia
[2] Novosibirsk State University, 2, Pirogov Ave., 630090, Novosibirsk, Russia
[3] Novosibirsk State Agrarian University, 160, Dobrolyubov Ave., 630039, Novosibirsk, Russia

Investigation of heat transfer from a local heat source becomes one of the most important problems in thermophysics. The problems are closely connected to the cooling of microelectronic equipment. One of the promising methods for removing the high heat fluxes from a local heat source is technology based on evaporation of a thin liquid layer. Dynamics of evaporation essentially depends on the conditions in the layer. In particular, the breakdown of liquid layer leads to dramatic decreasing of heat transfer from a local heat source (Lyulin et al. 2015). The goal of the present work is to study the breakdown dynamics of a horizontal evaporating liquid layer when heated from a localized hot spot.

A schematic of the experimental rig is shown in Fig. 1. Experiments were conducted respectively at atmospheric pressure, temperature and relative humidity of 28 ± 2 °C and 25 ± 3%. The thickness of the liquid layer varied from 300 to 700 μm. Ethanol was used as a working fluid. The temperature of the heater ranged from 20 to 82 °C. The density of heat flux varied from 0 to 120 W/cm$^2$. Diameter of the heater was 1.6 mm. The injection flow rate of the liquid was 0-200 μl/min. Visualization and control of the liquid layer were carried out using schlieren and shadowgraph techniques.

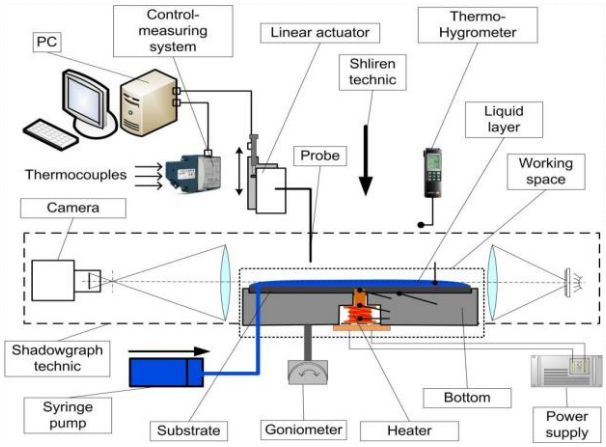


**Figure 1:** Scheme of the experimental rig.

It was found that breakdown process consists of several steps. At the beginning, thinning of the liquid layer over the heating area (Fig. 2 a) due to the effect of thermocapillary forces (Marchuk 2015) and evaporation is observed. Further thinning leads to the formation of residual liquid layer in the area of the local heating, Fig. 2 b). Then the residual layer evaporates until its thickness reaches the critical and breakdown of the liquid layer occurs, Fig. 2 c), (Zaitsev et al. 2007). After the breakdown the whole area of the local heating rapidly dries and quite symmetrical circular dry spot is formed Fig. 2 d). Influences of the layer thickness, intensity of heating and type of substrate on the breakdown dynamics of liquid layer were studied. The existence of residual liquid layer over the heating area before the breakdown has been proved. Velocity of dry spots formation increased when the local heating intensity is increased. One of the main factors that influence the breakdown of residual liquid layer and dry spot formation is evaporation. Significant influence of the surface properties on breakdown dynamics of liquid layer has been found. In case of the rough substrate dry spots were arisen in various points simultaneously and dewetting process was observed. For the smooth surface the residual layer ruptures in one place.

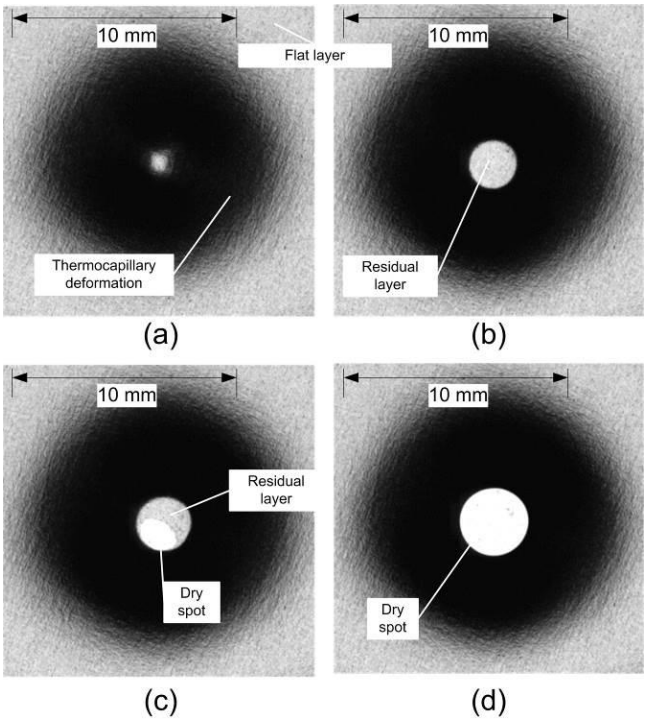


**Figure 2:** Visualization of breakdown dynamics and formation of the dry spots.

**Acknowledgements** The study was financially supported by the Russian Science Foundation (Project 15-19-20049).

## References

Lyulin Yu.V., Spesivtsev S.E., Marchuk I.V., Kabov O.A., Investigation of breakdown dynamics of a horizontal liquid layer with a point heat source, Technical Physics Letters, 41, pp. 22-29 (2015)

Marchuk I. V., Thermocapillary deformation of a horizontal liquid layer under flash local surface heating, Journal of Engineering Thermophysics, V. 24, N. 4. pp. 381-385 (2015)

Zaitsev D.V., Rodionov D.A., Kabov O.A., Study of thermocapillary film rupture using a fiber optical thickness probe, Microgravity sci. technol., XIX-3/4, pp. 100-103 (2007)

# Experimental investigation on the multi-scale heat transfer at pool boiling

Anton Surtaev, Vladimir Serdyukov, Aleksandr Pavlenko

Kutateladze Institute of Thermophysics
Acad. Lavrentiev ave. 1, Novosibirsk, 630090, Russia
surtaevas@gmail.com

Nucleate boiling is a common and one of the most effective heat transfer mechanisms, it is widely used in various technological and industrial applications: energy and chemical industry, nuclear plants, electronics cooling system, etc. At the same time the majority of the models used to calculate heat transfer at boiling are semi-empirical, due to the complexity of full mathematical description of the process (Yagov, 2014). For construction of new theoretical boiling models free of empirical parameters, and for verification of present models it is required to have quality experimental data on the heat transfer and local characteristics of boiling such as nucleation site density and frequency, the intensity of heat transfer in the vicinity of three phases line at the base of a vapor bubble, etc. (Kim, 2014). The main aim of this work is to study local and integral characteristics of pool boiling heat transfer with the use of high-speed digital and IR recordings.

The test fluids were saturated ethanol and deionized water boiling at atmospheric pressure. As the heater in the experiments thin film of indium-tin-oxide (ITO) was used. The 1 μm thick ITO layer was vacuum deposited onto sapphire substrates that were 0.4 mm thick. Boiling occurred on the upward facing side of this film which had an exposed area of 30×20 mm$^2$. Samples were resistively heated by a DC power supply via thin silver electrodes. The temperature fields of the heater were obtained with the use of high-speed thermographic recording with frequency of 1 kHz and resolution up to 0.015 mm/px. High-speed visualization was performed with frequency varied from 1 to 5 kHz and 640×480 (1 px ≈ 0.1 mm) resolution.

Obtained thermograms revealed that during nucleate boiling "dark spot" with a lower temperature were appearing on the test surface. The analysis of temporal and spatial synchronized high-speed digital recording data has shown that these spots occurred, when vapor bubbles appeared on the heating surface. The increase in the heat flux led to increase in the nucleation site density. The analysis of the number of nucleation sites was carried out automatically by the algorithm developed in «Matlab» software.

Also based on the obtained thermograms integral boiling heat transfer was analyzed for different fluids. It is shown that the experimental data for DI water are consistent with those of other authors. At the same time, ethanol heat transfer data lie below reported in the literature data, but at high heat fluxes are consistent with the calculations by well-known models.

High temporal and spatial resolutions of the thermographic recording have allowed to investigate evolution of the surface temperature under single vapor bubbles. This made possible to analyze the temporal characteristics of vapor bubbles growth and separation and to obtain new experimental data on nucleation frequency at different heat flux density for various liquids.

Figure 1 shows evolution of the surface temperature under single nucleation site and corresponding frames of the macro thermographic recording. It can be seen that appearance of the microlayer region led to surface temperature decrease. This data were used to evaluate size of the microlayer evaporation region and heat transfer intensity in the vicinity of three phases line at the base of a vapor bubble.

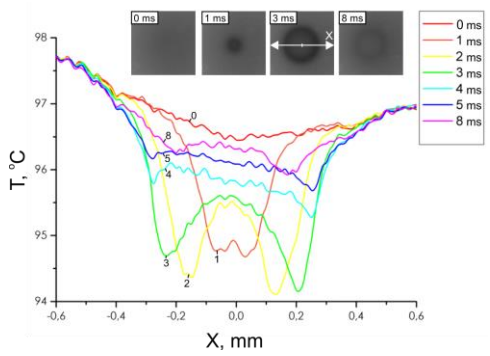


**Figure 1:** Temperature distribution on the heater surface underneath a growing bubble.

The dynamics of vapor-liquid-heater contact line and new data on bubbles departure diameters at ethanol boiling were investigated with the use of high-speed digital recording. The analysis revealed that the experimental data on the bubbles departure diameters were consistent with data from other authors, but couldn't be described by existing semi-empirical models.

Present study has shown high efficiency of the synchronized high-speed visualization and thermography for investigation of the most important local and integral characteristics of boiling heat transfer. Obtained experimental data can be used to calculate heat transfer due to the microlayer evaporation and to identify the relationship between local and integral characteristics of heat transfer at pool boiling.

The reported study was funded by RFBR, research project No. 14-08-00635.

## References

Yagov V.V. Heat Transfer in Single Phase Media and Phase Transitions (in Russian), MPEI Publish, 541 p. (2014)

S. Jung, H. Kim, An experimental method to simultaneously measure the dynamics and heat transfer associated with a single bubble during nucleate boiling on a horizontal surface, Int. Journal of Heat and Mass Transfer, vol. 73 pp. 365–375 (2014)

# Heat transfer enhancement at boiling on the longitudinal finned surfaces

Evgeniy Shatskiy, Evgeny Chinnov

Kutateladze Institute of Thermophysics SB RAS, Lavrent'ev av. 1, Novosibirsk, 630090, Russia
Novosibirsk State University, 630090 Novosibirsk, Russia
E-mail: shatskiy.itp@gmail.com

The future of a number of sectors of the economy is linked with the technology of solid-state light sources and one of the main characteristics of uptime is the removal of heat. Study of the evaporation mechanism on the surfaces of small size was started in Moor and Mesler (1961). The main objective was to study the temperature fields of the heating surface and liquid, and to study conditions for the formation and existence of a thin film of liquid at the base of the vapor bubble. In this work, as in the follow-up, dedicated to the study of a single center of vaporization (Borisov and Kirillov 1970), the heat flux limited with value at which there is a steady generation of a single center of evaporation, that is relatively modest values. A review of studies on heat transfer during vaporization at the surface of the small size is contained in Tolubinskiy et. al. (1987).

In this study, we carried out experiments for the conditions of a large volume of fluid (H> 10 mm) and maintaining the temperature of the fluid at saturation temperature. For these purposes, the work area was covered with additional heater and a protective insulation. Curves of boiling for heaters with D=5 and 1 mm on a smooth and finned surfaces are presented (fig. 1 and 2).

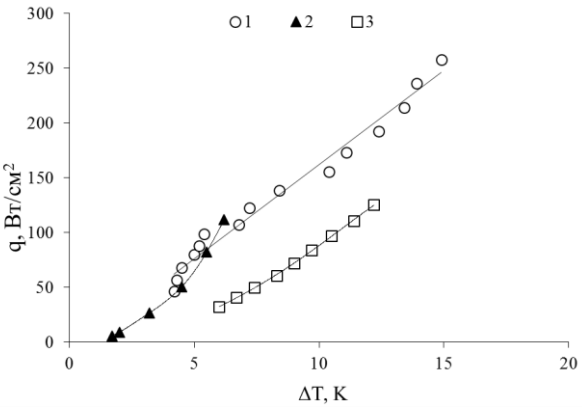


**Figure 1:** The dependence of the heat flux from the temperature difference for the heater for D = 5 mm. 1 - large fins, 2 - small fins 3 - smooth surface.

The boiling curves for the finned surfaces are higher than smooth. Experiments on the heaters D=5 mm with a smooth and finned surfaces showed that overheating on the ribbed surfaces is three times smaller (Fig. 1). And the heat transfer coefficient increases up to two times on the finned surface compared with the smooth. The crisis of heat transfer has been registered on the heater with large fins (Fig. 1) and amounted to 256 W/cm$^2$.

The studies of heat transfer during boiling on a heater with a diameter of 1 mm are shown on fig. 2. On the smooth surface overheating temperature reached about 200 C. The heat flux density before the onset of critical phenomena reaches 900 W/cm$^2$.

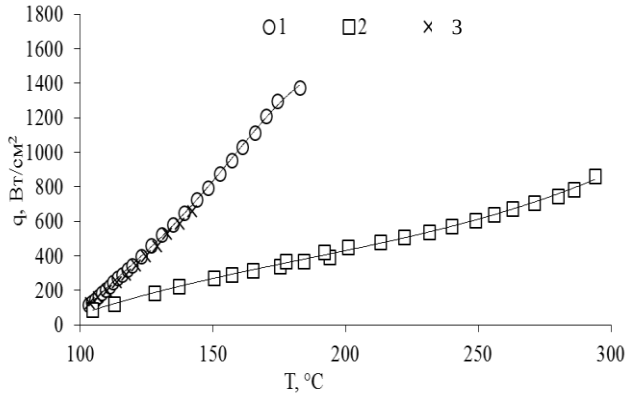


**Figure 2:** Dependence of the heat flux density from the temperature of the heater with a diameter D = 1 mm. 1 - head with large fins, 2 - smooth surface, 3 - head with small fins.

On the ribbed surfaces overheating relative to saturation temperature decreases up to four times. More than three times increases the heat transfer coefficient on the finned surface compared with the smooth. It should be noted that the type of finning has no significant effect on the boiling curve. As a result of the experimental work the density of heat flux reached 1400 W/cm$^2$.

Authors gratefully acknowledge support of this work by the Ministry of Education and Science of Russia (project identifier RFMEFI60414X0053).

**References**

Moor F. D., Mesler R. B. The measurement of rapid surface temperature fluctuation during nucleate boiling of water // AIChE Journal.- 1961 . – Vol. 7, N 4.- P. 620 – 624

Borisov V. Z., Kirillov P. L. Experimental study of the mechanism of heat transfer at a single center of bubble generation // Journal of Engineering Physics and Thermophysics – 1970 – V.28 – No. 4 – pp. 910

Tolubinskiy et. al. Heat transfer during vaporization at the surface of the small size // Industr. Heat Engineering – 1987 – V.9 – No.4 – pp. 3.

# Temperature Measurement inside a Passive Direct Methanol Fuel Cell

Jia Xing LIU[1], Hang GUO[1,2,*], Shuo Wu[1], Fang YE[1], Chong Fang MA[1]

1. MOE Key Laboratory of Enhanced Heat Transfer and Energy Conservation, and Beijing Key Laboratory of Heat Transfer and Energy Conversion, College of Environmental and Energy Engineering, Beijing University of Technology, Beijing 100124, China
2. Collaborative Innovation Center of Electric Vehicles in Beijing, Beijing 100081
*Address all corresponding to Hang GUO, E-mail: hangguo@sohu.com

The direct methanol fuel cell (DMFC) is considered as one of the promising power source for portable power supply because of the advantages such as simple structure, quick recharging, and high power density (Zhao et al. 2009). Although the performance of an active DMFC is higher than that of a passive DMFC, the auxiliary devices such as pump have been eliminated by passive DMFCs, which reduces the cost, the power consume, volume, and weight of the system. Therefore, passive DMFC is still one of the alternative power devices for portable power supply. Temperature plays a vital role in the performance of DMFCs. The cathode of a passive DMFC is normally exposed to ambient environment, thus the generated heat is directly transferred to the ambient environment. As a result, the operating temperature of a DMFC is quite low, which slows the dynamic of electrochemical reaction and therefore deteriorates the performance of cell. It is necessary to monitor the temperature in DMFC for better cell performance and reasonable heat management.

Four self-made thin film thermocouples were inserted into a passive MDFC to measure the temperature. Cobalt and stibium were selected as the metal materials of the thermocouples, and a silicon dioxide slice with a dimensional of 8 mm × 8 mm × 0.1 mm was chosen for the substrate of the thermocouples. More details about the fabrication and calibration of the thermocouple can be found in the work of Guo et al. (2012). The thermocouples were placed on the surface of cathode flow field. Figure 1 shows the placement of thin film thermocouples on the flow field. Once the flow field is assembled in the DMFC, the thermocouples are contact with the surface of MEA at the cathode side. The cathode rather than the anode side of the MEA was chosen for the measurement because methanol solution was fed in the anode methanol cavity, which would affect the temperature measurement by disabling the thermocouples. To insulate the thermocouples and the DMFC, a polyimide film was placed in the area for the arrangement of thermocouples. The thermocouples and lead wires were positioned on the polyimide film, and then another polyimide film was used to fix the thermocouples and lead wires.

The DMFC is tested with a methanol solution of 2 M and an operating temperature of 60 ℃. Figure 2 shows the comparison of cell performance with and without thermocouples. Because current density is used as the comparison parameter, the area occupied by polyimide film has been eliminated when calculating the current density of DMFC with thermocouples. As can be seen, the performance of DMFC with thermocouples has not been significantly deteriorated by the thermocouples. On the contrary, the DMFC with thermocouples shows better performance at high current density.

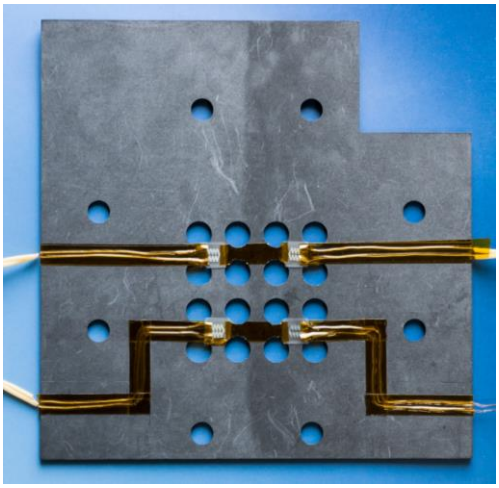

**Figure 1:** Arrangement diagram of thin film thermocouple on the flow field.

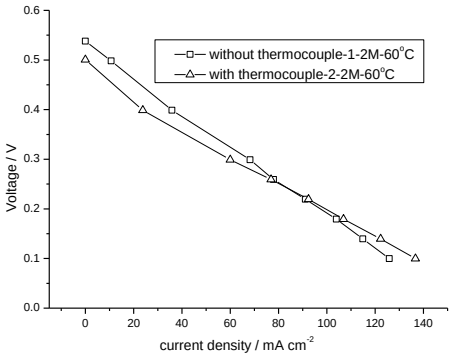


**Figure 2:** Polarization curve of fuel cell with or without thermocouple.

**Acknowledgement**
The authors are grateful to the National Natural Science Foundation of China (Grant No.: 50976006) and Specialized Research Fund for the Doctoral Program of Higher Education (Grant No.: 20121103110009) for the financial support.

**References**

Guo H., Jiang J. Y., Liu J. X., Ye F., and Ma C. F., Fabrication and calibration of Cu-Ni thin film thermocouples, Advanced Materials Research, Vol. 512-515 pp. 2068-2071 (2012)

Zhao T. S., Chen R., Yang W. W., and Xu C. Small direct methanol fuel cells with passive supply of reactants, Journal of Power Sources, Vol.191 pp. 185-202 (2009)

# Phase changes of water droplets with single metallic and nonmetallic inclusions in a high-temperature gas environment

Maxim Piskunov, Anastasia Borisova and Pavel Strizhak

National Research Tomsk Polytechnic University, Institute of Power Engineering, Department of Heat and Power Process Automation
30, Lenin Avenue, Tomsk, 634050, Russia
piskunovmv@tpu.ru

Experimental investigation of evaporation and boiling was carried out on fixed water droplet containing a single nonmetallic (pure graphite; 2–4 mm in size) or metallic (Al, Cu, Ti, Ni, carbon steel, stainless steel, brass, bronze; 1 and 2 mm in size) inclusion and placed in gaseous environment at a temperature of 300–1000 K.

For the heterogeneous liquid droplets with the graphite particles, we discovered a new phenomenon of explosive disintegration occurred with some of the droplets when heated. Furthermore, we revealed different steps such as free surface evaporation of the droplet, bubble boiling at the solid inclusion / liquid interface, explosive disintegration of a droplet into a group of small droplets and evaporation of small droplets. Lifetimes ($\tau_h$) of the droplets and times of each steps were recorded. In addition, we measured influence of gas temperature and inclusion sizes. On the whole, we found conditions for intensive vaporization at solid / liquid interface inside droplets and explosive breakup. This conditions were discussed in detail in Kuznetsov et al. 2016. Additionally, to explain the explosive vapor formation phenomenon and to predict the conditions allowing this process, we developed a simplified model heat and mass transfer.

Experimentally, we found that the addition of small graphite inclusions (0.05 mm in size; 2 % mass concentration) in a heterogeneous liquid droplet with single large graphite particle decreased $\tau_h$ by 50 % in comparison with $\tau_h$ for water droplets without small particles. In this case, a temperature of gas environment is in the range of 350–600 K. However, at a high temperature of 850 K, $\tau_h$ for heterogeneous droplets (15 μl in volume) with small graphite inclusions (0.05 mm in size; 2 % mass concentration) increased by 8 % in comparison with $\tau_h$ for droplets of the same volume without small inclusions. Then, we formulated hypothesis on the formation of vapor film (at a temperature of 850 K) in the surface layer of the heterogeneous liquid droplets (10 and 15 μl in volume) containing small graphite particles. This vapor film influences $\tau_h$ of heterogeneous droplets, in particular, slows down the evaporation process.

For the heterogeneous liquid droplets containing metallic inclusions, we determined lifetimes when increasing the gas temperature from ~298 to ~900 K. Further, to define in detail the evaporation mechanism of the heterogeneous water droplets under study, we proposed hypotheses that explain the random distribution of lifetimes in our tests. Moreover, conditions for the effective cooling of metallic particles were revealed using the balance equations, the calculated warm-up times of inclusions and the differences between phase transfer energy, energy absorbed by water, as well as energy absorbed by metallic particles.

To carry out the present research, we used an experimental setup similar to the one applied in Kuznetsov et al. 2016 and Volkov et al. 2016. Behavior of the heterogeneous liquid droplets was recorded by high-speed (up to $10^5$ frames per second) Phantom video cameras. PIV technique was applied to measure the flow rate of high-temperature gas. Metallic and graphite inclusions were weighed by analytical balance VIBRA AF 225DRCE with an accuracy of 0.001 g. Type K thermocouples were used to measure the temperature of gas environment. To generate water droplets (5, 10 and 15 μl), we used an electronic dosing devise Finnpipette Novus with variation step of 0.1 μl. To do a gas analysis, we used a device Testo 300XXL. Moreover, we applied mechatronic mechanism to move solid-liquid system under study in a high-temperature gas.

We note that the findings contribute to the development of the theory on the evaporation mechanisms of water droplets containing different metallic and nonmetallic inclusions at high temperatures of heating. In particular, the obtained results can be useful to develop such technologies as fire suppression using heterogeneous flows; thermal or flame cleaning of water, emulsions and suspensions on its base; heat carriers on the base of smoke gases, water droplets or emulsions and water vapors; defrosting of granular media by gas-vapor-droplet flows; effective cooling of the heated surfaces.

This work was supported by the Foundation of Russian Federation President (project MD–2806.2015.8).

**References**

Kuznetsov G.V., Piskunov M.V. and Strizhak P.A., Evaporation, boiling and explosive breakup of heterogeneous droplet in a high-temperature gas, Int. J. Heat Mass Transfer, Vol. 92 pp. 360-369 (2016)

Volkov R.S., Piskunov M.V., Strizhak P.A. and Kuznetsov G.V., Water droplet with carbon particles moving through high temperature gases, J. Heat Transfer, Vol. 138 (1) pp. 1-5 (2016)

# DEPOSITION FLUOROPOLYMER FILM WITH ACTIVATING PRECURSOR ON A HOT FILAMENT OF NICHROME

Kubrak K.V.[1], Safonov A.I.[1], Sulyaeva V.S.[2], Starinskiy S.V.[1], Timoshenko N.I.[1]
[1]*Kutateladze Institute of Thermophysics SB RAS, Lavrent'ev ave. 1, Novosibirsk, 630090, Russia*
[2]*Nikolaev Institute of Inorganic Chemistry SB RAS, Lavrent'ev ave. 3, Novosibirsk, 630090 Russia*
vika@itp.nsc.ru

Dependence of surface wettability on roughness can be obtained from the Cassie and Baxter law [1], which defines the value of macroscopic equilibrium contact angle $\theta_c$ in the case of inhomogeneous surface:

$$\cos(\theta_c) = \gamma(\cos\theta + 1) - 1 \qquad (1)$$

where $\theta$ is the contact angle for a smooth surface, $\gamma$ is a part of surface contacting with a droplet of wetting liquid. It is obvious that for low $\gamma$ and high $\theta$, the high contact angles surface can be created. Therefore, roughness amplifies the hydrophilic nature of the surface due to the capillary effect and makes the hydrophobic surface even more hydrophobic.

We used HWCVD (Hot Wire Chemical Vapor Deposition) method [2, 3] for the deposition of thin films of a fluoropolymer. The method consists in the activation of the precursor gas hexafluoropropylene oxide ($C_3F_6O$) on a hot filament of catalyst (nichrome). The activated gas forms the fluoropolymer film on the surface. The method allows control the fluoropolymer film structure by changing the parameters of the deposition process. The film structure determines coating properties, including wetting. The deposition parameters were as follows: the precursor pressure was 0.5 Torr, the activator filament temperature was in range 580 - 900 °C, the filament diameter was 0.5 mm, the substrate temperature was 30 °C, the precursor flow rate was 100 sccm, the wire-substrate distance was 50 mm, and the deposition time was 2 minutes.

The surface morphology of coatings was observed by Scanning Electron Microscope (SEM) JEOL JSM6700F.

The presented research shows a significant influence of the temperature activator on the structure of the fluoropolymer coating.

The fluoropolymer coating forms at the activator temperature over 580°C. The deposition rate increases with temperature increasing. The continuous, smooth and homogeneous films are formed at a temperature 660°C. The deposition rate is 3 - 6 nm/min for this temperature (Fig. 1). Increasing temperature an activator to 700°C leads to rise of the deposition rate to 14 nm/min and formation of globules with average diameter of 10 nm. The cluster globules forms at higher filament temperature in range 700-810 °C. The film becomes porous. The deposition rate increases and reaches a maximum 1.5 μm/min at 770°C. The fluoropolymer film deposits like a powder and consists of particles with a size several tens nanometers at 900°C (temperature limit of the activator).

It has been previously shown [4], HWCVD method allows control the structure of the coating, including wettability.

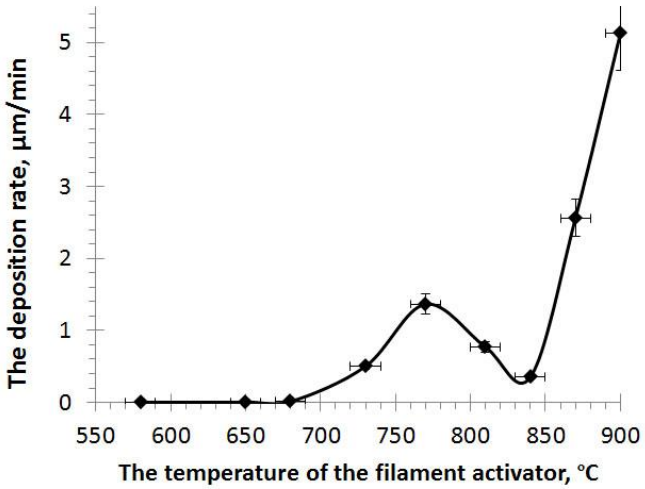


**Figure 1**: The film deposition rate at different activator temperatures.

It was shown that the influence of activating temperature mesh on the coating morphology and deposition rate.

The filament temperature required for formation of fluorpolymer film was determined.

It is found that film with smooth uniform structure are formed when temperature of filament is about 600°C. At the temperature about 900°C film has powder structure.

It is shown that management of the coating structure allows us to control its properties, including wettability.

*The work was supported by the RFBR grant 15-38-20411*

**References**

1. A. Cassie, S. Baxter, Trans. Faraday Soc., **40**, 546 (1944)
2. K. Lau, Y. Mao, H. Lewis, S. Murthy, B. Olsen, L. Loo, K. Gleason, Thin Solid Films, **501**, 211 (2006)
3. A.K. Rebrov, A.I. Safonov and N.I. Timoshenko, Technical Physics Letters, **35** (9), 395 (2009)
4. A. Safonov, V. Sulyaeva, N. Timoshenko, E. Gatapova, O. Kabov, E. Kirichenko, A. Semenov. «Deposition and investigation of hydrophobic coatings» // MATEC Web of Conferences, 37, 01047 (2015). DOI: 10.1051/matecconf/20153701047

# The investigation of boiling crisis of nanofluids

Andrey Minakov, Maxim Pryazhnikov and Valery Rudyak

Institute of Thermophysics SB RAS, Lavrentiev avenue, 1, 630090 Novosibirsk, Russian Federation
Siberian Federal University, Kirensky 26, 660074, Krasnoyarsk, Russian Federation
Novosibirsk State University of Civil Engineering, Leningradskaya 113, 630008, Russian Federation
tov-andrey@yandex.ru

Studies of the last two decades have shown that nanofluids have unusual transfer properties. In particular, small adds of nanoparticles into carrying liquid can considerably increase its heat conductivity and viscosity. This stimulated many thermophysical applications of nanofluids, particularly, aimed at intensification of heat exchange. It has been found that nanofluids have really enhanced coefficients of heat transfer. The further intention to increase this coefficient stimulated the study of heat transfer of nanofluids during boiling. These works have been performed quite intensely during the last decade. Nevertheless, the obtained results are rather contradictory. For example, in [1] it is noted that adding of nanoparticles does not change heat transport considerably, with an even decrease in the heat transfer coefficient during boiling been seen in [2]. Conversely, in [3], this coefficient rose.

In this paper an experimental study of saturated boiling of nanofluids on cylindrical heaters micro sizes. The aim of this study was to study the effect of nanoparticles on critical heat flux (CHF) during boiling. And also study the effect of the size of the heater. As the heater used nichrome wire of various diameters. Heater diameter ranged from 100 microns to 300 microns. Nanofluids were prepared on the basis of distilled water with diamond, silica and iron oxide (III) nanoparticle with a concentration of from 0.25 to 1%. For the preparation of nanofluids used a standard two-step method. After adding the required amount of water in a container with nanopowder, nanofluids for half an hour to destroy conglomerates nanoparticles placed in an ultrasonic disperser.

The critical heat load of the nanofluids changes considerably with an increase in the volume concentration of nanoparticles. Analysis of heat flux density behavior during boiling of nanofluids shows that the use of nanoparticles brings about a considerable increase in the critical thermal load. Especially for nanoparticle $SiO_2$. As early as at a volume particle concentration of 0.25%, the critical density of the heat flow increases by more than 100% and continues to rise with further increase in the concentration of nanoparticles. Hence, use of nanofluids can significantly increase the value of the thermal load as compared to a conventional heat carrier and, consequently, this can increase the energy efficiency of setups in which the main process is boiling.

It was further investigated the influence of the diameter of the heater on the value of the critical heat flux at the boiling. These studies were conducted for $SiO_2$ nanofluids, because it showed the best results in the previous experiments. For these studies, a series of experiments with different diameters of the heaters was performed. As a heater used nichrome wire diameter 100 and 300 microns. It is seen that with decreasing diameter of the heater ratio increases dramatically for all concentrations. CHF increase is considered to be caused by a well-supply of fluids into the surroundings of the departing bubbles near the heater surface. In nanofluids, namely, grown-up micro-convection contribution affected the rise of heat flux. Accordingly, micro-convection worked more effectively, and CHF is delayed in pool boiling of nanofluids, compared with pure water. Apparently, it is caused by the fact that micro convection could have a more dominant effect in small heaters. Therefore, the expansions of the heating area are thought to have diminished the CHF enhancement in pool boiling.

Also we investigated the influence of the diameter of the nanoparticle on the value of the critical heat flux at the boiling. These studies were conducted for $SiO_2$ nanofluids and heater diameter 200 microns. The particle diameters ranged from 25 nm to 100 nm. It is evident that with decreasing particle diameter ratio is reduced. We think that this is due to the deposition of particles on the wall heater. During deposition of particles on the surface of the formed roughened surface. With increase of the particle diameter size of the heater surface roughness increases. By electron microscopy the studied heater surface after boiling nanofluids. It is shown that the main factor determining the boiling crisis of nanofluids is the deposition of nanoparticles on the surface of the heater, which causes an improvement in the wetting surface of the heater, preventing the formation of dry spots

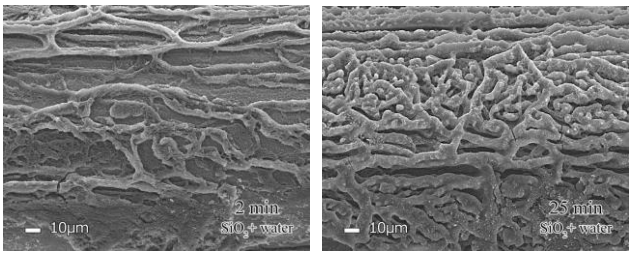


**Figure 1:** Electron microscopy images of the surface of heater after 5 and 25 minutes of boiling SiO nanofluids.

This paper is supported by the Russian Science Foundation (Contract No. 14-19-00312).

**References**

S. M. Kwark, R. Kumar, G. Moreno, J. Yoo, and S. M. You, Int. J. Heat Mass Transfer 53 (5–6), 972 (2009).
S. K. Das, G. Narayan, and Baby A. K. Prakash, J. Nanopart. Res. 10 (7), 1099 (2008).
J. S. Coursey and J. Kim, Int. J. Heat Fluid Flow, 29 (6), 1577 (2008).
M. H. Shi, M. Q. Shuai, Z. Q. Chen, Q. Li, and Y. Xuan, J. Enhanced Heat Transfer 14 (3), 223 (2007).

# Effect of the Kapitza temperature jump on thermal processes in nanofluids

Sergey Novopashin, Marina Serebryakova and Gennadiy Sukhinin

Kutateladze Institute of Thermophysics, 1, Ac. Lavrentieva ave., Novosibirsk, 630090, Russia
serebriakova.marina@gmail.com

A temperature jump at an interface between two media was detected by Kapitza in experiments on the thermal conductivity of superfluid helium. This phenomenon is often referred to as the Kapitza interfacial thermal resistance (KITR). Since the KITR is low, it is observed for systems having small dimensions or a high thermal conductivity. The development of nanotechnologies initiated investigations of this phenomenon in a wide temperature range and for various pairs of solids and at a fluid–solid interface. The Kapitza temperature jump can affect thermal processes in suspensions with nanoparticles (nanofluids), because the characteristic distance between particles in nanofluids with characteristic volume content of about 1% is larger than the diameter of a particle by a factor of 3–5.

We indicate two thermal problems for which the presence of the Kapitza temperature jump can be important. The first problem is the effect of the KITR on the thermal conductivity of nanofluids. This problem has been already solved. Complex research has shown that the Maxwell theory is valid for suspensions based on nanoparticles. It is noteworthy that the effect of the KITR was disregarded when analyzing experimental data. The second problem is heat transfer between a particle and a medium at the release of heat in nanoparticles, e.g., at hyperthermia with the heating of magnetic nanoparticles by an ac magnetic field or at a phase transition in the material of a nanoparticle used for the intensification of heat transfer. We solve the steady-state inhomogeneous heat conduction equation with a heat source $q$ = const inside a sphere with the radius a in an unbounded fluid taking into account the Kapitza temperature jump at the boundary of the sphere:

$$T_p(a) - T_f(a) = Gq = -G\frac{\partial T_p}{\partial r}\,\kappa_p = -G\frac{\partial T_f}{\partial r}\,\kappa_f, \quad T_f(\infty) = T_\infty,$$

where G is the KITR, $T\infty$ is the temperature at infinity, and the subscripts $f$ and $p$ refer to the fluid and particle, respectively. The solution is easily obtained analytically:

$$T_p(r) - T_\infty = \frac{1}{6}\frac{q}{\kappa_p}(a^2 - r^2) + \frac{a^2 q}{3\kappa_f}\left(1 + \frac{G\kappa_f}{a}\right), \ (r < a)$$

$$T_f(r) - T_\infty = \frac{1}{r}\frac{a^3 q}{3\kappa_f}, \ (r > a)$$

If the temperature of the sphere and the temperature at infinity are given, we obtain the solution

$$T_f(r) - T_\infty = \frac{a}{r}\frac{(T_p - T_\infty)}{(\frac{G\kappa_f}{a}+1)},$$

The heat flux in this case is

$$q = \frac{a\kappa_f}{r^2}\frac{(T_p - T_\infty)}{(\frac{G\kappa_f}{a}+1)}.$$

For both cases considered above, the effect of the KITR is characterized by the dimensionless parameter $\gamma = G\kappa_f/a$ expressed in terms of the interfacial resistance, radius of the nanoparticle, and thermal conductivity of the fluid.

The figure 1 shows the dependences of the temperature of the particle at a given thermal flux and the thermal flux at a given temperature difference between the particle and infinity on the parameter γ. The temperature and thermal flux are normalized to the values in the absence of the Kapitza temperature jump (in figure, $\Delta T = Tp(a) - T_\infty$).

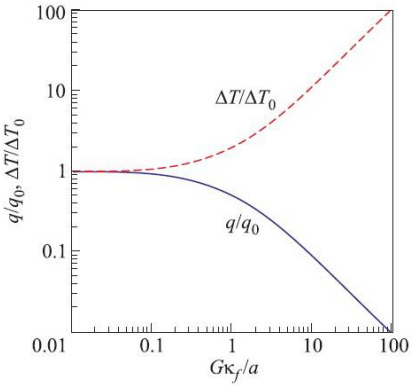


**Figure 1:** Thermal flux (at given temperatures) and the temperature at the boundary of the particle at a given thermal flux versus the Kapitza temperature jump.

According to the figure, the Kapitza temperature jump should be taken into account when considering thermal processes in nanofluids at the parameter $\gamma > 1$. It is worth noting that nanoparticles used both in hyperthermia and at the intensification of heat transfer owing to the heat of a phase transition are particles in shell (core–shell). In this case, there are two contact surfaces and, correspondingly, two Kapitza temperature jumps. Furthermore, the finiteness of the shell also contributes to additional thermal resistance.

For this reason, the total contribution can be significant when solving particular problems. To conclude, we present the following formula for the relative increase in the thermal conductivity of nanofluids $\kappa_{nf}/\kappa_f$ at the volume concentration of nanoparticles $\varphi$:

$$\frac{\kappa_{nf}}{\kappa_f} = \frac{2\kappa_f + \kappa_p(1+2\gamma) - 2\varphi[\kappa_f + \kappa_p(\gamma-1)]}{2\kappa_f + \kappa_p(1+2\gamma) + \varphi[\kappa_f + \kappa_p(\gamma-1)]},$$

It is seen that a change in the thermal conductivity of nanofluids can be characterized by the parameter $\gamma = G\kappa_f/a$ coinciding with the parameter obtained in this work for the description of heat transfer between the nanoparticle and fluid. The general character of this dimensionless parameter makes it possible to treat it as a similarity parameter when describing thermal processes in nanofluids with allowance for the Kapitza temperature jump.

This work was supported by the Russian Science Foundation (project no. 14-19-01379).

# Thermal conductivity, viscosity and rheology of nanofluids based on $Al_2O_3$ nanoparticles and ethylene glykol-water mixtures

Marina Serebryakova, Sergey Dimov, Sergey Bardakhanov and Sergey Novopashin

Kutateladze Institute of Thermophysics
1, Ac. Lavrentieva ave., Novosibirsk, 630090, Russia
serebriakova.marina@gmail.com

The nanofluids are the two-phase media, which include liquid and solid particles with sizes of the nanometer range. The interest to these systems relates to the fact that even low concentrations of nanoparticles can change significantly the thermal-physical properties of basic liquids. Practical application of nanofluids is connected with a possibility to create the high-performance liquid heat carrier. However, when nanoparticles are introduced into the liquid, together with a change in thermal conductivity some other thermal-physical properties change. The most important characteristic is viscosity because a gain obtained due to an increase in thermal conductivity can be lost through a rise of energy spent for liquid pumping. Therefore, it is reasonable to measure thermal conductivity and viscosity of nanofluids, simultaneously.

The current study presents the measurements of thermal conductivity, viscosity and rheological properties of nanofluids based on $Al_2O_3$ nanoparticles in the mixture of 90% EG and 10% water. We used nanoparticles of aluminum oxide $\gamma$-$Al_2O_3$ (Degussa, Germany) with average particle size of 13 nm. To synthesize nanofluids, we used ultrasonic dispersion for an hour. Measurements were carried out at room temperature (25°C) and nanoparticles volume fraction of 0 – 1.5%.

Thermal conductivity was measured by the non-stationary method of a heated wire. We used the device with a platinum wire of 5-μm diameter and 3-mm length. According to analysis, dependence of thermal conductivity on volume concentration of nanoparticles is properly described by the Maxwell theory (Fig.1).

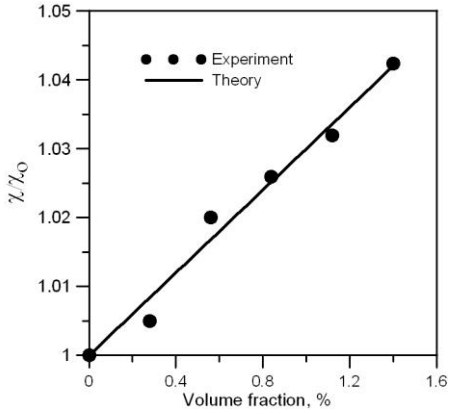


**Figure 1:** Relative thermal conductivity versus nanoparticles volume fraction.

Viscosity was measured by the rotation viscometer and by the homemade capillary viscometer. The rheological properties have been measured by varying Reynolds number. It was found that viscosity differs significantly from both theoretical values and data of other authors (Fig.2). Moreover, the rheological properties have been observed for the volume fraction of nanoparticles higher than 1% (Fig.3).

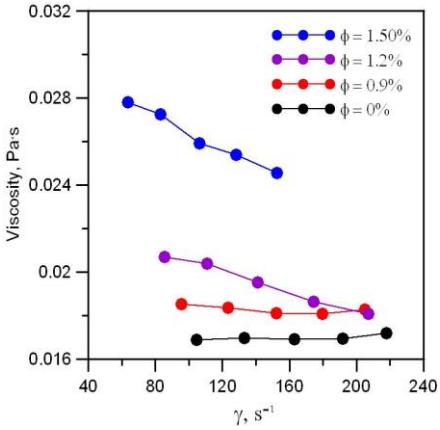


**Figure 2:** Rheological properties of nanofluids.

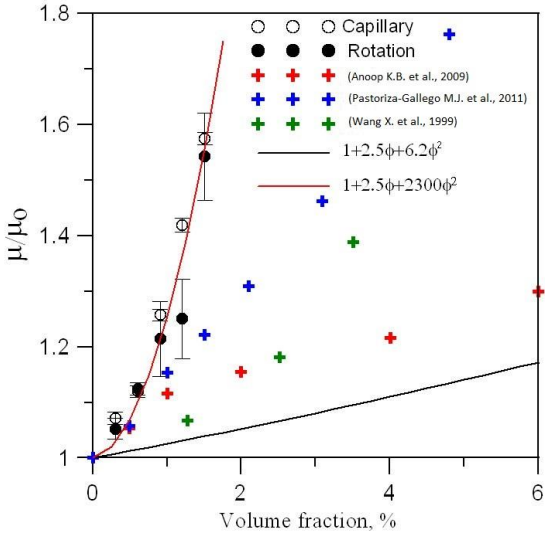


**Figure 3:** Viscosity increasing with volume fraction of nanoparticles.

At maximal volume fraction of nanoparticles (1.5%) used in the current study, an increase in thermal conductivity was about 5% and in viscosity it was about 50%. These values indicate that the studied nanofluids have no prospects for use as an effective heat carrier in comparison with the basic liquid.

This research was funded by Russian Scientific Foundation, Project No 14-19-01379.

# Experimental investigation of the evaporating meniscus dynamics near contact line

Elizaveta Gatapova and Oleg Kabov

Kutateladze Institute of Thermophysics SB RAS, Lavrentyev Ave., 1, Novosibirsk, 630090, Russia
E-mail gatapova@itp.nsc.ru

The wettability of a surface is usually described by the contact angle, measured within the liquid at the three phase contact line. Due to the topographical peculiarities of the solid surfaces, in reality the contact angle does not exhibit a unique value. The contact angle hysteresis (CAH), which is the difference between advancing and receding contact angles, plays an important role on wetting and dewetting processes (Chen et al. 2015).

The processes of liquid transfer between two solid surfaces, formation of liquid bridge and finally formation and evaporation of droplet occur an important in many industrial processes. We conduct with the experiments studying evaporation and dynamics of meniscus for configurations illustrated in Fig. 1, where liquid is confined between two surfaces. To study the dynamics of the evaporating meniscus the test section is installed to observe using microscope Olympus BX51 and high-speed monochrome camera PointGrey (Fig. 2). Super clean MilliQ water and ethanol are used as a working fluid. The microscope is placed on antivibration table system with compressor. The liquid is injected by a high-precision syringe pump (Cole Parmer) and liquid meniscus is formed (Fig. 1). Experiments are conducted at atmospheric pressure, humidity and temperature in vicinity of the working area controlled by Testo device.

**Figure 1:** Configuration of the problem.

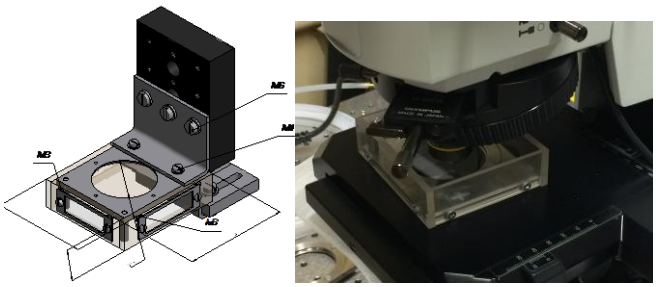

**Figure 2:** Sketch of the test section and photo of the test section mounted on the microscope Olympus BX51.

The formation of the so-called “fingers” of a certain wavelength is observed during the evaporation of ethanol on N-BK7 glass surface (Fig. 3). The wavelength, the time of evaporation as well as the last stage of the evaporation including the wetting and dewetting phenomena are monitored and some characteristic parameters are specified for the smooth glass surface.

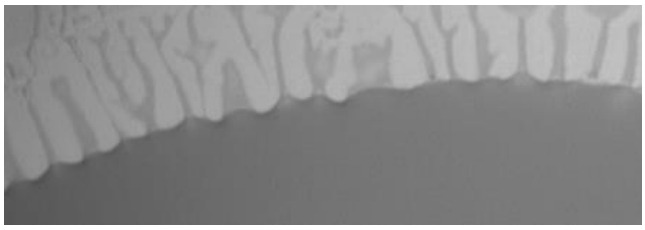

**Figure 3:** “Fingers” formation during evaporation of Ethanol meniscus on N-BK7 glass surface. Air humidity 7%, temperature 24 ºC, pressure 101 kPa.

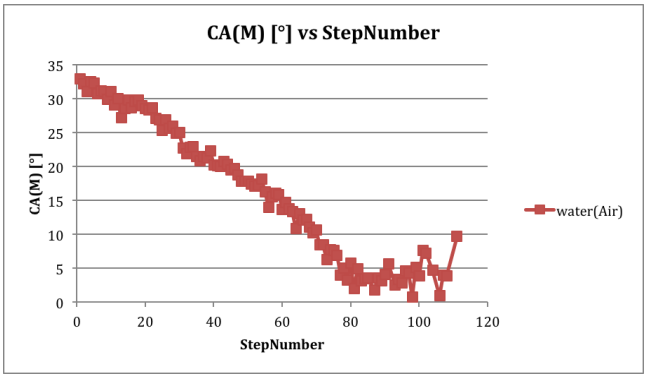


**Figure 4:** Contact angle dynamics during water evaporation. Water-Air system, surface glass N-BK7. Temperature of substrate 50 ºC, air temperature near liquid-gas interface 44 ºC.

Experiments are also conducted to study the contact angle dynamics during the evaporation of droplet under non-isothermal conditions. The contact angle of water on the same glass N-BK7 substrate is measured by KRUSS DSA-100. The work area is placed in the Peltier-chamber (KRUSS), which supports the definition of the constant wall temperature. Fig. 4 shows the evolution of the contact angle for the substrate temperature 50 ° C, the liquid - water. The temperature difference between the substrate and the gas near the liquid is 5 - 6 ° C. The contact angle under mentioned above conditions decreases almost linearly, Fig. 4.

The work is supported by the Ministry of Education and Science of Russia (project identifier RFMEFI61614X0016).

## References

Chen H., Tang T., Amirfazli A., Effect of contact angle hysteresis on breakage of a liquid bridge, Eur. Phys. J. Special Topics, 224, 277–288 (2015)

# Micro-droplet cluster dynamics in a heated layer of liquid at dry spots formation

Zaitsev D.V.[1], Kirichenko D.P.[1,2], Kabov O.A.[1,2]

[1]Kutateladze Institute of Thermophysics SB RAS, Novosibirsk, Russia
[2]Novosibirsk State University, Novosibirsk, Russia
Email: zaitsev@itp.nsc.ru

A micro-droplet cluster is a spatially ordered structure of micro-droplets, discovered in [1] over the surface of liquid layer spot-heated from below. The cluster consists of several of hundreds of drops packed into one layer, forming a hexagonal structure. The drop diameter is on the order of 10 microns; the distance between the drops is of several drop diameters, while the drops levitation height over the liquid surface is comparable to the drop diameter. The possible mechanism of drops levitation is the Stokes force acting onto a drop from the steam flow arising from the heated liquid surface [2].

In this work the micro-droplet cluster was observed at a relatively large heater, under the condition when the liquid layer ruptures and dry spots form on the heater. The basis of the test section is a stainless steel plate with a flush-embedded 10×10 mm$^2$ copper rod, electrically heated by a nichrome wire. Distilled water with the initial temperature of 25°C is used as the working liquid. The test section is opened into atmosphere and installed horizontally. Before conducting experiment, a given volume of liquid is put onto the working surface by means of a syringe. The initial thickness of the liquid layer is $h_0$=0.40 mm. To register dynamics of cluster formation, the Schlieren method with the high-speed camera FASTCAM SA1.1 (5400 fps, resolution of 1024x1024 pixel, optic resolution of up to 10 micron/pixel) is used.

In our experiments we have shown that the micro-droplet cluster can form when the liquid layer is heated from a relatively large heater of 10x10 mm$^2$ size (in previous works [1-3] the heater size was around 1 mm). It has been found, that the drops can levitate not only over the evaporating liquid surface, Fig. 1a, but also over a “dry” surface of the heater, when the rupture of the liquid layer occurs, Fig. 1b. The drops can move over the "dry" surface as far as 3 mm away from the contact line, and can exist for up to 3.5 seconds after the rupture, Fig. 2a.

It has been found that in the region of the contact line there is a so called "forbidden zone" where the drops do not exist (see Fig. 1b). The width of this zone is up to 120 microns during the first 1 sec after the rupture, but then it decreases to approximately 50 microns, Fig. 2b. The existence of such "forbidden zone" may be indicative of the intense evaporation in the vicinity of the contact line.

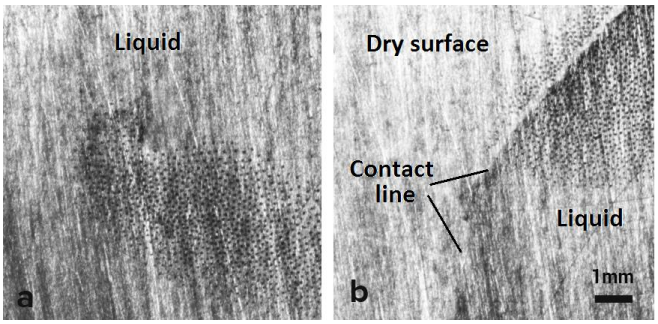


**Figure 1:** Micro-drops levitating over a layer of water heated from below (heat flux is 27.0 W/cm$^2$, heater surface temperature is 85±3°C.) a) Before the rupture of liquid layer; b) after the rupture.

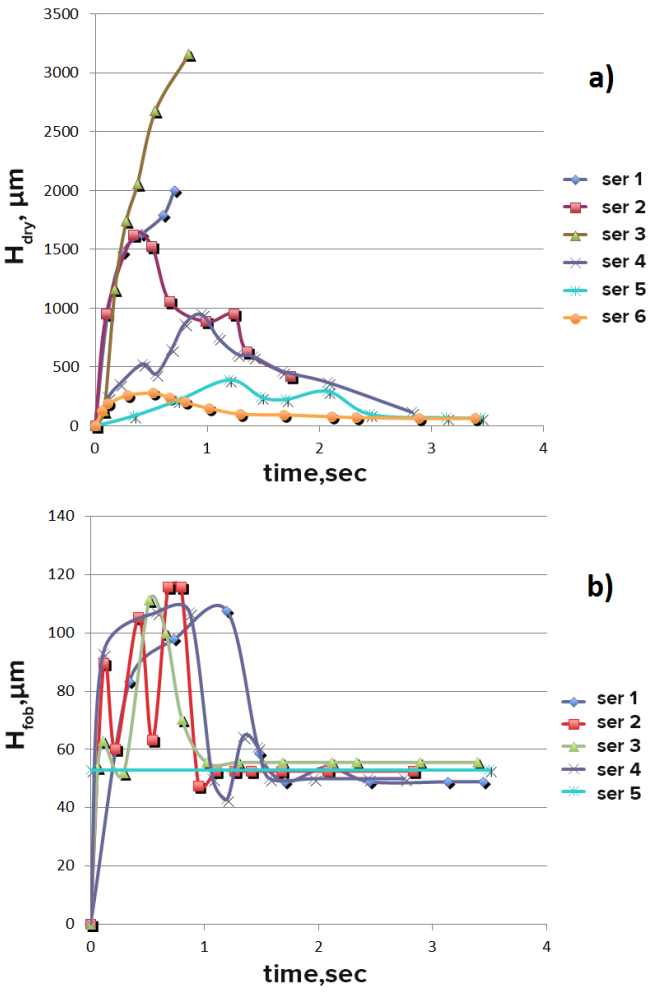


**Figure 2:** Distance to where the drops can move over the “dry” surface (a), and the width of the “forbidden zone” (b) versus time after the moment of the layer rupture.

## References

1. A. A. Fedorets, JETP Lett. 79 , 372 (2004).
2. A.A. Fedorets, I.V. Marchuk and O.A. Kabov, Technical Physics Letters, 37 (2), 116 (2011).
3. A.A. Fedorets, I.V. Marchuk and O.A. Kabov, JETP Lett. 99, 266 (2014).

# Wavy structure and liquid entrainment in annular flows

Dmitriy Markovich, Sergey Alekseenko, Andrey Cherdantsev, Mikhail Cherdantsev and Sergey Isaenkov

Kutateladze Institute of Thermophysics
1 Lavrentiev ave., Novosibirsk 630090, Russia
Novosibirsk State University, Pirogova St. 2, Novosibirsk 630090, Russia
cherdantsev@itp.nsc.ru

In annular gas-liquid flow liquid flows as a film along walls of a duct being sheared by high-velocity gas stream in the duct's core. Due to interaction between gas and liquid so-called disturbance waves appear on the film surface. These waves represent huge lumps of liquid traveling with high speed over long distances. They increase roughness of the interface and, hence, the pressure drop in the channel. They serve as the main source of entrainment of liquid droplets into the gas core. Experimental study of these waves is of high practical and scientific importance; though, it is a challenging task because of highly agitated interface, covered by waves of small spatial scale, high and irregular velocity, steep slopes, high curvature, strong degree of three-dimensionality and complex interactions between the waves. Measurement techniques must satisfy to strong requirements: the measurements should be spatially and temporally resolved with high spatial and temporal resolution and large area of interrogation. Comparative analysis of the available experimental techniques shows how few of them are able to fit the requirements. On this reason, knowledge of structure and dynamics of disturbance waves remains incomplete despite the intensive efforts of experimentalists for over 60 years. It is even unclear if the term "waves" is applicable to these objects.

The main amount of the results presented in this paper is obtained with brightness-based laser-induced fluorescence technique. This method was used intensively by our group to study gas-sheared liquid films for over eight years. The processes of generation of ripple waves of different spatiotemporal behavior were studied systematically for the first time. The ripples are generated at the rear slopes of disturbance waves; they can move either faster or slower than the parent disturbance wave depending on the position of the point of inception of a ripple. Slow ripples decelerate and move over thin base film layer behind the disturbance wave until the following disturbance wave absorbs them. Fast ripples move across the top of disturbance wave towards its front until either being decayed at the steep front of the disturbance wave or being broken by the gas stream into droplets. Presence of fast ripples is necessary for liquid entrainment. Fast ripples may be broken in two mechanisms, known as bag break-up and ligament break-up. Bifurcation in spatiotemporal evolution of the ripples may be explained by existence of eddy motion under the humps of disturbance waves.

A method of automatic identification of spatiotemporal trajectories of individual disturbance waves was devised. This method allowed us to analyze the disturbance waves and also the properties and evolution of fast and slow ripples in a reference system of parent disturbance wave. The average spatial length of crest and rear slope of disturbance waves was measured together with the length required for stabilization of slow ripples properties (the latter could be referred to as "wake" of a disturbance wave).

One of the ways to understand the nature of disturbance waves is to study how they are created. It was shown that the disturbance waves are formed near the inlet due to coalescence of high-frequency initial waves which appear due to Kelvin-Helmholtz instability of gas-sheared film. This mechanism was also found to occur far from the inlet, where so-called ephemeral disturbance waves are generated and where transition to entrainment occurs. Thus, the mechanism is universal and it is not defined by the inlet configuration. The initial waves were shown to be two-dimensional; not far from the inlet they are broken into localized 3D waves. Multiple coalescence of such waves leads to formation of the disturbance waves. After the disturbance waves are formed, the transverse coherence of the flow starts to increase downstream. The disturbance waves undergo strong individual acceleration at the initial stage of their evolution. The value of acceleration strongly correlates with the value of gas shear. Further downstream, acceleration decreases and can even become slightly negative. This can be explained by start of massive entrainment of liquid from the disturbance waves, which decreases the height of disturbance waves and their interaction with the gas flow.

The entrainment was studied by both sampling probes and LIF method. The former allowed us to estimate the amount of liquid entrained from an individual disturbance wave and compare it to the deceleration of the waves. The latter was used to study the parameters of entrained droplets at the initial stage of their evolution, since the droplets contain the fluorescent dye and are also detectable in LIF data. It was shown that the initial velocity of the droplet is 1.5-2 times higher than the velocity of the fast ripples, which implies that a droplet gains large momentum in process of ripples break-up. The size of the entrained droplets was found to be much larger than the average size of the droplets in the gas stream; this can be explained by faster deposition of the larger droplets back onto the film and creation of smaller droplets due to secondary entrainment. Impact of depositing droplets causes formation of craters on film surface which travel with the same speed as the slow ripples. The maximum size of the craters was found to be limited by the wavelength of the slow ripples. In some cases - presumably, when the angle between the droplet and the film is small - impacting droplets create bubbles trapped inside liquid film. It was also found that the coalescence of disturbance waves may be accompanied by massive entrainment. Thorough examination of such events shows that entrainment still occurs due to bag and ligament break-up mechanisms. Thus, coalescence of disturbance waves is not a separate mechanism of entrainment, but just a mechanism of entrainment enhancement.

# Interfacial Thermal Fluid Phenomena in Shear – Driven Thin Liquid Films

Oleg A. Kabov

Institute of Thermophysics, SB RAS, prosp. Lavrentyev 1, Novosibirsk, 630090, Russia

One of the global problems of thermal physics is the problem of finding new methods for improving the energy efficiency of technologies, including finding some new methods of significant enhancement of heat transfer. Today the problem of cooling of high-performance electronic systems, such as computers, RF electronics, and solid-state lasers is one of the most complex problems of thermal physics. Technical processes with a resolution of 20-28 nm (Qualcomm's Snapdragon processors 808/810, 20 nm) are used in the production of modern processors. The number of transistors in a chip reaches several billion (e.g. in NVIDIA GTX-TITAN it is $7x10^9$). The heat flux density in electronic converters and inverters of hybrid cars now reaches values of up to 100-200 W/cm$^2$. The average heat flux density in chips of commercially available computers and other electronic devices is up to 200-300 W/cm$^2$ [1]. For some military electronic systems heat removal is needed on the chip-level in excess of 1 kW/cm$^2$ heat flux and 1 kW/cm$^3$ heat density with thermal control of local submillimeter hot spots with heat flux exceeding 5 kW/cm$^2$ [2].

It should be noted that the heat flux density at the surface of the Sun is about 10 kW/cm$^2$, i.e. quite close to the values mentioned above. However, the heat transfer on the surface of the Sun occurs at a temperature of about 6000 K, while in chips the heat have to be removed, as a rule, at a temperature of 80-90 °C, and at a temperature of about 120-200 °C in special applications. The situation with heat removal becomes even more complicated due to the transition of the electronic industry to production of 3D chips, where several substrates with electronic components are installed in parallel with a distance of 50-100 microns. In March 2014 GLOBALFOUNDRIES has already announced the creation of three-dimensional processors architecture.

Even the most effective conventional cooling systems are unable to provide heat removal from the above mentioned microelectronic components, which is a kind of technological barrier preventing the further development of high-performance microelectronics. It is expected that these thermal limitations will be alleviated by integrating some new thermal management techniques into the chip layout, substrate structure, and/or package design. To implement a new concept of cooling, achieving a new level of understanding of interfacial phenomena under conditions of high and ultrahigh surface and/or volumetric heat generation is essential, as well as achieving a better understanding of the fundamental laws of functioning of multiphase systems with phase transitions in mini and micro sizes.

One of the major working hypothesis to improve the heat transfer efficiency can be a creation of specifically structured self-organized flows in mini- and microchannels that can be achieved by applying the relevant micro- and/or nanostructured surfaces, Fig. 1. Two-phase flows in general have to ensure the flow of a given amount of liquid that allows to avoid heat transfer crisis (burnout) in case of complete or almost complete evaporation of the liquid. The scope of the problem lies in the major objective to develop a new generation of highly efficient two-phase heat exchanging micro-systems using “smart interfaces”. Such systems can be called *intelligent*, since they are based on an adjustable and controlled two-phase flow providing minimum flow resistance and maximum rate of evaporation.

Thin liquid films driven by a forced gas/vapor flow are a promising candidate for the thermal management of advanced semiconductor devices in earth and space applications. The present work gives an overview of the achievements in this field obtained by a team led by the author of the lecture, over the past few years. The challenges of new research are being discussed.

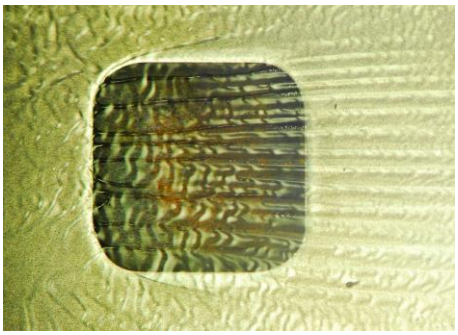

Fig. 1. Photograph of the flow structure in a horizontal flat 170 μm height and 30 mm width micro gap with a flush-mounted heated copper rod with a 1×1 cm square head, $Re_l$ = 18, $U_{Sg}$ = 19.5 m/s, $q$ = 150 W/cm$^2$.

Two-sided three-dimensional non-stationary mathematical model has been developed [3]. For a deformable gas-liquid interface, convection heat transfer in the liquid and the *gas* phases and temperature dependence of surface tension and liquid viscosity are taken into account. The problem has been reduced to five governing equations for the film thickness, temperature fields in the gas and liquid, vapor concentration in the gas phase and gas pressure. Numerical code has been tested by comparison with exact solutions. Systematic numerical investigations of evaporation, free interface deformations as well as evolution of heater size effect and temperature dependence of physical properties have been performed [4,5,6]. In addition 3D, non-stationary, two-sided mathematical model of joint motion of liquid film and co-current *vapor* flow in a microchannel with local heating has been developed [7]. For given calculation parameters, evaporation of liquid film sheared by the inert gas is several times higher than for the liquid film sheared by the vapor flow.

The isothermal two-phase flow structure in a narrow short horizontal channel of a rectangular cross-section with the height of 100 - 1000 micrometers and width of 9-30 mm has been studied experimentally. The use of the Schliren and

fluorescent methods made it possible to reveal the flow of liquid in the channel and to determine its characteristics quantitatively [8]. It was found that in the microchannels studied there is an area of the stable separate flow with a thin liquid film. The features of churn, jet and drop flow patterns were studied. It is shown that instability of the liquid flow near the lateral walls has a significant effect on the transition between different regimes of the two-phase flow. In particular, it is defined that formation of the liquid droplets is the feature of the gas-liquid flow in the channels with the height of below 500 μm. Two regimes have been distinguished: formation of the fixed drops on the channel wall due to liquid film breakdown and formation of mobile drops because of instability of the two-phase flow. It is determined that intensity of droplet formation increases with a decrease in the channel height. It is shown that a change in the height and width of the horizontal channels has a substantial effect on the boundaries between the regimes.

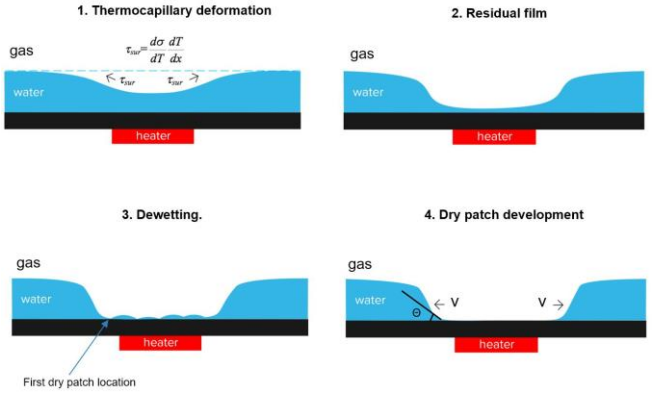


Fig. 2. Film rupture at local heating.

Dynamics and heat transfer of evaporating locally heated thin liquid film driven by the action of the pure nitrogen gas flow in a narrow channel have been investigated [9]. Experiments with water and FC-72 in flat channels (height 0.17 - 2.0 mm) and width 30-40 mm have been conducted. Schlieren technique, high-speed visualization and infrared thermography have been used in experimental investigations. The critical heat flux for a shear driven film of water may reach more than 500 W/cm$^2$. Thermocapillary effect can be considered as one of the most important reasons for the film rupture and crisis phenomenon for small and a moderate velocities of the gas [10].

The effect of a contact angle on the critical heat flux has been studied for water in [11]. Different methods of working surface processing were applied; this allowed variations of the equilibrium contact angle from 27±6° to 74±9° without a change in thermal properties of the system. The effect of equilibrium contact angle on dynamics of dry spot spreading at disruption of a horizontal water layer heated locally from the substrate was studied using the high-speed Schlieren technique in [12]. It is found that substrate wettability significantly affects the propagation velocity of dry spot and its final size. For the conditions of both good and poor wettability, the velocity of contact line propagation is higher in the substrate zones with a higher temperature.

Stable thin residual film may occur before the break up of the liquid layer with the local heating [13] (see Fig.2). It is a new and most likely important fact for better understanding of film rupture. The diameter of the thin residual film may reach up to 3 mm. Characteristic velocities of rupture of residual layer increase with intensity of local heating. The residual film mechanisms of stabilization can be London-van der Waals disjoining pressure; electrostatic repulsion; local temperature decrease in the wall. For the modeling of the evaporation process in thin residual film the pressure and the temperature jump conditions with coefficients derived from the kinetics theory can be important [14].

**Acknowledgements** The study was financially supported by the Russian Science Foundation, project no. 14_19_01755.

**References**

[1] Mahajan et al., Cooling a Microprocessor Chip, Proceedings of the IEEE 94 (8), 1476, 2006.
[2] A. Bar-Cohen, Intrachip/Interchip Enhanced Cooling Fundamentals, DARPA, Microsystems Technology Office, June 7, 2012, http://www.fedbizopps.gov/
[3] Kabova Yu.O., Kuznetsov V.V., Kabov O.A., Gambaryan-Roisman T. and Stephan P., Evaporation of a thin viscous liquid film sheared by gas in a minichannel, *Int. J. of Heat and Mass Transfer*, Vol. 68, pp. 527-541, 2014.
[4] Kabova Yu., Kuznetsov V.V., and Kabov O., Gravity Effect on Evaporation and Interfacial Deformations in Nonisothermal Liquid Film Moved by a Gas Flow in a Microgap, *Interfacial Phenomena and Heat Transfer*, 2 (1), pp. 85–102, 2014.
[5] Yu. O. Kabova, V. V. Kuznetsov, O.A. Kabov, Effect of temperature dependence of physical properties of fluid on flow and evaporation of film with concurrent gas flow in a microchannel, *Doklady Physics*, Vol. 60(6) pp. 259–262, 2015.
[6] O. A. Kabov and Yu. O. Kabova, Effect of heater sizes on evaporation of a liquid film entrained by the gas flow in a microchannel with local heating, *Thermophysics and Aeromechanics*, 2015. Vol.22, No.4, pp. 539-542.
[7] Yu. O. Kabova, V. V. Kuznetsov, O. A. Kabov, Flow and evaporation of non-isothermal liquid film with concurrent vapor flow in a microchannel with considerations of heat and mass transfer on the gas-liquid interface, *Doklady Physics*, 2016.
[8] Chinnov E. A., Ron'shin F. V., Kabov O. A. Two-Phase Flow Patterns in Short Horizontal Rectangular Microchannels, *Int. Journal of Multiphase Flow*, Vol. 80, pp. 57-68, 2016.
[9] Oleg A. Kabov, Dmitry V. Zaitsev, Yulia O. Kabova, Vechaslav V. Cheverda, Evaporation, dynamics and crisis phenomena in thin liquid films sheared by gas in a narrow channel, Proceedings of the 15th International Heat Transfer Conference, IHTC-15, August 10-15, Kyoto, Japan, paper IHTC15- 9537, 15 pages, 2014.
[10] V.S. Ajaev, E. Ya. Gatapova, O. A. Kabov, Stability and break-up of thin liquid films on patterned and structured surfaces, *Adv. in Colloid and Interface Science*, Vol. 228, pp. 92-104, 2016.
[11] D.V. Zaitsev, D.P. Kirichenko, O.A. Kabov, The Effect of Substrate Wettability on the Breakdown of a Locally Heated Fluid Film, *Technical Physics Letters*, Vol. 41. No. 6. P. 551–553, 2015.
[12] Zaitsev D.V., Kirichenko D.P., Orlik E.V., Kabov O.A., The effect of contact angle on dynamics of dry spots spreading in a horizontal layer of liquid at local heating, *Matec Web of Conference*, Vol. 37, 01063, p.1-5, 2015.
[13] Yu. V. Lyulin, S. E. Spesivtsev, I. V. Marchuk, and O. A. Kabov, Investigation of Disruption Dynamics of the Horizontal Liquid Layer with Spot Heating from the Substrate Side, *Technical Physics Letters*, Vol. 41, No. 11, pp. 1034–1037, 2015.
[14] Elizaveta Ya. Gatapova, Irina A. Graur, Felix Sharipov, Oleg A. Kabov, The temperature and pressure jumps at the vapor-liquid interface: application to a two-phase cooling system, *Int. J. of Heat and Mass Transfer*, Vol. 83, pp. 235 – 243, 2015.

# Understanding Pulsating Heat Pipes: The Way Ahead

Sameer Khandekar

Department of Mechanical Engineering, Indian Institute of Technology Kanpur
G. T. Road, Kalyanpur, Kanpur (UP), 208016, India
samkhan@iitk.ac.in

Research on Pulsating Heat Pipe (PHP) has received substantial attention in the recent past, due to its unique operating characteristics and potential applications in many passive heat transport situations, including space and terrestrial domains. A PHP is a capillary tube (with no wick structure) bent into many U-turns and partially filled with a working fluid, forming a natural distribution of Taylor bubbles and liquid plugs inside it, as shown in Figure 1 (Akachi, 1993; Akachi, 1996; Akachi et al., 1996, Khandekar, 2004; Mameli 2012). When the temperature difference between the heat source and the heat sink exceeds a certain threshold, thermally induced self-sustained oscillations of the vapor bubbles and liquid plugs commences. Heat is thus transferred, not only by the latent heat exchange like in conventional heat pipes, but also by sensible heat transfer between the wall and the fluid. Compared to other passive heat transfer solutions, PHPs are quite simple in construction, and thus, potentially more reliable and cheaper.

Mathematical modeling of pulsating heat pipes through 'first' principles is a contemporary problem which remains quite elusive. Simplifications and assumptions made in all the modeling approaches developed so far render them unsuitable for engineering design because the abstractions contained therein are not in sync with the real time transport processes taking place in the device. At present there are no theoretical models or correlations available that can predict the complex thermo-hydrodynamic transport behavior of PHPs. This prevents their widespread use in industrial applications.

Research in the last decade has highlighted the following new facts about the working principle and its modeling strategies:

- It has been conjectured that non-equilibrium states of liquid and vapor are quite likely to coexist during the normal operation of PHPs. Conclusive experimental evidence is yet to come, however initial results do point towards this fact. It requires very precise and repeatable dynamic temperature measurements of local vapor and fluid film temperature so as to ascertain non-equilibrium condition and/or metastability. On one asymptote is the assumption that vapor and liquid in the Taylor bubbles are always under thermodynamic equilibrium. This essentially means that the relaxation time-scales of the phase-change by heat addition/subtraction are much faster than the typical characteristics time-scales of internal fluid flow and heat transfer through the walls in the PHP system. However, the essence of the entire PHP thermal phenomena lies in its transient thermo-fluidic characteristics. While one can talk about a 'quasi-steady' state in a global or lumped sense, nothing is, in fact, steady on the local level inside an operating PHP. Hence, the assumption of thermodynamic equilibrium between adjacent vapor bubbles and liquid plugs may not be the most appropriate postulation. The rapid inertial flow transients vis-à-vis evaporation and condensation time scales may lead to situations wherein superheated vapor and/or sub-cooled liquid co-exists for finite metastable timescales (Khandekar 2004; Nikolayev 2013; Rao et al., 2015).
- The frictional pressure drop required to sustain the flow, especially in the liquid plugs may be substantially higher than what is predicted by assuming a simple Poiseuille flow inside them. The fluid flow pattern in the oscillating two-phase 'unit-cell' system (that is, one Taylor bubble with adjoining liquid plug, as has been depicted in Figure 2) is rather complex leading to high viscous dissipation. Moreover, three-phase contact lines tend to form inside the system, especially in the evaporator subsection, which lead to very high local dissipation (Srinivasan et al, 2015a, 2015b; Janeček and Nikolayev, 2013).
- Thin film evaporation and condensation plays a very crucial role in the overall dynamics. Unless this is included in the global model, realistic predictions cannot be made. Corollary to this is the fact that unless mass addition/removal from the vapor space is considered, the amplitude of oscillations which are observed in actual experiments cannot be predicted. Treating the vapor as an ideal gas with only sensible heating/cooling is not sufficient (Rao et al., 2015; Mameli et al., 2014).
- Inertia forces play a significant role in the manifestation of flow physics of the device. Sudden acceleration and deceleration of the 'unit-cell' and its interaction with surface and capillary forces lead to complex flow phenomena, including breakage of liquid plugs into smaller fragments. While most hydrodynamic theories of visco-capillary flows are valid for low Capillary number (less than $10^{-3}$) situations and high wettability conditions, engineering scale PHP devices do not pose such ideal situations. Partial wetting and relatively large Capillary numbers are routinely prevalent (Khandekar et al., 2010; Rana et al., 2014; Mehta and Khandekar, 2014).
- The radial heat transfer to/from the liquid-vapor system must happen via the capillary tube material. Unlike a conventional heat pipe which attains a quasi-steady state, the transient oscillatory flow patterns inside a PHP manifests itself as a conjugate (conduction–convection) problem. Hence, the interplay of diffusional and convective time-scales of the system strongly affects the ensuing thermal-hydraulic response. In effect, thermal properties of the tube material is vital in predicting the overall system dynamical response (Nikolayev, 2016; Rao et al. 2013; Rao et al., 2015).

In this background, this paper will highlight the state of the art on PHPs, by delineating a comprehensive approach to comprehend the underlying phenomena by experimental and modeling strategies, and by summarizing the contemporary efforts in furthering the understanding of physics governing the complex thermo-fluidic transport.

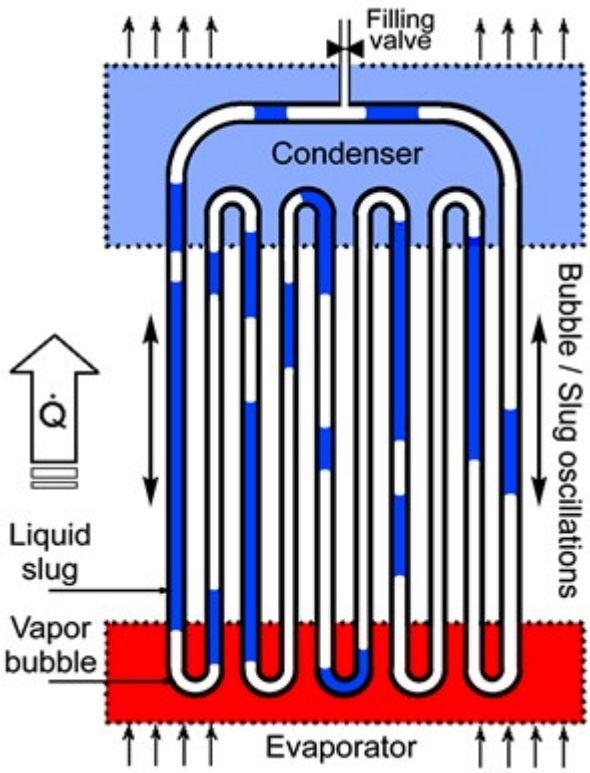


**Figure 1:** Schematic of a closed loop pulsating heat pipe

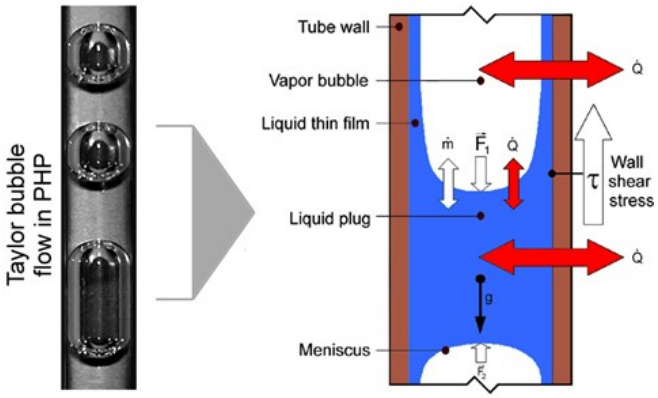


**Figure 2:** Transport processes in a 'unit-cell' of a PHP

## References

Akachi H., Polášek F. and Štulc P., Pulsating Heat Pipes, Proc. 5th Int. Heat Pipe Symp., Melbourne, pp. 208-217, (1996).

Akachi H., U. S. patent, Patent Number 5219020, (1993).

Akachi H., U. S. patent, Patent Number 5490558, (1996).

Janeček, V., Nikolayev, V.S., Apparent-contact-angle model at partial wetting and evaporation: Impact of surface forces, Phy. Rev.-E, 87 (1), #012404, (2013).

Khandekar S., Thermo-Hydrodynamics of Closed Loop Pulsating Heat Pipes, Doctoral dissertation, University of Stuttgart, Stuttgart-Vaihingen, Germany, (2004) (available at: http://elib.uni-stuttgart.de/opus/volltexte/2004/1939/

Khandekar S., Panigrahi P. K., Lefèvre F. and Bonjour J., Local Hydrodynamics of Flow in a Pulsating Heat Pipe: A Review, Frontiers in Heat Pipes, 1, pp. 023003(1-20), 2010.

Mameli M., Pulsating Heat Pipes: Numerical Modeling and Experimental Assessment, Doctoral dissertation, University Bergamo, Italy, (2012).

Mameli M., Marengo M. and Khandekar S., Local Heat Transfer Measurement and Thermo-fluid Characterization of a Pulsating Heat Pipe, Int. J. Therm. Sc., 75, pp. 140-152, (2014a).

Mehta B. and Khandekar S., Taylor Bubble-train Flow and Heat Transfer in the Context of Pulsating Heat Pipes, Int. J. Heat Mass Trans., 79, pp. 279-290, (2014).

Nikolayev, V.S., Effect of tube heat conduction on the single branch pulsating heat pipe start-up, Int. J. Heat Mass Transf. 95, pp. 477-487, (2016).

Nikolayev, V.S., Oscillatory instability of the gas-liquid meniscus in a capillary under the imposed temperature difference, Int. J. Heat Mass Transf., 64, pp. 313-321, (2013).

Rana G. R., Sikarwar B. S., Khandekar S., Panigrahi P. K., Hydrodynamics of a Confined Meniscus in a Square Capillary Tube at Low Capillary Numbers, Front. Heat Pipes, 5 (1), (2014).

Rao M., Lefèvre F., Khandekar S. and Bonjour J., Heat and Mass Transfer Mechanisms of a Self-Sustained Thermally Driven Oscillating Liquid Vapor Meniscus, Int. J. Heat and Mass Trans., 86, pp. 519-530, (2015).

Rao M., Lefèvre F., Khandekar S. and Bonjour J., Understanding Transport Mechanism of a Self-sustained Thermally Driven Oscillating Two-phase System in a Capillary Tube, Int. J. Heat Mass Trans., 65, pp. 451-459, (2013).

Srinivasan V., Marty-Jourjon V., Khandekar S., Lefèvre F. and Bonjour J., Evaporation of an Isolated Liquid Plug Moving Inside a Capillary Tube, Int. J. Heat Mass Trans., 89, pp. 176-185, (2015a).

Srinivasan V., Khandekar S., Bouamrane N., Lefèvre F. and Bonjour J., Motion of an Isolated Liquid Plug inside a Capillary Tube: Effect of Contact Angle Hysteresis, Exp. in Fluids, 56:14 (6 pages), (2015b).

# Effect of surface structure on DNB of subcooled flow boiling in a narrow channel

Tomohiko Nakamura, Jumpei Yoshidome, Taisaku Gomyo and Hitoshi Asano

Department of Mechanical Engineering, Kobe University
1-1, Rokkodai, Nada, Kobe, 657-8501, Japan
asano@mech.kobe-u.ac.jp

Boiling heat transfer is effective for cooling devices. However, burnout caused by departure from nucleate boiling (DNB) should be avoided. Asano et al. (2012) reported that a porous surface made by thermal spraying could produce higher boiling heat transfer enhancement and higher critical heat flux (CHF) in subcooled flow boiling. The purpose of this study is to clarify the effect of surface structure on DNB of subcooled flow boiling in a rectangular narrow channel. A smooth and thermal spray coated surfaces were used as the heating surface. Wall temperatures, pressure and void fraction were measured.

FC-72 was used as the working fluid. The working fluid was circulated by a gear pump. Figure 1 shows the detail of the test section. The test section with the channel gap of 4 mm, channel width of 20 mm, and heated length of 50 mm at the center of the channel was placed horizontally. The coating surface was made by a vacuum plasma spraying method. Six thermocouples were inserted in the copper heating wall at 2 and 7 mm in depth and 10, 25, and 40 mm from the inlet of the heating section. Void fraction was measured by a capacitance probe at the nearest temperature measure point to the exit. The sensing electrode had a rectangular cross-section with the same width as the channel. Volumetric average void fraction, $\alpha$, was measured from the capacitance, $C$, by using the capacitance for vapor single-phase, $C_G$, and liquid single-phase, $C_L$, in this equation, $\alpha = (C_L - C) / (C_L - C_G)$.

The experiments were carried out at the constant inlet pressure of 155 kPa and mass flux of $G$ = 800 kg/(m$^2$·s). The inlet subcooling, $\Delta T_{sub}$, was varied from 20 to 50 K.

Boiling curves for each heat transfer surface are shown in Figure 2. The coating produced about double boiling heat transfer coefficient of the smooth surface. Furthermore, the CHFs were increased by applying the coating.

At just during DNB, a large fluctuation of void fraction and pressure was observed as shown in Figure 3. Figure 3 shows transient changes of void fraction, the inlet pressure, wall temperatures, $T_w$ and mass flux, $G$ for the coating with $\Delta T_{sub}$ = 40 K. Before the fluctuation, the boiling mode was a nucleate boiling with small void fraction fluctuation due to bubble flows. At 4 seconds in the figure, the large fluctuation started. The pressure fluctuation was well synchronized with the void fraction fluctuation. At 15 seconds, the void fraction became stable at a lower value. Since the wall temperature continued to increase, a stable vapor film might be formed. The maximum and minimum void fractions during the fluctuation were close to the values before and after the fluctuation, respectively. It could be said that the fluctuation were caused by the cycle of nucleate and film boiling. Therefore, the wall temperature gradually increased during the fluctuation. The mass flux slightly decreased a few seconds later from the start of the fluctuation due to the increase in the flow resistance. For the smooth surface with the inlet subcooling lower than or equal to 30 K and the coating with every inlet subcooling, the same fluctuation was observed. The period of the fluctuation for the coating was longer than the smooth surface. The frequency was almost the same.

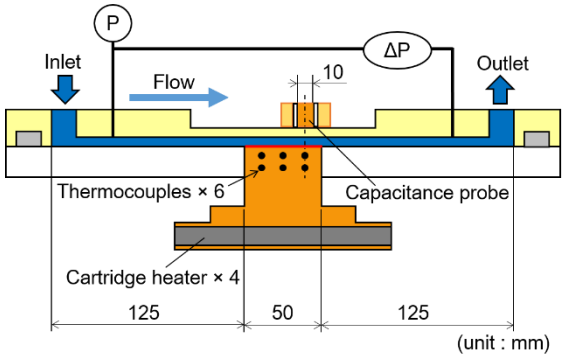


**Figure 1:** Detail of test section.

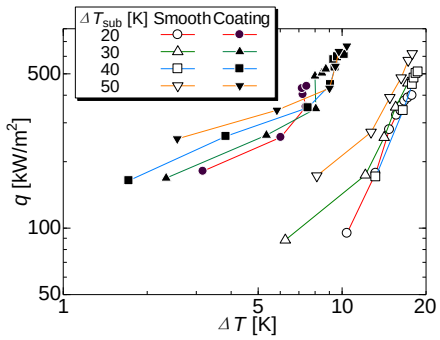


**Figure 2:** Comparison in boiling curves.

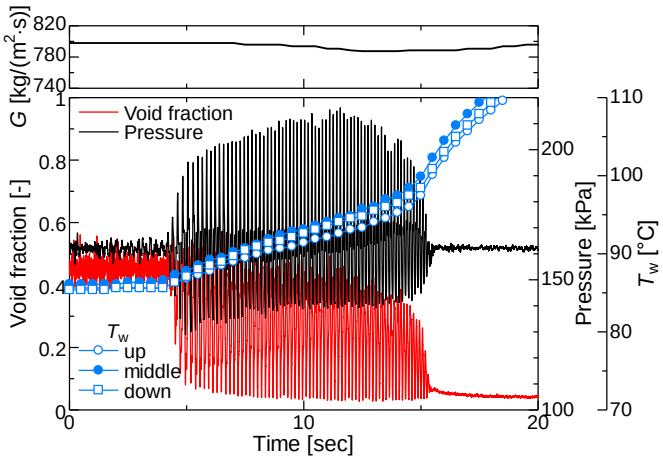


**Figure 3:** Transient changes during DNB.

## Reference

H. Asano, K. Kawasaki, N. Takenaka, Effect of heat-transfer surface structure on critical heat flux, Multiphase Science and Technology, 24(3), pp. 181-196 (2012).

# The effect of the channel height on the CHF in a shear-driven liquid film

D. Zaitsev[1], E. Orlik[1,2], O. Kabov[1,2]

[1] Institute of Thermophysics SB RAS, 1, Lavrentiev Ave, 630090, Novosibirsk, Russia
[2] National Research Tomsk Polytechnic University, 634050, Tomsk, Russia
Email: zaitsev@itp.nsc.ru

The fast development in semiconductor technology has led to increasingly higher chip power dissipation and greater non-uniformity of the heat dissipation with the result of localized hot spots, often exceeding 1kW/cm$^2$ in heat flux [1]. As was shown in previous works of the authors, thin and very thin liquid films driven by a forced gas/vapor flow (stratified or annular flows), i.e. shear-driven liquid films in a narrow channel are promising candidate for an innovative cooling technique optimizing the tradeoffs between performance and cost [2]. The goal of the present work is to study the effect of the channel height on the critical heat flux (CHF) in a locally heated liquid film driven by the shear stress of gas in a channel.

The test section consists of a thin and flat stainless steel plate with a flush-mounted copper rod with a 1×1 cm square head, serving as a heater (Fig. 1). The rod is heated by a nichrome spiral coiled around its bottom part. The test section is covered with a transparent cover (not shown in Fig. 1) so that a channel with variable height is formed. The liquid film supplied from the liquid nozzle is driven by the shear stress of gas in the channel. The heat flux is determined by the electrical power dissipated on the nichrome spiral. Water and air with initial temperature of about 25°C were used as the working liquid and gas, respectively. The channel is oriented horizontally. The channel height, $H$, varies from 170 to 2000 μm.

Figures 2 and 3 show the flow prior to heat transfer crisis for $H$=250 and 2000 μm, respectively. For $H$=250 μm the heater is covered with nonstable, evaporating liquid film at both $U_{Sg}$=5 and 30 m/s (where $U_{Sg}$ is the superficial gas velocity). However, for $H$=2000 μm the heater is covered with nonstable liquid film only at relatively high gas velocity ($U_{Sg}$=33 m/s), while for smaller gas velocity ($U_{Sg}$=2.5 m/s) the first dry patch propagates all over the heater, causing dryout and thus the occurrence of the heat transfer crisis.

Figure 4 shows the effect of $H$ on the CHF for different $U_{Sg}$. It is seen that for $H$=170-250 μm the CHF is weakly dependent on $U_{Sg}$, while for $H$=1-2 mm the CHF strongly decreases with decrease of $U_{Sg}$. Thus microchannels seem to be more suitable for cooling applications.

**Acknowledgements:**
We gratefully acknowledge the support from the Ministry of Education and Science of Russia (Project identifier RFMEFI60414X0053).

**References:**

1. Bar-Cohen A, Wang P. Thermal Management of On-Chip Hot Spot // ASME. J. Heat Transfer, 134(5), 051017, 2012.
2. Kabov O.A., Zaitsev D.V., Cheverda V.V. and Bar-Cohen A. Evaporation and flow dynamics of thin, shear-driven liquid films in microgap channels // Experimental Thermal and Fluid Science, 35(5), p. 825-831, 2011.

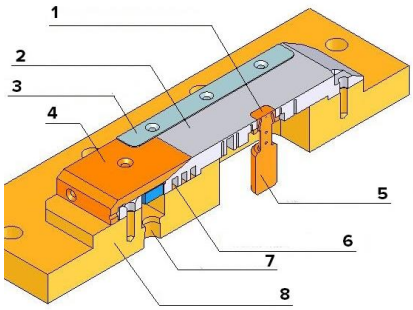


**Figure 1:** Scheme of test section. 1- 10×10 mm heater, 2- stainless steel substrate, 3- plate to adjust the channel height, 4- liquid nozzle, 5- copper rod, 6- thermal stabilization contour, 7- liquid inlet, 8- textolite base.

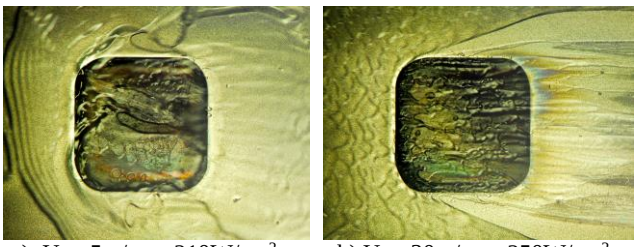

a) $U_{Sg}$=5m/s, $q$=210W/cm$^2$ b) $U_{Sg}$=30m/s, $q$=250W/cm$^2$

**Figure 2:** Photograph of the flow prior to CHF for $H$=250 μm, $Re_l$=18. The flow directed from left to right.

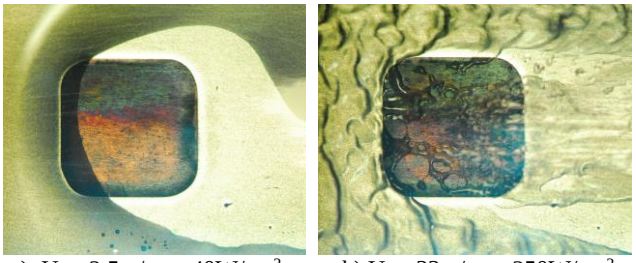

a) $U_{Sg}$=2.5m/s, $q$=40W/cm$^2$ b) $U_{Sg}$=33m/s, $q$=250W/cm$^2$

**Figure 3:** Photograph of the flow prior to CHF for $H$=2000 μm, $Re_l$=18. The flow directed from left to right.

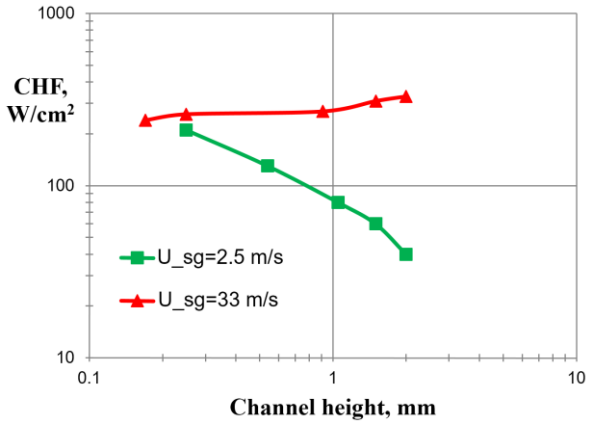


**Figure 4:** Critical heat flux vs. channel height for different superficial gas velocities, $Re_l$=18.

# Subcooled flow boiling in a rectangular macro-channel at high mass flow rates: Performance of horizontal and vertical orientation

Maria C. Vlachou[1], John S. Lioumbas[1], Constantine David[2], Thodoris D. Karapantsios[1]

[1]Division of Chemical Technology, School of Chemistry, Aristotle University of Thessaloniki
Univ. Box 116, Thessaloniki, 54124, Greece
marvlach@gmail.com, lioumbas@gmail.com, karapant@chem.auth.gr
[2]Mechanical Engineering Department, Technical University of Serres
Serres, 62124, Greece
david@teiser.gr

Flow boiling is one of the most efficient ways of cooling, because through the latent heat of vaporization of the fluid it absorbs large amounts of heat and through the inertial forces it removes the formed bubbles. The present work focuses on the investigation of a specific range of experimental parameters that refer to extreme conditions such as the fast cooling of very hot walls, e.g. walls exposed to gas flames. Parameters under investigation are (a) high subcooling level and (b) high mass flow rate (figure 1).

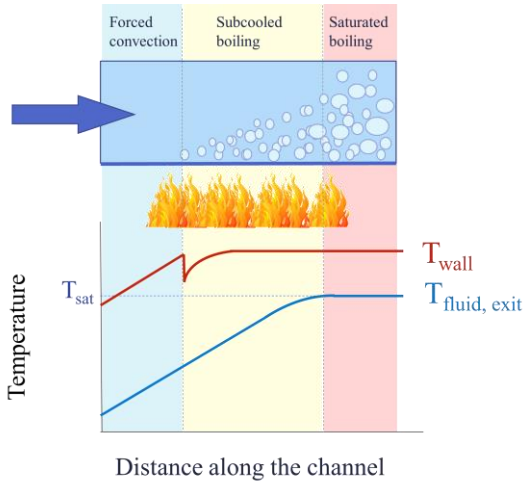


**Figure 1:** Temperature profiles of fluid and heated wall during flow boiling over a hot surface.

This study addresses the effect of channel's orientation on the removed heat flux and the heat transfer coefficient. Experiments are conducted with water as the working fluid. A device has been constructed with a macro-channel (figure 2), which permits simultaneous monitoring of the heated surface temperature and bubble dynamics in order to correlate boiling regimes with heat transfer results. Other measurements that take place include: bulk liquid's temperature & flow rate, pressure drop along the channel and void fraction at the exit of the text section via a patented custom-made non-intrusive impedance technique (IVED).

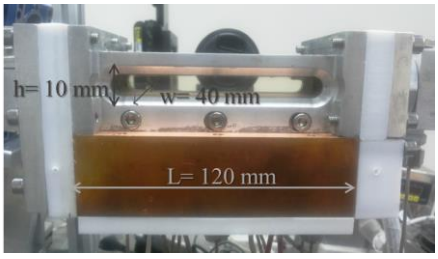


**Figure 2:** Macro-channel.

Experimental results provide evidence that vertical orientation increases heat removal for the same working conditions compared to the horizontal, which is in accordance with pertinent literature (Akhavan-Behabadi and Esmailpour, 2014, Kundu et al., 2014). An insight of the bubble dynamics is going to provide more information for assessing the flow boiling heat transfer mechanisms and the two phase heat transfer coefficient.

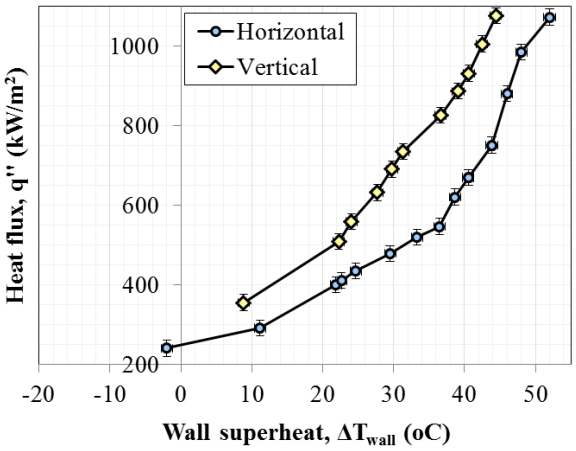


**Figure 3:** Effect of channel's orientation on the boiling curve for water mass flux 340 kg/m$^2$s.

## References

Akhavan-Behabadi M. A., Esmailpour M., Experimental study of evaporation heat transfer of R-134a inside a corrugated tube with different tube inclinations, Int. Commun. Heat Mass, Vol. 55 pp. 8-14 (2014)

Kundu A., Kumar R., Gupta A., Flow boiling heat transfer characteristics of R407C inside a smooth tube with different tube inclinations, Int. Journal of Refrig., Vol. 45 pp. 1-12 (2014)

**Acknowledgements:** The work is performed with the support of (1) "Highly efficient flow boiling macro-structured/ macro-porous channels" funded by the European Space Agency (Co. No. 4000106405/12/NL/PA) (2) IKY Fellowships of excellence for postgraduate studies in Greece – SIEMENS program. The work is performed under the umbrella of COST Action MP1106.

# Modelling of the joint motion of nonisothermal liquid film and gas in a microchannel: direct numerical simulation of Navier-Stokes equations

Kuznetsov V.V. [1], Kabova Yu. [2]

[1] Lavrentyev Institute of Hydrodynamics, SB RAS, prosp. Lavrentyev 15, Novosibirsk, 630090 Russia, kuznetsov@hydro.nsc.ru

[2]Institute of Thermophysics, SB RAS, prosp. Lavrentyev 1, Novosibirsk, 630090 Russia
kabova@itp.nsc.ru

Thermocapillary convection in nonisothermal thin liquid films with deformable or nondeformable liquid-gas interfaces is intensively studied in the past decades. Significant progress has been achieved, in both theoretical and experimental investigations. In theoretical and numerical studies of two-phase flows with the free boundaries kinematic and thermal characteristics of the film pattern and structures appearing due to the thermocapillary effects is studied. During these years big variety of mathematical models taking into account different features of the liquid heating and motion has been developed in the long-wave approximation (Scheid B. et al. 2002, Kabov O.A. 2010), and also direct numerical simulation of the Navier-Stokes equations under certain conditions (Frank A.M. and Kabov O.A. 2006) has been performed. Method of the integral proportions proposed by Prof. Shkadov V.Ya., also gives good results (Kalliadasis S. et al. 2003), but the question about impact of the gas phase on the free surface phenomena remains poorly studied. Generally, investigations of joint influence of thermocapillary and mass forces is conducted within the framework of generally accepted models, while full understanding of mechanisms of the structures formation and of influence of heat and mass transfer effects requires the use of new and more complex mathematical models taking into account the convective terms of equations. The first model of joint liquid and gas motion taking into account convective heat transfer in liquid and gas phases, as well as evaporation, which has been described by the convective diffusion equation in the gas phase has been proposed in (Gatapova E. Ya. et al. 2005) for laminar stratify flow with nondeformable free interface. Numerical study of the three-dimensional deformations of free interface in two-phase joint motion of the liquid film and gas in mini and microchannels in the thin layer approximation has been performed later in (Kabova Y. et al. 2014). It should be noted that full statement three-dimensional models, describing the liquid films motion taking into account the gas phase and the phase changes at the free boundaries are still very rare in literature. The authors of the abstract performed an extensive program of research aimed at studying and understanding hydrodynamics and heat and mass transfer at joint motion of evaporating liquid films and gas/pair in microchannels at the local heating. And in the present work new three-dimensional mathematical model of joint motion of a viscous liquid film and gas in a microchannel at local heating developed by taking into account the heat transfer by flows, evaporation and condensation, as well as the heat transfer at the gas-liquid interface is presented. The model is based on the full system of the Navier-Stokes equations, taking into account the convective terms of motion equations in the phases, gas compressibility is neglected. Influence of the liquid and gas Reynolds numbers on the main process characteristics including free interface deformations, heat transfer and evaporation has been investigated numerically. Reynolds numbers in phases are varied from 2 to 15 and from 15 to 150, correspondingly. In addition, comparison of the numerical results obtained using the model based on the full Navier-Stokes equations and using the simplified model developed in the framework of the thin layer approximation has been performed. The comparison shows that at low Reynolds numbers, simplified model well describes all the main characteristics of the gas and liquid motion. The difference between the calculated parameters for both models does not exceed 4%. With the gas Reynolds number significant increase differences between numerical results starts to grow.

**Acknowledgements** The study was financially supported by the Russian Science Foundation, project no. 14_19_01755.

**References**

Scheid B., Oron A., Colinet P., Thiele U. and Legros J-C., Nonlinear evolution of non-uniformly heated falling liquid films // Phys. Fluids 2002.V. 14, No. 12. pp. 4130-4151.

Kabov O.A., Interfacial Thermal Fluid Phenomena in Thin Liquid Films //Intern. Journal of Emerging Multidisciplinary Fluid Sciences 2010 Vol. 2, No. 2-3. pp. 87–121.

Frank A. M., Kabov O. A. Thermocapillary structure formation in a falling film: experiment and calculations // Phys. Fluids. 2006. Vol. 18, pp. 032107 (10 P).

Kalliadasis S., Kiyashko A. and Demekhin E.A., Marangoni instability of a thin liquid film heated from below by a local heat source// J. Fluid Mech. 2003, V. 475 pp. 377-408.

Gatapova E.Ya., Kabov O.A., Kuznetsov V.V., and Legros J.-C. Evaporating shear-driven liquid film flow in minichannel with local heat source// Journal of Engineering Thermophysics 2005. V. 13. No. 2, pp. 179-197.

Kabova, Y., Kuznetsov, V.V., Kabov, O., Gambaryan-Roisman, T., Stephan, P., Evaporation of a thin viscous liquid film sheared by gas in a microchannel// International Journal of Heat and Mass Transfer 2014, 68, pp. 527-541.

# Three-dimensional investigation of liquid film structure at the initial area of annular-dispersed flow

Sergey Alekseenko, Andrey Cherdantsev, Mikhail Cherdantsev, Sergey Isaenkov and Dmitriy Markovich

Kutateladze Institute of Thermophysics SB RAS
Lavrentiev ave.,1 , Novosibirsk, 630090, Russia
mikhail.cherdantsev@gmail.com

In annular-dispersed flow liquid film flows on the inner wall of the pipe sheared by high velocity gas stream flowing in the center of the pipe. In such a flow large-scale disturbance waves are formed on film surface. Presence of disturbance waves is necessary for liquid entrainment into the gas core. These waves cause enhancement of pressure drop and heat transfer. Modeling of wavy structure of liquid film is complicated by multi-scale nonlinear wavy processes and strong turbulence in both phases. To verify the existing models and to create new models detailed experimental information describing the interactions of waves is required.

Experiments by local conductivity probes showed that near the inlet film surface is covered by high-frequency small-amplitude waves (Zhao et al. 2013). In recent article (Alekseenko et al. 2015) longitudinal film thickness profile near the inlet of 15 mm i.d. pipe has been obtained using laser-induced fluorescence technique. It has been concluded that disturbance waves are formed due to multiple coalescence~~s~~ of initial high frequency waves that appear due to Kelvin-Helmholtz instability (see fig. 1a). At low gas velocities initial waves do not coalesce.

For more detailed investigation of waves shape and process of interaction three-dimensional measurement of film thickness are required. Pipe geometry doesn't allow obtaining three-dimensional film thickness profile on whole pipe perimeter. Three-dimensional measurements are possible only in a restricted area along transverse coordinate of the pipe.

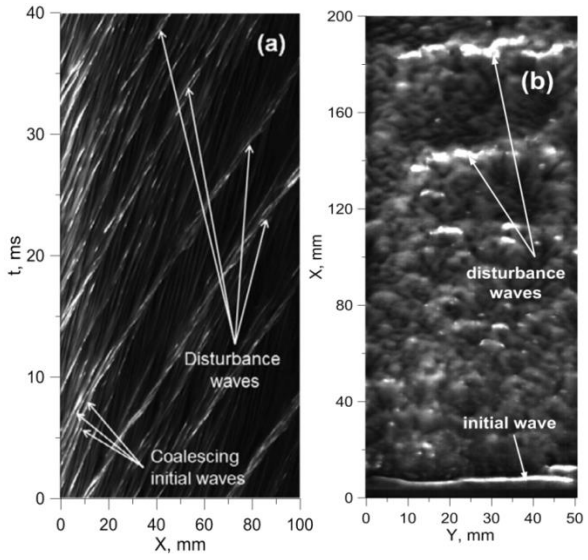


**Figure 1:** (a) Spatiotemporal evolution of film thickness near the inlet. $V_g$ = 50 m/s. $Re_L$ = 140. (b) Instantaneous three-dimensional film thickness profile. $Re_L$ = 220, $V_g$ = 26 m/s.

A new duct with rectangular cross-section 50 mm * 5 mm has been designed to have clear optical access to the whole width of the channel. Liquid film is formed by 0.5 mm tangential slot between one of the long walls and a thin stainless steel plate.

Laser-induced fluorescence technique was used for field measurements of film thickness. Frame rate of high speed camera is 1 KHz. Spatial resolution is 0.2x0.2 $mm^2$ for each pixel.

It can be seen from figure 1b that ~~at~~ very close~~ness~~ to the inlet initial waves are two-dimensional with transverse size equal to that of the whole channel. With increasing distance from the inlet these waves are disrupted into many small-scaled waves. Further downstream they tend to rejoin with each other and form disturbance waves. With increasing gas velocity disruption of initial waves and formation of disturbance waves occurs sufficiently faster. And at very high gas velocities initial waves are disrupted immediately after the tangential slot. On the other hand, at low gas velocities ($V_g \leq 18$ m/s) initial waves lose two-dimensionality very gradually, splitting into small-scale waves that do not form disturbance waves.

The work was supported by Russian Foundation for Basic Research (project number 15-58-10059-KO_a).

**References**

Alekseenko S.V., Cherdantsev A.V., Cherdantsev M.V., Isaenkov S.V. and Markovich, D.M., Study of formation and development of disturbance waves in annular gas–liquid flow, Int. J. Multiphase Flow, Vol. 77 pp. 65–75 (2015)

Zhao Y., Markides C.N., Matar O.K., Hewitt G.F., Disturbance wave development in two-phase gas–liquid upwards vertical annular flow, Int. J. Multiphase Flow, Vol. 55, pp. 111–129 (2013)

# Convective flows study by PIV method within a horizontal fluid layer under the action of gas flow

Yuriy Lyulin[1], Aleksei Kreta[1,2], Artur Bilsky[1], Dmitriy Markovich[1], Oleg Kabov[1,2] and Jean-Claude Legros[1]

[1] Institute of Thermophysics SB RAS (IT SB RAS), 1, Lavrentiev Ave, 630090, Novosibirsk, Russia, lyulin@itp.nsc.ru
[2] Novosibirsk State University, 2, Pirogov Ave, 630090, Novosibirsk, Russia

The processes of convection, accompanied by evaporation at the interface, are actively studied experimentally, numerically and theoretically in the present time (Scheid et al. 2012; Goncharova and Kabov 2013). Scientific activity in this direction is determined by the experiments in the frame of the CIMEX project of the European Space Agency (Lyulin and Kabov 2014). The experiments devoted to study of the features of the convective fluid flows in a horizontal layer under the action of gas flow is the aim of the present study.

The evaporation process under the action of the inert gas flow induces an intensive heat and mass transfer through the gas-liquid interface. The liquid surface is cooled. It causes a temperature gradient between the heated bottom and the gas-liquid interface. The temperature gradient leads to the appearance of the buoyancy convection within the liquid layer. The inert gas flow induces the shear-stress at the gas-liquid interface. The liquid surface can be moved in the co-current direction of the gas flow. A strong evaporation at the initial section of the gas-liquid interface leads to an interfacial temperature gradient. Thermocapillary effect due to the interfacial temperature gradient induces motion of the liquid at the interface countercurrent to the gas flow. Thus, there is a quite complicated convection within the liquid layer. It is evident that the structure of the convective flow within the liquid layer should significantly depend on the various parameters of experiment like the inert gas flow rate, the gas and liquid temperature and the size of the liquid layer. In the future experiments under microgravity condition on the International Space Station the buoyancy convection is excluded and the cross influence of the gas shear-stress, the vapor recoil and the thermocapillary effect on the dynamics of evaporation and convection in the liquid layer is considered. Thus, the task is simplified.

A schematic of the experimental rig is shown in Fig. 1. The experimental rig consists of the fluid cell, gas/liquid supply circuits, the data acquisition system, thermal stabilization system and optical systems. The pure gas arrives into the inlet of the gas channel of the test cell from the compressor. The flow controller maintains the flow rate at the inlet of the fluid cell. To supply the working liquid into the fluid cell the syringe pump is used. The liquid is evaporated into the gas phase. The flow rate of the gas-vapor mixture is measured by the flow meter at the outlet of the test cell. Temperature in the experimental rig is measured by thermistors and thermocouples. The temperature difference between the liquid and the gas flows at the entrance to the test cell is maintained less than 0.1°C. An optical Shlieren technique is used for the observation of the flow patterns on the gas-liquid interface and control of the flatness of the liquid surface. Optical PIV method is used for the visualization of convection in the liquid layer (Akhmetbekov et al. 2006).

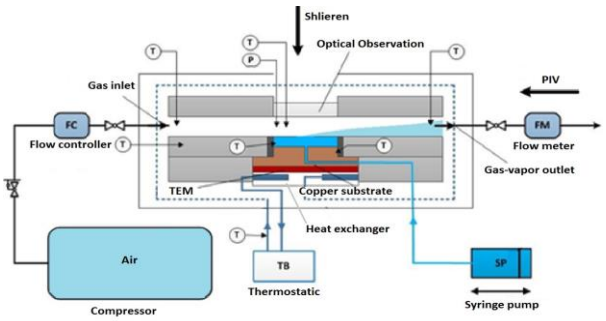


**Figure 1:** Scheme of the experimental rig.

In Fig. 2 the distribution of the two-dimensional velocity field is presented. The iterative cross-correlation method is used for calculation of the velocity field. The gas flow rate was 100 ml/min (gas velocity - 0.013 m/s). The temperature of the system "Ethanol –Air" was equal to 25°C. The area of evaporation was 400 mm$^2$. As one can see in Fig. 2 a convective vortex in the initial area of contact of the liquid and gas is observed. Gas-liquid interface and the convective vortex are moving in counter-current direction of the gas flow. Governing factor of the convective vortex is the thermocapillary effect due to the intensive evaporation, i.e. temperature decreasing near the attack border of the liquid.

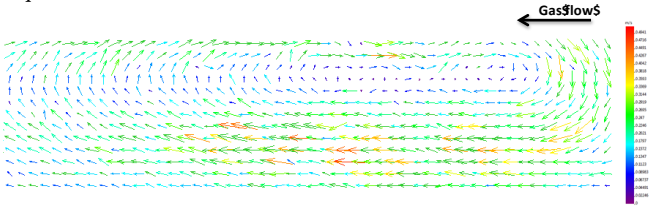


**Figure 2:** Convective flow in the liquid layer.

**Acknowledgements** The study was financially supported by the Russian Science Foundation (Project 15-19-20049).

## References

Scheid B., Margerit, J., Iorio, C.S., Joannes, L., Heraud, M., Queeckers, P., Dauby, P.C., Colinet, P., Onset of thermal ripples at the interface of an evaporating liquid under a flow of inert gas, *Experiments in Fluids*, 52(5), 1107-1119 (2012).

Goncharova O. and Kabov O., Numerical investigation of the tangential stress effects on a fluid flow structure in a partially open cavity, *J. Eng. Thermophys*, Vol. 22(3), pp. 216-225, 2013.

Lyulin Y., Kabov O., Evaporative convection in a horizontal liquid layer under shear–stress gas flow// *Int. J. Heat Mass Transfer* 70, 599-609 (2014).

Akhmetbekov Ye.K., Bilsky A.V., Lozhkin Yu.A., Markovich D.M., Tokarev M.P., Tyuryushkin A.N., Software for experiment management and processing of data obtained by digital flow visualization techniques (ActualFlow) // Vychisl. Metody Programm., V.7, 79-85 (2006).

# Liquid rivulet moved by a gas flow in a microchannel

Kabova Yu. [1], Kuznetsov V.V. [2], Kabov O.A. [1]

[1] Institute of Thermophysics, SB RAS, prosp. Lavrentyev 1, Novosibirsk, 630090 Russia, kabova@itp.nsc.ru

[2] Lavrentyev Institute of Hydrodynamics, SB RAS, prosp. Lavrentyev 15, Novosibirsk, 630090 Russia, kuznetsov@hydro.nsc.ru

Rivulet flows with and without phase-change are abundant in nature and play an important role in our daily life. Fast development in semiconductor technology, including shrinking feature size, increasing transistor density and faster circuit speeds have resulted in greater non-uniformity of on-chip power dissipation, generating localized submillimeter hot spots often exceeding 1 kW/cm$^2$ in heat flux. Rivulets driven by forced gas/vapor flow in narrow channels (100–300 μm) are assumed to provide very high heat transfer intensity especially near the contact line area of the fluid on the heated surface (Stephan and Brandt 2003, Rednikov and Colinet 2011). Rivulet flows represent a promising approach to thermal management of advanced semiconductor devices with high power dissipation, in particularly for space applications: energy production, electronic cooling devices, life support systems and waste water treatment for long duration space exploration missions. Understanding of fundamental aspects of rivulet dynamics might provide a way to control these flows. The rivulet and gas flow in minichannel were theoretically investigated under conditions of variable gravity in Bartashevich et al. (2009, 2010). The mathematical model describes steady-state isothermal rivulets. In general it was found that the flow dynamics at microgravity differs significantly from that at normal gravity. Profile of the rivulet and gas-liquid interface deformations are affected significantly by the liquid and the gas flow rates and gravity level.

In the present work we consider an incompressible and nonisothermal liquid rivulet moved by a gas flow in an inclined or horizontal microchannel. Action of wetting, gravity and tangential stress at the gas-liquid interface are taking into account. The liquid and gas Reynolds numbers are assumed to be constant. The liquid and gas motion are assumed to be steady state. This becomes possible if temperature distribution on a bottom wall of the channel is permanent along the entire length of the rivulet. The lubrication-type mathematical model based on the predominant velocity direction approach was built. Heat exchange is most high near the triple contact line formed by the liquid rivulet, substrate and gas phase, that is why the rivulets with two contact lines are of particular interest. Modeling of the rivulet form and main features of the flow near the three-phase contact line depends significantly on the thin liquid film appearing in the vicinity of the contact line, where the action of van der Waals forces is significant. In the present model calculations are carried out in the entire field of flow, including the thin film zones. Numerically it is found out that existence of thin liquid film zones near the contact lines gives a significant disturbing effect on the gas velocity distribution. It is shown that in the case of normal gravity and at low inclination of the channel to the horizon increasing Reynolds numbers leads to rivulets with almost flat boundary, which is curved only near the three phases contact lines. Figure 1 shows calculated rivulet profiles in cross section at different values of the number δ, which specifies the relation of the van der Waals and capillary forces.

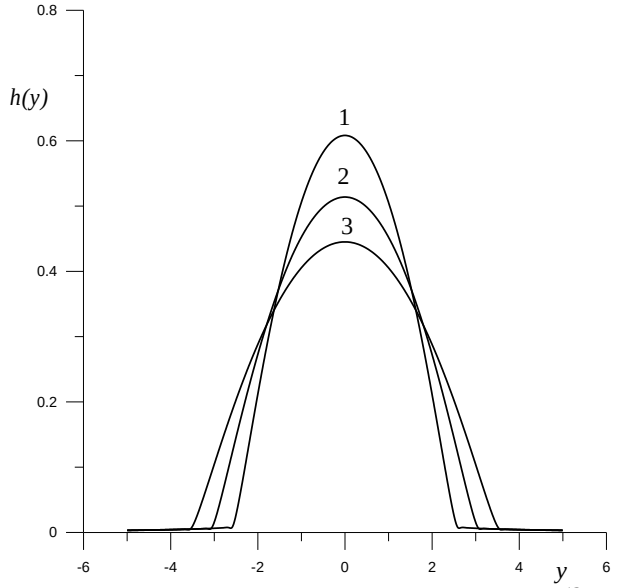


Fig. 1. Rivulet profile in cross-section. 1 – $\delta = 0{,}7\cdot10^{-12}$, 2 – $\delta = 1{,}0\cdot10^{-12}$, 3 – $\delta = 1{,}3\cdot10^{-12}$.

**Acknowledgements** The study was financially supported by the Russian Science Foundation, project no. 14_19_01755.

## References

Stephan, P., Brandt, C.: Advanced capillary structures for high performance heat pipes. In: Kandlikar, S.G. (ed.) Proc. I Int. Conf. on Microchannels and Minichannels, pp. 69–75. Rochester, NY, 24–25 April (2003)

Rednikov, A.Ye., Colinet, P., Truncated versus extended microfilms at a vapor-liquid contact line on a heated substrate // Langmuir (2011) **27**(5), pp. 1758–1769

Bartashevich,M.V., Kuznetsov, V.V., Kabov, O.A,. The rivulet flowing in inclined minichannel with co-current gas flow in conditions of variable gravity.// Sib. J. Ind. Math. (Sibirskii Zhurnal Industrial'noi Matematiki) (2009) **12**(2), pp. 3–16 (in Russian)

Bartashevich, M.V., Kabov, O.A., Kuznetsov, V.V., Dynamics of a finite-width liquid film in a co-current microchannel gas flow // Fluid Dyn. (2010) **45**(6), pp. 924–929

# Influence of substrate temperature on the wettability of the silicon oxide nanowires synthesized by gas-jet electron beam plasma chemical vapor deposition method

Evgeniy Baranov, Sergey Khmel and Alexandr Zamchiy

Kutateladze Institute of Thermophysics SB RAS
Ac. Lavrentiev ave. 1, 630090, Novosibirsk, Russia
itpbaranov@gmail.com

Functionalized silicon oxide nanowires are used to control surface wettability [Coffinier et al. 2007], which is important for biological applications and for the enhancement of boiling heat transfer on nanostructured surfaces [Kim et al. 2015].

Surface wettability is determined by the contact angle. In this study, contact angles of silicon oxide nanowire surfaces were measured using deionized water with a Kruss DSA 100E drop shape analyzer. The accuracy was about 3°. All measurements were made in ambient atmosphere at a temperature of 20°C.

Wettability is a very important property of nanostructured surfaces. It depends on the chemical composition, roughness, method of preparation and surface cleanliness. Wettability is characterized by the contact angle of liquid with solid surface. Usually, the formation of a contact angle at a solid–liquid–gas boundary can be described by two models, namely the Wenzel's equation and the Cassie and Baxter law [Kumar et al. 2011]. A hydrophilic surface has a contact angle less than 90°.

Analysis of the photograph of the water droplet on the $SiO_x$NW film grown on c-Si substrate shows the measured contact angle was <35° for all samples. This confirms that the $SiO_x$NW films surface, synthesized in this work, is hydrophilic in nature. The measured contact angle was different for the left and right side of the drop. We can explain this phenomenon by the fact that microropes are not perpendicular to the surface, and have a different angle of inclination. In addition, it was observed that the droplets on the surface have a very large precursor line [Shin et al. 2014]. We assume that water penetrate easily into grooves constituting the relief in case of Cassie impregnating wetting [Bormashenko et al. 2013].

The contact angle of $SiO_x$ nanowire films deposited at various substrate temperatures is shown in Fig. 1. The contact angle was measured for the left and right sides of the drop. Two typical regions can be distinguished: region 1 with a contact angle <15° for samples synthesized at a temperature of 200, 245, and 270°C; region 2 with a contact angle >20° for samples synthesized at a temperature of 335 and 415°C.

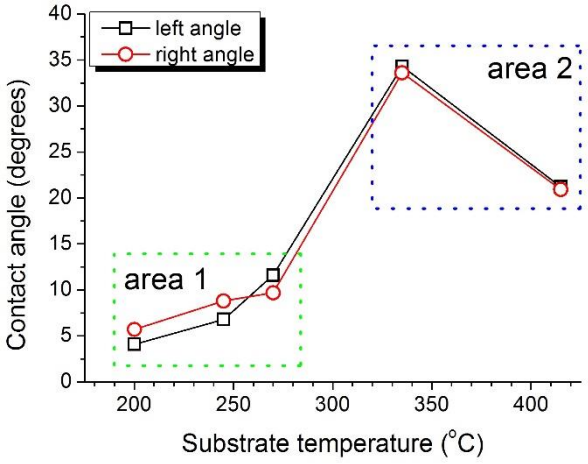


**Figure 1:** Dependence of the contact angle on the substrate temperature. Shows the contact angle for the left and right side of the drop. We can highlight two typical areas: area 1 with the contact angle <15°; area 2 with the contact angle >20°.

The identified regions are in good agreement with the morphology of the obtained nanostructures. When structuring involves the oriented growth of silicon oxide microropes, the contact angle is about 20–35°. The change in the morphology due to a decrease in the density of microropes and formation of cocoon-like structures leads to a decrease in the contact angle to 4–12°. Moreover, the larger the number of cocoon-like structures are the smaller the contact angle.

**Acknowledgements**

This work was supported by grant of the Russian Scientific Foundation #15-19-30038.

The authors thank Ekaterina Kirichenko for the contact angles measurements.

**References**

Y. Coffinier, S. Janel, A. Addad, R. Blossey, L. Gengembre, E. Payen, and R. Boukherroub, Langmuir Vol. 23, p. 1608 (2007)

D. Kim, D. Yu, D. Jerng, M. Kim, and H. Ahn, Exp. Therm. Fluid Sci. Vol. 66 p. 173 (2015)

R. Kumar, N. Rao, and Phani, Appl. Nanosci. Vol. 1 p. 211 (2011)

S. Shin, G. Choi, B. Kim, and H. Cho, Energy Vol. 76 p. 428 (2014)

E. Bormashenko, R. Grynyov, G. Chaniel, H. Taitelbaum, and Y. Bormashenko, Appl. Surf. Sci. Vol. 270 p. 98 (2013)

# The heat flux near the contact line of the droplets on heated foil

Vyacheslav Cheverda[1, 4], Igor Marchuk[1,2], Andrey Karchevsky[2,3], Oleg Kabov[1,4]

1 - Kutateladze Institute of Thermophysics SB RAS, Novosibirsk 630090, Russia
2 - Novosibirsk State University, Novosibirsk 630090, Russia
3 - Sobolev Institute of Mathematics SB RAS, Novosibirsk 630090, Russia
4 - Tomsk Polytechnic University, Tomsk 634050, Russia
* Slava.cheverda@gmail.com

Liquid droplets on the substrate are widely distributed in nature, techniques, and technology. The wetting angle is a fundamental macroscopic characteristic of the contact line. This angle is determined by the Young equation, (Ababneh et al., 2006). The heat flux near with a contact line could exceed 1 kW/cm$^2$ (Stephan and Brandt, 2004). The heat flux distribution was obtained by numerical solution of the Cauchy problem for elliptic equations (see, e.g., Marchuk et al., 2015).

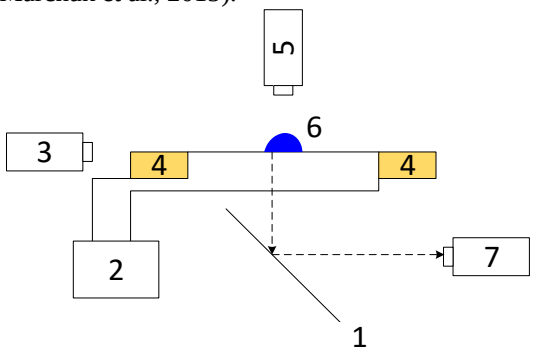


**Figure 1:** The principal scheme of the experimental setup:
1 – gold mirror, 2 – power supply, 3 – Nikon D300,
4 – electrodes with constantan foil, 5 – video camera,
6 – liquid drop, 7 – IR camera

In the present work the evaporating sessile water drops on a horizontal heated substrate were studied experimentally using the setup shown in Fig. 1. The constantan foil (CuNi) of the thickness of 25 $\mu$m, size of 80 × 35mm$^2$ and heat conductivity $\lambda$ of 23W/mK was used as the substrate. The substrate was heated by Joule heating. The temperature of the bottom foil surface was measured by IR camera Titanium 570M. The average coefficient of heat transfer from the foil surface to surrounding air $\alpha_{av}$ was found to be within 25 W/m$^2$ K. These measurements were performed without droplets on the foil surface.

The heat flux on the side of IR-scanner of the foil is estimated by equation: $q_b=\alpha_{av}(T_w-T_a)$, $T_W$ – temperature measured by IR-scanner, $T_a$ – ambient temperature, $\alpha_{av}$ – average heat transfer coefficient. The heat flux on the drop side of the foil is calculated by equation $q_t=2q_{av}-q_b$ with neglecting the heat conductivity along the foil, $q_{av}=P/S$, P is electrical power, S=2 l w is the total surface area of the foil.

Using the Cauchy problem solution, the distributions of heat flux density on the wetted foil surface have been obtained, Fig. 2 c), d) curve 1. The infrared data were used. The measured temperature field, calculated distribution of the heat flux density on the substrate, and heat flux density along the central drop cross section are shown in Fig. 2. The results show that the maximum of the heat flux density is near the contact line and it exceeds the average heat flux density by several times.

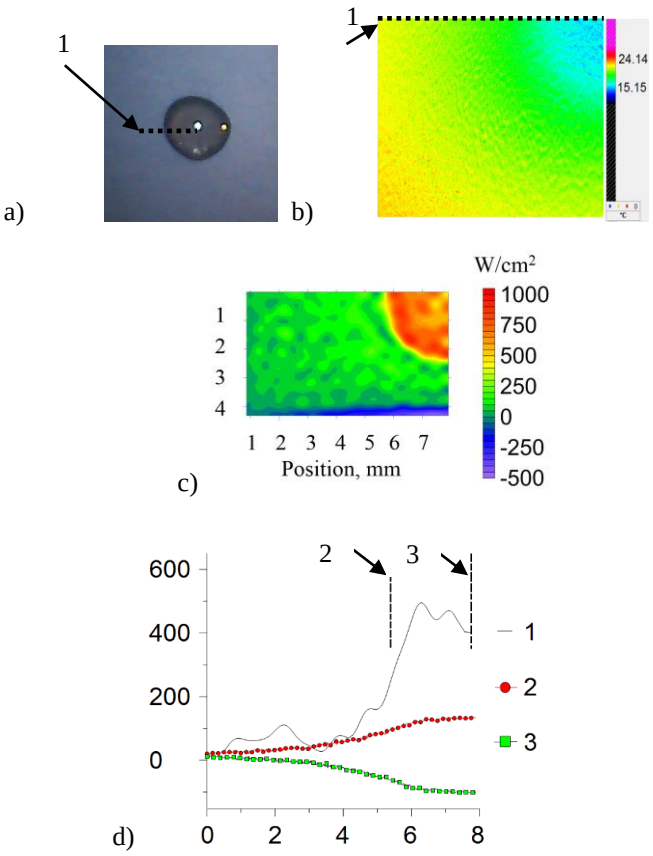


**Figure 2**: The experimental results: a – water drop with diameter 3 mm, heat flux 16.23 W/cm$^2$, b – quarter of the IR image of the foil from the opposite side to the drop where line 1 – is the line for data on graph d, 2 –left contact line of the drop, 3 – center of the drop, c – heat flux density, Cauchy problem solution, d – 1 - Cauchy problem solution, 2 - Calculation with neglecting of heat flux redistribution in the foil $q_t$, 3 - on the bottom side of wall $q_b$.

## References

A. Ababneh, A. Amirfazli, and J. A. W. Elliott, Effect of gravity on the macroscopic advancing contact angle of sessile drops Canadian Journal of Chemical Engineering, vol. 84,no. 1, pp. 39–43, (2006).

P. Stephan, C. Brandt, Advanced capillary structures for high performance heat pipes, Heat Transfer Engineering, Vol. 25(3), pp. 78 – 85, (2004).

I. Marchuk, A. Karchevsky, A. Surtaev, O. Kabov, Heat Flux at the Surface of Metal Foil Heater under Evaporating Sessile Droplets, International Journal of Aerospace Engineering, Vol. 2015, 5 pages, (2015).

# Interfacial phenomena in films of monoliquids and binary mixes in vacuum

Yuri Vyazov, Victor Prihodko, Igor Yarygin and Vyacheslav Yarygin

Kutateladze Institute of Thermophysics SR RAS
Lavrentiev Ave.1, Novosibirsk 630090, Russia
E-mail:yarygin@itp.nsc.ru

The gas outflow into vacuum was the subject of many experimental and theoretical researches; however, the problem of joint outflow of gas and wall liquid film is still studied insufficiently.

Early works of the authors have been devoted to solving the problem of external contamination of the International Space Station (ISS) by the jets from orientation thrusters, where the fuel film is used to cool the nozzle walls. It was found (Prikhodko et al. 2004) that when entering vacuum, the wall liquid film at the trailing edge not only disintegrates into droplets, but also flows to the outer surface of the nozzle and starts moving in the opposite direction, even against gravity. It was also shown experimentally (Yarygin et al. 2003) that the film turn on the trailing edge of the nozzle and its outflow to the outer surface occurs under the action of a co-current gas flow, when it turns in the Prandtl–Mayer flow, and the further rise of the film occurs due to the inertial forces. Ethanol was used as the working liquid because by its basic physical properties (density, saturated vapor pressure, latent heat of vaporization, viscosity, and surface tension coefficient) it is close to the unsymmetrical dimethylhydrazine (UDMH), currently used as the fuel in orientation thrusters of the ISS.

The present work deals with experimental investigation of interfacial phenomena under liquid film outflow from cylindrical channel with high-velocity gas flow into vacuum. In our experiments we used ethanol, water and their binary mixes as working liquid, and air at room temperature was used as working gas.

The experiments were carried out performed in pulse mode on a large-scale (the volume of about 150 $m^3$) vacuum gas-dynamic setup "VIKING" developed at Kutateladze Institute of Thermophysics SB RAS. The typical time of gas and liquid outflow equaled 5 s, wherein the time of outflow stabilization was less than 1 s and an increase in pressure in the vacuum chamber was less than 10 Pa. Stagnation pressure of gas in experiments was $p_0 \approx 37$ kPa ($\mathrm{Re}_{gas} = 4.8 \cdot 10^4$), liquid film flow rate was about 0.6 ml/s ($\mathrm{Re}_{liq} = 20$).

In our experiments we measured the temperature of the near wall liquid film on the outer surface of the tube. Measurement results allowed us to see how the liquid films are cooled under the considered conditions at different absolute pressures in the vacuum chamber. Fig. 1 illustrates the effect of pressure in the vacuum chamber on the final temperature of ethanol and water films. This result has a clear explanation, assuming that the film of ethanol is cooled to the temperature, at which the pressure of saturated ethanol vapors becomes close to the pressure in the vacuum chamber. It can be seen in Fig. 1 that at the pressure in vacuum chamber $p_k$ = 130 Pa, the ethanol film is cooled to the temperature of about –28 °C, and this correlates with the temperature dependence of the pressure of saturated ethanol vapors. For water the situation differs due to the water parameters at the triple point ($T$ = 0 °C and $p$ = 611.7 Pa) and its high specific heat of vaporization. Snapshots of wall water film ejection process into vacuum chamber shows that the film on the outer surface of the tube freezes and starts to move in opposite direction. Although transformation of the water film into ice or snow was expected, its rise to the full height of the tube was unanticipated. According to experimental data, at $p_k$ = 130 Pa the water film is cooled to $T \approx$ –5.5 °C, and this qualitatively contradicts the above considerations. Experimental results on water-ethanol mixture (volumetric concentration of ethanol is 50%) film temperature show that the film is cooled to $T \approx$ –22 °C. At the same time its freezing is not observed in experiments.

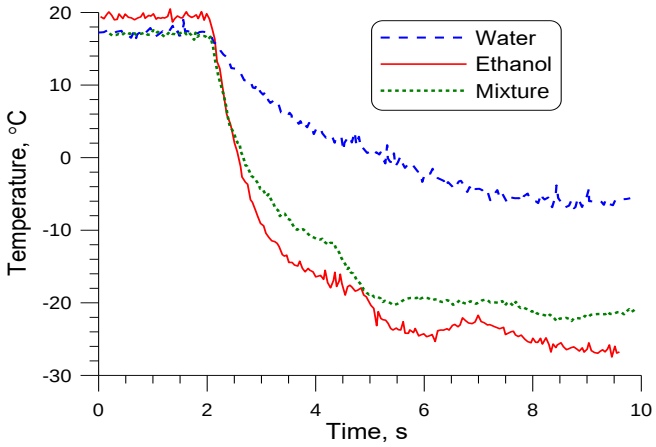


**Figure 1:** Temperature of liquid films

In conclusion, we should note that the considered experiments allow better understanding for the phase transition effect on the character of the wall liquid film outflow with the co-current gas flow into vacuum.

The study was supported by RFBR, research project No. 16-08-00436.

## References

V.G. Prikhodko, S.F. Chekmarev, V.N. Yarygin, and I.V. Yarygin, Rise of a near-wall liquid film over the outer surface of a nozzle accompanying supersonic gas flow into vacuum, Doklady Physics, Vol. 49, No. 2, pp. 119–121 (2004)

V.N. Yarygin, V.G. Prikhodko, I.V. Yarygin, Yu.I. Gerasimov, and A.N. Krylov, Gas-dynamic aspects of the contamination problem at the International Space Station. 1. Model experiments, Thermophysics and Aeromechanics, Vol. 10, No. 2, pp. 269–286 (2003)

# Interphase interaction of near-wall liquid film with co-current gas flow inside a nozzle and under ejection into vacuum.

Yuri Vyazov, Victor Prihodko, Igor Yarygin and Vyacheslav Yarygin

Kutateladze Institute of Thermophysics SR RAS
Lavrentiev Ave.1, Novosibirsk 630090, Russia
E-mail:yarygin@itp.nsc.ru

Expansion of liquids and gas-liquid mixtures into vacuum is of great interest both from the fundamental and practical points of view. From the fundamental science perspective studies of physical processes and the phenomena accompanying expansion of a liquid into vacuum - instant boiling, disintegration into droplets, phase transitions on surfaces and inside droplets, interaction of droplets with a supersonic gas flow, etc. are important. For practical applications ejection of a liquid into vacuum is of interest in particular in the field of space technology, where a problem of space vehicle surface contamination by orientation thrusters, drainage devices, and refueling systems is of great importance

In our previous experiments we studied problem of external contamination of space vehicles (including the ISS) surfaces by jets of orientation and control thrusters, in which a fuel film is used for nozzle walls cooling. Fuel was modeled by ethanol because its main physical properties are close to unsymmetrical dimethylhydrazine, which is currently used as a fuel for ISS orientation thrusters.

The present work deals with experimental investigation of interphase interaction of near-wall liquid films with co-current gas (air) flow in a nozzle and under ejection into vacuum for working liquids, whose physical properties differ significantly from ethanol.

Experiments were carried out on a VIKING vacuum gas-dynamic setup of the Kutateladze Institute of Thermophysics. The large volume of the working chamber (150 m3) allowed to carry out operation in the pulse mode with high flow rates of gas and liquid. The nozzle (cylindrical tube with 5 mm diameter, 20 mm length) was mounted vertically in the vacuum chamber, with exit part facing downwards. The liquid entered through a circular gap into stagnation chamber of the nozzle and moved down the nozzle walls as a film. Simultaneously, gas was blown through the nozzle. At the nozzle exit, a freely expanding gas jet with dispersed liquid droplets was formed. Snapshots of near-wall film ejection process into vacuum chamber with initial pressure of about 1 Pa for ethanol and water are shown in Fig. 1 (Yarygin et al. 2014).

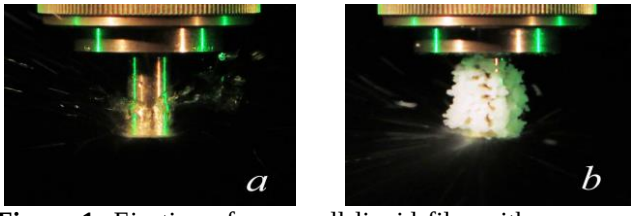


**Figure 1:** Ejection of near-wall liquid film with co-current gas flow into vacuum. *a* - ethanol, *b* - water.

It should be noted that the ejection of near-wall liquid film into vacuum and into atmosphere is drastically different. Under ejection into vacuum near-wall liquid film emerges on the external surface of the nozzle, moving backwards on it against gravity. The snapshots in Fig. 1 show the maximum recorded film rise. A special feature of water near-wall film ejection into vacuum is formation of the ice/snow layer on the external surface of the nozzle. Let's consider the results obtained in more detail.

Saturated vapor pressure of ethanol at room temperature is equal to 5.9 kPa. Therefore under ejection into vacuum chamber with pressure of about 1 Pa ethanol film becomes instantly overheated. This leads to partial disintegration of liquid film into droplets during its movement on the external surface of the nozzle. The process of intensive droplet detachment from external surface during experiments with ethanol is shown in Fig. 1.

The results obtained (Fig. 1b), namely transformation of the water film into ice or snow under ejection into vacuum, were expected. However its rise to the full height of the tube was unanticipated. At the same time it is shown that relation of liquid film height and vacuum chamber pressure is not universal and depends on properties of liquid.

Along with acceleration of near-wall film under effect of co-current gas flow another process is observed in experiments – detachment of liquid in the form of droplets from the liquid film surface and their entrainment in the co-current flow. Experiments have shown (Prikhodko et al. 2009) that the amount of the liquid detached by co-current gas flow can reach 70% of initial liquid flow rate. Corresponding results are shown in Fig. 2.

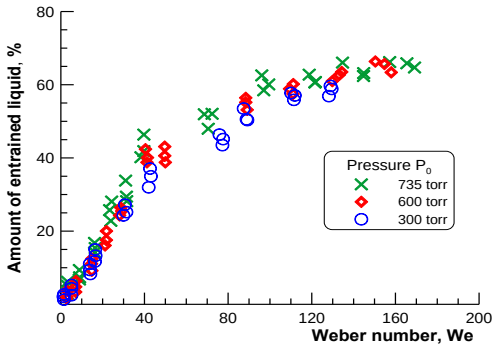


**Figure 2:** Dependence of entrained liquid on Weber number.

The study was supported by RFBR, research project No. 16-08-00436.

## References

V.N. Yarygin, V.G. Prikhodko, I.V. Yarygin, Yu.N. Vyazov. Near-wall liquid film ejection with co-current gas flow from nozzle into vacuum, Vacuum, Vol. 109, pp. 401-404 (2014)

Victor Prikhodko, Igor Yarygin and Vyacheslav Yarygin. Mass transfer and friction in near-wall film flows in conditions of high-velocity co-current gas flow, Microgravity Science and Technology. Vol. 21, pp. S277-S281 (2009)

# Two-phase flow patterns in horizontal rectangular minichannel

Fedor V. Ronshin, Evgeny A. Chinnov and Oleg A. Kabov

Kutateladze Institute of Thermophysics, Siberian Branch, Russian Academy of Sciences
Lavrentiev ave. 1, Novosibirsk, 630090, Russia
E-mail: f.ronshin@gmail.com

Gas–liquid and vapor–liquid flows exist in various applications under the conditions of normal and reduced gravity. The tendency to minimization of devices in various fields of technology, including aerospace industry, electronics, transport, power engineering, and medicine accounts for a growing interest in hydrodynamics of gas–liquid flows and heat transfer in microsystems and microchannels.

The use of two-phase mechanical pumped loops offers a significant reduction in weight and size due to powerful heat transfer by latent heat. Many experiments on heat transfer in two-phase flows have been performed in the past using the channels with various geometry.

The current work is aimed at the study of the two-phase flow regimes in a short (80 mm) horizontal minichannel with the width of 10 mm and height of 1mm. The main regimes of the two-phase flow were studied experimentally, the boundaries between them were determined, and the regime map of the studied process for the studied channel has been developed. The boundaries of the flow regimes for the channel with cross-section $1\times10$ mm$^2$ are shown in Fig. 1 by the solid lines. The following main flow regimes are distinguished: bubble, slug, jet, stratified, churn and annular.

The stationary jet regime was observed at low superficial velocities of liquid and gas, when gas moves in the central part of the channel, while the liquid moves along lateral walls of the channel. The gas flow occupies no more than a half of the channel cross-section. The jet regime is specific for the flat minichannels. Increasing the superficial liquid velocity leads to an increase in the frequency and amplitude of pulsations and stability loss of the jet regime of the two-phase flow. The slug regime is observed at low superficial velocities of liquid and gas. The slug regime is characterized by the large bullet-shape bubbles passing along the channel. The diameter of bubbles is about the channel width. With an increase in superficial velocity of liquid the transition to the bubble flow occurs. In this regime, liquid comprising many small gas bubbles moves along the channel. The size and number of bubbles vary depending on liquid and gas flow rates, but the sizes of the bubble are always much smaller than the channel width. At low superficial liquid velocities and high superficial gas velocity, the stratified regime was observed. In this regime, a part of the liquid moves along the bottom wall of the channel in the form of a film entrained by the gas flow. The upper wall of the canal is dry. Gas in this regime occupies more than a half of the channel cross-section. The stratified regime is characteristic only for the non-round minichannels because in the round channels the film closes forming the annular flow. At high superficial liquid velocities, the churn regime is observed. This regime is characteristic to the vertical channels, where it occurs due to gravity, and it is also observed in the wide horizontal minichannels, where it is caused by the capillary forces. The broken bridges are characteristic of this regime. It is caused by the development of instability of the jet regime and increasing frequency of pulsations of liquid moving along the lateral walls of the channel under the influence of the gas flow. The churn flow occupies a large area on the map (Figure 1).

Authors gratefully acknowledge support of this work by the Ministry of Education and Science of Russia (project identifier RFMEFI60414X0053).

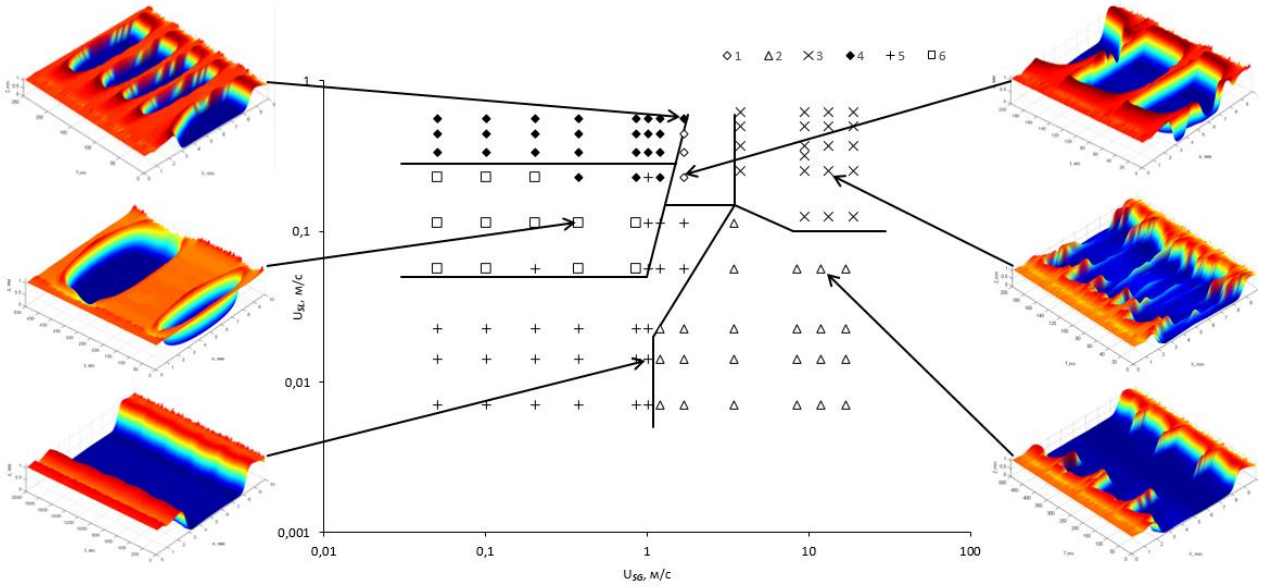


Figure 1: Regime map for the channel with cross-section of $0.1\times10$ mm$^2$. Flow regimes: 1 – churn, 2 –stratified, 3 – annular, 4 – bubble, 5 – jet, 6 – slug.

# Study of heat transfer in the bubble meniscus with an array of temperature micro-sensors

E. Orlik[1,2], D. Zaitsev[1], H. Ohta[3], O. Kabov[1,2]

[1] Institute of Thermophysics SB RAS, 1, Lavrentiev Ave, 630090, Novosibirsk, Russia
[2] National Research Tomsk Polytechnic University, 634050, Tomsk, Russia
[3] Kyushu University, Dept. Aeronautics and Astronautics, 744 Motooka, Nishi-ku, Fukuoka 813-0044, Japan
Email: orlik.evgeniy@gmail.com

The goal of the experiment is to study the boiling and condensation of vapor in the bubble, and also the process of evaporation at the meniscus, under the control of the heating from the substrate. These studies are performed in collaboration with Kyushu University, where a unique technology of manufacturing micro-sensors (micro-heaters) have been developed that provide high accuracy of heat transfer measurements (Kawanami et al., 2009). Micro-sensors create relief on surface, which may significantly affect the behavior of the contact line and the evaporation. Analysis of the effect of patterned and structured surfaces on contact line and its dynamic has been reviewed in (Ajaev et al., 2016).

Experimental setup consists of three elements (Fig. 1): a transparent test cell with inner size of 60×60×8mm, a pressure damper connected to the test cell and a transparent cover box with air fan electrically heated to control surround temperature. A pressure damper is mounted on a platform which allows changing hydrostatic pressure and equipped with Peltier elements controlling the temperature in a liquid. Two types of substrates are used: 1) 3 mm thick sapphire plate with a uniform transparent thin film heater (Fig. 2) made of indium tin oxide (ITO). Thickness of the ITO layer is 1.1 micron, which has been coated by 450 nm silicon dioxide (SiO2) layer to prevent electrolysis. 2) Substrate for heat transfer measurements near the contact line using temperature platinum micro-sensors is shown in Fig 3. The surface area of a single sensor is 3×0.5mm$^2$. Distance between sensors is 0.1mm.

The bubble shape is visualized from the top and from the side with the help of the shadow technique with resolution of 6 μm/pix (as shown in Fig. 4). The images from the side are processed in the Drop Shape Analysis software by KRÜSS. The measurement of the contact angle hysteresis of water on the uniform transparent heater is shown in Fig. 5.

**Acknowledgements:**
We gratefully acknowledge the support from the Ministry of Education and Science of Russia (Project identifier RFMEFI61314X0011).

**References:**

Kawanami O., Ohta H., Kabov O., Sakata Y., Kotani Y., Asada Y., Nagayasu T., Shinmoto Y., Chikov S., Queeckers P. and Straub J., Heat Transfer and Bubble Behaviors in Microgravity Pool Boiling in ESA Parabolic Flight Experiment, *Microgravity sci. technol.*, Vol. 21, Suppl. 1, p. S3-S8, (2009).

V.S. Ajaev, E.Ya. Gatapova, O.A. Kabov, Stability and break-up of thin liquid films on patterned and structured surfaces, *Advances in Colloid and Interface Science*, vol. 228, pp. 92–104, (2016).

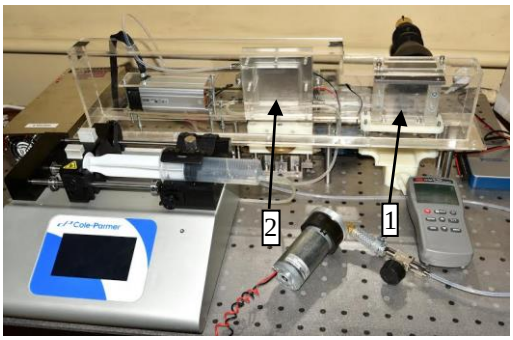


**Figure 1:** Photograph of experimental setup: 1 –test sell, 2 – pressure damper.

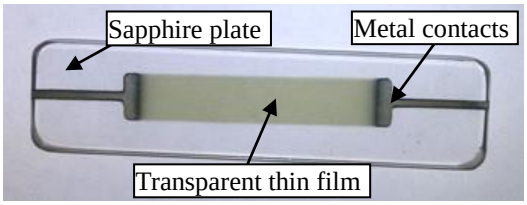


**Figure 2:** Photograph of thin film heater.

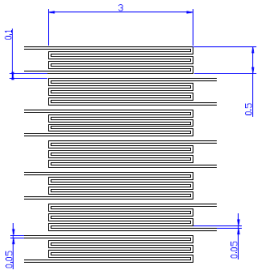

**Figure 3:** Scheme of platinum resistance thermometers.

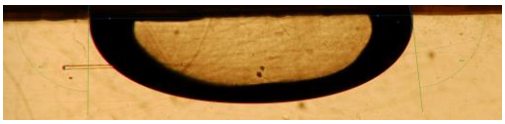

**Figure 4:** Photograph of the bubble in water on the transparent heater.

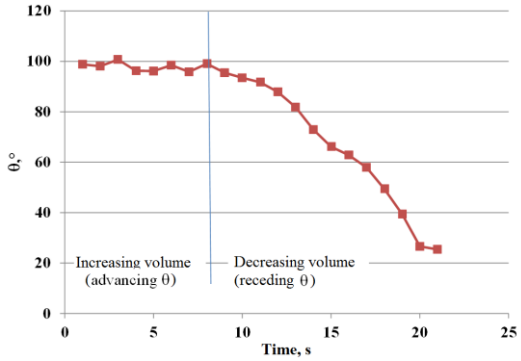


**Figure 5:** Contact angle hysteresis measurement of water on the transparent heater at room temperature.

# Superhydrophobic microfluidics

Olga I. Vinogradova

A.N.Frumkin Institute of Physical Chemistry and Electrochemistry RAS
31 Leninsky Prospect, 119071 Moscow, Russia and Faculty of Physics, M. V. Lomonosov Moscow State University, 119991 Moscow, Russia
E-mail: oivinograd@yahoo.com

Superhydrophobic Cassie surfaces, which trap dissolved gas, have opened a whole new field of investigation, with both fundamental and practical perspectives. Research on these materials has mostly focused on their extreme non-wettability, which has large-scale implications in the context of self-cleaning and impact processes. However, implications of superhydrophobicity for transport phenomena, which are especially important at the micro- and nanoscale, remain largely unexplored. In my talk I summarize some recent advances in this field, including a current switch in focus from wetting to related areas, such a remarkable drag-reducing ability of superhydrophobic materials (Vinogradova & Dubov 2012).

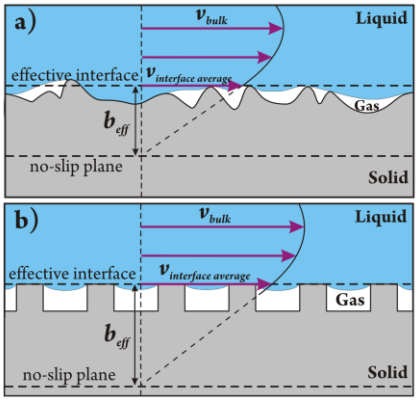


Figure 1: Schematic representation of velocity profiles and effective slip lengths, $b_{eff}$, near randomly rough (a) and periodic (b) superhydropic surfaces. Disordered surfaces display a broad spectrum of scales and a poorly defined location of the effective interface. Instead, periodic surfaces are typically characterized by a characteristic length of a texture, $L$, local slip at the gas area, $b$, and a fraction of the liquid-solid interface, $\varphi_s$

In particular, I show that superhydrophobic surfaces induce novel hydrodynamic properties, such as giant effective slip (Fig.1). In contrast to wetting studies, the major focus was on surfaces with directional patterns, such as arrays of parallel superhydrophobic grooves that generate anisotropic effective slip in the Cassie regime. The hydrodynamic slip is different along and perpendicular to the stripes. Axial motion is preferred, and such designs are appropriate when liquid must be guided. The flow anisotropy is characterized by the second-rank effective slip tensor, $\mathbf{b}_{\mathbf{eff}} \equiv \{b_{ij}^{eff}\}$, and is represented by a symmetric, positive definite $2\times 2$ matrix diagonalized by a rotation (Bazant & Vinogradova 2008):

$$\mathbf{b}_{\mathbf{eff}} = S_\alpha \begin{pmatrix} b_{eff}^{\parallel} & 0 \\ 0 & b_{eff}^{\perp} \end{pmatrix} S_{-\alpha}, \quad S_\alpha = \begin{pmatrix} \cos\alpha & \sin\alpha \\ -\sin\alpha & \cos\alpha \end{pmatrix} \qquad (1)$$

Therefore the flow along any direction of the anisotropic surface can be determined, once the eigenvalues of the effective slip tensor are found from the known spatially non-uniform scalar slip. For all anisotropic surfaces the eigenvalues $b_{eff}^{\parallel}$ and $b_{eff}^{\perp}$ of the slip-length tensor correspond to the fastest (greatest forward slip) and slowest (least forward slip) orthogonal directions. In the general case of any direction $\alpha$, this means that the flow past such surfaces becomes misaligned with the driving force (Fig.2), which is due to a generation of a secondary (transverse) flow (Vinogradova & Belyaev 2011).

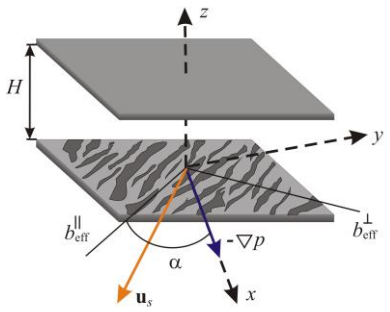


**Figure 2**: Sketch of a flat channel of a thickness H with notation for directions along the plates. One wall represents an anisotropic superhydrophobic texture.

The quantitative understanding of liquid slippage (where $H >> L$) past even in case of a single anisotropic superhydrophobic surface is still challenging. However, recent work suggested that for any anisotropic surface with arbitrary scalar slip b(y), varying in only one direction, the transverse component of the effective slip-length tensor is equal to half of the longitudinal one, with a two times larger local slip (Asmolov & Vinogradova 2012):

$$b_{eff}^{\perp}[b(y)/L] = \frac{b_{eff}^{\parallel}[2b(y)/L]}{2} \qquad (2)$$

This result opened the possibility of solving a broad class of hydrodynamic problems for one-dimensional single textured surfaces. For a patterns composed of no-slip and partial slip stripes (i.e. flat liquid-gas interface), reads

(Belyaev & Vinogradova 2010):

$$b_{eff}^{\parallel} \approx \frac{L}{\pi} \frac{\ln\left[\sec\left(\frac{\pi(1-\phi_s)}{2}\right)\right]}{1+\frac{L}{\pi b}\ln\left[\sec\left(\frac{\pi(1-\phi_s)}{2}\right)+\tan\left(\frac{\pi(1-\phi_s)}{2}\right)\right]}, \quad (4)$$

These effective tensorial slip is responsible for transverse hydrodynamic phenomena, which allowed us to suggest new methods of mixing in microfluidic devices (Nizkaya et al. 2015) as illustrated in Fig.3.

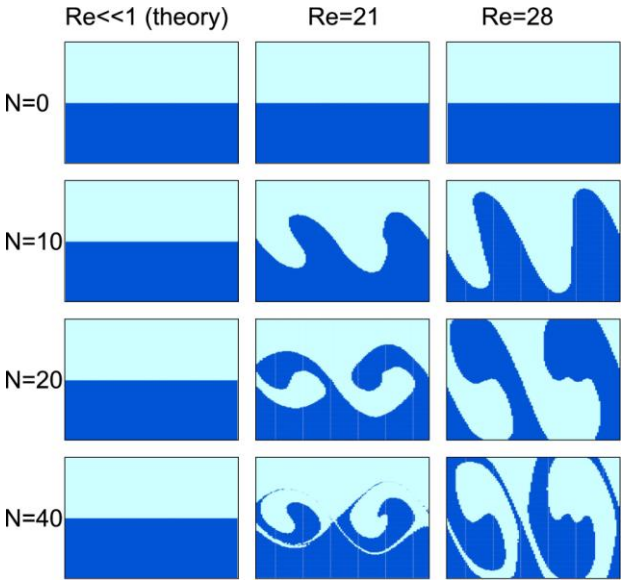


**Figure 3**: Displacements of colored fluids over N periods obtained for several Re.

Moreover, we have suggested a new concept of continuous lateral separation of microparticles (Asmolov et al. 2015) in the channel with a striped wall (see Fig.4).

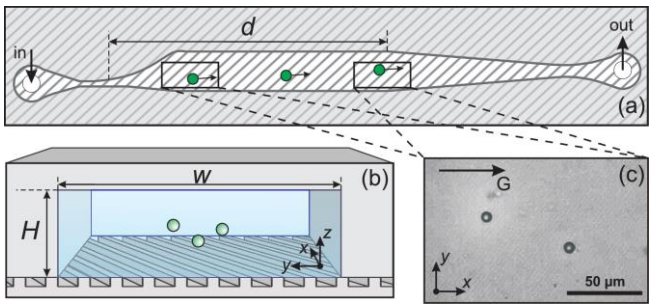


**Figure 4**: (a) Sketch of the microfluidic device (top view), the boxes indicate the regions of interest at the start and end of the active separation zone of length d = 6 mm; (b) sketch of the active zone of a microchannel (front view); (c) typical micrograph showing 2.5 μm particles moving in the vicinity of the striped superhydrophobic surface.

Finally in my talk I will suggest several remaining challenges in the field.

This research was supported by the Russian Foundation for Basic Research (grant 15-01-03069)

**References**

Asmolov E.S., Vinogradova O,I., Effective slip boundary conditions for arbitrary one- dimensional surfaces. J. Fluid Mech., Vol.706, pp.108--117 (2012)

Asmolov E.S., Dubov A.L., Nizkaya T.V., Kuehne A.J.C., Vinogradova O.I., Principles of transverse flow fractionation of microparticles in superhydrophobic channels. Lab Chip, Vol.15, pp.2835-2841 (2015)

Bazant M.Z, Vinogradova O.I., Tensorial hydrodynamic slip, J. Fluid Mech., Vol. 613 pp. 125-134 (2008).

Belyaev A.V., Vinogradova O.I., Effective slip in pressure-driven flow past superhydrophobic stripes, J. Fluid Mech., Vol.652, p.489-499 (2010)

Vinogradova O.I., Dubov A.L., Superhydrophobic textures for microfluidics. Mendeleev Commun., Vol.22, pp.229–236 (2012)

Nizkaya T.V., Asmolov E.S., Zhou J., Schmid F., Vinogradova O.I., Flows and mixing in channels with misaligned superhydrophobic walls. Phys. Rev. E, Vol.91, Art. 033020 (2015).

Vinogradova O.I., Belyaev A.V., Wetting, roughness and flow boundary conditions, J. Phys.: Condens. Matter, Vol.23, Art. 184104 (2011).

# Mechanical Properties of Complex Fluid Interfaces: Underlying Mechanisms at Molecular Scale and Effects on Drop Dynamics

Bofeng Bai, Zhengyuan Luo, Chengzhen Sun

State Key Laboratory of Multiphase Flow in Power Engineering, Xi'an Jiaotong University
Xi'an 710049, China
E-mail: bfbai@mail.xjtu.edu.cn

Studying interfacial phenomena in multiphase flow has been an important branch of the discipline of thermophysics. Usually, the interface between two immiscible fluids consists of the same molecules as the two fluids, and the interface structure is simple and uniform. Notably, complex fluid interfaces consisting of various types of molecules that are different from the surrounding fluids are also extensively found in nature and engineering applications[1,2]. For instance, surfactants or nanoparticles can appear on oil−water interfaces in petroleum engineering; biological membranes consist of lipid bilayers supported by a network of spectrin proteins. The presence of various molecules confers interfaces special mechanical properties, such as resistances to shear deformation, area dilatation and bending. On the other hand, droplets surrounded by complex liquid interfaces are widely used for encapsulation, transport and release of active agents in numerous engineering and biomedical applications and are also employed as a model system for biological cells. Under this condition, coupling effects among viscous stresses of surrounding flow, elastic stresses of the complex liquid interface and specific or non-specific adhesion forces of the walls confer the droplets complex dynamical behaviors of deformation, motion and adhesion in shear flows. Therefore, we systematically investigated the mechanical properties of complex liquid interfaces by focusing on the underlying mechanisms at molecular level and also studied the deformation, motion and adhesion of droplets surrounded by complex interfaces. Our methods and results may be helpful for understanding interfacial phenomena in complex multiphase flows and for further developing related technologies such as surfactants or nanoparticles assisted enhanced oil recovery technologies in petroleum engineering and capsules or vesicles assisted substance delivery in chemical and biomedical engineering.

We developed a microscopic model to study the mechanical properties of complex fluid interfaces and reveal the underlying mechanisms from molecular point of view. In this model, molecular dynamics simulation is used to model the adsorption and motion of surfactant molecules at the oil-water interface and statistical mechanical method is employed to obtain the mechanical properties of the interface such as surface tension and interfacial viscoelasticity. Using this model, we demonstrated that the adsorption, molecular conformation and movement of specific substances (e.g. surfactants) at the oil-water interface have remarkable effects on the interface mechanical properties, for example, reducing the tension of the oil-water interface and altering the interfacial viscoelasticity. We expect that these mechanisms could provide guidance for developing and selecting oil-displacing agent in the enhanced oil recovery technologies.

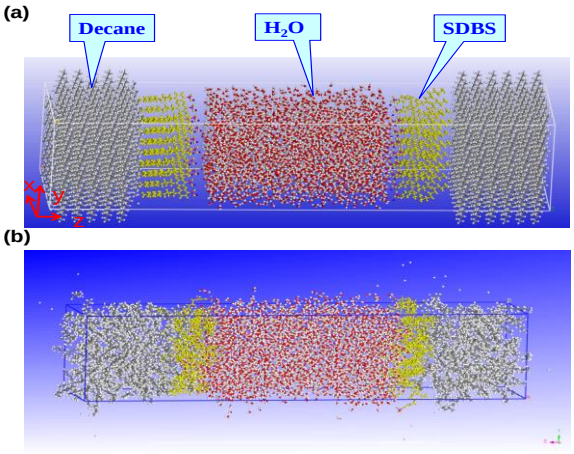


**Figure 1:** (a) Problem description. The simulation box is 4 nm×4 nm×16 nm. The water and oil phase is placed in the middle and at the two sides, respectively. Surfactants are initially close to the water phase. Molecular dynamics simulations are performed in NVT and NPT ensembles. A Nose–Hoover thermostat is used to maintain the system temperature at 300 K and Andersen method is used to keep the pressure at 1 atm. Periodic boundary conditions are applied in the x, y and z-directions, and the time step is 1 fs. (b) A molecular view of the equilibrium state. Surfactants are adsorbed at the decane-water interfaces.

We developed a front tracking−finite element method to investigate the deformation and dynamics of droplets enclosed by complex liquid interfaces under shear flow. This method is based on the coupling of the front tracking method (for the flow inside and outside the capsule and for the tracking of the membrane) and the finite element method (for the special mechanical properties of drop interface including resistances to shear deformation, area dilatation and bending). A fully three-dimensional finite difference code is developed to solve the governing equations and hence the nonlinear term can be included for the inertial effect. Using this model, we found that the deformation and dynamics of complex droplets are significantly affected by the fluid inertia and the internal structures inside the droplets. For instance, the drop deformation is greatly enhanced by the fluid inertia and the dynamical states of drops can be altered from tumbling motion to swinging motion by increasing the Reynolds number. Besides, the presence of a smaller drop inside reduces the deformation of compound drops and the increase of the inner drop size can induce the transition of drop dynamics from swinging motion to rumbling motion. The underlying mechanisms are also discussed by analyze the distributions of viscous stresses and pressure inside and outside the drop.

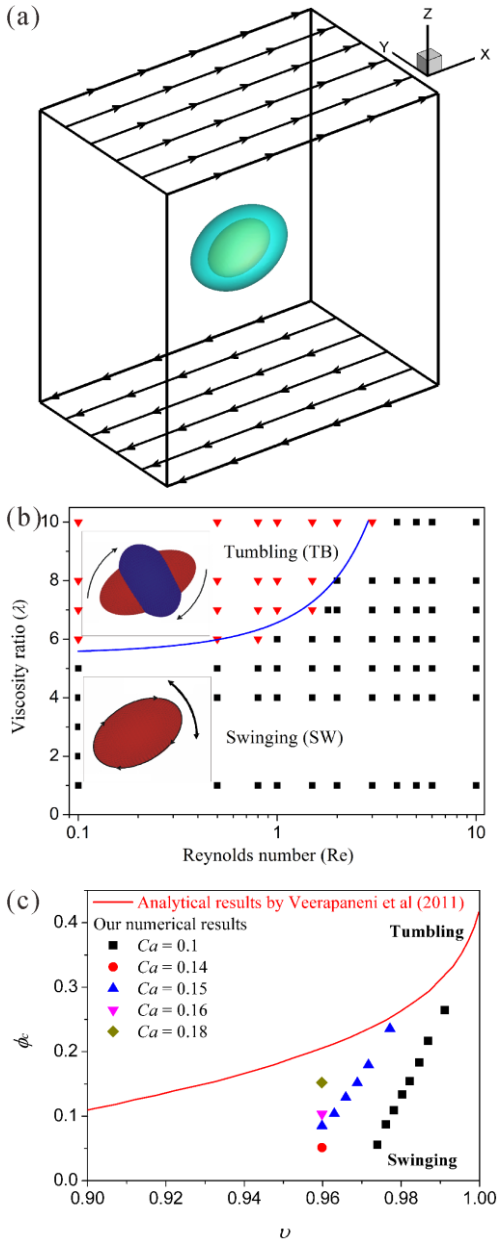


**Figure 2:** (a) A droplet enclosed by a complex liquid interface that possesses special mechanical properties including resistances to shear deformation, area dilatation and bending is subjected to a simple shear flow produced by moving the upper and bottom plates with the same velocity in opposite directions. (b) Phase diagram is plotted as a function of the viscosity ratio of the internal and external fluids and the Reynolds number for the occurrence of different drop dynamical states such as the swinging motion and the tumbling motion. (c) Phase diagram of compound drop dynamics. The critical value of the inner drop volume ratio ($\phi_c$) is plotted as a function of the reduced volume $\upsilon$ for the swinging to tumbling transition [3,4]. The solid line is the analytical result from the small-deformation theory by Veerapaneni et al. [5].

When droplets contact with solid walls, the moving contact line problem is crucial for droplet static spreading, droplet adhesion and detachment from the solid surface. Based on the front tracking−finite difference method that we developed for complex droplets under infinite shear flow, the generalized Navier boundary condition is further combined to consider the moving contact line. The front tracking method requires several special treatments to capture the interface near the moving contact line. For instance, the indicator function for updating the distribution of fluid density and viscosity must be modified to ensure the computational accuracy of the flow field near the moving contact line. Besides, the front restructuring operation near the moving contact line and the marker points advecting at the contact line are also modified to capture the accurate movement of the interface. Using this model, we simulated the deformation, motion and detachment of droplets with viscoelastic interfaces on solid walls with inhomogeneous wetting property under various flow conditions.

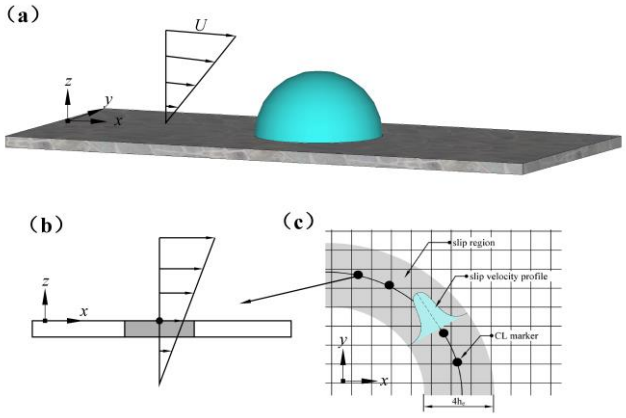


**Figure 3:** (a) Droplet is placed on a solid wall with inhomogeneous wetting property under shear flow. X-axis is in the flow (horizontal) direction; y-axis is in the lateral direction and z-axis is in the height (perpendicular to the wall) direction. (b) The generalized Navier boundary condition at the wall for the velocity at the moving contact line. (c) The slip velocity distribution near the moving contact line handled in the front tracking method.

**Acknowledgement**
This work was supported by the China National Funds for Distinguished Young Scientists (51425603).

**References**

[1] Langevin, D.. Rheology of adsorbed surfactant monolayers at fluid surfaces. Ann. Rev. Fluid Mech., 46: 47-65 (2014).
[2] Cui M, Emrick T and Russell TP. Stabilizing liquid drops in nonequilibrium shapes by the interfacial jamming of nanoparticles. Science, 342: 460-463 (2013).
[3] ZY Luo, SQ Wang, L He, F Xu and BF Bai. Inertia-dependent dynamics of three-dimensional vesicles and red blood cells in shear flow. Soft Matter, 9. 9651-9660 (2013)
[4] ZY Luo, L He and BF Bai. Deformation of spherical compound capsules in simple shear flow. J. Fluid Mech., 775. 77-104 (2015)
[5] S Veerapaneni, Y Young, P Vlahovska and J Blawzdziewicz. Dynamics of a compound vesicle in shear flow. Phys. Rev. Lett., 106. 158103 (2011)

# Moving contact lines

Stephen H. Davis

Department ESAM, Northwestern University Evanston, IL 60208 USA
sdavis@northwestern.edu

A contact line (CL), the curve common to three phases of material occurs in many industrial and natural contexts ranging from ink-dot printing and the coating of a substrate by a liquid, to the shedding of water from a penguin's fur to a droplet on a leaf. When it moves relative to the substrate, a macroscopic description of its motion requires a boundary condition between liquid and solid. The classical no-slip condition fails because the solution of the Navier- Stokes equation near the CL has a non-integrable singularity in the rate-of-strain tensor resulting in it requiring an infinite force to move the CL. Hence moving contact lines represent a non-standard fluid-mechanics problem.

The study of moving CL's is 45 years old and much progress has been made resulting in well -defined theoretical results that match experiments in common liquids. This is the HYDRODYNAMIC THEORY (HDT). However, there have been large sets of experiments on the spreading of liquid metals, necessarily at high temperatures, that diverge sharply from HDT, but instead follow a theory that ignores fluid flow completely but finds that CL's can move by molecules hopping across the CL onto the substrate effectively causing motion of the line. This is the MOLECULAR - KINETIC THEORY (MKT).

The talk to be presented will give an overview of the HDT, its kinematics and extensions, and its applications, showing its fundamentals in physical terms. It will then focus on the MKT and its properties.

Finally, it will be shown that the two theories, applied to the same system, yield a cross-over when the macroscopic contact angle is plotted verses the speed of the contact lines as shown in the Figure. At 'high' speeds one expects that the HDT will prevail because fluid flow should be dominant. At 'low' speeds the MKT theory should dominate. A large spectrum of experiments are examined and a criterion is extracted that demarks when each theory should hold even before the experiment is done.

One implication of the comparisons discussed above is that in principle every experiment should display both theoretical behaviors. To see this one should recognize that a spreading drop slows at it spreads. When the spreading begins, the CL moves most rapidly and the HDT should apply. As time proceeds, the CL speed slows beyond a (predictable) critical value and the MKT takes over. Whereas this crossover is in principle present, it may occur at such low speeds that the observer cannot perceive it.

The present state of the theories and experiment well describe the macroscopic state of moving contact lines. Much of the present research regards the microscopic underpinnings of the subject. For example, what determines the slip law for the HDT? What is the meaning of a contact line or contact angle at nanoscale dimension? How can one match molecular-dynamic predictions to continuum functions? Now, patching is in use.

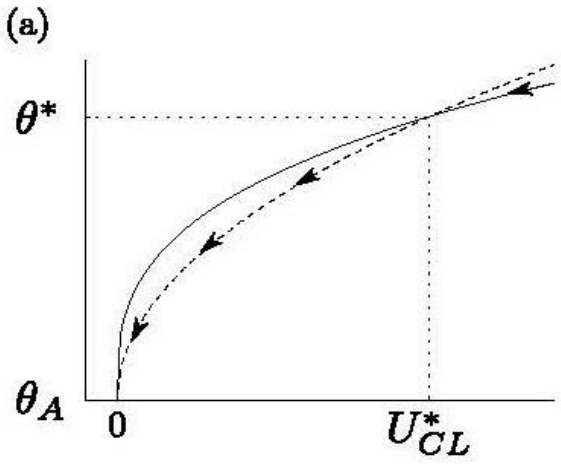


**Figure 1.**

# Dynamics of droplets moving on solid surface: Lattice Boltzmann simulations

Alexander Kupershtokh

Lavrentyev Institute of Hydrodynamics SB RAS
Acad. Lavrentyev ave., 15, Novosibirsk, 630090, Russia
E-mail: skn@hydro.nsc.ru

The behavior of thin liquid films and droplets placed on the surface of solid substrates are very important in modern technologies.

A static contact angle is closely related with forces of interaction of molecules of fluid and solid substrate. Even for sessile and pendant drops on inclined surface, a contact angle depends on azimuthal angle and changes from advancing point to receding point. In general case, the contact angle depends on a local curvature radius of contact line. For the shape of 3D static drop on inclined surface, the Young–Laplace equation is valid

$$2\sigma\kappa_{\mathrm{m}} = \Delta p_* + (\rho_{\text{ж}} - \rho_{\text{г}})(\mathbf{g}\cdot\mathbf{z} + \mathbf{g}\cdot\mathbf{x}), \qquad (1)$$

where $\sigma$ is the surface tension of liquid, $\kappa_{\mathrm{m}} = (\kappa_1 + \kappa_2)/2$ is the mean curvature of liquid-air interface, $\mathbf{z} = \mathbf{n}z$, $\mathbf{x} = \boldsymbol{\tau}x$, $\mathbf{n}$ and $\boldsymbol{\tau}$ are the vectors normal and tangent to the solid surface.

A large number of experiments showed that for motion of contact line along the horizontal solid substrate, the advancing contact angle is greater than receding angle (hysteresis). In general case, the contact angles depend on velocity of a contact line. Moreover, in several works, the phenomenon of dynamic contact angles and singularity at a contact line were investigated.

A non-stationary motion of a drop can only be simulated numerically. The viscous flow of fluid with surface tension of liquid and interaction of a liquid with a solid wall should be described in computer simulations. The most important problem is the interaction forces between fluid and solid at the interface. This phenomenon can be described better using the mesoscopic methods that closer to the nature of such interaction.

The lattice Boltzmann method (LBM) was successfully implemented for computer simulation of these three-dimensional problems. The lattice Boltzmann method describes the viscous flows of fluids with an arbitrary equation of state and simulates the interfaces between vapor and liquid phases with a surface tension.

The three-dimensional version of lattice Boltzmann method D3Q19 (Qian 1992) with nineteen vectors $\mathbf{c}_k$ of pseudo-particle velocities on a cubic lattice is realized. The evolution equation for the distribution functions $N_k$ can be written in the form

$$N_k(\mathbf{x} + \mathbf{c}_k\Delta t, t + \Delta t) = N_k(\mathbf{x}, t) + \Omega_k(N) + \Delta N_k, \qquad (2)$$

where $\Delta t$ is the time step, $\Omega_k$ is the collision operator, and $\Delta N_k$ is the change of the distribution functions due to the action of the internal and external body forces.

The hydrodynamic variables (the density $\rho$ and the velocity $\mathbf{u}$ of fluid) in a node are calculated as

$$\rho = \sum_{k=0}^{b} N_k \quad \text{and} \quad \rho\mathbf{u} = \sum_{k=1}^{b} \mathbf{c}_k N_k \qquad (3)$$

The collision operator is usually used in Bhatnagar–Gross–Krook (BGK) form

$$\Omega_k = (N_k^{eq}(\rho, \mathbf{u}) - N_k(\mathbf{x}, t))/\tau, \qquad (4)$$

where $\tau$ is the dimensionless relaxation time.

The Exact Difference Method (EDM) (Kupershtokh 2010) is used for the implementation of the body forces (internal forces and gravity) in the LBM:

$$\Delta N_k(\mathbf{x}, t) = N_k^{eq}(\rho, \mathbf{u} + \Delta\mathbf{u}) - N_k^{eq}(\rho, \mathbf{u}), \qquad (5)$$

where the value of the velocity after the action of the total force $\mathbf{F}$ on a node is equal to $\mathbf{u} + \Delta\mathbf{u} = \mathbf{u} + \mathbf{F}\Delta t/\rho$. The corresponding equilibrium distribution functions $N_k^{eq}$ are calculated as

$$N_k^{eq}(\rho, \mathbf{u}) = \rho w_k \left(1 + \frac{\mathbf{c}_k\mathbf{u}}{\theta} + \frac{(\mathbf{c}_k\mathbf{u})^2}{2\theta^2} - \frac{\mathbf{u}^2}{2\theta}\right). \qquad (6)$$

For equation of state $P(\rho, T)$, the total force acting on a node was introduced by Qian (1997) as a gradient of pseudopotential $\mathbf{F} = -\nabla U$, where $U(\rho, T) = P(\rho, T) - \rho\theta$. The isotropic finite-difference approximation of the gradient operator was proposed by Kupershtokh et al. (2009).

The van der Waals interaction forces between two flat surfaces is equal to $F = -A/(6\pi D^3)$, where $A$ is the Hamaker constant. For two different materials of densities $\rho_1$ and $\rho_2$, the Hamaker constant is proportional to the density of fluid near the solid surface $A = C\pi^2\rho_1\rho_2$ (see review by Leite et al. 2012). Hence, the effect of solid walls on fluids is simulated by special forces acting on a node $\mathbf{x}$ belonging to the fluid from the nearest nodes $\mathbf{x} + \mathbf{e}_k$ representing the solid boundaries (Kupershtokh 2010)

$$\mathbf{F}_k = w_k\rho(\mathbf{x})C(\mathbf{x} + \mathbf{e}_k)\,\mathbf{e}_k. \qquad (7)$$

Thus, contact angles are not prescribed in lattice Boltzmann method but are simulated in natural way.

For all computer simulations the Graphics Processing Units (GPUs) were exploited.

The three-dimensional dynamics of droplets on inclined and vertical walls in gravity was simulated. We use the quite simple well-known “bounce-back” rule to implement in the LBM no-slip boundary conditions at the solid walls.

The results of computer simulations for the droplet on inclined substrate ($\alpha = 40^\circ$) are shown in Fig. 1. The important parameter for the problem is the Bond number $\mathrm{Bo} = \rho g H^2/\sigma$. It represents a dimensionless parameter used to characterize the ratio of gravity force to surface tension force. Here $\rho$ is the density of liquid droplet. The Bond number in dimensionless variables has the form

$\mathrm{Bo} = \tilde{\rho}\tilde{H}^2\tilde{g}\cos\alpha/(k\tilde{\sigma})$. Here $k = P_{\mathrm{cr}}\Delta t^2/(\rho_{\mathrm{cr}}h^2)$ is the dimensionless parameter. The values $\tilde{\rho} = 1.93$, $\tilde{g}\cos\alpha = 0.000007$, $\tilde{\sigma} = 1.8$ were chosen. The initial height of droplet was $\tilde{H} = \tilde{R}_0 \approx 115$. Hence, the initial value of the Bond number was $\mathrm{Bo} \approx 10$. At the final stage of simulations (Fig. 1,*b*), the Bond number $\mathrm{Bo} \approx 1$.

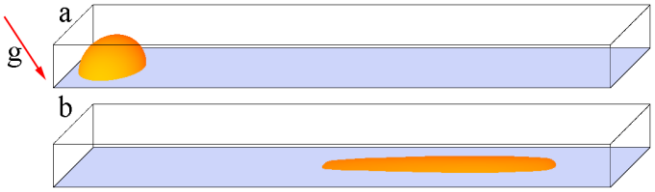


**Figure 1:** Droplet flowing down inclined surface ($\alpha = 40^\circ$). $\tilde{R}_0 = 115$.Grid 2048×368×160.

The second parameter is the ratio of gravity force to viscous forces $\mathrm{Ga}/\mathrm{Re} = \tilde{g}\sin\alpha\,\tilde{H}^2/(\tilde{\nu}\tilde{U})$. Here $\tilde{\nu}$ is the dimensionless kinematic viscosity, $\tilde{U}$ is the dimensionless characteristic velocity of liquid along the surface.

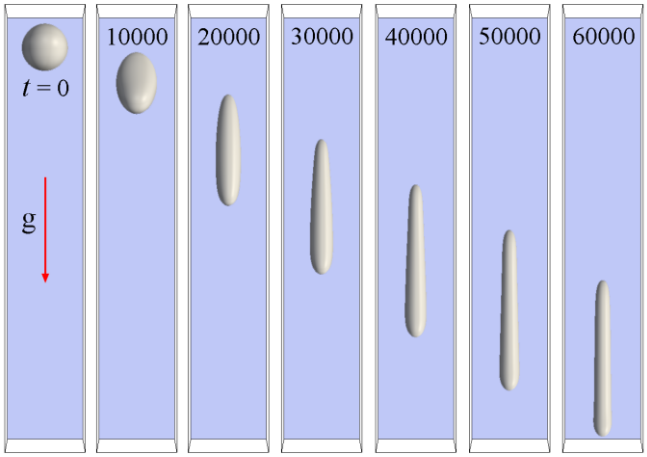


**Figure 2:** Droplet flowing down vertical wall in gravity. $\tilde{R}_0 = 115$. Grid 368×2048×160.

The results of three-dimensional computer simulations for the droplet flowing down vertical wall in gravity are shown in Fig. 2. The initial spreading of the droplet on the surface is determined by the Bond number. The steady velocity of the droplet is determined by the parameter $\mathrm{W} = \mathrm{Ga}/\mathrm{Re}$ (the ratio of the Galilei number to the Reynolds number). The initial value $W \approx 15$. At the end of simulations ($t = 60000$, $W \approx 3$), the flow tends to the quasi-stationary velocity.

The simulations of a rupture of the liquid films on the nonwettable solid substrate due to the thermocapillary effect (Marangoni effect) were also carried out. For the prescribed axisymmetric temperature distribution with a flattened vertex, a diverging flow in the film in the vicinity of the hot spot is generated because of the gradients of the surface tension along the film (Fig. 3). The rupture of the liquid film occurs not in the center of symmetry but along some circle where the gradient of the temperature is more pronounced (Kupershtokh et al. 2015). As a result, a central liquid disk is formed (Fig. 3*a*,*b*). The disk transforms initially into the toroidal figure due to surface tension (Fig. 3*c*,*d*) and then into an oscillating droplet (Fig. 3*e*,*f*).

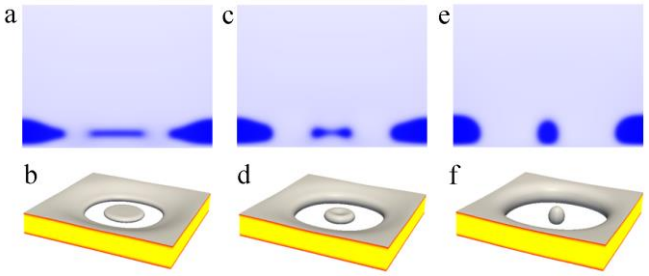


**Figure 3:** Marangoni effect (Kupershtokh et al. 2015). Thin film on nonwettable solid substrate. Periodic boundary conditions are used along the $x$ and $y$ directions.

For the non-axisymmetric temperature distribution, the rupture of free-hanging thin film is shown in Fig. 4.

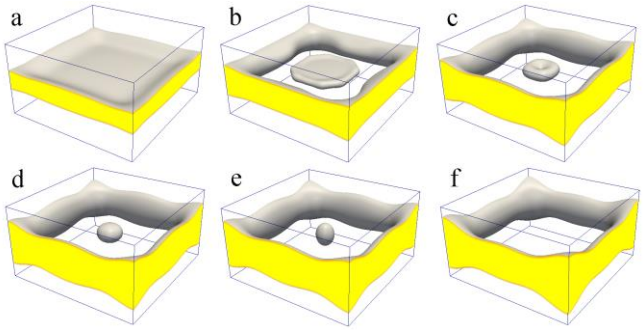


**Figure 4:** Marangoni effect. Free-hanging thin film at prescribed non-axisymmetric temperature distribution.

**References**

Qian Y.H., d'Humières D. and Lallemand P., Lattice BGK models for Navier – Stokes equation, Europhys. Lett., Vol. 17 pp. 479-484 (1992).

Kupershtokh A.L., Criterion of numerical instability of liquid state in LBE simulations, Computers and Mathematics with Applications, Vol. 59 pp. 2236-2245 (2010).

Qian Y.H. and Chen S. Finite size effect in lattice-BGK models, International Journal of Modern Physics C, Vol. 8 pp. 763-771 (1997).

Kupershtokh A.L., Medvedev D.A. and Karpov D.I., On equations of state in a lattice Boltzmann method, Computers and Mathematics with Applications, Vol. 58 pp. 965-974 (2009).

F. L. Leite, C. C. Bueno, A. L. Da Róz, E. C. Ziemath and O. N. Oliveira Jr., Theoretical models for surface forces and adhesion and their measurement using atomic force microscopy (Review), Int. J. Mol. Sci., Vol. 13 pp. 12773-12856 (2012),

Kupershtokh A.L., Ermanyuk E.V. and Gavrilov N.V., The rupture of thin liquid films placed on solid and liquid substrates in gravity body forces, Communications in Computational Physics, Vol. 17 pp. 1301-1319 (2015).

# Local hydrodynamic boundary conditions at a grooved superhydrophobic surface.

Tatiana V. Nizkaya*, Eugeny S. Asmolov and Olga I. Vinogradova

A.N. Frumkin Institute of Physical Chemistry and Electrochemistry RAS,
31 Leninsky Prospect, 119071 Moscow, Russia
*E-mail: nizkaya@gmail.com

A superhydrophobic (SH) surface combines chemical hydrophobicity and artificial or natural roughness, which leads trapping of air in its recessions when in contact with water (Cassie state). Such surfaces have first attracted attention because of their remarkable wetting properties: very large contact angles and extremely high droplet mobility. However, in the last decade the focus has shifted to hydrodynamic properties of SH surfaces and their possible applications in microfluidics (Rothstein, 2010).

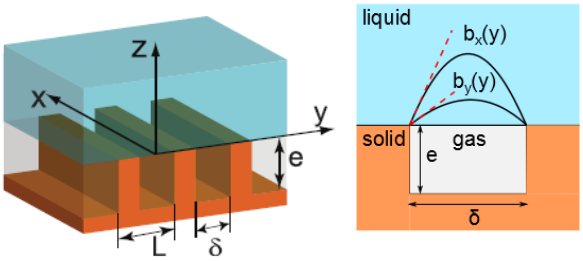


**Figure 1:** *Sketch of an anisotropic superhydrophobic texture with parallel grooves and a local slip length profile at liquid/gas interface for longitudinal and transverse flow.*

From hydrodynamical point of view a SH surface can be seen as a composite system with liquid/gas and liquid/solid parts of the interface. On solid parts the no-slip boundary condition is applied (if hydrophobic slip is neglected), but at liquid/gas interface the fluid can slip with some finite velocity. Existing models use the free shear condition at this interface, completely neglecting dissipation in gas, or consider a partial slip boundary condition with a constant slip length b, considered as an external model parameter (Belyaev and Vinogradova, 2010). Deriving boundary conditions that would account for the flow in gas and connect the slip with the shape of the groove is, therefore, an important problem.

We consider an anisotropic superhydrophobic texture consisting of an array of periodic parallel grooves completely filled with gas (see Fig.1). Assuming that the liquid/gas interface is flat, we derive non-local boundary conditions for fluid velocity based on Dirichlet-to-Neumann map for the Stokes equations in gas (Nizkaya et al., 2014):

$$\frac{\partial u_{//,\perp}}{\partial z} = \frac{\mu_g}{\mu}\mathbf{P}_{//,\perp}[u_{//,\perp}],$$

where $\mu, \mu_g$ are dynamic viscosities of liquid and gas, $//,\perp$ correspond to flow direction along or across the grooves and linear operators $\mathbf{P}_{//,\perp}$ take a matrix form when discretized on a grid. For rectangular grooves, these matrices have been calculated semi-analytically and the boundary condition has been implemented for a shear flow over the surface in both longitudinal and transverse directions.

Analysis of numerical results shows that the velocity at liquid/gas interface satisfies partial slip boundary condition:

$$u_{//,\perp} - b_{x,y}(y)\frac{\partial u_{//,\perp}}{\partial z} = 0,$$

with the local slip length obeying the following scaling:

$$b_{x,y}(y) = \delta\frac{\mu}{\mu_g}\beta_{x,y}(y/\delta).$$

The rescaled slip length profiles $\beta_{x,y}(y/\delta)$ depends only on the aspect ratio $e/\delta$ of the groove, but not the gas fraction $\phi = \delta/L$ or viscosity ratio $\mu/\mu_g$ (see Fig.2). The red dash-dotted lines in Fig. 2 correspond to an asymptotic solution that was obtained by considering flow singularities at the groove's edge (Nizkaya et al., 2014):

$$b_x' \approx 2\frac{\mu}{\mu_g}, \qquad b_y' \approx \frac{\mu}{2\mu_g}.$$

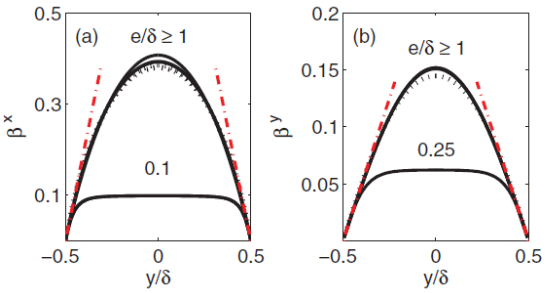


**Figure 2:** *Profiles of rescaled local slip length at the liquid/gas interface for deep and shallow grooves. Curves for different $\phi$ and viscosity ratios $\mu/\mu_g$ nearly overlap.*

Such an analysis can be performed for arbitrary slopes of the groove's edge and suggests that universal local slip length profiles exist for a wide range of groove shapes. The operators $\mathbf{P}_{//,\perp}$ for arbitrary groove shapes can also be obtained using boundary integral equations, which opens wide perspectives for generalization of this work.

This research is partly supported by the Russian Foundation for Basic Research (Grant No. 16-31-00457)

**References**

J.P. Rothstein, Slip on superhydrophobic surfaces. Annu. Rev. Fluid Mech, 2010, V. 42, pp. 89-109.

O.I.Vinogradova and A.V.Belyaev, Wetting, roughness and flow boundary conditions, J. Phys.: Condens. Matter, 2011, V.23, 184104.

T.V. Nizkaya, E.S. Asmolov, O.I. Vinogradova, Gas cushion model and hydrodynamic boundary conditions for superhydrophobic textures. Phys. Rev. E, 2014, V.90, 043017.

# Contact angle hysteresis and wetting transition on superhydrophobic striped surfaces

Alexander Dubov[1] and Olga Vinogradova[1,2]

[1] - A.N. Frumkin Institute of Physical Chemistry and Electrochemistry, Russian Academy of Sciences
Leninsky Prospect 31, 119071 Moscow, Russia
[2] - Department of Physics, M.V. Lomonosov Moscow State University
Leninskie Gory 1, 119991 Moscow, Russia

alexander.dubov@gmail.com

The ability of superhydrophobic Cassie surfaces to trap air at the liquid-solid interface leads to remarkable properties such as a high water contact angle and a water slippage. Such properties make these surfaces perspective for use in anti-wetting or self-cleaning systems and microfluidic lab-on-a-chip devices. The application of superhydrophobic textures for microfluidics attracts high attention since large effective slip over gas layer can significantly lower the viscous drag and direct the liquid flow.

For enhancement of efficiency and better control of hydrodynamic properties in thin channel the most effective is use of anisotropic patterns with moderate or high solid-liquid fraction, $\varphi_S$, on interface. They allow optimization of effective slip, robust transverse flows in superhydrophobic devices, droplet or particle sorting, or passive mixing. The wetting properties of such textures (e.g. contact angle hysteresis and robustness of Cassie wetting state) are also of great importance for microfluidics since they determine the stability conditions for slippery gas layer. However the earlier research of superhydrophobic wetting has been mostly dedicated to isotropic patterns with low solid fraction. Therefore exploration of wetting on `denser' anisotropic surfaces is an important and timely step in study of microfluidics-oriented superhydrophobicity.

The present work combines experimental study and analytical modeling of wetting of the most anisotropic superhydrophobic *stripe* textures in entire range of solid fraction $0<\varphi_S<1$.

In the first part of our research we study experimentally and discuss quantitatively the contact angle hysteresis on striped superhydrophobic surfaces as a function of a solid fraction $\varphi_S$. The advancing and receding contact angle are measured and explained theoretically accounting for mechanisms of water motion and pinning of contact line on weak defects of smooth solid areas and borders of superhydrophobic stripes. The advancing contact angle is found to be anisotropic, and its value is shown to be determined by the rolling motion of the water. The cosine of the longitudinal advancing angle depends linearly on $\varphi_S$, and a satisfactory fit of the data can be provided by generalizing of the Cassie equation to account for weak defects. The cosine of the transverse advancing angle is much smaller and is maximized at $\varphi_S\approx0.5$. Its value can be explained by invoking an additional energy due to strong defects in this direction, which is shown to be caused by the adhesion of the water on solid areas and is proportional to $\varphi^2_S$. Unlike advancing contact angle the receding contact angle is shown to be determined by a longitudinal sliding motion of the deformed contact line. Despite an anisotropy of the texture the receding contact angle remains isotropic, i.e. it is practically the same in the longitudinal and transverse directions. The cosine of the receding angle grows nonlinearly with solid-liquid fraction. A theoretical model developed for interpretation of experimental observations shows that the value of the receding angle is determined by pinning of contact line on both weak defects at smooth solid areas and borders of superhydrophobic stripes. The shape of pinned contact line can be described in terms of elastic deformation with energy which scales as $\varphi^2_S \ln \varphi_S$. The contact angle hysteresis for superhydrophobic striped surfaces with moderate $\varphi_S$ is found to be quite large and generally anisotropic, but it becomes isotropic when $\varphi_S \leq 0.2$.

The second part of our research is study of Cassie state robustness and influence of contact angle hysteresis on it. We discuss an evaporation-induced breakdown of Cassie wetting state on superhydrophobic stripes and show that mechanism of transition depends on the elastic energy of the deformed contact line, which determines the value of an instantaneous apparent contact angle due to receding of contact line. For dilute stripe textures the receding angle is above 90°, and Cassie state is metastable. On such textures sudden impalement transition to Wenzel state happens due to an increase of Laplace pressure in an evaporating drop. For dense stripe patterns the breakdown of Cassie state is caused by additional energy introduced by receding motion of contact line. For these surfaces slow impregnation transition commences when the apparent angle reaches 90° and represents the impregnation of the grooves starting from the triple contact line towards the drop center (Fig. 1).

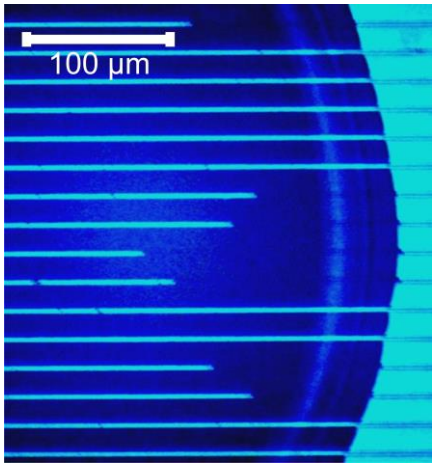


**Figure 1:** The bottom view of water drop during Cassie-Wenzel transition on stripe pattern with $\varphi_S$=0.86 by impregnation from the triple line.

# APPLICATION OF BOUNDARY INTEGRAL METHOD FOR STOKES FLOW OVER A CAVITY ON A SUPERHYDROPHOBIC SURFACE CONTAINING A GAS BUBBLE

Alexey Ageev, Alexander Osiptsov

M.V. Lomonosov Moscow State University, Institute of Mechanics
Michurinskii Prospekt, 1, Moscow, 119192, Russia
E-mail: aaiageev@mail.ru, osiptsov@imec.msu.ru

Within the Stokes hydrodynamics, several problems of a steady-state flow over a two-dimensional cavity and a group of cavities containing gas bubbles are considered, as applied to modeling the flows near microtexture of superhydrophobic surfaces. For the solution of the problem, a numerical algorithm based on the method of boundary integral equations is developed (Pozrikidis 1992). In contrast to previous publications, the method proposed makes it possible to study the situation in which the cavity is only partially filled with gas, and the edges of a curved phase interface do not coincide with the cavity corners (Fig. 1). The method is validated by the solution of known problems for a cavity completely filled with the fluid (Higdon 1985) and a cavity completely occupied by a gas bubble with a flat phase interface (Vinogradova and Belyaev 2011). A good agreement of the calculations with the data known in the literature is demonstrated.

Using periodic boundary conditions for the velocity, the flows with pure-shear and parabolic velocity profiles, and also the flow over a group of cavities were considered. The aim of the study was to calculate the effective (average) slip velocity $b_{\text{eff}}$ over a microcavity, as applied to the effective Navier slip condition in macroscale modeling of flows near superhydrophobic surfaces with periodic striped textures. The effective slip length scaled to the period $L$ of texture.

A parametric numerical study of the problem of a shear flow over a cavity with the gas bubble having the shape of an arc of a circle is performed for a general case, when the edges of the interface do no coincide with the cavity corners and the gas bubble occupies only a part of the cavity. The effective (averaged) slip length of the fluid over the cavity as the function of the geometrical parameters of the cavity and the curvature of the phase interface is investigated. The restructuring in the streamline patterns with the variation of the interface position and curvature is investigated. It is shown that the maximum average slip is attained in the case when the gas completely occupies the cavity and the interface is flat (Fig. 2). The results are generalized to the case of the flow over a group of cavities and the flow near a superhydrophobic surface with a periodic array of cavities. The velocity profiles, which are formed between the cavities and satisfy the conditions of flow periodicity are calculated (Ageev and Osiptsov 2015).

The work received financial support from the Russian Foundation for Basic Research (project No. 16-31-00069).

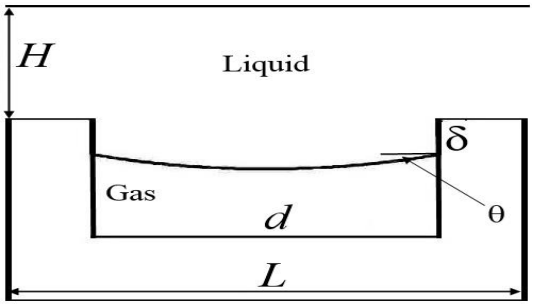


**Figure 1:** Flow domain over the cavity partially filled with a gas bubble.

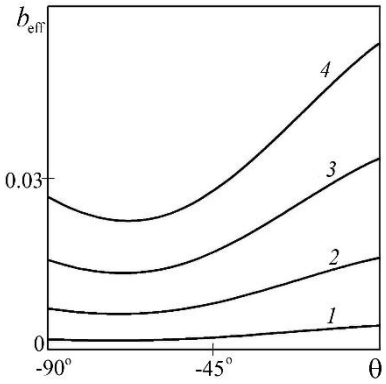


**Figure 2:** Effective slip length as a function of the protrusion angle of the bubble into the fluid for the pure-shear velocity profile, $\delta/L = 0$, $d/L = 0.15, 0.30, 0.45, 0.60$ (*1-4*).

## References

Pozrikidis C. Boundary integral and singularity methods for linearized viscous flows // Cambridge University Press. 1992. 259 p.

Higdon J.J.L. Stokes flow in arbitrary two-dimensional domains: shear flows over ridge and cavities // J. Fluid Mech. 1985. V. 159. P. 195—226.

Vinogradova O.I., Belyaev A.V. Wetting, roughness and flow boundary conditions // J. Phys.: Condens. Matter. 2011. V. 23. 184104.

Ageev A.I., Osiptsov A.N. Stokes flow over a cavity on a superhydrophobic surface containing a gas bubble // Fluid Dynamics. 2015. V. 50. N. 6. P. 748-758.

# Flow visualization in evaporating droplet on a substrate by means of Micro-PIV technique

Anna Yagodnitsyna[1, 2], Artur Bilsky[1, 2], Mina Roudgar[3], Joël De Coninck[3] and Oleg Kabov[1, 2]

[1] Institute of Thermophysics SB RAS, 1, Lavrentev ave., Novosibirsk, 630090, Russia
[2] Novosibirsk State University, 2, Pirogova str., Novosibirsk, 630090, Russia
[3] Laboratory of Surface and Interfacial Physics. Université de Mons, Belgium
yagodnitsinaaa@gmail.com

The interest towards droplet evaporation is connected with number of scientific and technological processes such as DNA molecules visualization, ink-jet printers, spray cooling and so on (Erbil 2012). Flow structure in evaporating droplets can dramatically influence the heat and mass transfer processes and particle deposition on a substrate. In the present work in order to visualize flow structure in evaporating droplets Micro-PIV technique was applied.

Experiments were performed for two substrates with different contact angles (RCA) and contact angle hysteresis (CAH): the substrate with OTS surface (RCA 110-130º, CAH 10-15º) and the substrate with SU-8 surface (RCA 45-60º, CAH 30-40º). Experimental setup is made of Zeiss inverted microscope with 10x/0.25 lens, double-pulsed Nd:YAG green laser and double exposure CCD camera. The working fluid is ultra-pure water seeded with 3.2 μm fluorescent polystyrene particles. Droplets were created by high precision micropipette. The droplet volume was equal to 1.5 μl. During experiments environment temperature and humidity were controlled. Evaporation time for each droplet was also measured.

Velocity field measurements were performed in 9 cross-sections parallel to the substrate plane located at different distances from the substrate ranging from 13 μm to 465 μm. For each cross-section several measurements for different droplets were done in order to obtain sufficient statistical information. The measurements were carried from the beginning of droplet evaporation up to the end.

In-house software package “ActualFlow” was used to process the acquired data. Image preprocessing included masking and minimum intensity subtraction calculated for every 20 particle images. These procedures allowed eliminating background noise and decreasing out-of-focus particles influence. Instantaneous velocity fields were calculated using iterative cross-correlation algorithm. Final spatial resolution of measured instantaneous velocity fields was equal to 30 μm per velocity vector.

Analysis of instantaneous velocity fields showed that flow structure in evaporating droplet changed significantly during the evaporation process. At the first stage of evaporation two vortices were found in the droplet (see Figure 1). Similar vortices were obtained for droplets on both substrates. At the second stage of evaporation droplet height decreases and velocity fields become radial with higher velocities near the edges of the droplets. Experimental data obtained can be useful for numerical models verification.

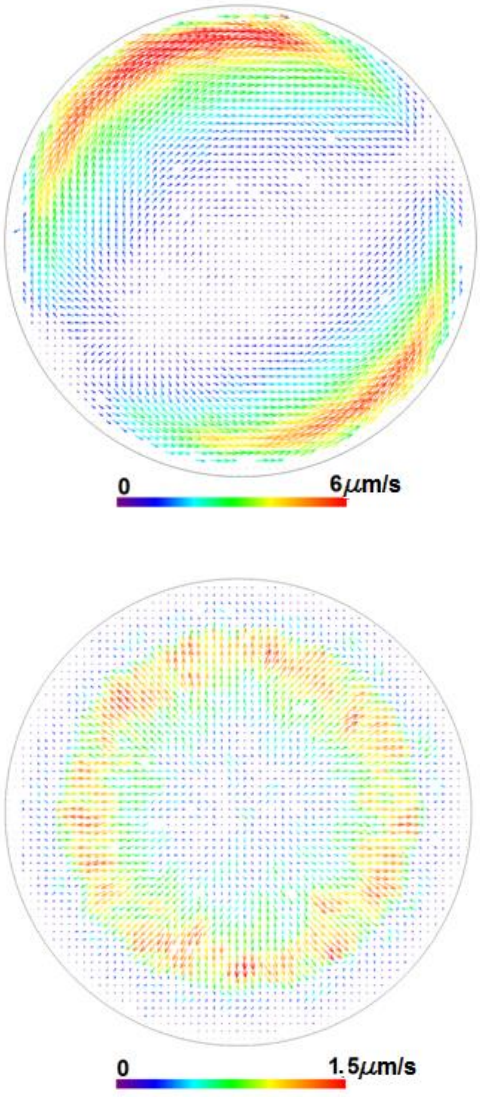


**Figure 1:** Instantaneous velocity fields in a droplet cross-section located at the distance 93 μm from the substrate surface made of SU-8. Top: 78s after the beginning of evaporation. Bottom: 220 s after the beginning of evaporation. Full evaporation time was equal to 558 s.

This work was supported by a grant from the Russian Science Foundation (project Nr. 14-19-01755).

**References**

H.Y. Erbil Evaporation of pure liquid sessile and spherical suspended drops: A review // Advances in Colloid and Interface Science – 2012 – V.170 – P. 67–86.

# Evaporation modes of a water drop on copper substrates

Geniy Kuznetsov, Dmitry Feoktistov and Evgeniya Orlova

National Research Tomsk Polytechnic University, Tomsk, 634050, Russia
lafleur@tpu.ru

Study of the physical mechanisms of drop spreading and evaporation is usually accompanied by indicating different modes. Spreading modes in the initial period of time (when a drop and surface are in contact) are the most studied. The basic physical mechanisms occurring during this period were obtained for liquid metals spreading on solid substrates by Sorokin and Hlynov (1967). Drop spreading is found to begin from the kinetic mode. The inertial mode comes after kinetic, when the contact line movement is mainly determined by the inertial forces acting on the drop. Force of viscous (internal) friction prevails in the third mode (viscous). After conducting experimental and numerical investigations of drop evaporation (Erbil et al., 2002; Anantharaju et al., 2009) several modes (from one to four) have been detected depending on wetting characteristics (contact angle and diameter) and evaporation rate.

This paper presents the results of experimental studies of distilled water drop evaporation on the copper substrate with detecting spreading modes following after the viscous mode.

Investigations were conducted on the experimental setup with using shadow optical system (Kuznetsov et al., 2014). A drop was placed on the surface of heated substrates (55, 62, 70°C) by electronic dosing device Single Channel Pipette (Thermo Scientific). Three copper substrates with different surface roughness were used in the experiment. The surface of the one substrate was not finished (sample No 1). Two rough surfaces are obtained by bombarding a smooth surface with $Al_2O_3$ particles sizes of 10 and 100 microns (sample No 2 and 3, respectively).

According to the analysis of contact diameter change (Fig. 1) three modes of distilled water drop spreading on copper surfaces were detected (following after the viscous mode). The first one is an increase of the contact area; then it is pinning of a drop with constant contact area (Yoo and Kim, 2015); the third mode is depinning or drop shrinking (reduction in the contact diameter).

It is known (Abkhalimov and Ershov, 2014) that the effect of the temperature on the wetting depends on the nature of the interaction forces between a liquid and a solid. If adhesion between the liquid and the substrate is performed by molecular forces (physical wetting) then the contact angles decrease with increasing temperature.

Experiments were conducted to analyze the effect of the copper substrate temperature in the range from 55 to 70 °C on the wetting process. The contact angle is found to decrease monotonically during evaporation process. It indicates that there are no chemical and structural transformations in the liquid, and also that the adhesion work remained practically unchanged. Calculated temperature coefficient $d\theta/dT$ (Summ et al., 1976) in these experiments has negative value and decreases linearly during drop evaporation, i.e. wetting is enhanced with increasing the temperature.

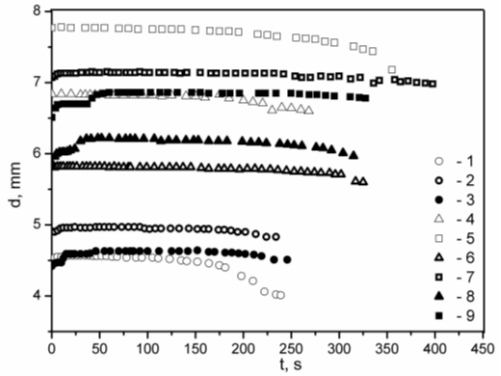


**Figure 1:** Contact diameter versus time at substrate temperature 55 °C. Sample No 1: 1 – V=0.02 ml; 2 – V=0.04 ml; 3 – V=0.06 ml. Sample No 2: 4 – V=0.02 ml; 5 –V=0.04 ml; 6 – V=0.06 ml. Sample No 3: 7 – V=0.02 ml; 8 – V=0.04 ml; 9 – V=0.06 ml.

The results obtained in the experiments approve the ability to "control" the process of drop spreading by changing the substrate roughness.

**References**

Abkhalimov E.V., Ershov B.G., The size effect in the catalytic activity of agcorept shell nanoparticles, Colloid J., Vol.76 pp. 381-386 (2014)

Anantharaju N., Panchagnula M., Neti S., Evaporating drops on patterned surfaces: transition from pinned to moving triple line, J Colloid Interface Sci., Vol. 337 pp. 176-182 (2009)

Erbil H.Y., McHale G., Newton M.I., Drop evaporation on solid surfaces: constant contact angle mode, Langmuir, Vol. 18 pp 2636-2641 (2002)

Kuznetsov G.V., Orlova E.G., Feoktistov D.V., The evaporation of the water-sodium chlorides solutiondroplets on the heated substrate, EPJ Web of Conferences, Vol. 76 pp 1-8 (2014)

Sorokin Yu.V., Khlynov V.V., Esin O.A., Study of the spreading kinetics of melts over the surface of the solid oxides, Russ. J. Phys. Ch. A, Vol. 41 pp. 1764-1769 (1967)

Summ B.D., Goryunov Yu.V. *Physical and chemical bases of wetting and spreading* (Khimia, Moscow, Russia, 1976) [in Russian]

Yoo H., Kim C., Experimental studies on formation, spreading and drying of inkjet drop of colloidal suspensions, Colloid Surfaces A, Vol. 468 pp. 234–245 (2015)

# Size dependence of the contact angle of water droplets under the natural evaporation

Yukihiro Yonemoto[1], Tomoaki Kunugi[2]

[1]Priority Organization for Innovation and Excellence, Kumamoto University
2-39-1, Kurokami, Chuo-ku, Kumamoto-shi, Kumamoto, 860-8555, Japan
yonemoto@mech.kumamoto-u.ac.jp
[2]Department of Nuclear Engineering, Kyoto University
C3-d2S06, Kyoto Daigaku-Katsura, Nishikyo-ku, Kyoto, 615-8540, Japan
kunugi@nucleng.kyoto-u.ac.jp

A droplet wetting behavior is important because wettability is related to the improvement of energy efficiency in industrial applications such as heat exchanger, ink-jet printing and spray cooling[1-3]. Especially, in heat removal systems which are related to heat and mass transfer, control of the droplet wetting behavior leads to development of high performance devices. Therefore, accurate prediction of the droplet behavior during volume variation process is very important. In such the situation, however, the contact angle is not constant and exhibits a complex behavior. Thus, the problem is not so simple.

In general, wettability between a liquid and a solid is characterized by a contact angle. The contact angle varies depending on the combination of the liquid and solid. The Young equation is a horizontal equilibrium condition at the contact line. According to this equation, the contact angle is determined from the surface energy densities of the solid-gas, solid-liquid and liquid-gas interfaces as follows.

$$\sigma_{sg} = \sigma_{lg}\cos\theta + \sigma_{sl}, \quad (1)$$

where $\sigma_{sg}$, $\sigma_{lg}$, and $\sigma_{sl}$ represent the surface energy densities of solid-gas, liquid-gas and solid-liquid interfaces, respectively. However, the actual wetting behavior cannot be simply explained by this equation. For example, two processes such as contact angle hysteresis and the size dependence of the contact angle[4] are observed when a droplet volume decreases due to phase change or extraction using microsyringe. Although many researchers try to explain those complex wetting behaviors, the problem remains unresolved at the present time. In light of actual applications such as heat exchanger and heat removal system, prediction and control of such kind of the complex wetting behavior are very important.

In this study, natural evaporation of water droplets is experimentally measured to understand the fundamental wetting behaviors under the volume reduction process. The droplet behavior in the process of the size dependence of the contact angle is discussed on the basis of our new wettability model[5].

In the experiment, several sized water droplets are deposited on low-surface energy solid. Then, the radius, height and contact angle were mainly measured. The droplets images were captured using a CCD camera.

Figure 1 shows results of the relationship between the contact area radius ($r$) and the droplet height ($h$) for different water droplet volumes on polycarbonate (PC). The initial droplet volumes of empty and black circles are 0.024 μL and 1.2 μL, respectively. The data are normalized using the initial contact area radii and the droplet heights for each case. The time advances along the dashed arrow. From this figure, two processes are mainly observed such as constant contact area process and the simultaneous changes in the contact area radius and the droplet height. In the present study, the relationship between the contact area radius and the contact angle after the constant contact area process is also discussed theoretically. The result indicates that the process of the size dependence of the contact angle may be predicted without the line tension concept.

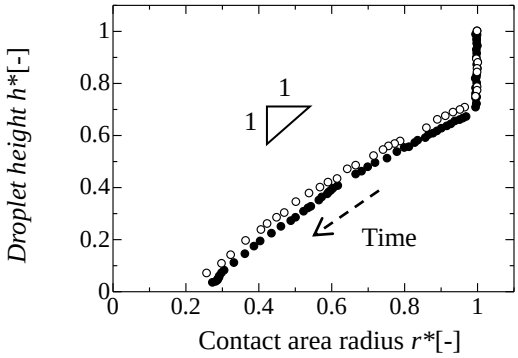


Figure 1: Relationship between the contact area radius and the droplet height of water droplets.

**References**

[1]P. Vlasogiannis, G. Karagiannis, P. Argyropoulos and V. Bontozoglou, Air-water two-phase flow and heat transfer in a plate heat exchanger, Int. J. Multiphase Flow, Vol. 28, pp. 757-772 (2002)

[2]S.-S. Hsieh, S.-Y. Luo, R.-Y. Lee and H.-H. Liu, Spray cooling heat transfer on microstructured thin film enhanced surfaces, Exp. Therm. Fluid Sci., Vol 68, pp. 123-134 (2015)

[3]O. Schneider, P. Epple, E. Teuber, B. Meyer, M. P. M. Jank, C. Rauh and A. Delgado, Jet printing of colloidal solutions-Numerical modeling and experimental verification of the influence of ink and surface parameters on droplet spreading, Adv. Powder Technol., Vol. 22, pp. 266-270 (2011)

[4]Y. Yonemoto and T. Kunugi, Experimental investigation on variations in geometric variables of a droplet on a low-surface energy solid, Int. J. Heat Mass Transfer, Vol. 73, pp. 810-818 (2014)

[5]Y. Yonemoto and T. Kunugi, Wettability model for various-sized droplets on solid surfaces, Phys. Fluids, Vol. 26, pp. 082110-1-082110-19 (2014)

# Evaporation dynamics and Marangoni number estimation for sessile picoliter liquid drop of binary mixture solution

Peter Lebedev-Stepanov*, Alexander Kobelev and Sergey Efimov

Lab of nanoparticle self-organization, Photochemistry Center of Russian Academy of Sciences
Novatorov St., 7a/1, Moscow, 119421, Russia;
Condensed matter physics department, National Research Nuclear University "MEPhI"
Kashirskoe Shosse St., 31, Moscow, 115409, Russia,
E-mail*: petrls@yandex.ru

The evaporating picoliter liquid sessile drop of axis-symmetric shape is an interesting object of theoretical and experimental investigations due to its important fundamental and practice applications (inkjet printing, eletronics, sensorics, photonics). J.C. Maxwell has elaborated the simple model of slow evaporation of spherical drop of single (one component) liquid at normal condition. Evaporation process is controlled by diffusion of the saturated vapor from surface of drop in surrounded air.

The evaporation rate is described by equation $-\frac{dN}{dt} = 4\pi RD(n_S - n_\infty)$, where $N = \frac{4}{3}\pi R^3 n_L$ is quantity of molecules in liquid drop with radius of *R*, volume concentration of molecules of $n_L$, *D* is diffusion coefficient of drop molecules in air, $n_S$ and $n_\infty$ are the volume concentrations of saturated vapor of considered liquid and asymptotic concentration of this vapor in atmosphere far from the drop surface. The important assumption of this model is $n_S k_B T << p_A$, where $k_B$ is Boltzmann constant, $p_A$ is atmospheric pressure.

Popov (2005), Hu and Larson (2002) have elaborated the models of evaporation of sessile drop of single liquid based on Maxwell diffusion model of evaporation.

We developed the evaporation model of picoliter sessile drop of binary solvent mixture (with infinitely soluble in each other components) based on Hu and Larson solution for single solvent sessile drop and Raoult law for saturated vapor density of components of binary mixture in wide range of undimensional molar binary concentration of the components *c*. (The Raoult law declares that saturated vapor density of first component has a linear reducing dependence on the percent of second component presence in binary solution if this addition of second one is small enough).

There are two characteristic times in this system: drop evaporation time, $t_e \propto \frac{L^2 n_L}{D(n_S - n_\infty)}$, and relaxation time, $t_r \propto \frac{L^2}{D_L}$, where *L* is characteristic size of drop; *D*, $D_L$ are the diffusion coefficient of molecule in air and in liquid respectively. Obviously, non-depending on *L* ratio $\frac{t_r}{t_e} = \frac{D(n_S - n_\infty)}{D_L n_L}$ ( $n_s, n_L, n_\infty$ are the concentrations of saturated vapor, liquid and vapor far from the drop respectively) is the criterion of concentration relaxation rate into drop.

If $\frac{t_r}{t_e} << 1$ then *c=const* inside the liquid drop is good assumption, due to there is fast relaxation of concentration of binary components in the liquid drop of solution.

With account of these approximations we obtain the next equations of evaporation dynamics

$$\frac{d\phi}{dt} = -\frac{2\phi(1+\cos\phi)^2}{\pi R^2 \sin\phi}(K_1(c-h) + K_2(1-c))$$

$$\frac{dc}{dt} = \frac{2\phi\sin^2\phi}{\pi R^2\left(\frac{2}{3} - \cos\phi + \frac{\cos^3\phi}{3}\right)}(K_1(c-h)(c-1) + K_2 c(1-c))$$

where

$$K_1 = 2D_1\frac{n_{S10}}{n_{L10}}, K_2 = 2D_2\frac{n_{S20}}{n_{L20}}$$

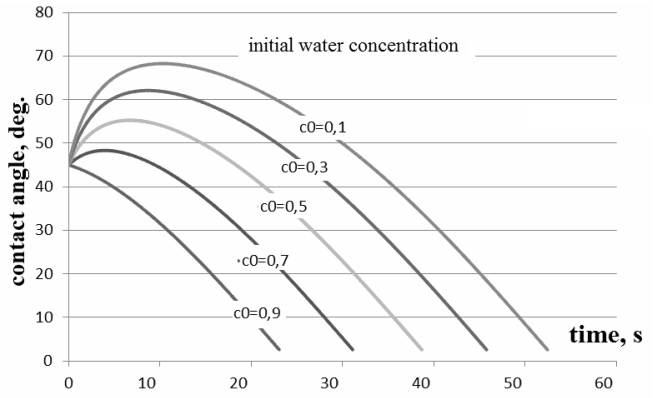


**Figure 1:** Evaporation of water-metoxipropanol binary mixture drop with pinned radius of 0.05 mm, initial contact angle 45° and relative humidity 0.9 (calculation result).

Concentration Marangoni number estimation for such a system is also considered for prediction of liquid flows structure for further applications in dissipative particle dynamics in binary mixture evaporating drop.

**References**

Hu H., Larson R.G. Evaporation of a Sessile Droplet on a Substrate. J. Phys. Chem. B, Vol. 106 (6), pp. 1334-1344 (2002)

Popov Yu.O. Evaporative deposition patterns: Spatial dimensions of the deposit. Phys. Rev. E, Vol. 71, p. 036313 (2005)

# Experimental investigation of the feature of polydisperse droplet flow evaporation while motion through high-temperature combustion products

Roman Volkov, Geniy Kuznetsov and Pavel Strizhak

National Research Tomsk Polytechnic University, Institute of Power Engineering
30, Lenin Avenue, Tomsk, 634050, Russia
romanvolkov@tpu.ru

By cross-correlation recording complex (Volkov et al. 2015) based on double pulse Nd:YAG lasers and cross-correlation CCD video cameras, it was carried out the cycle of experimental investigations of the features of polydisperse droplet flow displacement and evaporation while droplet motion in a flow of high-temperature (1100 K) combustion products. In experiments we used modern panoramic optical methods Particle Image Velocimetry (PIV), Particle Tracking Velocimetry (PTV), Shadow Photography (SP) and Interferometric Particle Imaging (IPI) for diagnostic of multiphase medium. A detailed description of the setup and experimental procedure is given in the works Volkov et al. 2014*a*, Volkov et al. 2014*b* and Volkov et al. 2015.

The limited values of gas velocities ($U_g$), as well as speeds ($U_d$) and sizes ($R_d$) of liquid droplets were determined. These values correspond to parameters at which it is reached a complete droplet evaporation in an area of high-temperature combustion products. Also, the phase transformation speeds of corresponding values were calculated. We added the parameter $\Delta R$ under consideration. It characterizes the relative decrease in droplet size after it traverses a distance of 1 m in a flow of high-temperature combustion products. Several regimes of droplet motion in gas flow were identified under conditions of intensive vaporization and the dependences allowing to predict these regimes were obtained.

It was defined that to preserve the conditions of initial motion trajectories of liquid droplets in a channel of high-temperature gases with corresponding $U_g$, it is necessary to make a provision of liquid dispersability when the inequality $R_d$>0,16 mm will be realized. At the same time it was found that about 85% of the droplets evaporated, and the droplets with sizes $R_d$<0,175 mm evaporated completely when water droplets with characteristic dimensions of 0,175<$R_d$<0,275 mm pass the distance of 1 m through the high-temperature gas flow. The conducted experiments illustrated that droplets with initial sizes 0,16<$R_d$<0,175 mm were not “taking away” by gases and evaporated almost completely.

We defined the ranges of the influence of motion velocities of gas and droplet flows on its evaporation characteristics. It was shown that the values of parameter $\Delta R$ decrease by 20-25 % upon the average with increasing the initial speeds of droplet flow within the range 0,5-3 m/s. The limited velocities of droplet flow (for $U_g$≈1,5 m/s) were determined when the conditions of complete deceleration and following turn of droplets of atomized liquid were reached. It was identified that the next values are the limited initial speeds of droplets when high-temperature gases “took away” them under considered conditions: $U_d^{lim}$=0,25 m/s at $R_d$=0,04÷0,09 mm; $U_d^{lim}$=0,35 m/s at $R_d$=0,09÷0,16 mm; $U_d^{lim}$=0,7 m/s at $R_d$=0,16÷0,23 mm; $U_d^{lim}$=1,05 m/s at $R_d$=0,23÷0,3 mm. Motion trajectories of droplets with sizes $R_d$=0,3÷0,4 mm did not changed mostly in a considered high-temperature gas medium.

We defined from the conducted experimental investigations that the flow of high-temperature gases had a determining influence on vaporization intensity if $U_g$>$U_m$. The dependences $U_d$=$f$($U_g$), $\Delta R$=$f$($R_d$), $\Delta R$=$f$($U_d$) obtained from approximations of experimental data allow predicting the main characteristics of mixing the considered mediums and determining the conditions which are necessary and sufficient for reaching the set values of the required parameters for a big group of applications.

It was also established in experiments that the initial concentration ($\gamma$) of droplets played the determining role in the displacement and evaporation of droplet flow. Thus, the growth of the volume concentration of droplets in the flow leads to slower evaporation in the area of high temperature combustion products. This effect is enhanced with increasing the initial droplet sizes. For example, the values of parameter $\Delta R$ at concentrations $\gamma$ corresponding to $1\cdot10^{-5}$ and $2\cdot10^{-5}$ m$^3$ of droplet/m$^3$ of gas for droplets with sizes $R_d$≈150 μm equal to 0.55 and 0.47, and the parameter $\Delta R$ at the same values of $\gamma$ for droplets with sizes $R_d$≈250 μm is 0.24 and 0.1, correspondingly.

The study was supported by the Russian Science Foundation (project No. 14–39–00003)

**References**

Volkov R.S., Kuznetsov G.V., Strizhak P.A. Analysis of the effect exerted by the initial temperature of atomized water on the integral characteristics of its evaporation during motion through the zone of "hot" gases, J. Eng. Phys. Thermophys., Vol. 87 (2) pp. 450-458 (2014*a*).

Volkov R.S., Kuznetsov G.V., Strizhak P.A. The influence of initial sizes and velocities of water droplets on transfer characteristics at high-temperature gas flow, Int. J. Heat Mass Transfer, Vol. 79 pp. 838-845 (2014*b*).

Volkov R.S., Kuznetsov G.V., Strizhak P.A. Experimental investigation of mixtures and foreign inclusions in water droplets influence on integral characteristics of their evaporation during motion through high-temperature gas area, Int. J. Therm. Sci., Vol. 88 pp. 193-200 (2015).

# Features of the deformation of liquid droplets while moving in a gaseous medium

Roman Volkov, Geniy Kuznetsov and Pavel Strizhak

National Research Tomsk Polytechnic University, Institute of Power Engineering
30, Lenin Avenue, Tomsk, 634050, Russia
romanvolkov@tpu.ru

By the tools of high-speed (up to $6 \cdot 10^5$ frames per second) video recording and cross-correlation recording complex, it was performed a cycle of experimental investigations of liquid droplet evaporation while their motion in a gaseous medium. For the first time, we identified two typical regimes of droplet deformation and defined the ranges of influence of motion speeds and droplet sizes, liquid properties (viscosity, surface-tension) and temperature of gas medium ($T_g$) and water droplets ($T_w$) on studying processes (under various heat exchange conditions). Characteristic times ($\tau_d$) and durations ($l_d$) of "deformation cycles" were determined. Maximum rangeabilities of droplet sizes were established while deformation. We completed dimensionless processing of the results of experiments using the similarity criteria of Re and We.

The experimental setup described in detail in Volkov et al. 2014 and Volkov et al. 2015*b* was used in investigating the liquid droplet deformation. In the experiments the following parameters were varied: the size (2-6 mm) and the initial droplet velocity (1-5 m/s), the initial liquid temperature (278-353 C) and the gas medium (283-800 K). We used several typical liquids with different properties: distilled water, ethyl hydroxide, kerosene.

It was determined that the droplet motion process was a fixed sequence of "deformation cycles" characterizing by the repetition of their shapes. We identified two deformation regimes – "oscillative" and "vertical". Typical droplet shapes typical to each deformation regime were determined. It was revealed that periods ($\tau_d$) and durations ($l_d$) of "deformation cycles" for the second regime is more by 15-20 % upon the average than for the first one.

While analyzing the changes in the droplet shapes within each "deformation cycle", we defined the law consisting of differences in time periods of transition from spherical to ellipsoidal shapes (and vice versa). At the same time, the periods of transition from spherical to ellipsoidal shapes higher than the times of reverse transitions by 18-30%.

It was settled that the main characteristics (times, durations and amplitudes) of "deformation cycles" of droplets are quite significantly changed while their motion through gas medium. This is due to increase of droplet speeds at their gravity sedimentation.

We defined that that with increasing the initial droplet sizes, times of "deformation cycles'' growths nonlinearly. At increasing the initial speeds of the droplets, on the contrary, there was some reduction in the relevant times.

While investigations the influence of liquid properties in characteristics of "deformation cycles" was analyzed. Thus, it was determined if close values of density and viscosity of considered liquids (differences are 4–7 %) that with increasing values of the surface tension ($\sigma$), there was a decrease of characteristic times of "deformation cycles". The parameter $\sigma$ for water exceeds the values of $\sigma$ for kerosene and ethyl hydroxide by two-three times. As a consequence, the periods $\tau_d$ in experiments with water are significantly shorter than values of $\tau_d$ for droplets of spirit and kerosene under identical conditions.

We estimated the influence of temperatures $T_w$ and $T_g$ on characteristics of considered deformation processes. Conducted experiments allowed defining that temperature gradient at the "liquid – gas" boundary has an influence on deformation characteristics of water droplets, while their motion in a gas medium, which is not significantly less than droplet speeds and sizes. This is due to the intensification of phase transformations and formation of a vapor layer around the droplets. Whereby, the determining effect of $T_w$ and $T_g$ on deformation characteristics was established for two revealed regimes of deformation (Volkov et al. 2015*a*).

Obtained results scale up the modern ideas in processes of liquid droplet motion through gas mediums and can be used for developing such technologies as water cooling in the working area of cooling towers and high-temperature water purification at power engineering facilities, defrosting the granular mediums by gas-vapor-liquid flows, purification of drossed surfaces of power equipment by gas-vapor-liquid mixtures, polydisperse vapor-droplet fire extinguishing.

The study was supported by the Russian Science Foundation (project No. 14–39–00003)

**References**

Volkov R.S., Kuznetsov G.V., Strizhak P.A. Water droplet deformation in gas stream: Impact of temperature difference between liquid and gas, Int. J. Heat Mass Transfer, Vol. 85 pp. 1-11 (2015*a*).

Volkov R.S., Vysokomornaya O.V., Kuznetsov G.V., Strizhak P.A. Experimental determination of times, amplitudes, and lengths of cycles of water droplet deformation in air, Tech. Phys. Lett., Vol. 41 (2) pp. 128–131 (2015*b*).

Volkov R.S., Zhdanova A.O., Vysokomornaya O.V., Kuznetsov G.V., Strizhak P.A. Mechanism of Liquid Drop Deformation in Subsonic Motion in a Gaseous Medium, J. Eng. Phys. Thermophys., Vol. 87 (6) pp. 1351-1361 (2014).

# Experimental investigation of droplet evaporation on a heated solid surface

A. Semenov[1,2], D. Zaitsev[1], E. Gatapova[1]

[1] Institute of Thermophysics SB RAS, 1, Lavrentiev Ave, 630090, Novosibirsk, Russia
[2]Novosibirsk State University, 2, Pirogova str, 630090, Novosibirsk, Russia
E-mail: Semenov.itp@gmail.com

The process of liquid drop evaporation, which takes place in a variety of technological systems in power engineering, medicine, chemical and other industries, has been actively investigated in the last decade [1, 2].

The goal of the present experiment is to study evaporation of a liquid drop into the open atmosphere. We use four different surfaces: silicon wafer, glass with Teflon spin coating (contact angle hysteresis, CAH= 122.5°-112.7°=9.8°), glass with Teflon spray coating (CAH=119.9°-90.6°=29.3°) and textured stainless steel with roughness of about 5 μm. Distilled deionized nano-filtered water was used as the working liquid. Initial drop volume $V_0$ was varied from 1 to 100 μl. The substrate temperature $T_s$ was varied from 55±1 to 85±1 ºC. The drop shape is visualized from the top with the help of a 5 Mpix CCD camera, and from the side with the help of a high accuracy shadow technique with resolution of up to 0.5 μm/pix. The images from the side are processed in the Drop Shape Analysis software by KRÜSS.

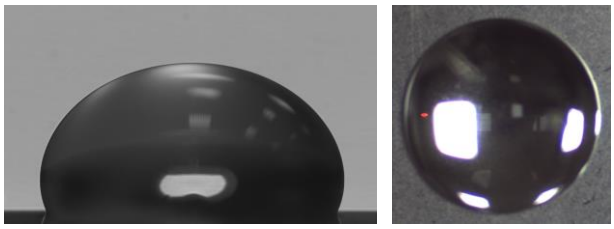

**Figure 1:** Visualization of drop from side and from top on Spray Teflon substrate, V=88.4 μl, $T_s$=65±1.

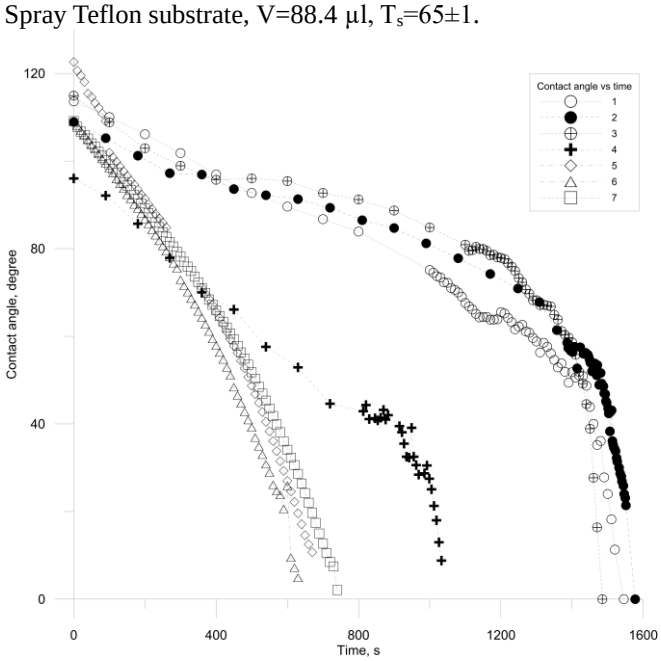


**Figure 2:** CA vs time for different substrates. 1-3 Spray Teflon (3 runs), 4 – Spin Teflon, 5-7 Stainless steel (3 runs). $T_s$=65±1 ºC.

Dependences of CA on evaporation time are shown in Fig. 2 for three different substrates. The initial drop volume was 100 μl. In the case of textured stainless steel substrate, CA is steadily decreasing because droplet contact line is pinned. Evaporation on the substrates with low and medium CAH (Spin Teflon and Spray Teflon coating) occurs with moving contact line. Figure 3 presents data on the specific evaporation rate (mass loss by evaporation per unit time per unit surface area) versus CA. On textured stainless steel substrate, the dependence is almost linear, but on Spin Teflon and Spray Teflon substrates the evaporation rate is increasing more sharply with decreasing CA, especially for small CA (at the end of drop life time).

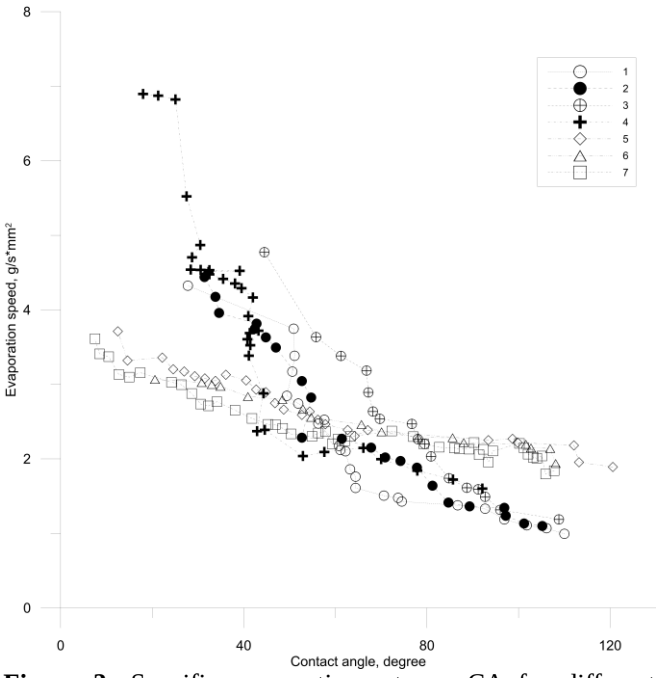


**Figure 3:** Specific evaporation rate vs CA for different substrates. See legend in Fig. 2.

**Acknowledgment**

The study was supported by a grant from the Russian Science Foundation (project Nr. 14-19-01755).

**References**

[1] B. Sobac and D. Brutin, Langmuir, 2011, Vol. 27, P. 14999-15007.
[2] E.Ya. Gatapova, A.A. Semenov, D.V. Zaitsev, and O.A. Kabov, Colloids and Surfaces A: Physicochemical and Engng Aspects, 2014, Vol. 441, P. 776–785.

# Flow patterns inside an evaporating water sessile droplet

Chafea Bouchenna[1,2a], Mebrouk Ait Saada[1b], Salah Chikh[1c], Lounès Tadrist[2d]

[1]USTHB, Faculty of Mechanical and Process Engineering, LTPMP, Alger 16111, Algeria
[2]Aix-Marseille Université, CNRS, Laboratoire IUSTI, UMR 7343, 13453 Marseille, France
[a]bouchennachafea@hotmail.fr, [b]m_aitsaada@yahoo.fr, [c]salahchikh@yahoo.fr, [d]lounes.tadrist@uni-amu.fr

Evaporation of droplets on substrates is a phenomena encountered in different applications of biochemical assays, thin film coating, spray cooling and microelectronics. It is a complex physical problem which involves fluid flow, heat and mass transfer in presence of three interfaces and a contact line. In particular, the internal flow of the evaporating sessile drops is induced by the effects of non-uniform evaporation flux and tension gradient due to temperature variation along the liquid-gas interface as well as the effect of thermal buoyancy in the liquid.

Xu and Luo [1] showed the existence of the thermo-capillary flow by using fluorescent nanoparticles. Ristenpart et al. [2] demonstrated theoretically and experimentally that thermo-capillary flow depends sensitively on the ratio of thermal conductivities of the liquid and substrate. The numerical simulations of Barash et al. [3] allowed identifying a sequence of early dynamical stages of the thermo-capillary convection in the drop, containing an array of near-surface cells which then transforms to the state with three bulk cells. Brutin et al. [4] used the infrared visualization technique and showed three evaporation steps: first a warm-up phase, second a principal phase of evaporation with thermal-convective instabilities, and finally a phase of film evaporation. Lu et al. [5] developed a numerical model and showed that the internal flow pattern changes during evaporation and Bénard-Marangoni instabilities eventually occur for a small droplet.

The present work studies the convective flow inside an evaporating water drop on substrates of different natures and in heated or non-heated cases. A numerical model is developed by taking into account (1) the radial flow induced by the strong liquid loss at the contact line, (2) the thermo-capillary flow resulting from the surface tension gradient at the drop surface, and (3) the flow induced by the thermal buoyancy due to variation of liquid density with temperature. The objective is to analyze the flow pattern resulting from the competition of these effects. The description of the different flow patterns is deduced partly from the temperature profile at the drop surface, which is determined as a function of three controlling parameters: the relative humidity of the surrounding air, the wall temperature and the thermo-physical properties of the substrate.

Results show that the wall temperature of the heated substrate can introduce multi-cellular pattern in the thermo-capillary flow for the contact angles from 11° to 20°. The substrate thermal conductivity can reverse the thermo-capillary flow direction at low contact angles (≤ 11°). Figure 1 represents flow patterns during evaporation on an isothermal solid surface at 40° and for two values of the air relative humidity. Results show that the beginning of each flow structure phase depends on the air relative humidity (Ha). For Ha = 0%, the appearance of the 3-cell structure is at the evaporation step where the ratio of the height to the contact radius of the drop h / R is equal to 0.26, whereas it is delayed at h / R = 0.17 for Ha = 40%.

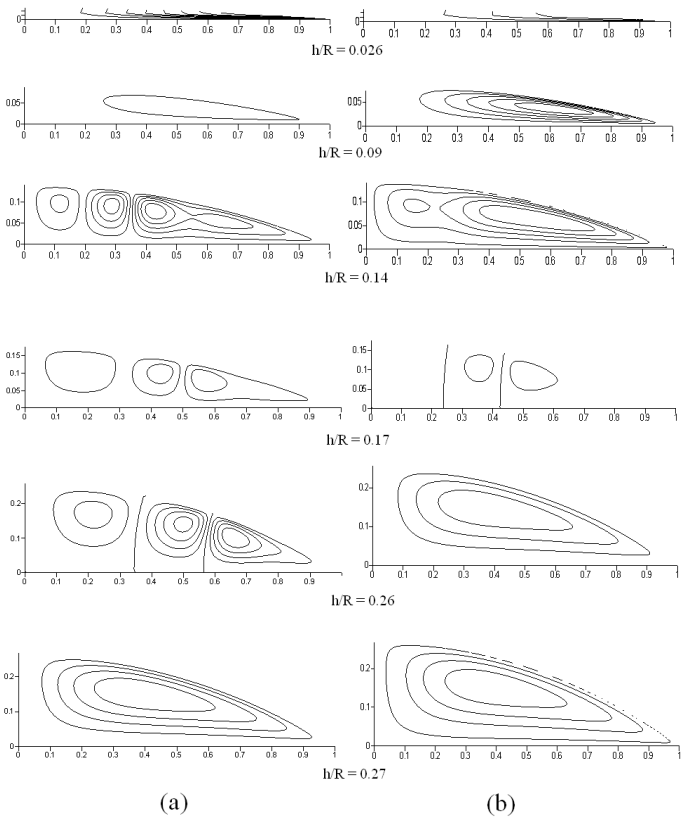


**Figure 1:** Streamlines and flow patterns for an evaporating sessile drop on an isothermal solid surface at 40°C: (a) Ha = 0% and (b) Ha = 40%.

**References**

[1] Xu, X.,Luo, J., (2007), Marangoni flow in an evaporating water droplet, *Appl. Phys. Lett.* 91, 124102.

[2] Ristenpart, W.D., Kim, P.G., Domingues, C., Wan, J., Stone, H.A., (2007),Influence of substrate conductivity on circulation reversal in evaporating drops, *Phys. Rev. Lett.*99, 234502.

[3] Barash, L. Yu., Bigioni, T. P., Vinokur, V. M., Shchur, L. N., (2009), Evaporation and fluid dynamics of a sessile drop of capillary size, *Phys. Rev.* E 79, 046301.

[4] Brutin, D., Sobac, B., Rigollet, F., Le Niliot, C., (2011), Infrared visualization of thermal motion inside a sessile drop deposited onto a heated surface, *Experimental Thermal and Fluid Science* 35, 521–530.

[5] Lu, G., Duan, Y., Wang, X., Lee, D., (2011),Internal flow in evaporating droplet on heated solid surface, *Int. J. Heat Mass Transfer* 54, 4437-4447.

# The liquid bridge: A paradigm for thermocapillary flow

Kuhlmann Hendrik C.

TU Wien, Institute of Fluid Mechnics and Heat Transfer,
Getreidemarkt 9, Vienna, 1060, Austria
Hendrik.kuhlmann@tuwien.ac.at

Surface-tension-driven flows have been puzzling scientists since the early investigations of Thomson (1855), Marangoni (1871), and others. About 100 years later renewed interest in the subject was stimulated by Scriven (1960). At about the same time the zone-melting technique of crystal growth was introduced. Owing to the thermocapillary effect a vigorous flow arises from cold to hot regions of the free surface. Such flow was computed numerically in a simplified cylindrical geometry by Chang and Wilcox (1975). Not much later the thermocapillary mechanism was experimentally confirmed by Schwabe et al. (1978) in the reduced model of a half-zone.

Since that time the half-zone problem, or thermocapillary liquid bridge, has been investigated quite extensively. To some extent the research has been driven by controversies. Initially, there was a debate about the existence of thermocapillary versus buoyant flow in millimetric systems. As soon as oscillatory thermocapillary flows were confirmed to exist different hypotheses regarding the mechanism of oscillation were discussed. A more recent controversy concerns the role of inertia in the transport of small particles suspended in the thermocapillary liquid bridge.

An overview of the evolution of the half-zone is given. Moreover, two current trends are addressed. One is the quest for an improved characterization of the system by controlling of the ambient gas-phase conditions. To that end several groups have joined their efforts in the JEREMI experiment. Shielding the liquid bridge from undesired perturbations in the ambient atmosphere by means of a concentric tube enables a certain control of the liquid flow by imposing a defined gas flow in the annular gap, but also introduced new instabilities. A contemporary review was given by Shevtsova et al. (2014).

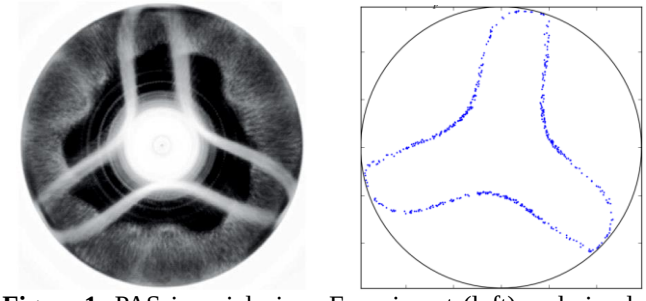

**Figure 1:** PAS in axial view. Experiment (left) and simulation (right).

The other problem under current investigation concerns the motion of suspended finite-size particles which Schwabe (1996) found to rapidly form particle accumulation structures (PAS, Fig. 1). Curiously enough, the clustering was observed to be fastest for particles whose density is matched to the mean density of the liquid (Schwabe 2007). This is a hint that particle inertia, the natural candidate for clustering, is not the primary reason for PAS. A closer consideration of the mechanism of PAS also reveals a fresh view on the flow structure of hydrothermal waves (Mukin and Kuhlmann, 2013).

**Acknowledgments**
The author gratefully acknowledges the collaboration with many coworkers and material support through DFG, DLR, FFG, ESA, JAXA, and TU Wien.

**References**

Chang C. E. & Wilcox, W. R. Inhomogeneities due to thermocapillary flow in floating zone melting J. Crystal Growth **28**, 8-12 (1975).

Marangoni C., Ueber die Ausbreitung der Tropfen einer Flüssigkeit auf der Oberfläche einer anderen, Ann. Phys. Chem. **143**, 337-354 (1871).

Schwabe D., Scharmann A., Preisser F. and Oeder, F., Experiments on surface tension driven flow in floating zone melting, J. Crystal Growth **43**, 305-312 (1978).

Schwabe D., Hintz P. and Frank S., New Features of thermocapillary convection in floating zones revealed by tracer particle accumulation structures (PAS), Microgravity Sci. Technol. **9**, 163-168 (1996).

Schwabe D., Mizev A. I., Udhayasankar M. and Tanaka S., Formation of dynamic particle accumulation structures in oscillatory thermocapillary flow in liquid bridges, Phys. Fluids **19**, 072102 (2007).

Scriven L. E., Dynamics of a fluid interface, Chem. Eng. Sci. **12**, 98-108 (1960).

Shevtsova V., Gaponenko Y., Kuhlmann H. C., Lappa M., Lukasser M., Matsumoto S., Mialdun A., Montanero J. M., Nishino K. and Ueno I., The JEREMI-Project on thermocapillary convection in liquid bridges. Part B: Overview on impact of co-axial gas flow, Fluid Dyn. Mat. Proc. **10**, 197-240 (2014).

Thomson J., On certain curious motions observable at the surfaces of wine and other alcoholic liquors, London Edinburgh Dublin Phil. Mag. J. Sci. **10**, 330-333 (1855).

Mukin R. V. and Kuhlmann H. C., Topology of hydrothermal waves in liquid bridges and dissipative structures of transported particles, Phys. Rev. E **88**, 053016 (2013).

# Thermocapillary flows and their stability in pure fluids and binary mixtures

Ilya I. Ryzhkov

Institute of Computational Modelling SB RAS
Akademgorodok 50-44, 660036 Krasnoyarsk, Russia
rii@icm.krasn.ru

The dynamics of fluid systems with interfaces remains a challenging problem of modern physics. In such systems, the variation of surface tension due to thermal or compositional gradient along the interface can cause convective flows in the bulk fluid. This effect is especially important in weightlessness, where buoyancy convection is absent and thermocapillary forces often constitute the sole cause of motion. Thermocapillary flows play an important role in many natural and technological processes, such as propagation of liquid jets, motion of thin liquid films, evolution of ocean waves, etc.

Thermocapillary effect essentially affects the process of crystal growth by *floating-zone method* (Kuhlmann, 1999). To study the motion of melt in the full floating zone between the feed material and crystal, the so-called *half-zone* or *liquid bridge model* is often used. In this model, the fluid is placed between two rods (hot and cold), see Fig. 1. Liquid bridge has become a paradigm of a complex dynamical system and is often used for investigating the thermocapillary effect. In the liquid bridge, the surface tension gradient due to temperature variations along the free surface drives thermocapillary flow from hot to cold rod near the free surface and in the opposite direction at the central axis (Fig. 1). This flow is stationary for small temperature differences ΔT between the rods. When ΔT reaches some critical value, the instability sets in as a standing or axially running hydrothermal wave.

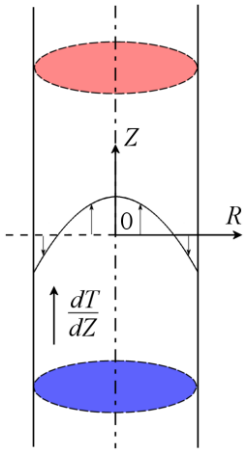


**Figure 1:** Liquid column

Linear stability analysis of stationary thermocapillary flow in an infinite liquid bridge was first performed by Xu & Davis (1984). The free surface of the liquid was assumed to be non-deformable. The authors determined the critical Marangoni number *Ma* (which is proportional to ΔT) for the appearance of instability. It was shown that for small Prandtl numbers, the critical mode has the azimuthal wave number *m=1*. The instability develops in the form of two waves traveling in opposite circumferential directions *along* the basic flow on the interface (from hot to cold plate). For large Pr numbers, the critical mode was found to be *m=0*.

The linear stability analysis of steady thermocapillary flow in an infinite liquid bridge was revisited by Ryzhkov (2011). The previous results of Xu & Davis (1984) for the mode *m=1* were confirmed in the range of low Prandtl number. However, for large Pr, the true stability boundary on the plane (*Pr*, *Ma*) was found to be below the previously reported one

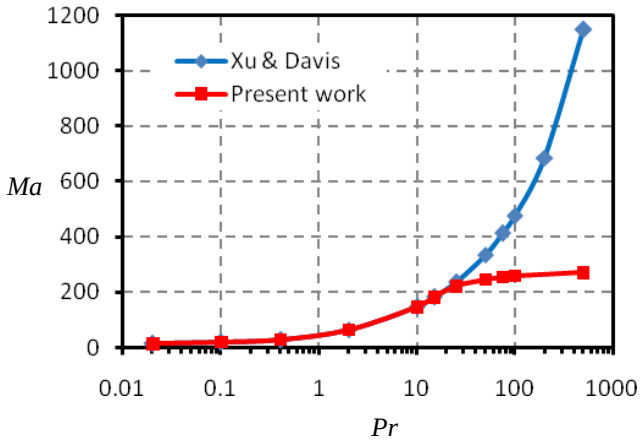


**Figure 2:** The dependence of critical Marangoni number on Pr.

(Fig. 2). It is associated with a new instability mode in the form of two waves traveling in opposite circumferential directions *opposite* to the basic flow on the interface (from cold to hot plate). A comparison with the experimental results (Schwabe 2005) showed that the corrected stability boundary was closer to the experimental values. In contrast to the work of Xu & Davis (1984), Ryzhkov (2011) showed that the mode *m=1* is always critical and there is no transition to *m=0* in with increasing the Prandtl number.

Thermocapillary instability in long liquid bridges was recently investigated experimentally in microgravity conditions on the International Space Station by Yano et al (2015). The experiments confirmed the existence of new instability mode predicted theoretically by Ryzhkov (2011). This mode was observed in a liquid bridge, which height was two times larger than its diameter. The liquid was 5 cSt silicon oil (Pr=67). A detailed comparison of experimental data with the results of linear stability analysis was performed.

The flows driven by interfacial tension can appear not only in liquid-gas, but also in liquid-liquid systems. The systematic studies of interfacial convection in multilayer systems of pure fluids were summarized by Nepomnyashchy et al (2006). Multilayer systems can be also formed by binary or multicomponent fluids, which exhibit phase separation when their composition or temperature are changing. In particular, phase diagrams for many binary and ternary liquids contain both one–phase and two–phase regions. If different phases of the same mixture have different densities, then this mixture forms a two–layer system in the gravity field with less dense phase in the upper layer and more dense phase in the lower layer. With increasing temperature, the interfacial tension between the phases typically decreases and becomes zero at some critical temperature. At this point, the difference between phases disappear and one-phase liquid is formed.

An example of binary fluid with phase separation provides the mixture of cyclohexane and methanol. Its phase

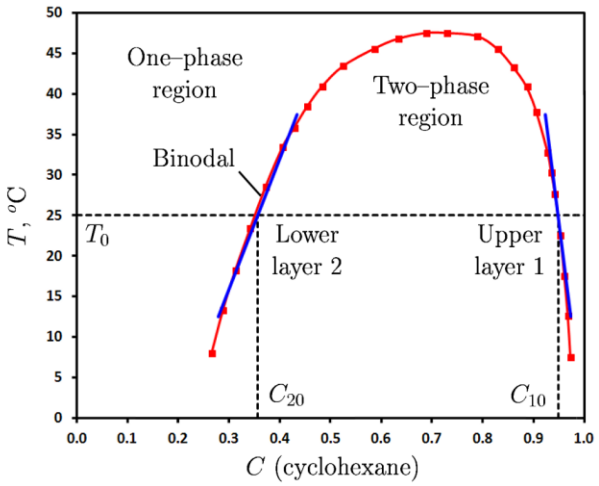


**Figure 3:** Phase diagram of cyclohexane-methanol binary mixture. Blue lines show the linear approximation of the binodal.

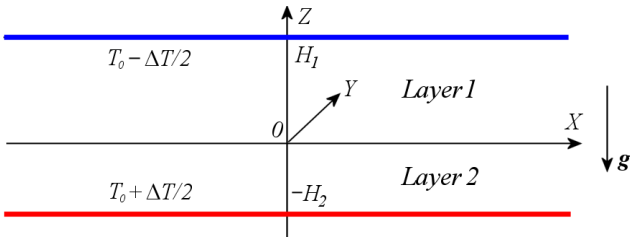


**Figure 4:** Geometry of the two-layer system.

diagram is shown in Fig. 3. The geometry of two-layer system, which is formed by this binary fluid in the two-phase region, is sketched in Fig. 4.

When a temperature gradient is applied to this system, the concentration gradients can form in the layers due to the thermal diffusion (or the Soret effect). This effect relates to mass transfer driven by temperature gradient. Convection in a two–layer system can be induced by buoyancy forces and surface tension forces on the interface. These forces depend on the inhomogeneities of temperature and concentrations of the mixture components. Ryzhkov and Tsarev (2015) studied the stability of mechanical equilibrium in a two–layer system formed by cyclohexane – methanol binary mixture. The temperature difference was applied to the layers by heating and cooling the opposite rigid boundaries.

The values of concentrations on the interface are determined according to the phase diagram and linearly depend on temperature, see Fig. 3. The conservation of mass for the mixture components leads to the dependence of layer thicknesses on the applied temperature difference. The linear stability of mechanical equilibrium with respect to small perturbations is investigated. The main mechanisms of instability are gravitational, thermocapillary (interfacial tension depends on temperature), and phase change (mass transfer through the interface and phase transition heat are taken into account). For the case of monotonic perturbations in the absence of gravity, Ryzhkov and Tsarev (2015) found analytical solution of amplitude equations and constructed the neutral curves describing the dependence of critical temperature difference on the wave number. The general case of monotonic and oscillatory perturbations was investigated numerically taking into account the dependence of layer thicknesses on the applied temperature difference. Different instability mechanisms were analyzed and stability maps in the parameter space were constructed.

The work is supported by the Russian Foundation for Basic Research Grant 15-01-03293.

**References**

Kuhlmann H.C. Thermocapillary Convection in Models of Crystal Growth. Springer, 1999.

Xu J.J. and Davis S.H. Convective thermocapillary instabilities in liquid bridges. Phys. Fluids, V. 27, 1102 (1984).

Schwabe D. Hydrothermal waves n a liquid bridge with aspect ratio near the Rayleigh limit under microgravity. Phys. Fluids, V. 17, 112104 (2005).

Ryzhkov I.I. Thermocapillary instabilities in liquid bridges revisited. Phys. Fluids, V. 23, 082103 (2011).

Yano T., Nishino K., Kawamura H., Ueno I., and Matsumoto S., Instability and associated roll structure of Marangoni convection in high Prandtl number liquid bridge with large aspect ratio. Phys. Fluids, V. 27, 024108 (2015).

Nepomnyashchy A.A., Simanovskii I.B., and Legros J.C. Interfacial convection in multilayer systems. Springer, 2006.

Ryzhkov I.I. and Tsarev S.P. Onset of convection in a two-phase binary mixture with the Soret effect in weightlessness. Phys. Fluids, V. 27, 072103 (2015).

# Rayleigh-Benard, Marangoni and Vibrational Instabilities in Two-Layer Systems with Deformable Interfaces

Tatyana Lyubimova

Computational Fluid Dynamics Laboratory Institute of Continuous Media Mechanics UB RAS
1, Koroleva Str., 614010, Perm, Russia
lubimova@psu.ru

The paper presents the results on the Rayleigh-Benard, Marangoni and vibrational instabilities in two-layer systems of fluids with deformable interfaces. Conventional Boussinesq approximation used in the theory of thermal buoyancy convection is related to the situation where the density differences are small and can be neglected everywhere except for the buoyancy force term. Formally this means that the limit transition $\varepsilon \to 0$ is performed simultaneously with the limit transition $G \to \infty$ ($\varepsilon$ is the Boussinesq parameter and $G$ is the dimensionless measure of gravitational acceleration) such that the product of these parameters $G\varepsilon$ which is the Rayleigh number remains finite. However in this case, as follows from the normal stress balance condition, the interface should be considered as non-deformable. Accounting for the interface deformations in the framework of the conventional Boussinesq approach for thermal buoyancy convection may lead to physically incorrect results.

However for some physical situations, approximation of non-deformable interface is not sufficient. For example, if difference in densities of two fluids $\delta$ is of the same order of magnitude as density inhomogeneities caused by non-isothermality, than at finite values of the Rayleigh number the gravity force is not able to keep the interface planar. In this case the interface deformations can be large enough and have to be taken into account in proper way. Generalized Boussinesq approach allowing correct accounting for the interface deformations for two-layer systems of fluids with close densities was developed by F. Busse (Rasenat et al. 1989) and D. Lyubimov Lobov et al. 1996) who showed that the effect of interface deformations can be included through the term proportional to the product of $Ga\delta$ with the deflection $\zeta$ of the interface from planarity but it is needed to treat the densities of two fluids as equal (i.e. $\delta \to 0$) in the momentum equations.

In (Rasenat et al. 1989) the Busse-Lyubimov model was implemented for the investigation of the onset of thermal buoyancy convection in a two-layer system with deformable interface where all properties of two fluids were similar except for the densities. The case of fluids with different properties was studied in the framework of the same model in (Lobov et al. 1996). It was found that in a wide range of parameters long-wave monotonic instability mode related to the interface deformations is most dangerous (this mode was not found in (Rasenat et al. 1989) since it does not exist in the case of model system in that paper).

Both in (Rasenat et al. 1989) and in (Lobov et al. 1996) the case of the external boundaries of perfect thermal conductivities was studied. In (Lyubimova et al. 2007) this problem was studied for the external boundaries with constant heat flux. It was found that the interaction of deformational long-wave instability mode with the long-wave instability mode existing in the case of constant heat flux at the boundary results in the existence of the oscillatory long-wave instability mode.

The influence of thermocapillary effect on the onset of Rayleigh–Benard convection in a two-layer system with a deformable interface with the imposed constant heat flux at the external boundaries was studied in (Lyubimova et al. 2015). Stabilization of conductive state to oscillatory perturbations with the increase of Marangoni number was observed such that at strong enough thermocapillary effect the oscillatory instability mode degenerates.

Vibrations are found to be very simple and powerful low-energy method to control the behaviour of inhomogeneous hydrodynamical systems. The effect of vibrations depends on their amplitude and frequency and on their orientations to the temperature gradient and to the interface. In the present paper the possibilities to control the onset and development of the Rayleigh-Benard convection in a system of two superposed horizontal fluid layers with deformable interface applying vertical vibrations and the interaction of thermocapillary and vibrational instability modes in a two-layer system of immiscible fluids subjected to the horizontal vibrations are analyzed.

The work was supported by Russian Science Foundation (grant 14-21-00090).

**References**

Rasenat S., Busse F.H., Rehberg I., A theoretical and experimental study of double-layer convection, J. Fluid Mech., Vol. 199, pp. 519-540 (1989).

Lobov N.I., Lyubimov D.V., Lyubimova T.P., Convective instability of a system of horizontal layers of inmiscible liquids with a deformable interfaces, Fluid Dynamics, Vol. 31 (2), pp. 186-192 (1996).

Lyubimova T. P., Parshakova Y. N., Stability of equilibrium of a double-layer system with a deformable interface and a prescribed heat flux on the external boundaries, Fluid Dynamics, Vol. 42, pp. 695–703 (2007).

Lyubimova T.P., Lyubimov D.V., Parshakova Y.N., Implications of the Marangoni effect on the onset of Rayleigh-Benard convection in a two-layer system with a deformable interface, European Physical Journal - Special Topics, Vol. 224 (2), pp. 249-259 (2015).

# Non-isothermal interfacial flows: more interest and intrigue

Omar K. Matar

Imperial College London, Department of Chemical Engineering
Prince Consort Road, London, SW7 2AZ, UK
o.matar@imperial.ac.uk

Interfacial flows involving non-isothermal effects and phase change are a constant source of intriguing phenomena, many of which remain poorly understood. Here, we present examples of novel phenomena associated with interfacial flows in the presence of thermocapillarity, buoyancy, and viscous, inertial, surfactant-induced, and phase change effects. We consider the three-dimensional (3D) dynamics of a gas bubble in a non-isothermal so-called "self-rewetting" fluid, whose surface tension exhibits a parabolic dependence on temperature. We show that the bubble ascent, retardation (and potential arrest), descent, and lateral migration, have no analogues in simple, "linear" fluids. We also show that the spreading of sessile drops of self-rewetting fluids on heated substrates can exhibit features associated with "super-spreading" phenomena, usually driven by surfactants or electric fields. Finally, we consider the 3D evaporation of non-axisymmetric drops of pure fluids and binary mixtures. We show that their life-time and bulk flow characteristics, including roll and hydrothermal wave-formation, depend on their size and shape, and the substrate non-uniform wettability.

In Fig. 1, we show a schematic of a gas bubble rising under the action of buoyancy in a square channel (see Fig. 1a, left) containing a so-called “self-rewetting” fluid. The surface tension of this fluid exhibits a parabolic dependence on temperature with a well-defined minimum (see Fig. 1a, right). A constant, positive temperature gradient is imposed in the vertical direction. In Fig. 1b, we demonstrate via three-dimensional numerical simulations that, for the self-rewetting case, the bubble exhibits flow reversal; this is in contrast to the isothermal case or for “linear” fluids, that is, for a linearly-decreasing dependence of surface tension on temperature. This behavior is related to the delicate interplay between buoyancy, Marangoni flow, and the self-rewetting nature of the fluid surrounding the bubble.

We have also studied the thermocapillary-driven spreading of a self-rewetting droplet on a non-uniformly heated substrate using lubrication theory. An interface equation is derived that accounts for capillarity and thermocapillarity, and the contact line singularity is relieved by using a slip model and a Cox-Voinov relation in which contact angles vary depending on the substrate wettability, which, in turn, is linked to the local temperature. For self-rewetting fluid cases wherein the surface tension minima are located within the droplet, the thermocapillary stresses drive rapid spreading away from the minima. The spreading characteristics resemble those associated with the “superspreading” of droplets on hydrophobic substrates, more often associated with the the presence of surfactant “superspreader” molecules. The mechanism underlying these phenomena is shown schematically in Fig. 2.

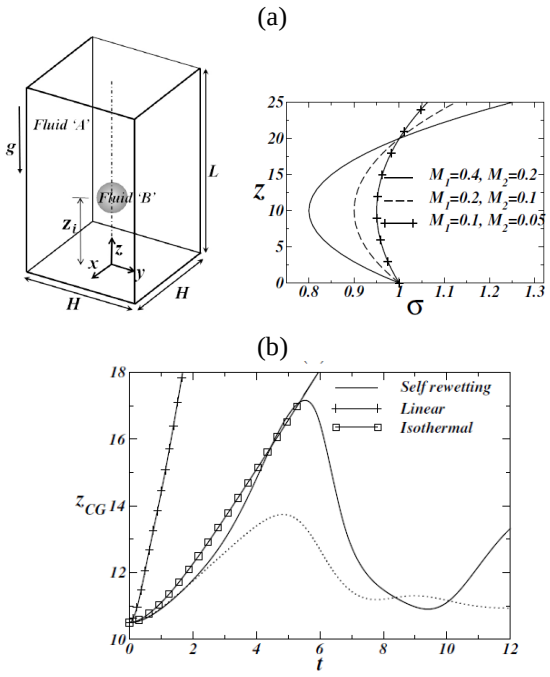


**Figure 1:** (a, left) Schematic diagram showing the initial configuration of a bubble (fluid `B') rising inside a medium (fluid `A') under the action of buoyancy. The bubble is placed at $z = z_i$ initially. The acceleration due to gravity, g acts in the negative $z$ direction. A linear temperature variation is imposed at the walls in the vertical direction with a constant gradient, γ. (a, right) the variation of the surface tension with $z$ for the self-rewetting fluid considered in this study; $M_1$ and $M_2$ are parameters that control the depth of the surface tension minimum. (b) Temporal variation of the centre of gravity for a bubble at very small Bond numbers. The solid and dotted lines indicate the three-dimensional and axisymmetric results, respectively (Premlata *et al.*, 2016)

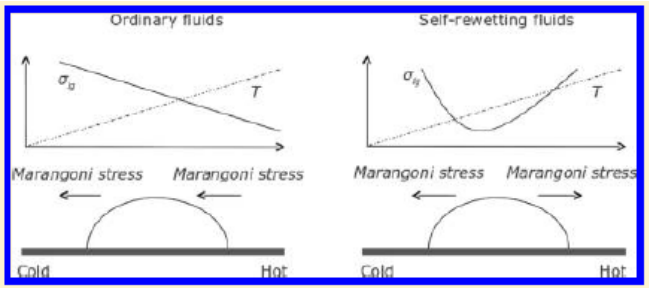


**Figure 2** The mechanism of thermally-enhanced spreading of “self-rewetting” fluids (from Karapetsas *et al*. 2014).

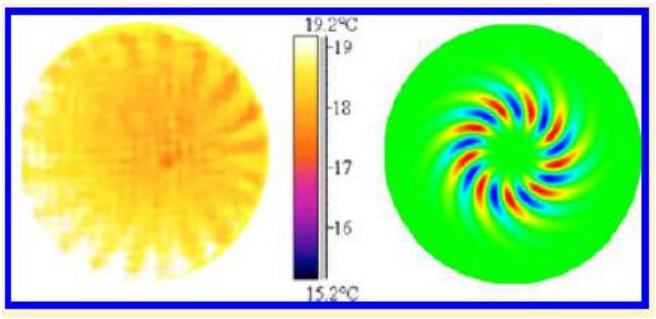


**Figure 3:** Hydrothermal waves observed in evaporating sessile drops of methanol on silicon substrates, left, obtained from IR thermography; predictions from a linear stability analysis carried out in the quasi-steady-state approximation, right (reproduced from Karapetsas *et al.*, 2012).

Next, we consider the dynamics of sessile drops. Recent experiments on these systems have revealed the spontaneous formation of rolls and hydrothermal waves; the latter were first discovered in the case of thin liquid layers with an imposed, uniform temperature gradient. In the case of an evaporating droplet, these gradients arise naturally due to evaporation and are not uniform but spatially- and temporally-varying. We show through the use of a linear stability analysis of an axisymmetric base state exhibiting roll formation, carried out in the quasi-steady-state approximation, that a transition to hydrothermal waves is possible. Our theoretical results are in qualitative agreement with experimental trends, as shown in Fig. 3.

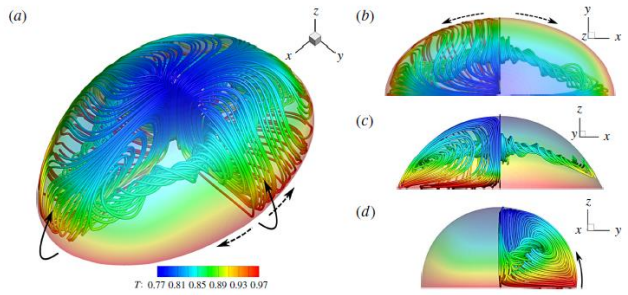


**Figure 4:** Structure of the three-dimensional flow within a non-circular sessile drop having an elliptic contact area. Here, (a)-(d) depict the plan, top, front, and side-views, respectively (from Saenz *et al.*, 2015).

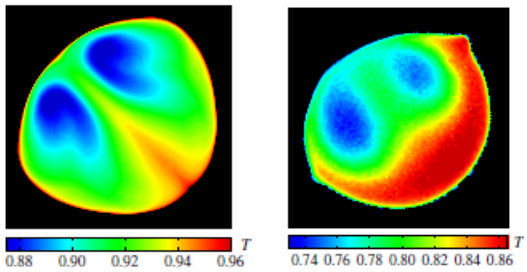


**Figure 5:** Interfacial temperature obtained from simulations (a) and infra-red imaging (b) showing the formation of counter-rotating vortices (from Saenz *et al.*2015).

Although the dynamics of evaporating drops has received considerable attention in the literature, the large majority of the studies involving these systems have focused on circular drops. We use three-dimensional direct numerical simulations to study the evaporation dynamics of non-circular drops. In Fig. 4, we show the rich flow structure that accompanies the evaporation process, while in Fig. 5, the emergence of counter-rotating vortices is clearly depicted with very good agreement between the numerical predictions and experimental measurements. For the case of three-dimensional drops evaporating with a moving contact line, we have studied the constant-angle (CA) and constant-radius (CR) modes. Our numerical results demonstrate that increasing the substrate heating results in a more rapid rise in the evaporation rate associated with the CR mode. Otherwise stated, the higher the temperature the larger the difference between the lifetimes of an evaporating drop in the CA mode in comparison to that evaporating in the CR mode.

In the presentation to be given at the Symposium, we will also discuss a number of other topics. For instance, we will show that evaporating self-rewetting droplets on uniformly-heated walls have spreading exponents that display an intriguing non-monotonic dependence on substrate temperature, as well as fingering instabilities near the contact line. We will also show how surfactants modify the evaporative flux in nano-particulate droplets of simple fluids, and influence their wall deposition patterns.

## Acknowledgements

OKM would like to express his profound thanks to Prof. Khellil Sefiane, Dr Prashant Valluri, and Dr Pedro Saenz (all from the University of Edinburgh – PS is now at MIT), Dr George Karapetsas (University of Thessaly), Prof. Kirti Sahu (ITT Hyderabad), and Prof. Richard Craster (Imperial College London) for their contribution to the work cited in this extended abstract. Thanks also to the Engineering and Physical Sciences Research Council, UK, for their funding through several grants (EP/J010502/1, EP/E056466, EP/E046029/1, and EP/L020564/1) including the MEMPHIS Programme Grant (EP/K003976/1).

## References

George Karapetsas, Omar K. Matar, Prashant Valluri and Khellil Sefiane, Convective rolls and hydrothermal waves in evaporating sessile drops, Langmuir, Vol. 28, pp. 11433-11439 (2012).

George Karapetsas, Kirti C. Sahu, Khellil Sefiane, and Omar K. Matar, Thermocapillary-driven motion of a sessile drop: effect of non-monotonic dependence of surface tension on temperature, Langmuir, Vol. 30, pp. 4310-4321 (2014).

A. R. Premlata, Manoj K. Tripathi and Kirti Sahu, George Karapetsas, Khellil Sefiane, Three-dimensionsl non-isothermal bubble rise in self-rewetting fluids, in preparation for submission to J. Fluid Mech.

Pedro J. Saenz, Khellil Sefiane, Jungo Kim, and Omar K. Matar and Prashant Valluri, Evaporation of sessile drops: a three-dimensional approach, J. Fluid Mech., Vol. 772, pp. 705-739 (2015).

# Traveling waves and structures in the Nakoryakov-Ostapenko-Bartashevich model of film flow with phase transitions

Frolovskaya O.A. and Pukhnachev V.V.

Lavrentyev Institute of Hydrodynamics of SD RAS and Novosibirsk State University
Lavrentyev Prospect 15, Novosibirsk, 630090, Russia
E-mail: pukhnachev@gmail.com

A mathematical model describing the motion of a thin layer along a vertical wall with condensation or evaporation was proposed and investigated in works by Nakoryakov, Ostapenko and Bartashevich (2012, 2014, 2015). This model describes planar quasi-stationary flows at small Reynolds number in terms of film thickness $h(x,t)$, which satisfies equation

$$\frac{\partial h}{\partial t}+\frac{\partial}{\partial x}\left[\frac{h^3}{3}\left(1+\alpha\frac{\partial^3 h}{\partial x^3}\right)\right]=\frac{\beta}{h}. \qquad (1)$$

Equation (1) is written in dimensionless variables. Two similarity criteria in equation (1), $\alpha$ and $\beta$, are proportional to surface tension coefficient and difference between the wall temperature and saturation temperature, respectively. In addition, both parameters $\alpha$ and $\beta$ were supposed to be constant. Case $\beta>0$ corresponds the condensation process while case $\beta<0$ corresponds to the evaporation one. Typical values of these parameters are $\alpha=5\cdot10^{-5}$, $|\beta|=1$.

Limiting transition $\alpha\to0$ transforms equation (1) into first-order quasi-linear hyperbolic equation

$$\frac{\partial h}{\partial t}+\frac{1}{3}\frac{\partial h^3}{\partial x}=\frac{\beta}{h}. \qquad (2)$$

In turn, equation (2) can be converted into the classical Hopf equation, $u_t+uu_z=0$, via change of variables

$$x=z+2\int_0^t(t-s)\beta(s)\,ds,\quad h^2(x,t)=u(z,t)+2\int_0^t\beta(s)\,ds.$$

Here it is not assumed that $\beta=const$ (it means that the wall temperature can be an arbitrary function of time but is does not depend on $x$). Different way for integration of equation (2) consists in transition to Lagrange variables. This allows us to reduce equation (2) to an ordinary differential equation and a quadrature.

Solutions of equation (2) with $\beta=const$ in form of combination of space-uniform flows, rarefaction waves and shock waves were constructed in (Nakoryakov et al, 2012, 2014, 2015). Here we present a number of solutions of equations (1) and (2), which describe traveling waves propagating with acceleration or retardation. Simplest example corresponds to the case $\beta=1,\alpha=0$ and has form

$$h=(u_-+2t)^{1/2},\ x<D(t);\ h=(u_++2t)^{1/2},\ x>D(t), \qquad (3)$$

where $u_-$ and $u_+$ are constant, $u_->u_+>0$, and velocity of condensation front $D=2t+(u_-+u_+)/2+O(t^{-1})$ as $t\to\infty$. Cauchy problem for equation (1) was numerically solved with initial data (3) as $t=1$. Its solution demonstrates small oscillation of function $h$ before and behind of discontinuity line in solution of limiting equation (1). Width of transient zone has order $\alpha^{-1/3}$ as $\alpha\to0$.

Let us put $2\beta=-(t+1)^{-2}$. In this case, solution of equation (2) is given by formula $h=(t+1)^{-1/2}(f+1)^{1/2}$, where function $f$ is the positive solution of equation

$$f+(1-W)\ln f=\varsigma,\ \varsigma\in\mathbb{R}, \qquad (4)$$

$W=const$, $\varsigma=x-W\ln(t+1)$. If $0<W<1$, then solution of equation (4) is unique, $f=\varsigma[1+o(1)]$, $\varsigma\to\infty$ and $f\to0$, $\varsigma\to-\infty$. If $W>1$, equation (2) has two solutions, which define for $\varsigma>\varsigma_*$ only, but we can to continue solution of equation (1) for $\varsigma<\varsigma_*$ putting $h=(t+1)^{-1/2}(f_*+1)^{1/2}$. We show as taking into account of capillarity in equation (1) smoothes a weak discontinuity in this solution for small $\alpha$

**References**

V.E. Nakoryakov, V.V. Ostapenko and M.V. Bartashevich, Heat and mass transfer in the liquid film on a vertical wall in roll-wave regime, Int. J. Heat Mass Transfer, Vol. 55 (23-24), pp. 6514-6518 (2012).

V.E. Nakoryakov, V.V. Ostapenko and M.V. Bartashevich, Investigation into rolling waves on the surface of a condensate falling film, Doklady Physics, Vol. 59, No. 2, pp. 94-98 (2014, translation from Doklady Akademii Nauk, 2014, Vol. 454, No. 5, pp. 540-544).

V.E. Nakoryakov, V.V. Ostapenko and M.V. Bartashevich, Rolling waves on the surface of a thin layer of viscous liquid at phase transition, Int. J. Heat Mass Transfer, Vol. 89, pp. 846-855 (2015).

V.V. Pukhnachev and O.A. Frolovskaya, Wave regimes of a film flow at the presence of phase transitions (model by Nakoryakov-Ostapenko-Bartashevich), In: Abstracts of 32th Siberian Thermophysics Seminar, p. 7-8, Novosibirsk, 2015.

# Two Dimensional Thermocapillary Motion of Immiscible Viscous Liquids in Layer

Victor K. Andreev

Department of Differential Equations of Mechanics, Institute of Computational Modeling SB RAS,
Akademgorodok, 50/44, Krasnoyarsk, 660036, Russia
e-mail: andr@icm.krasn.ru

The 2D motion of two immiscible incompressible viscous heat conducting liquids in a flat layer is considered. Four-dimensional Lie's subgroup was used to searching partially invariant solution of governing equations. Such solution has the velocity, pressure and temperature presentations

$$u_{1j} = u_j(y,t)x,\ \ u_{2j} = v_j(y,t),\ \ p_j = h_j(y,t) - f_j(t)\,x^2/2,$$
$$\theta_j = a_j(y,t)x^2 + b_j(y,t),\ \ h_{jy} = \eta_j v_{jyy} - v_{yt} - v_j v_{jy} - g,$$
$$v_{jy} = -u_j,$$

where $\eta_j$ is the kinematic viscosity of liquid ( $j = 1,2$ ), $g$ is the acceleration of gravity. It is assumed that motion arises under act of thermocapillary forces from state of rest and surface tension linearly depends on temperature, $\sigma = \sigma_0 - \kappa\theta_1$. Under these assumptions the equations of motion and heat transfer can be reduced to the coupled initial boundary value problem for unknowns $u_j(y,t)$, $a_j(y,t)$. This problem is inverse one since the functions $f_j(t)$ must be determined together with functions $u_j(y,t)$ and $a_j(y,t)$. As concerning to the functions $b_j(y,t)$, then the problem of its finding is separated. The following results are obtained for creeping motion when Marangoni and capillary numbers are small:

1) exact stationary solution $u_j^s(y)$, $a_j^s(y)$ and $f_j^s$ are found;

2) obtained a priori estimates of solution prove the convergence to stationary one. More exactly, the following estimates are valid:

$$\left|u_j(y,t) - u_j^s(y)\right| \le U_j e^{-\gamma t},\quad \left|a_j(y,t) - a_j^s(y)\right| \le A_j e^{-\gamma t},$$
$$\left|f_j(t) - f_j^s\right| \le F_j e^{-\gamma t} \qquad (1)$$

with positive constants $U_j$, $A_j$, $F_j$, $\gamma$ depending physical liquids properties and thickness of layer;

3) solution of the non-stationary problem in the form of final analytical formulas in the transforms of Laplace representation was found and some numerical results of velocities and temperatures behaviour in layers are shown.

For example, Figures 1, 2 show the horizontal dimensionless velocities $\bar{u}_j(\xi,\tau)$, $j = 1,2$, $\xi = y/l$, $\tau = \eta_1 t/l^2$. Liquid layers have the same thickness $l$ = 1 mm, the first liquid is a water and the second liquid is a air. The numerical results are presented in Figure 2 are good agreement with the estimates (1).

Some results were obtained for non-linear problem by using asymptotical methods. In that case the more general energy condition on interface $\Gamma = \{y = 0\}$ was used

$$\left[k\frac{\partial\theta}{\partial y}\right] = \kappa\theta_1 \mathrm{div}_\Gamma \mathbf{u}_1 \qquad (2)$$

where symbol [$f$] denotes the difference between $f_1$ and $f_2$ on interface. It means the jump of the heat flux into direction of the normal to $\Gamma$ is compensated by the change in the internal energy of interface. This change is related both to the change in temperature and to the change in the interface area: this circumstance is responsible for the emergence of term in the right – hand side of equation (2).

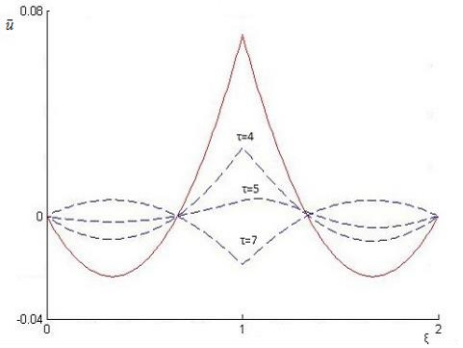


Fig. 1. Velocities evolution $\bar{u}_j$ for the case $a_1(-1,\tau) = a_{10}(\tau) = \sin\tau$, $a_2(1,\tau) = a_{20}(\tau) = 0$. The total line present the stationary velocities $\bar{u}_j^s(\xi)$

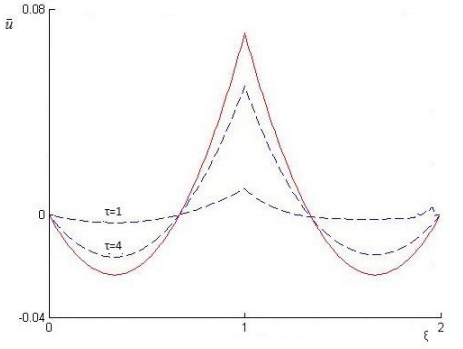


Fig. 2. Velocities evolution $\bar{u}_j$ for the case $a_1(-1,\tau) = a_{10}(\tau) = 1 + e^{-\tau}\cos(10\tau)$. The total line present the stationary velocities $\bar{u}_j^s(\xi)$

**Acknowledgments.** The research has been supported by the Russian Foundation for Basic Research (Project No. 14-01-00067).

# Investigation of behavior of the dynamic contact angle on the basis of the Oberbeck-Boussinesq approximation of the Navier-Stokes equations

Olga N. Goncharova[1,2] , Alla V. Zakuraeva[1,2]

[1]Department of Differential Equations, Altai State University, Barnaul, Russia
[2]Laboratory of Enhancement of Heat Transfer, Institute of Thermophysics SB RAS, Novosibirsk, Russia
gon@math.asu.ru

The problems of the fluid flows with a dynamic contact angle are very important at present. Such problems occur in many applications by study of the convective multi-phase flows, flows through porous medium, of evaporative liquid drops, wetting hydrodynamics etc (see, for example, Gatapova et al. (2014)). The contact angle is defined as an angle between the two surfaces, where the free boundary touches the solid boundary. The non-stationary problems remain to be rather difficult for investigations in connection with an open problem of the dynamic contact angle, due to an appearing problem of motion of the contact line of three phases, which do not have unique closure.

In the case if the boundary walls of a liquid containing domain are moving with constant speed, the contact angle will change with the velocity. Changing of this angle will also depend on a character of the thermal boundary regimes on the free and solid boundaries. Interaction of the gravitational and thermocapillry convection and their influence on a behavior of the contact angle and shape of the free boundary should be investigated. The mathematical models of the fluid flows with dynamic contact angle will be presented.

Two-dimensional motion of a viscous incompressible liquid with a thermocapillary boundary is investigated numerically on the basis of the mathematical model that consists of the Oberbeck-Boussinesq approximation of the Navier-Stokes equations, kinematic and dynamic conditions at free boundary and of the slip boundary conditions at solid walls (Doerfler et al. 2002). We assume that the constant temperature is supported on the solid walls. On the thermocapillary gas-liquid interface the condition of third order for temperature is imposed.

The numerical algorithm based on a finite-difference scheme of second order approximation on space and time has been constructed. The numerical experiments are performed for water under conditions of normal and low gravity for different values of the static contact angle ($\Phi_0$), different friction coefficients ($\gamma$, $\gamma_0$) and surface tensions and different interphase heat transfer coefficients (see on figures 1, 2 the examples of the dependence of the contact angle ($\Phi$) of the contact point velocity (S) and of the free boundary positions under normal gravity (g); the CGS-system is used; angle values are given in degrees). In this paper the velocity and temperature fields and the size of the contact angle, as a function of the velocity of the contact point, have been computed. Comparison with the results of the fluid flows with dynamic contact angle in the isothermal case (Doerfler et al. 2002) are presented.

**Acknowledgments.** The study was supported by the Russian Science Foundation (grant RSF 15-19-20049).

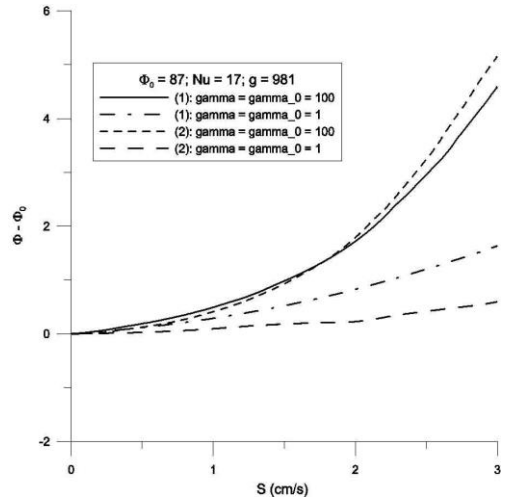


**Figure 1:** Dynamic contact angle (increasing contact angles $\Phi$ with increasing velocity S for different choices of the friction coefficients $\gamma$, $\gamma_0$ ).

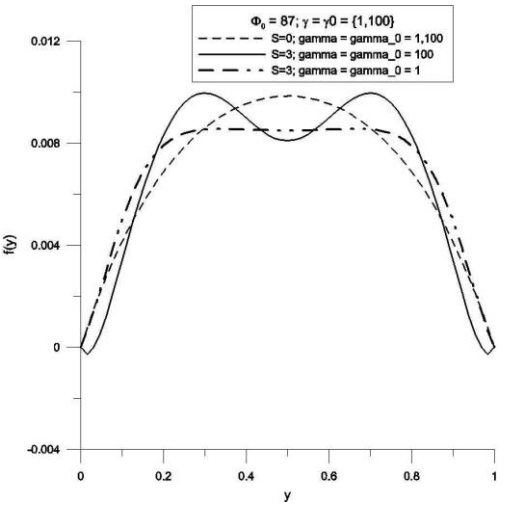


**Figure 2:** Free boundary (examples for the free boundaries f(y) for the velocities S at different values of the friction coefficients $\gamma$, $\gamma_0$).

**References**

Gatapova E. Ya., Semenov A.A., Zaitsev D.V., Kabov O.A., Evaporation of a sessile water drop on a heated surface with controlled wettability, Colloids and surfaces A, Psysicochem. Eng. Aspects, Vol. 441 pp. 776-785 (2014)

Doerfler W., Goncharova O., Kroener D., Fluid flow with dynamic contact angle: numerical simulation, ZAMM, Vol. 82 pp. 1-10 (2002)

# Characteristics of two-layer flows with evaporation depending on boundary thermal load

Ilya Shefer

Siberian Federal University, Institute of Mathematics and Computer Science,
Svobodny 79, Krasnoyarsk, 660041, Russia
Ilya.shefer@gmail.com

Dynamics and heat- and mass transfer processes in a two-layer system of liquid and gas are studied in the full problem statement with respect to evaporation at interface. The stationary joint flow of liquid and vapor-gas mixture in plane horizontal channel is described by the Boussinesq approximation of the Navier-Stokes equations. The governing equations include additional terms which correspond to the Dufour effect in the gas phase. On the thermocapillary interface, remaining undeformed, the following conditions are specified: kinematic and dynamic conditions, the heat transfer condition with a diffusive-type evaporation, continuity conditions for the velocity and temperature and the relation for the saturated vapor concentration. On the solid walls of the chanel the no-slip conditions and the linear temperature distribution with respect to the longitudinal coordinate are to be valid. Exact solutions of the considered problem were constructed in (Goncharova, Rezanova 2014). They allow to model processes in the two-layer system with zero vapor flux condition on the upper fixed boundary of the channel and to estimate influence of the Dufour effect on characteristics of flows and features of concentration and temperature fields. The investigation of the flow topology depending on longitudinal temperature gradients on the outer walls of channel and height of the liquid layer for the "HFE7100-nitrogen" system was performed (fig. 1). Conditions of appearance of reverse flows and dependence of evaporation intensity on the problem parameters were specified.

Stability of the main flow with regard to infinitesimal perturbances has been studied on the basis of normal wave method. For the system "HFE7100-nitrogen" influence of the intensity of thermal load on the channel walls on character and type of the arising perturbations is investigated numerically. It is found that the thermocapillary mechanism is potentially more dangerous. The disturbances are localized near interface and fade out or grow depending on linear sizes (thicknesses of media) and value of longitudinal temperture gradient. Co-existence of two non-uniformly scaled types of the convective flow can be observed.

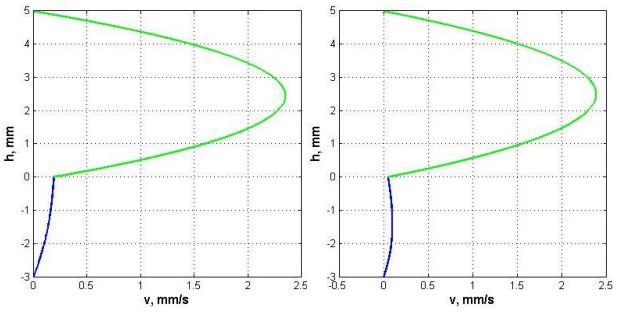


a) b)

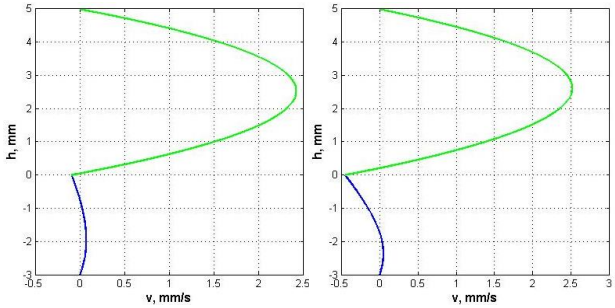


c) d)

**Figure 1:** Velocity profiles for different longitudinal temperature gradients: a) A = 0.2 K/m, b) A = 0.6 K/m, c) A = 1 K/m, d) A = 2 K/m.

This work was supported by Russian Foundation of Basic Researches (project 14-08-00163).

## References

Goncharova O.N., Rezanova E.V. Example of an exact solution of the stationary problem of two-layer flows with evaporation at the interface, J. Applied Mechanics and Technical Phys., Vol. 55(2), pp. 247-257 (2014)

# Convective Thermal Patterns and Evaporation Flux through an Evaporating Surface: parametric study

Hatim Machrafi, Pierre C. Dauby

Université de Liège, Faculty of Science, Institute of Physics, Thermodynamics of Irreversible Phenomena
Allée du 6-Août, 19, Liège, B-4000, Belgium
h.machrafi@ulg.ac.be

This work falls into a general framework which consists of observing the behavior of patterns and structures that can be formed after instability onset in an evaporating liquid layer under a gas flow. In previous work, such a configuration has been studied with regard to theoretical instability thresholds (Machrafi et al. (2013)). What is of interest here, is a three-dimensional numerical simulation of the transient temperature and fluid motion in the liquid for a liquid evaporating into a horizontal nitrogen gas flow. The chosen liquid is HFE7100. The numerical simulations (CFD) are performed using the software ComSol (finite elements method) (Machrafi et al. (2014)).

The numerical model in the present work is based on the evaporator part of an experimental setup of the European Space Agency (ESA), to be flown onboard the International Space Station (ISS) in the near future. This study takes part of a pre-flight analysis of the EVAPORATION PATTERNS (EP) (previously named CIMEX). The fluid is contained in a box whose horizontal dimensions are 50 by 50 mm. The height can be changed between 2 and 8 mm. The evaporating surface is a square hole in the upper wall with dimension 10.6 mm by 10.6 mm. Note also that the evaporated liquid is constantly replenished from the bottom, so that the liquid-gas interface remains at the same level. Above it, there is a gas channel, wherein nitrogen flows with a rate of 100 or 1000 ml/min. The ambient conditions are at a temperature of 293.15 K and a pressure of 1 atm.

The objectives are to study the evaporation flux and patterns at the liquid-gas interface for a set of experimental operating conditions. We will define the "reference situation" by the following values of the parameters: 2 mm liquid height, 100 ml/min gas flow, no gas humidity and no gravity. Then, the aforementioned parameters are separately altered and the difference with the reference situation is observed. The liquid height is changed to 4 mm, the gas flow to 1000 ml/min, the relative gas humidity to 50% of the saturation limit and the effect of absence of gravity is also considered.

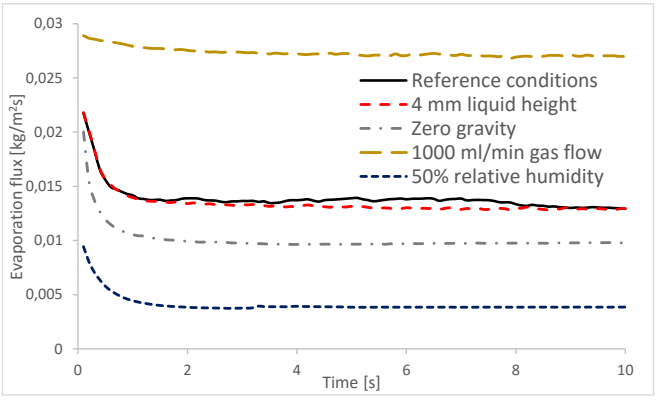


**Figure 1.** Evaporation flux as a function of time for several operating conditions

Figure 1 presents the evaporation flux for different experimental operating conditions. Figure 1 serves to show the range of the evaporation flux for the parameter ranges considered in this paper, which correspond to those of the EP experiment. Figure 1 also shows that for all the parameters ranges considered, the evaporation flux reaches a quasi-constant value at approximately the same time, i.e. t = 1s. We can see, furthermore, that the evaporation flux can be increased or decreased considerably with the parameters considered in this work.

**Figure 2.** Pattern formation at the reference conditions for times t=0.1 (left), 1 (middle) and 10 (right) s.

Figure 2 shows an example of the evaporation patterns at the liquid-gas interface at the previously defined reference point. The picture shows that at t = 0.1 s, many cells of approximately the same size and shape exist (quasi-regular). Then, at t = 1 s, the cells become somewhat more irregular. Finally, at t = 10 s, the evaporation patterns at the liquid-gas interface consists of cells that have no common size or shape (non-regular). When linking the evaporation patterns to the evaporation fluxes in figure 1, one observes that at first, the quasi-regular patterns correspond to a decreasing evaporation flux. However, very soon, the evaporation flux reaches a quasi-monotonic behavior that does not depend greatly on the different patterns, being associated to a transition from quasi-regular to non-regular patterns.

## Acknowledgements

BelSPo and ESA are acknowledged for financial support throught the PRODEX projects.

## References

Hatim Machrafi, Nacer Sadoun, Alexey Rednikov, Sam Dehaeck, Pierre C. Dauby, Pierre Colinet, Evaporation Rates and Bénard-Marangoni Supercriticality Levels for Liquid Layers Under an Inert Gas Flow, Micrograv. Sc. Tech. Vol. 25 pp. 251-265 (2013).

Hatim Machrafi, Carlo S. Iorio, Pierre C. Dauby, Relation between convective thermal patterns and heat flux through an evaporating surface via 2D and 3D numerical simulations, Interf. Phenom. Heat Trans. Vol. 2 pp. 199-209 (2014).

# Modeling of the liquid film flows with evaporation at thermocapillary interface

Ekaterina Rezanova

Altai State University, Faculty of Mathematics and Information Technologies, Department of Informatics
61 Lenina avenue, Barnaul, 656049, Russia
katerezanova@mail.ru

The processes of convection of the fluids, accompanied by evaporation at the interface, are studied analytically and numerically in the framework of the new mathematical models developed with the help of the long-wave approximation of the governing equations. The one-sided mathematical models of the evaporating liquid films are constructed on the basis of the Navier-Stokes equations (NSE) and their Boussinesq approximation (OBE) in the two-dimensional case . To model an evaporation process at the thermocapillary interface the general kinematic, dynamic and energetic conditions are used (Iorio et al. 2011, Goncharova 2012). The additional hypotheses concerning continuity of temperature and tangential velocity, the laws of the heat and mass fluxes, the phenomenological relations are to be fulfilled. To close the problem statement the initial position of the thermocapillary interface, the initial conditions for velocity and temperature and the conditions at infinity should be given.

The equations of the thin liquid films in the two-dimensional case are derived in detail in the cases of moderate (Re = O(1)) and high (Re = O(1/ε)) values of the Reynolds number ($\varepsilon$ is a small parameter equal to the ratio of the transverse and longitudinal characteristic sizes), see for example, Goncharova and Rezanova (2015). The nonlinear evolution equations of the shape of the thermocapillary interface take into account the effects of gravity, viscosity, capillarity, thermocapillarity, evaporation and of the additional tangential stresses at interface. The parametric analysis has been performed.

As usual in the problems of convection the evaporation effects are modeled with the help of the energy balance condition that is an analog of the Stefan condition; the local mass flux is determined by the Herzt-Knudsen equation. It has been shown that the taking into account even of one additional term in the thermal condition at the evaporative interface leads to the quantitative differences from the results, which can be obtained with use of the classical approach.

The results of testing of the numerical algorithm will be presented. The numerical investigations are carried out for the liquids like ethanol and HFE7100. Evolution of an uniformly or non-uniformly heated films flowing down an inclined substrate is investigated in the case of different values of the inclination angle and for selected values of the non-dimensional parameters. Comparison with the results of an alternative modeling of the evaporating falling films is presented. The periodic initial boundary value problem was solved in the interval [-L, L] with the initial disturbance taken to be a monochromatic wave with a small amplitude under conditions of normal gravity and microgravity. By decreasing of the values of the Galileo number (Ga) a more rapid thinning of the liquid layer due to evaporation is observed. Comparison of some results of the film flows calculating with the help of the models based on NSE and OBM, is presented in fig. 1, in the case Ga= 40. Qualitatively we have the similar wave-type flowing of the liquid layer but at the same time we observe the differences in the wave amplitude.

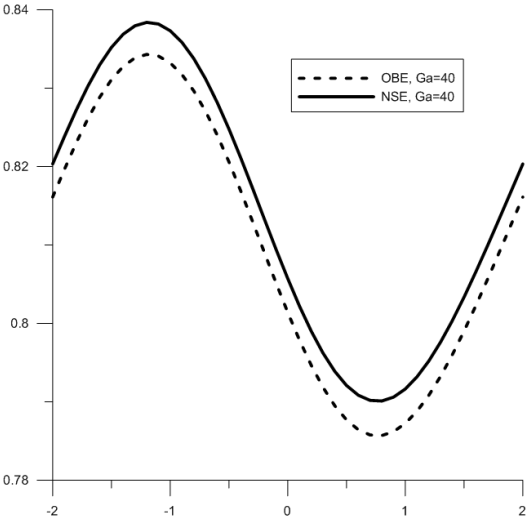


**Figure 1:** The behavior of the liquid layer thickness in the "ethanol-nitrogen"; the case of non-uniform heating.

**Acknowledgments.** The research has been supported by the Russian Foundation for Basic Research (Project No. 14-08-00163) and the Russian Ministry of Education and Science (project indicator RFMEFI61314X0011).

## References

Iorio C.S., Goncharova O.N., Kabov O.A., Heat and mass transfer control by evaporative thermal pattering of thin liquid layers, Computational Thermal Sci., Vol. 3 (4) pp. 333-342 (2011)

Goncharova, O.N., Modeling of flows under conditions of heat- and mass transfer at the interface, Proceedings of the Altai State University (Izvestiya Altaiskogo universiteta), N. 1/2 (73) pp. 12-18 (2012) (in Russian)

Goncharova, O.N., Rezanova, E.V., Construction of a mathematical model of in a thin liquid layer on the basis of the classical convection equations and generalized conditions on an interface, Proceedings of the Altai State University (Izvestiya Altaiskogo universiteta), N. 1/1 (85) pp. 70-74 (2015) (in Russian)

# Spatiotemporally resolved heat transfer measurements in falling-film flows down an inclined heated foil

Alexandros Charogiannis, Baptiste Heiles, Richard Mathie, Omar Matar and Christos N. Markides

Clean Energy Processes (CEP) Laboratory, Department of Chemical Engineering,
Imperial College London, London SW7 2AZ, United Kingdom
c.markides@imperial.ac.uk

We present experimental measurements of unsteady and conjugate heat-transfer in harmonically forced, gravity-driven liquid films flowing down a resistively-heated inclined titanium foil by simultaneous application of planar laser-induced fluorescence (PLIF) imaging and infrared (IR) thermography (Mathie, Nakamura & Markides 2013, Markides, Mathie & Charogiannis 2015). In particular, quantitative, spatiotemporally resolved and simultaneously conducted measurements are reported for the local and instantaneous film-height, film free-surface temperature, liquid-solid interface temperature, heat flux exchanged with the heated substrate, and finally the local and instantaneous heat transfer coefficient (HTC). The experimental campaign comprises two different liquids (water-ethanol and water-glycerol solutions) and two inclination angles (30° and 40°), as well as a wide range of heating and flow conditions (heat fluxes, forcing frequencies, forcing amplitudes and flow rates). The effort was motivated by the strong demand for spatiotemporally resolved heat-transfer data in planar falling films, which can be harnessed to further our understanding of the underlying heat-transfer mechanisms, facilitate the development and validation of advanced modeling tools, and ultimately improve the performance and reduce the cost of practical equipment.

The formation, interaction and spatiotemporal evolution of thermal rivulet structures on the film free-surface of water-ethanol films was examined as a function of the heat input to the flow, in the absence of as well as in response to film forcing. In addition, phenomenological observations pertinent to the formation and evolution of thermal rivulets on the free surface of glycerol-rich films are reported and compared to results from the water-ethanol solution experiments. Flat thermal rivulets (i.e. thermal rivulets not associated with film-height fluctuations) were identified by simultaneous and local PLIF and IR imaging, and linked to the emergence of Marangoni flows on the film free-surface. Local surface tension variations are believed to trigger instabilities and the ensuing mass transfer characterized by accumulation of liquid in the cooler film regions and thinning in the hotter ones. Flow pulsation instigates a pronounced mixing enhancement on these features, manifested by the development of strongly skewed and intertwined thermal rivulets (Figure 1).

Beyond this qualitative assessment, the interfacial characteristics of the examined film-flows were linked quantitatively to their heat-transfer performance in an effort to assess the effect of unsteadiness. Our results captured the overall HTC variation as a function of the film height, including the HTC enhancement at lower film heights; however, the magnitude of the true HTC was found to be significantly higher than HTC predictions based on the Nusselt theory, sometimes by up to a factor 3. The unsteady flow phenomena linked to the interface waviness are believed to contribute significantly towards the observed enhancement, most probably through enhanced convective heat transfer. The mean flow Nusselt number (*Nu*) at low mean flow Reynolds numbers (*Re*) was found to be around 2.5, in agreement with the steady flow prediction, while with increasing *Re*, the mean *Nu* was found to increase. For thicker film regions, the HTC appears to be decoupled from the film height, while for thinner ones, the anticipated HTC enhancement (based again on the steady flow analysis) is significantly more pronounced. Finally, the HTC coefficient of variation (HTC standard deviation normalized by the mean HTC) was found to increase as the film height coefficient of variation decreases, while the former was also found to correlate linearly with the coefficient of variation of the temperature difference across the film.

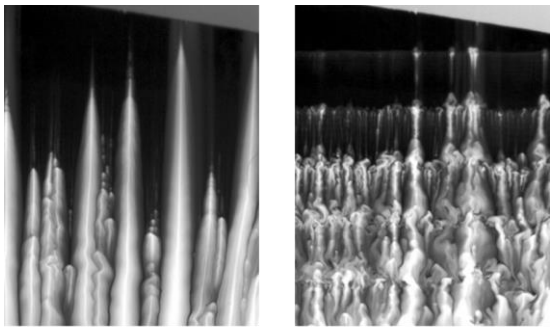

(a) (b)

**Figure 1:** (a) Instantaneous temperature distribution over the free surface of a liquid film with flow *Re* = 179, and a mean heat flux of 3.6 W cm$^{-2}$. (b) Instantaneous temperature distribution over the free surface of a liquid film with flow *Re* = 179, forcing frequency of 1.8 Hz, pulsation amplitude of 10% and a mean heat input of 1.5 W cm$^{-2}$.

## References

Mathie R., Nakamura H., and Markides C.N., Heat transfer augmentation in unsteady conjugate thermal systems – Part II: Applications. International Journal of Heat and Mass Transfer, Vol. 56 pp. 819–833 (2013)

Markides C.N., Mathie R. and Charogiannis A., An experimental study of spatiotemporally resolved heat transfer in thin liquid-film flows falling over an inclined heated foil, Accepted for publication in: International Journal of Heat and Mass Transfer, (2015)

# Sedimentation of deformable viscoplastic drops in a non-isothermal Newtonian fluid

Olga M. Lavrenteva, Irina Smagin and Avinoam Nir

Technion, Chemical Engineering Department
Haifa, 32000, Israel
ceolga@techunix.technion.ac.il

The slow sedimentation of deformable viscoplastic drops with temperature-dependent yield stress in non-isothermal Newtonian fluid is simulated making use of a variation of integral equation method. The Green function for the Stokes equation is used and the non-Newtonian stress is treated as a source term. Integration over the outer unbounded domain occupied by the viscous liquid is eliminated by satisfying the boundary condition and using the integral expressions for the adjoined domains. Thus, the problem is reduced to an integral equation in a bounded domain, which reduction is the main advantage of this method.

A regularized Bingham constitutive equation is used for the viscoplastic medium. The computations are carried out for a vertical temperature gradient, initially spherical and ellipsoidal drops, and for the values of governing parameters taken from Smagin *et al.* (2011), where sedimentation of viscoplastic drops in isothermal fluid was studied. Piecewise linear decreasing dependence of the yield stress on the temperature is assumed, while all the other physical parameters are taken to be temperature-independent.

The study revealed that initially spherical drop remains almost spherical, however the shape and size of unyielded zone considerably changes as the drop propagates to warmer or cooler regions. In the case of downward temperature gradient, the drop moves to the warmer regions, the yield stress decreases and the unyielded zone inside the drop shrinks. In the case of upward temperature gradient, the drop moves to the cooler regions, the yield stress increases and the unyielded zone inside the drop grows until the entire drop becomes solid and proceeds to move as a rigid body. The described above behavior is illustrated in Figure 1.

Initially deformed drop is known to return to spherical shape if the interfacial tension is strong enough (the capillary number, *Ca*, is small). If *Ca* exceeds some critical value (depending on initial deformation), eventually the drop breaks up. In Smagin *et al.* (2011), it was demonstrated in the case of constant yield stress, the increase of the Bingham number stabilizes the drop shape. Our present computations reveal that strong enough temperature dependence of the yield stress prevents the breakup of the drop settling in an upward temperature gradient. The terminal shape of the drop in this case is non spherical. On the other hand, a downward temperature gradient can destabilize the drop in near- critical situations.

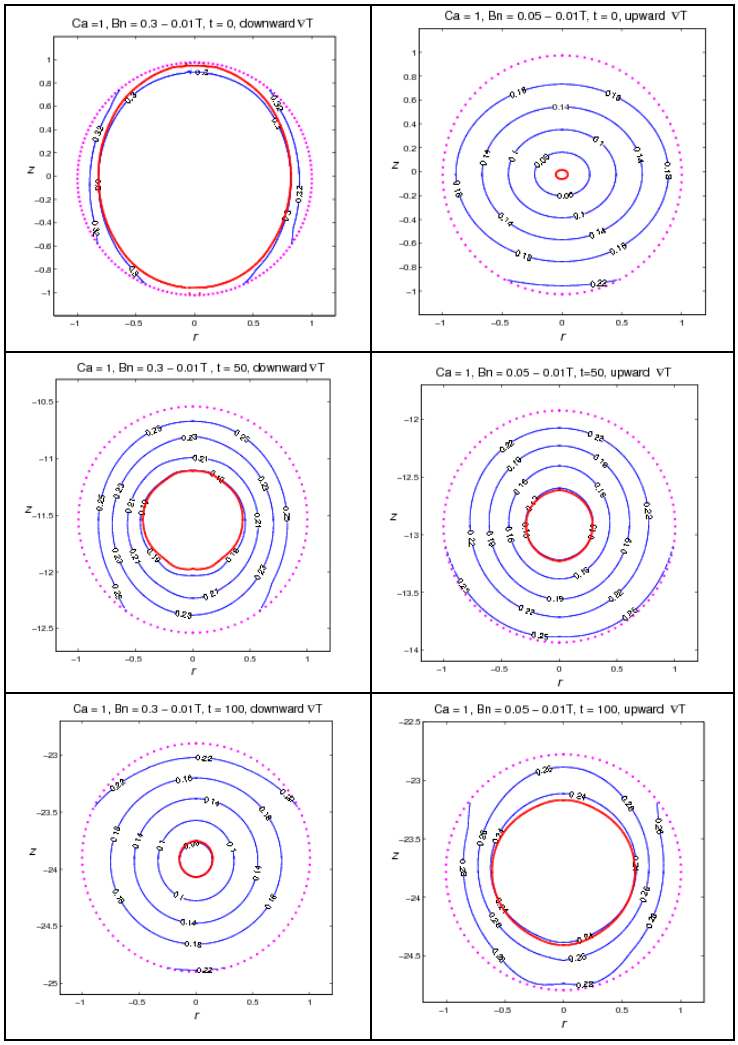


**Figure 1:** Evolution of unyielded zone (marked by thick red line) inside viscoplastic drop slowly settling in non-isothermal viscous fluid. Left- and right-hand columns correspond to downward and upward temperature gradient, respectively. Drop interface is shown by dotted line. Iso-lines of the stress tensor second invariant are depicted by thin blue lines.

## References

I. Smagin, M. Pathak, O. M. Lavrenteva, A. Nir, Motion and shape of an axisymmetric viscoplastic drop slowly falling through a viscous fluid. Rheol. Acta 50, 361--374 (2011).

# The Effect of Film Temperature on Transition Regimes and Crater Evolution from a Single Droplet

E. R. Underhill, A. Mitchell, D. B. Hann

Faculty of Engineering,
University of Nottingham, UK, NG7 2RD
David.Hann@nottingham.ac.uk

The heat transfer that occurs in lubrication systems is difficult to understand. Even simplifying to a single droplet impact problem still retains many unknowns. A few papers exist looking at this phenomena, and these do show an effect, (Manzello and Yang, 2003; Mitchell et al., 2015) but it is not clearly defined which liquid parameters should be used to define the impact, the liquid or the film. This paper attempts this understanding by carrying out an investigation into the heat transfer due to a single water droplet at 15°C impacting onto a liquid film at different temperature. The film temperature ($T_{film}$) is increased, from room temperature (15°C) to 60°C and the influence on the crater evolution and the splashing regimes according to the non-dimensional K parameter (Cossali et al., 1997) is demonstrated and compared to those in a static film. The results are obtained experimentally using droplets with a diameter (D) of 3±0.2 mm and Weber number (We) ranging between 75 - 240 impinging onto a film with a non-dimensional thickness (H*) of 2. The propagation of the droplet through the film and the splashing outcome is recorded using a high-speed camera and the heat transfer effects are observed from infrared images.

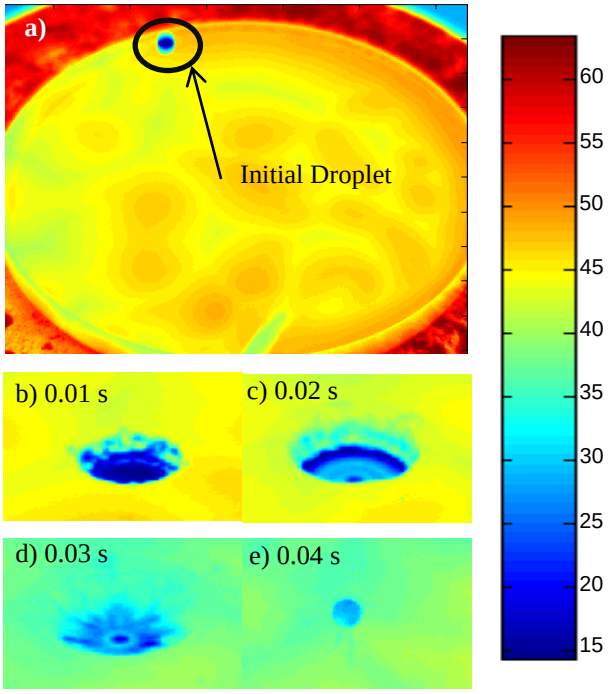


**Figure 1:** Infrared images before and after impact ($T_{film}$ = 50; We = 160): a) initial droplet and petri dish 0.01 s before impact; b-e) 0.01, 0.02, 0.03 and 0.04 s after impact. Right: Temperature calibration.

Results show that the number of secondary droplets increases with increasing film temperature. The results suggest that a higher film temperature causes an increase in the depth and width of the crater due to the decrease in viscosity and surface tension of the fluid film at higher temperatures. The infrared images show that droplet spreads into a lamella over the surface of the crater (Figure 1) and so thinning of the crater will enhance the heat transfer effect between the droplet and the wall if the wall is heated. It is demonstrated that the main mechanism of heat transfer is conduction for thin films and not convection mixing as occurs at thicker films.

## References

Cossali, G.E., Coghe, A., Marengo, M., 1997. The impact of a single drop on a wetted solid surface. Experiments in Fluids 22, 463-472.

Manzello, S.L., Yang, J.C., 2003. The influence of liquid pool temperature on the critical impact Weber number for splashing. Physics of Fluids 15, 257-260.

Mitchell, A., Simmons, K., Hann, D.B., 2015. Experimental Investigation Into Droplet Impingement Upon Supercritical Films Using High Speed Video And Thermal Imaging, International Mechanical Engeineering Congress and Exposition, Houston, Texas, pp. IMECE2015-51677.

# Waves interaction with thermocapillary structures in heated liquid films

Evgeny. A. Chinnov

Kutateladze Institute of Thermophysics, Siberian Branch, Russian Academy of Sciences, Novosibirsk, 630090, Russia
Novosibirsk State University of Architecture and Civil Engineering, Novosibirsk, Russia
Novosibirsk State University, 630090 Novosibirsk, Russia
e-mail: chinnov@itp.nsc.ru

Investigation of wave-thermocapillary structures interaction in heated liquid films is necessary for better understanding of the mechanisms of heat transfer and crisis phenomena in heated films. Besides the basic interest, this knowledge is important for increasing the efficiency of modern heat and mass transfer apparatuses.

Various regimes of the structures formation in a heated falling liquid film were detected in [1–3]. The structures in regimes A and B differ by the level of heat flux necessary for their formation and by the character of the wavelength dependence on the heat flux and the Reynolds number. Previously, the formation of regular structures in a thermocapillary regime A on the surface of a smooth liquid film flowing down a vertical wall containing heaters was discovered and studied at small Reynolds numbers. Under the action of thermocapillary forces directed against the flow (from heated to cold regions), the film exhibited thickening and, in the case of a threshold heat flux, the flow disintegrated into vertical rivulets separated by thin film. The formation of rivulets in regime B takes place on the wavy surface of liquid films under the action of thermocapillary forces directed from relatively hot to cold regions. The rivulet flow structure gradually develops with growing heat flux and increasing distance from the upper edge of the heater.

Results obtained for large Reynolds numbers showed that the relative amplitudes of waves in the regions between rivulets at high heat fluxes are much greater than those for small Reynolds numbers and in isothermal falling films [4]. The thermocapillary force effect across the film flow is characterized by the transverse deformation that increases as the film run length and the heat flux grow. In the second place, the thermocapillary force effect is also directed along the film flow and is characterized by the Marangoni number. As the film is heated, this parameter grows in the valley between rivulets and remains almost unchanged on the rivulet crest. Their effect in the valley, while the film heating increases, enhances more rapidly than that for small Re values.

Results obtained for large Reynolds numbers showed that the relative amplitudes of waves in the regions between rivulets at high heat fluxes are much greater than those for small Reynolds numbers and in isothermal falling films.

Interaction between waves and thermocapillary structures is investigated in heated liquid films for wide range of Reynolds numbers. An experimental study of the transformation of three-dimensional waves into thermocapillary-wave structures in the flow of water film on a vertical plate with a heater was carried out using the fluorescent thickness measurement technique and a high-speed infrared recording technique in order to measure the temperature field on the liquid film surface.

Two mechanisms of interaction between waves and thermocapillary structures are found. There are movement of small and medium-sized waves in the area of thermocapillary rivulets and the deformation and destruction of large waves. Mechanism of waves movement in the area of the rivulets applies to all sizes of waves that can be built into the regular ranks without destruction. During the movement of these waves, the thermocapillary forces change the distance between their crests, resulting in compliance with the distance between the emerging thermocapillary structures in the residual layer. In the second place, large waves break down into waves of lesser width that move in the direction of the rivulets, which are formed by thermocapillary forces.

The initial size of such waves considerably more distance between the rivulets of the thermocapillary structures. It is important to note that wave front lines deformation occurs not at a point corresponding to the maximum thermocapillary stresses, but in place of the local minimum of the film thickness where thermocapillary forces above fluid inertia forces. The collapse of large waves in the heated liquid film occurs as a result of the combination of thermocapillary and inertial effects.

**References**

1. Kabov O.A., Diatlov A.V., Marchuk I.V. Heat transfer from a vertical heat source to falling liquid film. Proceedings of the First International Symposium on Two-Phase Flow Modelling and Experimentation, Rome, Italy, October 9–11, 1995, Rome, Vol. l. p. 203(1995).
2. Kabov O.A., Chinnov E.A. Heat transfer from a local heart source to subcooled falling liquid film evaporating in a vapor-gas medium. Russ. J. Eng. Termophys., Vol. 7. pp. 1-34 (1997)
3. Chinnov E. A., Kabov O. A. Jet formation in gravitational flow of a heated wavy liquid film. J. Appl. Mech. Tech. Phys. Vol. 44. pp. 708-715 (2003).
4. Chinnov E. A. Wave - thermocapillary effects in heated liquid films at high Reynolds numbers. IJHMT, Vol. 71. pp. 106-116 (2014).

# Numerical Modelling of Thermocapillary deformation and dry spot formation in a locally heated thin horizontal volatile liquid layer

Igor Marchuk[1, 2], Ella Barakhovskaya[1], Yuriy Lyulin[2], Oleg Kabov[2], Jean Claude Legros[2]

[1]Novosibirsk State University, Pirogova Str. 2, Novosiborsk, 630090, Russia
[2]Institute of Thermophysics, Russian Academy of Sciences, Prosp. Lavrentyev 1, Novosibirsk, 630090, Russia
marchuk@itp.nsc.ru

Heat transfer and rupture in thin liquid layers with local heating is an important challenge of thermal stabilization technique of electronic equipment (Kabov, 2010). The problem of thermocapillary breakdown of the locally heated horizontal liquid layer has been solved numerically in axisymmetric statement, Fig. 1. The thin layer approximation model is used (Marchuk 2015). Capillary pressure, viscosity and gravity are taken into account. Evaporating rate is supposed to be proportional to the temperature difference between temperatures of the liquid surface and ambient. Heat transfer in the substrate is also simulated. The deformation of the free surface has been calculated for different values of the heating power and thickness of the liquid layer. The model predicts the formation of the thin residual layer of the liquid and film breakdown at sufficiently intensive heating. Fig. 2-3. A local decreasing of the liquid surface temperature is shown in Fig. 2b, curve 4. It caused by intense evaporation and decreasing of the thermal resistance of the liquid layer. A dry spot is formed in a ring shape because of the axial symmetry, Fig. 3. Surrounded by a dry ring liquid in the center is a drop, which tends to acquire an equilibrium shape, which is defined by Young–Laplace equation. The dynamics of the three phase contact line is calculated.

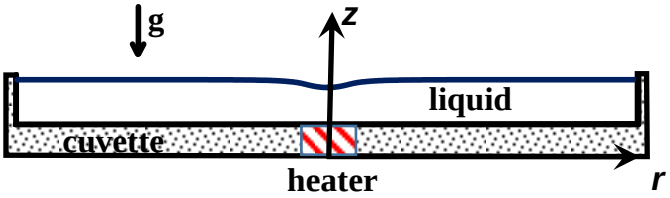


**Figure 1:** Scheme of the problem statement.

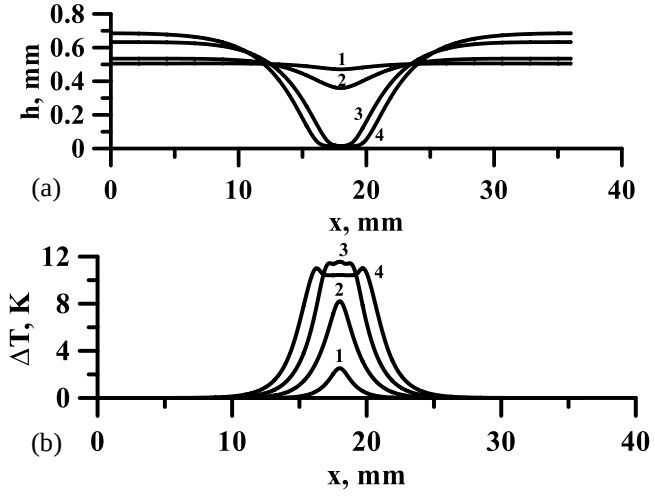


**Figure 2:** Calculated distributions of the liquid layer thicnkess (a) and surface temperature (b). 1 – 0.5 s; 2 – 1.0 s; 3 – 1.5 s; 4 – 2.0 s. Heating power 3 W, water.

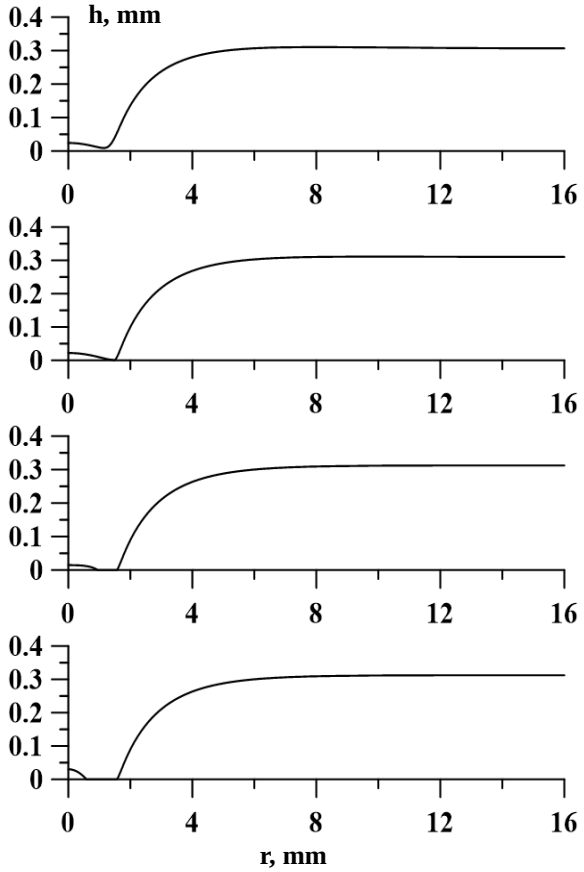


**Figure 3:** Liquid layer breakdown and contact line evolution. Ethanol, axisymmetric case.

The velocity of the contact line increases with the increase of the wetting contact angle value and of the surface tension coefficient. The calculations results are in a good qualitative agreement with the experimental ones (Lyulin, et. al. 2015).

**Acknowledgements** The study was financially supported by the Russian Science Foundation (Project 15-19-20049).

**References**

Kabov O.A., Interfacial thermal fluid phenomena in thin liquid films, International Journal of Emerging Multidisciplinary Fluid Sciences, 2(2-3), pp. 87-121 (2010)

Marchuk I. V., Thermocapillary deformation of a horizontal liquid layer under flash local surface heating, Journal of Engineering Thermophysics, 24(4), pp. 381-385 (2015)

Lyulin Yu.V., Spesivtsev S.E., Marchuk I.V., Kabov O.A., Investigation of breakdown dynamics of a horizontal liquid layer with a point heat source, Technical Physics Letters, 41, pp. 22-29 (2015)

# The waves amplitudes increase due to interacting with thermocapillary structures

Evgeniy Shatskiy, Yuliya Koemets, Evgeny Chinnov

Kutateladze Institute of Thermophysics SB RAS, Lavrent'ev av. 1, Novosibirsk, 630090, Russia
Novosibirsk State University of Architecture and Civil Engineering, Novosibirsk, Russia
Novosibirsk State University, 630090 Novosibirsk, Russia
E-mail: shatskiy.itp@gmail.com

Fluid film flows are widely used in cooling of the heat-generating surfaces in many technological applications: heat exchangers, condensers, evaporators. The main characteristics of these flows are their wavy amplitudes and structures. It is known that two-dimensional hydrodynamic waves in an isothermal liquid film are unstable to three-dimensional disturbances. It was found that the wavelength of the instability to transverse three-dimensional perturbations decreases with increasing Reynolds number. During transformation of two-dimensional into three-dimensional waves in Joo S. W. and Davis S.H. (1992) and Liu J. et. al. (1995) it was shown that there are isolated synchronous wave when there is no phase shift in the transverse direction of waves and the subharmonic waves, when the phase shift occurs.

When the liquid film flow over the heated surface except hydrodynamic instability that leads to the development of three-dimensional waves, there is also a thermocapillary instability which results in the appearance on the film surface of the stationary three-dimensional structures in the form of a number of rivulets with a thin film between them. Depending on the heating conditions and the temperature gradient on the film surface there are two types of thermo-capillary structures. Two mechanisms of growth of the relative amplitudes of the waves when heated falling liquid film are known in the literature: in the residual layer of the liquid film because of its intensive evaporation (Pavlenko et. al. 2002) and the film thickness decreases in interrivulet region by the action of thermocapillary forces (Chinnov 2014).

In this paper, the analysis of experimental data on the simultaneous measurement of the thickness and temperature fields in the flowing heated liquid film at Re = 15 is presented. It is shown that increasing heat flux results in more expressed rivulet formation in the lower part of the heater (differential thicknesses in the rivulet and interrivulet area increases from 0.04 mm to 0.11 mm). It was found that the wave amplitude increase in the region where waves interact with the thermocapillary structures.

Fig. 1 shows the dependence of the amplitude of the incoming waves to the heater along the rivulet from the path length for several values of the heat flux. It is seen that with increasing of the heat flux there is a local maximum of the thickness in the initial part of the heater. Also it is seen that increase of the heat flux density results in shifting this maximum closer to the top of the heater (X = 0). This trend is related to the fact that when the heat flux reaches the threshold value at the upper edge of the heater in the residual layer there are thermocapillary periodic structures. These structures arise because of the high temperature gradients at the leading edge of the heater (up to 10 K/mm), resulting in occurrence of thermocapillary forces directed against the flow. These structures make a disturbance in the following wavefront, leading to an increase in the amplitude of the waves. It was found that the amplitude of hydrodynamic waves in the upper part of the heater (5 mm < X <30 mm) can be increased by more than half when interacting with the thermocapillary instability of type A (q= 2.55 W/cm$^2$). While moving along the heater the wave amplitude decreases, although the value is substantially higher than at lower heat flux (q = 0.98 W/cm$^2$) when thermocapillary structure type A is not yet formed. Also at high heat fluxes there is a transverse movement of the rivulets and in combination with an amplitude increase it results in an increase of the stability of the heated liquid film to rupture.

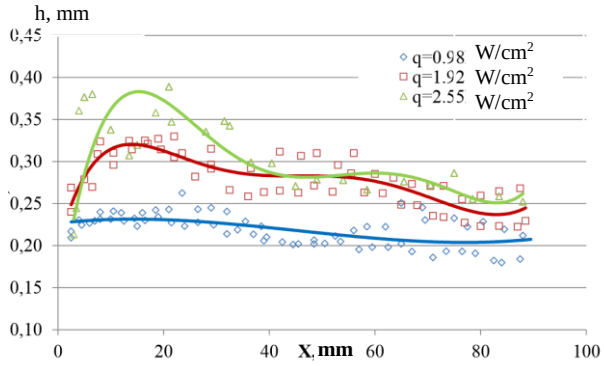


**Figure 1:** Dependence of the amplitude of the wave from the path length of the heater

This work was supported by the grant of Russian Science Foundation (Agreement No. 15-19-30038).

## References

Joo S. W., Davis S.H. Instabilities of Three-Dimensional Viscous Falling Films // J. Fluid Mech. 1992. V. 242. P. 529-547.

Liu J., Schneider J. B., Golub J.P. Three-dimensional Instabilities of Film Flows // Phys. Fluids. 1995. V. 7. N 1. P. 55–67.

Pavlenko A. N. et. al. // Journal of Engineering Thermophysics. 2002. V. 11, No. 4 – P. 321 – 333

Chinnov E. A. // IJHMT, 2014. V. 71. p. 106-116.

# Criterion of dry spot development in isothermal liquid film on a horizontal substrate

Leonid I. Maltsev and Oleg A. Kabov

Institute of Thermophysics, SB RAS, prosp. Lavrentyev 1, Novosibirsk, 630090, Russia

Studies of rupture of thin liquid films on solid surfaces are important for modeling of multiphase flows in microfluidic devices, heat exchange systems, mining industry, and for biomedical applications such as dynamics of the tear film in the eye, [1]. When the interface approaches the wall, the film can rupture, resulting in the formation of a three-phase contact line. The overall dynamics of many types of multiphase flows encountered in applications depends on these local phenomena, [2]. In cooling systems based on thin-film flows driven by either gravity or shear stresses at the liquid-gas interface, formation of dry spots results in significant reduction of heat flux from the heated wall, as shown experimentally in [3]. Liquid films flowing under gravity over a localized heater on vertical or inclined flat plates rupture for sufficiently high values of the heat flux generated by the heater, [4,5].

The present work presents a mathematical model to obtain the criterion of the emergence and development of the dry spots in isothermal liquid films. Isothermal liquid film on a horizontal solid substrate are considered. At some point in the film a dry spot in the shape of a circle occurs, Fig. 1. A characteristic liquid bump surrounds the dry spot that is in good agreement with the experimental results [4]. The cross-section of the bump is formed under the influence of gravity and surface tension forces, Fig. 2.

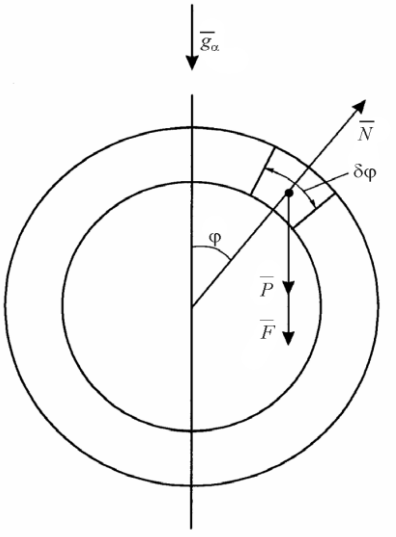


Fig. 1. Schematic of the flow.

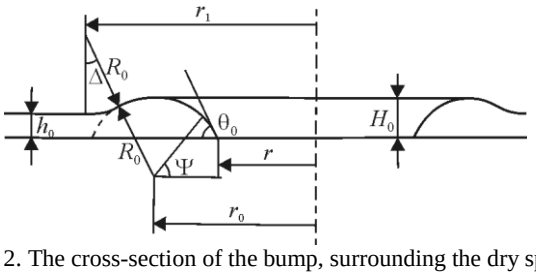


Fig. 2. The cross-section of the bump, surrounding the dry spot.

$$N = \sigma(-K + 1 - \cos\theta_0) r_0 \delta\varphi.$$

$$K = \int_{(L)} \frac{\cos^2\psi}{r(\psi)} R(\psi) d\psi.$$

Force $N$ is the only active force on each element of bump in the direction of bump radii in case of neglecting by gravity force. Bump begins to grow symmetrically, absorbing film of liquid, or shrink. Let us neglect the fluid redistribution inside the bump. Then the sign of $N$ determine behavior of the initial small dry spot in the film. The criterion $N(r_0) = 0$ is a condition of equilibrium, motionless position of the hole in the film of liquid. For a given geometry of the bump, the critical value of $r_0$ is determined by the thickness of fluid film and by the equilibrium contact angle, Fig. 3.

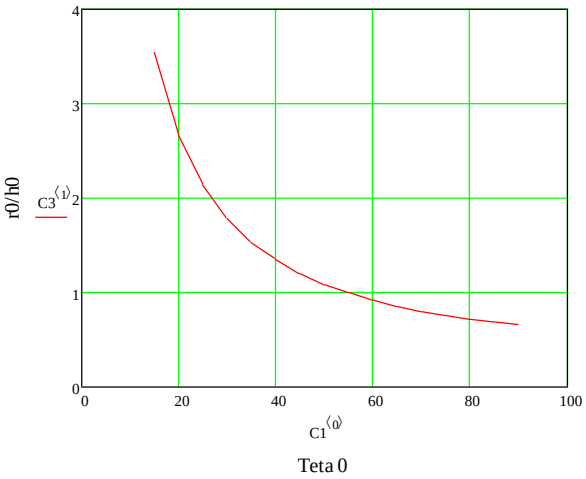


Fig. 3. Dependence $r_0/h_0$ vs $\theta_0$.

**Acknowledgements** The study was financially supported by the Ministry of Education and Science of Russia (Project identifier RFMEFI61314X0011).

**References**

[1] V.S. Ajaev, Instability and Rupture of Thin Liquid Films on Solid Substrates, *Interfacial Phenomena and Heat Transfer*, 1(1), pp. 81 – 92, 2013.

[2] Vladimir S. Ajaev, Elizaveta Ya. Gatapova, Oleg A. Kabov, Stability and break-up of thin liquid films on patterned and structured surfaces, *Advances in Colloid and Interface Science*, Vol. 228, February, pp. 92-104, 2016.

[3] Kabov, O. A., Breakdown of a liquid film flowing over the surface with a local heat source, *Thermophys. Aeromech.*, vol. 7, pp. 513–520, 2000.

[4] D.V. Zaitsev, D.P. Kirichenko, O.A. Kabov, The Effect of Substrate Wettability on the Breakdown of a Locally Heated Fluid Film, *Technical Physics Letters*, Vol. 41. No. 6. P. 551–553, 2015.

[5] Yu. V. Lyulin, S. E. Spesivtsev, I. V. Marchuk, and O. A. Kabov, Investigation of Disruption Dynamics of the Horizontal Liquid Layer with Spot Heating from the Substrate Side, *Technical Physics Letters*, Vol. 41, No. 11, pp. 1034–1037, 2015.

# Effect of Tube Diameter on Void Fraction Characteristics of One-Component Vertically Upward Two-Phase Flow

Taisaku GOMYO, Hitoshi ASANO

Department of Mechanical Engineering, Kobe University
1-1, Rokkodai, Nada, Kobe, 657-8501, Japan
E-mail : asano@mech.kobe-u.ac.jp

The purpose of this study is to clarify the transition boundaries in the dominant force map, especially to clarify the condition in which the effect of gravity becomes little in comparison with the effect of surface tension. This study focuses on void fraction characteristics of vertically upward flows in small circular tubes using FC-72 as the working fluid. The effect of the tube diameter was examined for 4.0, 2.0, 1.1 and 0.5 mm diameter tubes.

The test section was consisted of the heating section and observation section as shown in Fig. 1. In the heating section, the refrigerant became a two-phase flow by Joule heating and local heat transfer coefficients were measured by K-type thermocouples mounted on the thin wall stainless steel tube. In the observation section, void fraction measurements by a capacitance sensor and flow behavior observations by a high frame rate camera were conducted simultaneously. The detail of the observation section is shown in Figure 2. A parallel plate type capacitance sensor was selected as the electrode arrangement. For each tube diameter, $D_{in}$, the length of the sensing area, $L$, was unified in $L/D_{in}$=4.0. Volumetric average void fraction, $\alpha$, was measured from the capacitance, $C$, by using the capacitance for vapor single-phase, $C_G$, and liquid single-phase, $C_L$, in this equation, $\alpha = (C_L - C) / (C_L - C_G)$. The experimental conditions are shown in Table 2. To make mass flux stable, in the experiments for 0.5 mm tube a syringe pump was used.

From the flow observation, churn flows were not observed in the 1.1 and 0.5 mm tubes. The measured void fractions are plotted against vapor quality for varied mass flux conditions in Fig. 3. The Cioncolini's model overestimated the void fractions. The void fraction became lower with decreasing the mass flux and decreasing the tube diameter.

To examine the liquid film structures in annular flows, the void fraction fluctuations were compared for almost the same vapor quality conditions with 200 kg/m$^2$s, as shown in Fig. 4. The void fraction for the 0.5 mm tube was lower than the other tubes, because the base liquid film thickness for the 0.5 mm tube was thicker. The passing frequency of disturbance waves became higher with decreasing the tube diameter, and the wave height increased with decreasing the tube diameter due to the increase in the effect of surface tension.

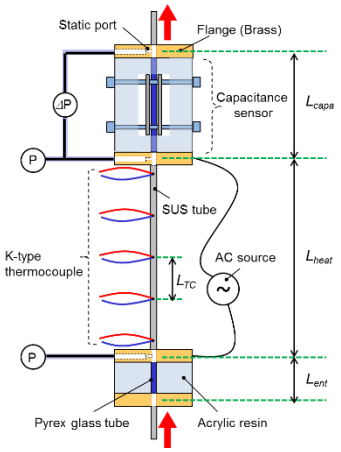


**Figure 1:** Detail of the test section.

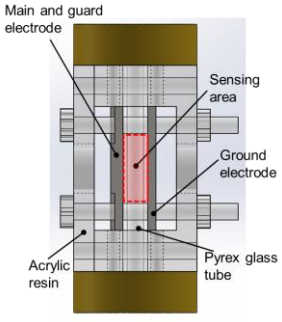


**Figure 2:** Detail of the capacitance sensor.

**Table2**: Experimental conditions.

| $D_{in}$ | Mass flux $G$ [kg/(m$^2$s)] | Vapor quality $x$ [-] | Pressure $P$ [kPa] |
|---|---|---|---|
| 4.0 | 30 ~ 600 | -0.1 ~ 0.8 | 100 ~ 140 |
| 2.0 | 100 ~ 600 | -0.1 ~ 0.8 | 100 ~ 180 |
| 1.1 | 70 ~ 600 | -0.1 ~ 0.8 | 100 ~ 160 |
| 0.5 | 200 ~ 600 | -0.1 ~ 0.8 | 100 ~ 180 |

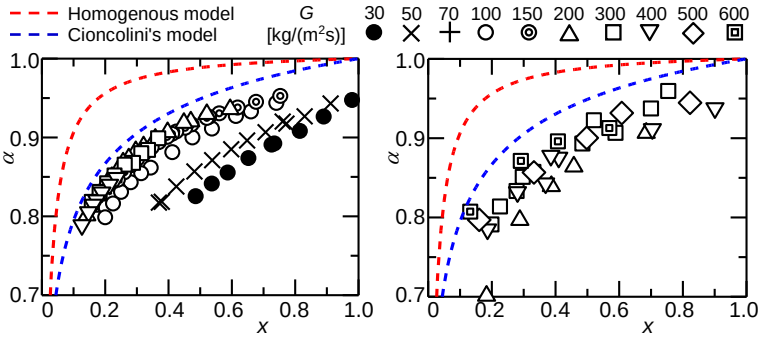


(a) $D_{in}$ = 4.0 mm (b) $D_{in}$ = 0.5 mm

**Figure 3 :** Comparison of measured void fractions with predicted results by the homogeneous and Cioncolini and Thome (2012) model for annular flow.

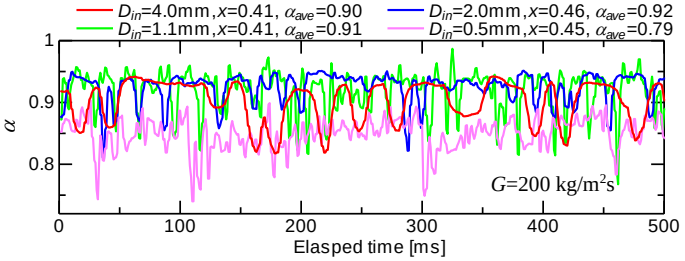


**Figure 4 :** Void fraction fluctuation of annular flow.

## References

Cioncolini, A. and Thome, J.R., Void Fraction Prediction in Annular Two-Phase Flow, Int. J. of Multiphase Flow, Vol. 43, pp. 72-84, (2012).

# Two-Layer Fluid Flows With Evaporation: Analytical Methods and Comparison with Experiments

Victoria B. Bekezhanova[1], Olga N. Goncharova[2,3]

[1]Department of Differential Equations of Mechanics, Institute of Computational Modeling SB RAS, Academgorodok 50/44, Krasnoyarsk, 660036, Russia
[2]Department of Differential Equations, Altai State University, Lenina 61, Barnaul, 656049, Russia
[3]Laboratory of Enhancement of Heat Transfer, Institute of Thermophysics SB RAS, Lavrentyev 1, 630090, Novosibirsk, Russia
bekezhanova@mail.ru, gon@math.asu.ru

The modern technologies and experimental methods of investigation of the features of the joint convective liquid flows and cocurrent gas fluxes at normal and microgravity are actively developed at the present time. Improvement of the existing techniques and development of new experiments are often based on theoretical results obtained as a results of mathematical modeling of the two-layer flows with interfaces. Such factors as media flow rates, their thermophysical properties, type of a thermal load on the flow domain boundaries and linear scales influence the character of the convective flows (Lyulin and Kabov 2013, 2014).

By mathematical modeling a special attention is paid to construction and investigation of the exact solutions describing the convective flow and taking into account the mass transfer at interface, in particular, due to evaporation. The importance of exact solutions (solutions of special type) is explained by opportunities of a rapid, sensitive and effective analysis of the physical factors, acting on the main flow mechanisms. In the case of a multiparameter problem we can examine the degree of influence of the different physical factors on the flow characteristics and criteria of its stability. The result of such analysis can lead to the refinement of the mathematical model in order to describe the investigated flows more adequately.

In the present work an overview of the analytical methods used for study of the problems on two-layer flows and appearing difficulties are presented. The methods include formulation of the physically meaningful and correct mathematical models, analysis and interpretation of the exact solutions and their generalization in the framework of the models, investigation of stability of these solutions.

We managed to construct a generalization of one of the exact solutions of the Oberbeck- Boussinesq equations. The solution is the analogue of the Birikh-Octroumov solution and describes a joint flow of an evaporating viscous heat-conducting liquid and gas-vapor mixture in the horizontal channel. The basic equations in the gas phase and the interface conditions have additionally terms responsible for the effects of thermodiffusion and diffusive heat conductivity. In this solution the temperature, pressure and concentration of the vapor in the upper gas phase linearly depend on the longitudinal coordinate. Only longitudinal components of the velocity vectors in the upper and lower layers are not equal to zero and depend on the transverse coordinate. This solution has a group nature and describes different classes of flows. Variety of the flow types is explained by properties of the solution. Influence of the boundary conditions and physical effects on the properties of the solution and, consequently, on the characteristics of the two-layer flows are investigated. Classification of the flow types depending on boundary conditions for concentration function and given parameters of the problem is proposed. The obtained results are compared with experimental data. The qualitative and in some cases quantitative coincidence of the theoretical and experimental results has been justified.

Methods of the stability theory allow us to describe and to clarify a formation of the thermocapillary and vortex structures in the considered system. In the case of equal thermal load on the boundaries of the flow domain the normal mode method can be used for investigation of the linear stability due to the properties of basic equations and constructed exact solution. In the case of different thermal load on the channel walls a transition to the “stream function – vorticity” terms and numerical solution of the spatial-temporal problem allow to predict the dynamics of the disturbances and to obtain the conditions when we can guarantee the stability of the basic flow regimes.

Influence of the external disturbing actions, such as gas flow rates and thermal load, on flow characteristics is investigated. Typical forms of appearing disturbances are defined and critical values of the flow rates and longitudinal temperature gradients are obtained. Thus we can point out the most dangerous mechanisms in the space of the problem parameters. Furthermore, influence of evaporation on stability characteristics is studied. In the system the high frequency regimes can be formed.

The proposed analytical methods enable to improve the theoretical and experimental modeling of the two-layer fluid flows with interfacial processes.

**Acknowledgments.** The research has been supported by the Russian Foundation for Basic Research (Project No. 14-08-00163).

**References**

Lyulin Y., Kabov O., Measurement of the evaporation mass flow rate in a horizontal liquid layer partly opened into flowing gas, Technical Physics Letters, 39(9), 795-797 (2013)

Lyulin Y., Kabov O., Evaporative convection in a horizontal liquid layer under shear-stress gas flow Int. J. Heat Mass Transfer, 70, 599-609 (2014)

Goncharova, O.N., Rezanova, E.V., Example of an exact solution of the stationary problem of two-layer flows with evaporation at the interface, Journal of Applied Mechanics and Technical Physics, 55 (2), 247-257 (2014)

# Thermofluid Characteristics of High Quality Microgap Flow

Avram Bar-Cohen, Caleb A. Holloway

University of Maryland, College Park, MD 20742, USA

The ongoing demand for greater compactness, higher functionality, and higher feature count in electronic components, as well as the emergence of the three-dimensional packaging paradigm, continue to drive chip power dissipation, heat flux, and heat density to higher values. High-quality, microfluidic evaporative cooling, with dielectric liquids flowing in a microgap adjacent to a single active chip or in the microgaps between chips in a chips stack, offers highly potent thermal management capability and is the foundation for the emerging "embedded cooling" paradigm of electronic cooling. While the thermofluid characteristics of such flows are intimately tied to distinct forms of vapor-liquid aggregation, insufficient attention has been paid to characterizing the regimes, sub-regimes, and interfacial wave patterns in high-quality microgap channel flow.

This Keynote presentation will open with a review of the thermophysical phenomena underpinning two-phase microgap flow and heat transfer, followed by a brief survey of microgap studies underway around the world. Attention will then be focused on 3 recent studies in the TherPES Laboratory at UMD: a fundamental study of flow patterns and thin film behavior in a “long” microgap channel, a fundamental visualization study of a “chip-scale” microgap channel using visible and IR wavelengths, and an applied study of microgap thermal management, using a thermally-simulated microprocesor chip.

# Copper-Water Loop Heat Pipes – Highly Efficient Two-Phase Heat Transfer Devices

Yury F. Maydanik

Institute of Thermal Physics
Ural Branch of Russian Academy of Science
Amundsen St. 105A, Ekaterinburg, 620016, Russia
maidanik@etel.ru

Copper-water loop heat pipes (LHPs) are promising devices for providing an effective thermal link between a heat source and a heat sink in cooling systems of powerful heat sources having relatively small dimensions and operating in the temperature range from 50 to 100 °C [1-6]. Thermophysical properties of water as a working fluid and high thermal conductivity of copper as a constructional material for a body and a wick as well as their good compatibility make it possible to achieve an extremely high heat flux and low thermal resistance of such LHPs. Today the obtained values of these parameters are close to 1000 W/cm$^2$ and 0.05 °C/W, respectively. However, making copper-water LHPs one has to overcome a serious contradiction between the high thermal conductivity of copper and the low value of $dP/dT$ which water has at temperature below 100 °C. The last circumstance is connected with the so called thermodynamic condition of an LHP serviceability which may be written as follows:

$$\Delta T \frac{dP}{dT} = \sum \Delta P - \Delta P_w ,$$

where $\Delta T$ and $\Delta P$ is the difference of temperatures and pressures of the saturated vapor above the wick evaporating surface and the liquid-vapor interface in the compensation chamber, $\Delta P_w$ is the pressure losses in the wick, $dP/dT$ is the is the derivative that characterizes the slope of the saturation line of the working fluid at a given temperature.

Computer simulations and experimental investigations of copper-water LHPs have shown that despite the mentioned contradiction achievement of high performance characteristics is possible with the optimal choice of design parameters of the devices.

The paper presents the results of numerical and experimental investigations of copper-water LHPs with cylindrical evaporators 6-8 mm in diameter and flat evaporators 3-7 mm thick as well as shows example use of the given devices in cooling systems of different electronics.

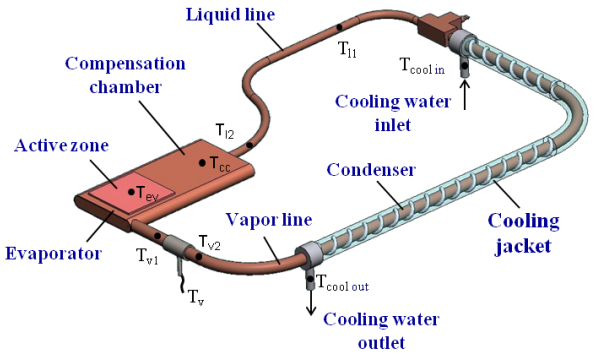


**Figure 1:** Copper-water LHP

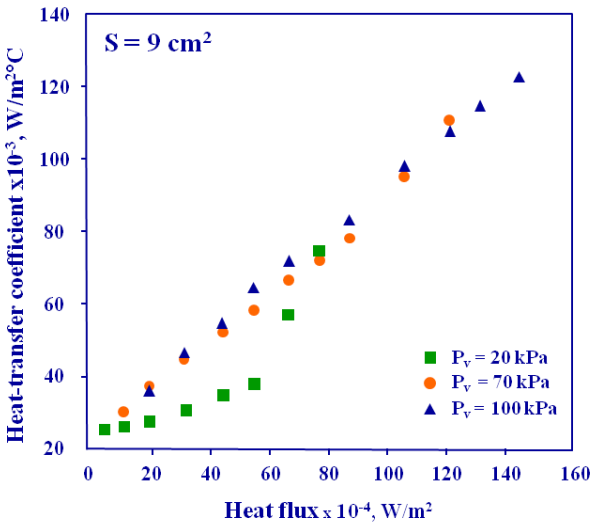


**Figure 2:** Heat-transfer coeff. in the evaporation zone vs Heat flux

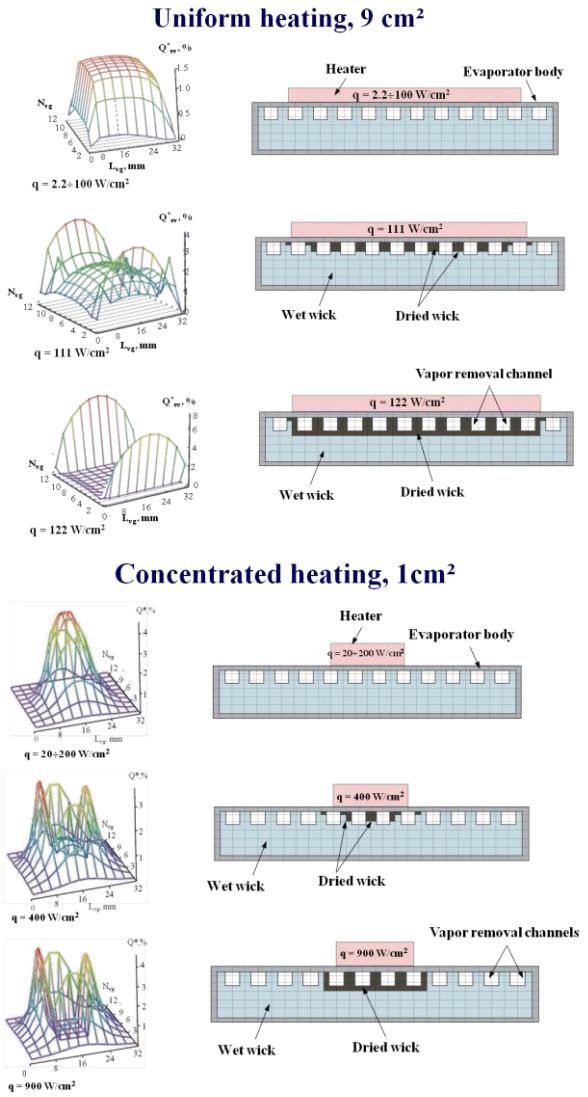


**Figure 3:** Evolution of evaporating wick surface

## References

Maydanik Yu.F., Miniature loop heat pipes, Keynote lecture, Proceedings of the 13th International Heat Pipe Conference, Shanghai, China, September 21-25, pp. 24-37 (2004)

Maydanik Yu.F., Vershinin S.V., Development and investigation of copper-water loop heat pipes with high operating characteristics, Heat Pipe Science and Technology, Vol. 1 pp. 151-162 (2010)

Maydanik Yu.F., Loop heat pipes – state-of-the-art and industrial application, Keynote lecture, Proceedings of the 9th International Heat Pipe Symposium, Kuala Lumpur, Malaysia, November 17-20, pp. 13-25 (2008)

Becker S., Vershinin S.V., Sartre V., Laurien E., Bonjour J., Maydanik Yu.F., Steady state operation of a copper–water LHP with a flat-oval evaporator, Applied Thermal Engineering, Vol. 31 pp. 686–695 (2011)

Maydanik Yu.F., Vershinin S.V., Chernysheva M.A., Yushakova S., Investigation of a compact copper–water loop heat pipe with a flat evaporator, Applied Thermal Engineering, Vol. 31 pp. 3533–3541 (2011)

Maydanik Yu.F., Chernysheva M.A., Pastukhov V.G., Review: Loop heat pipes with flat evaporators, Applied Thermal Engineering, Vol. 67 pp. 294–307 (2014)

# FILM THICKNESS MEASUREMENT FOR ELONGATED BUBBLE FLOW IN MICROCHANNEL USING LIF

Bartkus G. V.[1,2], Kuznetsov V. V.[1,2]

[1] Novosibirsk State University, 630090, Pirogova, 2, Russia
[2] Kutatelad3
.
ze Institute of Thermophysics, 630090, Academician Lavrentyev Avenue, 1, Russia
germanbartkus@gmail.com

Using high-speed video recording and method LIF the elongated bubble gas-liquid flow characterization in rectangular microchannels with aspect ratio of 1.5 was considered. The distributions of the phases in cross-section of the microchannel, with hydraulic diameter less then the capillary constant, were identified in a wide range of liquid and gas flow rates. Experiments were carried out for the flow of a water-nitrogen in vertical microchannel with cross section 420x280 μm. For gas-liquid flow formation T-mixer was used at the channel inlet.

The aim of this work was studying the mechanism of multi-scale two-phase gas-liquid flow formation in rectangular microchannel of the microfluidic devices. It was found that the regime with elongated gas bubbles, the transition and annular flow regimes are the main patterns of a flow for microchannel with hydraulic diameter substantially less than the capillary constant and aspect ratio of 1.5. Using high-speed video recording and method LIF, the rates of elongated bubble were measured and compared with mixture superficial velocities and capillary numbers.

Using laser-induced fluorescence (LIF) method, which provides high spatial resolution without making hydrodynamic disturbances, the distribution of local thickness of liquid film along a cross section was measured for elongated bubbles flow and transition flow in the vertical microchannel. Rhodamine 6G was used as a fluorescent dye in the experiments. Distribution of a liquid film thickness along the long side of microchannel measured by LIF is shown on Fig.1. The data are presented for three gas superficial velocities and fixed liquid superficial velocity. One can see that capillary forces deform the interface and maximal film thickness is observed in the middle of a long side of the microchannel. Accurate film thickness measurements for whole meniscus in the channel's corner using this technique are impossible.

The dependences of liquid film thickness on Capillary number and channel size were determined and compared with existing correlations. Figure 2 shows the dependence of dimensionless liquid film thickness in the middle of long side of the channel with length *a* (scaled by microchannel hydraulic diameter) on the capillary number. The experiments were done for elongated bubble flow and transition flow and liquid film thickness is presented for two dimensionless distances from the bubble head *L/a*. Using this method, it was found failure to comply with the Taylor law [1] in rectangular microchannel. Here the experimental data of [2] are presented also.

The work was supported in part by the grant RFBR №15-08-07506-A.

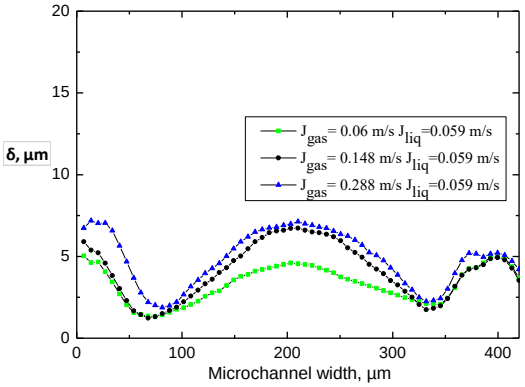


**Figure 1:** Distribution of a liquid film thickness along the long side of microchannel measured by LIF.

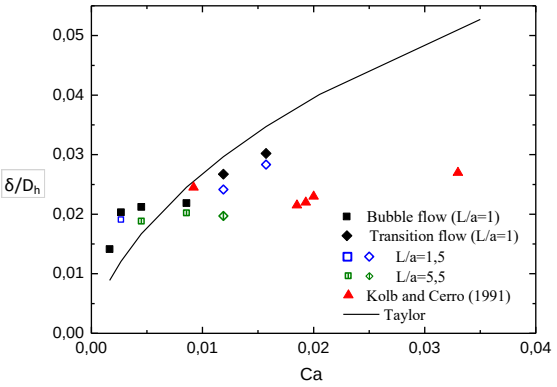


**Figure 2:** Dependence of dimensionless film thickness on the capillary number.

## References

1. *Aussilous P., Quere D.* Quick deposition of a fluid on the wall of a tube // Phys Fluids. 2000. Vol. 12 (10). P. 2367-2371.
2. *Kolb W.B., Cerro R.L.* Coating the inside of a capillary of square cross-section // Chemical Engineering Science. 1991. Vol. 46 (9). P. 2181–2195.

# Liquid-liquid two-phase flow patterns in T-junction rectangular micro-capillaries

A.A. Yagodnitsyna[1,2], A.V. Kovalev[1,2], A.V. Bilsky[1,2]

[1]Kutateladze Institute of Thermophysics of SB RAS, [2]Novosibirsk State University
[1]Lavrentiev ave., 1, 630090, Novosibirsk, Russia, [2]Pirogova str., 2, 630090, Novosibirsk, Russia
bilsky@itp.nsc.ru

In last decade microreactors have become alternative to traditional reactors in chemical industry and biotechnology. Channels with submillimeter hydraulic diameter have extremely large surface to volume ratio which leads to intensification of heat and mass transfer. Besides that microreactors have such advantages as small volume of reacting fluids and better reaction control. Flows of immiscible liquids in microchannels are important for different kinds of technical applications such as microreactors in chemistry, bioMEMS devices, extraction reactions, emulsions production etc. In the present paper experimental investigation of immiscible liquids flow in a T-shaped microchannel was carried out.

A flow of tree sets of immiscible liquids in a rectangular microchannel with T-junction made of SU-8 material was studied. Liquid-liquid sets were kerosene – water; paraffin oil – water; paraffin oil – castor oil. The size of inlet channels was 200x200 um, the size of outlet channel was 200x400 um. We used high speed camera (pco.1200 hs) and inverted microscope (Zeiss Axio Oberver.Z1) with 5x magnification to visualize flow patterns and interfacial dynamics. The flow of liquids was controlled by KDS Gemini 88 double syringe pump. Density, viscosity, interfacial tension and contact angles of all liquids were measured directly prior experiments.

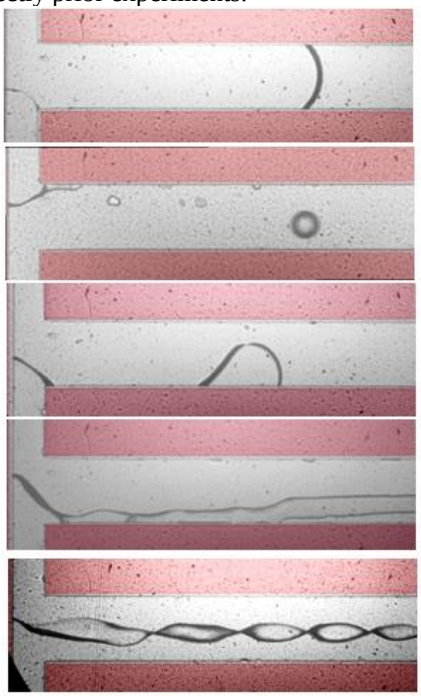

**Figure 1:** Typical flow patterns for kerosene and water near the T-junction. From top to bottom: plug flow, droplet flow, slug flow, rivulet flow and parallel flow with steady wavy interface.

For water-kerosene flow we observed following flow patterns: plug flow (water in kerosene), slug flow (for both liquids), droplet flow (water in kerosene), rivulet flow (for both liquids) and parallel flow. It is important to notice that we didn't observe annular flow because of low contact angle of both liquids. High surface wettability was the reason for occurrence of slug flow for both liquids and rivulet flow instead of annular flow. New flow pattern of parallel flow with steady wavy interface was found. Flow visualization of paraffin oil – water and paraffin oil – castor oil gave similar flow patterns.

As flow visualization was done we derived flow map using Weber number of both liquids (Fig. 2). The flow map was different from that obtained by Zhao et al. (2006). So we can conclude that Weber number is not the only parameter which defines flow regime. Comparison of flow maps for all liquid sets showed that those were similar to each other but pattern transition was on different Weber numbers. In order to take into account fluid viscosity we constructed new flow maps based on Weber number multiplied by liquid viscosity (Fig.2). After that flow maps coincided with each other.

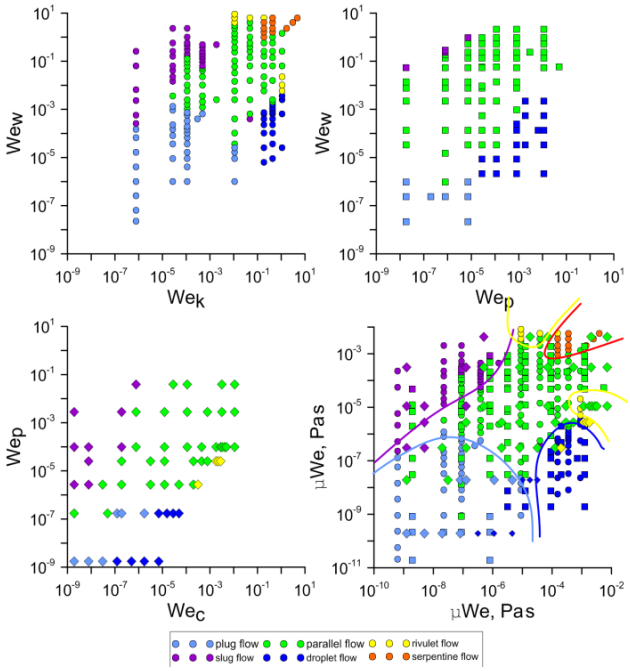


**Figure 2:** Flow pattern maps for kerosene-water (top left), paraffin oil-water (top right), paraffin oil – castor oil (bottom left). Modified joint flow map for all liquid systems (bottom right).

## References

Zhao, Y., Chen, G., Yuan, Q. Liquid–liquid two-phase flow patterns in a rectangular microchannel. // A.I.Ch.E. Journal 52 (2006) – PP. 4052–4060

# Mathematical modeling of motion of an isolated liquid plug inside a dry capillary tube

Vyas Srinivasan, Sameer Khandekar*
IIT Kanpur, Department of Mechanical Engineering
Kanpur, 208016, India
samkhan@iitk.ac.in

## Introduction

A mathematical model is developed to predict the pressure drop across an isolated, partially wetting liquid plug in a capillary tube (Bo < 2). The liquid plug (water) at rest with defined static contact angle $\theta_s$ is made to move by forcing air at constant flow rate from one end, while the other side is open to atmosphere, as reported in [1]. The model takes into account the pressure drop due to contact angle hysteresis and dissipation due to contact line motion, which has been missing from the previous literature [2].

## Flow physics and modeling

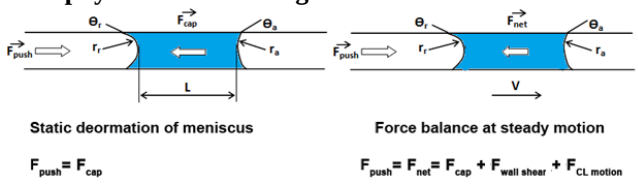


Figure 1 shows the forces acting on an isolated liquid plug of known *L/D*, during rest and motion.

- 0 to A: During this phase, $\theta_s < \theta_a < \theta_{a,cric}$ and $\theta_s > \theta_r > \theta_{r,cric}$. i.e., the liquid plug is still at rest and the meniscus deforms to satisfy Young's condition. 'A' corresponds to maximum deformation ($\theta_a = \theta_{a,cric}; \theta_r = \theta_{r,cric}$). If, $\theta_{a,cric}$ and $\theta_{r,cric}$ (which are independent of *L/D* ratio and depends on surface forces) are known, then the pressure drop can be modeled as (assuming air as ideal gas):

$$PV = mRT \qquad (1)$$ Taking time derivative,

$$PV' + VP' = m'RT \qquad (2)$$

when the liquid is at rest, and at known mass flow of pushing air, solving the below equation gives the pressure rise till the limiting pressure is reached at $t=t_{cric}$,

$$P' = m'\left(RT/V\right) \quad \because V' = 0 \qquad (3)$$ The limiting capillary pressure drop is given by:

$$\Delta P_{cap,cric} = 2\sigma/r\,(\cos\theta_{r,cric} - \cos\theta_{a,cric}) \qquad (4)$$

- A to B: Here, the liquid plug completely starts to move, i.e. $\theta_a > \theta_{a,cric}$ and $\theta_r < \theta_{r,cric}$. Once the motion commences, the pressure drop is found by:

$$P' = (m'RT - PV')/V \qquad (5)$$

$$x' = u \qquad (6)$$

$$u' = F_{net}/m_{liquid} \qquad (7)$$

solving coupled equations 4-6 with initial condition: $t = t_{cric}, P = \Delta P_{cap,cric}; x = x_{initial}; u = 0$. $F_{net}$ is the total force acting on the liquid during motion which is given by:

$$F_{net} = csa*(P - (P_{cap} + P_{flow} + P_{CL})) \qquad (8)$$ where, *P* is the pressure of pushing air and:

$$P_{cap} = 2\sigma/r\,(\cos\theta_r - \cos\theta_a) \qquad (9)$$ where, $\theta_r$ and $\theta_a$ are obtained from Tanner's law during motion.

$$P_{flow} = 8\mu uL/r^2 \qquad (10)$$ $P_{flow}$ is based on Poiseuille pressure drop for laminar fully developed flow and,

$$P_{CL} = \mu_{CL} u_{CL}/r \qquad (11)$$ $P_{CL}$ is the dissipation at contact line where, $\mu_{CL}$ is the apparent viscosity modeled in terms of capillary length scales and $u_{CL}$ is the contact line velocity at depinning transition [3], which are modeled as:

$$u_{CL} = u((P/P_{cap,cric}) - 1)^{\beta} \qquad (12)$$

$$\mu_{CL} = \mu(l_{cap}/r_c) \qquad (13)$$ where, $l_{cap} = \sqrt{\sigma/\rho g}$ and $r_c$ is the microscopic length scale ~ 10 Å. Neglecting this contact line motion leads to under-predict the observed pressure drop (Figure 2). This model is also tested for different wetting fluids (different contact angle hysteresis), where pinning of contact line is different and it provides a good fit, which is not reported here for brevity.

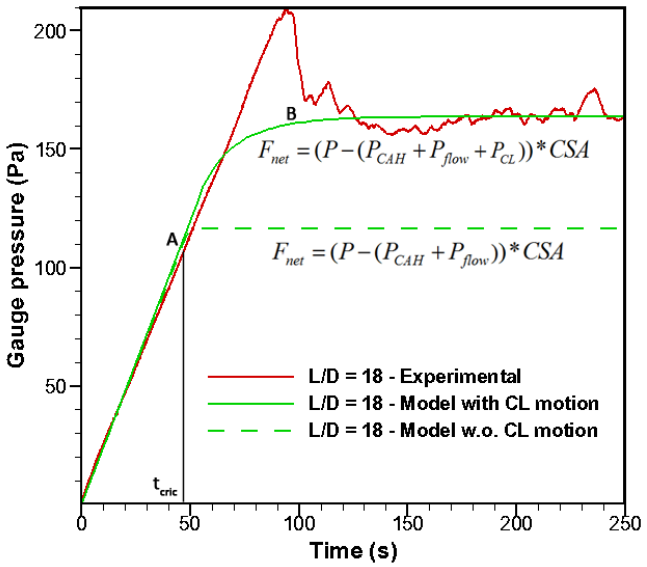


Figure 2: The comparison of model with experiment is shown. It is seen that excluding the contact line motion at start of the motion under-predicts the net pressure drop.

## References

Vyas S., Khandekar S., Bouamrane N., Lefevre F. and Bonjour J., Motion of an Isolated liquid plug inside a capillary tube: effect of contact angle hysteresis, Experiments in Fluids, Vol. 56:14 (2015).

Qu J, Wang Q, Li C, Han X, He Z, A simple model for Taylor flow induced contact angle hysteresis and capillary pressure inside mini/micro-scale capillary tubes. Int. Journal of Heat and Mass Transfer, Vol. 78:1 (2014).

Schaffer E, Wong P, Contact line dynamics near the pinning threshold: A capillary rise and fall experiment. Physical Review E, Vol. 61:5 (2000).

# Liquid flow over bubbles on hydrophobic surface with contrast wettability

Elizaveta Gatapova, Dmitry Gluzdov and Oleg Kabov

Kutateladze Institute of Thermophysics SB RAS, Lavrentyev Ave., 1, Novosibirsk, 630090, Russia
E-mail gatapova@itp.nsc.ru

One of the major obstacles to the development and use of microsystems with long microchannels is a significant pressure drop along the channel, which can reach 5-10 atmospheres. The need to maintain such a high pressure drop is associated with the problem of fluid transport in the small devices used in microfluidics and microsystems (Squires and Quake, 2005). Since the viscous resistance is high, very large pressure gradient is required for liquid transport in a microchannel. The solution to this problem could be to change the properties of the solid surface of the channel through which the fluid flows by using micro / nanostructuring. In this case, the flow rate should increase at a fixed pressure gradient (Rothstein 2010).

Recent experimental studies on two-phase channel flows past chemically patterned surface showed that the bubbles of gas phase in the liquid tend to accumulate in the regions of lower wettability. It has been proposed to use the effect of concentration of gas bubbles on hydrophobic segments of the surface of the channel with contrast wettability for ensuring drag reduction (Gatapova et al. 2015). Two regimes of flow with the concentration of bubbles in the hydrophobic region are analyzed (Fig. 1). The first one is a regime without heating, where small gas bubbles in the flow precipitate in the hydrophobic region. The nanocoating ensured the contrast of wettability of about 20°–25° between the surface of the silicon plate and coating. The second regime was produced specially for the enhancement of the effect: a heater mounted beneath the hydrophobic region was switched on and the process of nucleation of bubbles began.

The two-dimensional approach of NS equations is considered. A two–dimensional flow model with the Navier slip condition (Belyaev and Vinogradova 2010) in the region of the bubble layer gives criteria for drag reduction, depending on the slip length, dimension of bubbles, and dimension of the segment with nanocoating. The presence of the bubble layer on half of the surface of the channel can increase the flow rate of a liquid flowing through the channel by 40% at a fixed pressure gradient (Fig. 2).

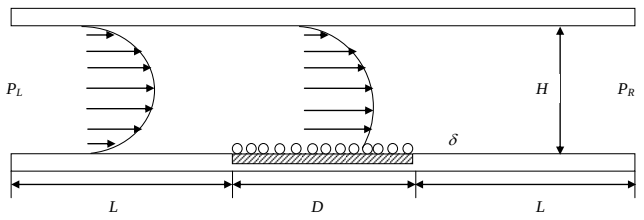


**Figure 1:** Sketch of the flow over bubbles.

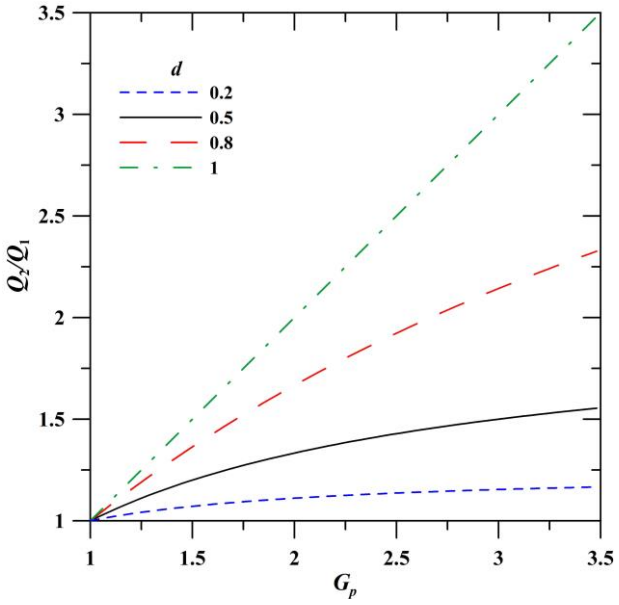


**Figure 2:** Ratio of the flow rates of the flowing liquid versus the ratio of the pressure gradients for the cases where the region with coating is 20, 50, 80, and 100%.

This work was supported by a grant from the Russian Science Foundation (project Nr. 14-19-01755).

## References

Squires T. M. and Quake S.R., Microfluidics: Fluid physics at the nanoliter scale// Rev. Mod. Phys. – 2005- 77 - 977.

Rothstein J. P., “Slip on superhydrophobic surfaces” Annu. Rev. Fluid Mech. 42: 89-109, 2010.

Gatapova E.Ya., Ajaev V.S., Kabov O.A. On drag reduction in a two–phase flow. JETP Letters 101(3). P. 176-180 (2015).

Belyaev A.V., Vinogradova O.I., Effective slip in pressure-driven flow past super-hydrophobic stripes. J. Fluid Mech., 652, 489-499 (2010).

.

# Features of two-phase flow patterns in horizontal rectangular microchannels of height 50 μm

Fedor V. Ronshin, Evgeny A. Chinnov, Vyacheslav V. Cheverda and Oleg A. Kabov

Kutateladze Institute of Thermophysics, Siberian Branch, Russian Academy of Sciences
Lavrentiev ave. 1, Novosibirsk, 630090, Russia
E-mail: f.ronshin@gmail.com

At present, there is revolutionary development in heat-exchange systems with micro- and nanosizes, which have proved to be much more energy efficient than macrosystems with the channel sizes of 3–100 mm. With a decrease in the thicknesses of flat channels, the surface to volume ratio of the channel increases inversely proportional to its minimum transverse size, this causes high intensity of heat transfer in the microsystems. Such systems are receiving increasingly wider application in microelectronics, aerospace industry, transport, and power engineering.

The studies on two-phase flows in channels with different geometries are reviewed in Chinnov and Kabov (2006). It is shown that in most publications relatively long channels, where the conditions of liquid and gas entry to the channel do not have a significant effect on the structure of two-phase flow, are considered. In such systems, the length of the channels is two or more orders of magnitude higher than their transverse dimension. The short channels have broader prospects of use in technical applications, for example, in biochips and cooling devices for microelectronics. In the heat exchangers on the basis of short microchannels, sufficiently small pressure drops can be achieved. Despite the relevance of the study of two-phase flows in the short channels, the number of publications on this subject is very limited. The gas-liquid flows in the short horizontal minichannels have been studied systematically in Chinnov et al. (2016). New flow regimes, which can be associated with new types of instability in the flow of water and Nitrogen gas in horizontal rectangular channels, have been determined.

The two-phase flow in a narrow short horizontal channel of a rectangular cross-section with the height of 50 micrometers and width of 40 mm has been studied experimentally in the present work. The main part of the test section is a stainless steel plate with the length of 160 mm and width of 60 mm. The plate has been covered with an optical glass lid. Figure 1 shows the test section with the channel. Air or nitrogen gas has been supplied from a balloon via flat nozzle (1). The liquid has been driven by a peristaltic pump and have introduced into the gas flow via flat nozzle (2). The use of the Schliren method has made it possible to reveal the flow of liquid in the channel and to determine its characteristics quantitatively. The two-phase flow regimes and transition between them have been studied. The classical patterns of two-phase flow in the channel (bubble, stratified, churn and annular) have been detected. Experimental information allows us to define the characteristics of the regimes and to determine precisely the boundaries between the patterns of the two-phase flows.

The feature of the channels height below of 200 μm in comparison with the higher channels is the presence of many drops in the gas jet. Drops appear for all two-phase flow patterns in the channel height of 50 μm. Two particular regimes that can be distinguished represent (i) formation of immobile drops on the channel wall due to liquid film or bridge breakage and (ii) appearance of mobile drops because of the two-phase flow instability. The second case is illustrated by the Schlieren image Figure 2, where the dark regions correspond to liquid filling the channel from the top to the bottom and the bright regions represent the liquid on the inner surface of the top cover. After the ejection of liquid towards the center (caused by perturbation) and its subsequent return, a fraction of ejected liquid separated in the form of a drop. The diameters of these drops exceeded the channel thickness and were typically is from 50 μm to several millimeters, while their shapes were nearly circular due to the action of capillary forces.

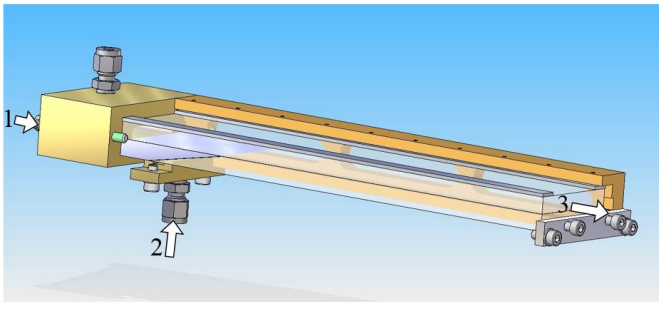


Figure 1: Test section with the channel height of 50 μm.
(1) gas flow inlet; (2) liquid flow inlet; (3) two-phase flow outlet

**References**

Chinnov E.A., Kabov O.A., Two phase flow in pipes and capillary channels, High Temperatures, Vol. 44, no. 5, pp. 773-791 (2006).

Chinnov E.A., Ron'shin F.V., Kabov O.A. Two-phase flow patterns in short horizontal rectangular microchannels // International Journal of Multiphase Flow, Vol. 80, pp. 57–68 (2016)

Figure 2: Mobile drops in the annular pattern, channel height=50 μm

# Two layer dielectric-electrolyte micro-flow with pressure gradient

Georgy Ganchenko[1], Abhishek Navarkar[2], Evgeny Demekhin[1], Michael Zhukov[3] and Sakir Amiroudine[2]

[1]Laboratory of Micro- and Nanoscale Electro- and Hydrodynamics for the Krasnodar Branch of Financial University,
34 Luzana st., Krasnodar, 350051, Russia
E-mail: EADemekhin@fa.ru
[2]Université Bordeaux, I2M, UMR CNRS 5295, 16 Av. Pey-Berland, 33607 Pessac, France
[3]Department of computational mathematics and mathematical physics, Southern Federal University,
8a Melchakova st., Rostov-on-Don, 344090, Russia

Phenomena of micro- and nanoscale moving of conductive and non-conductive liquids with an interface between them requires a great deal of attention because it has numerous practical applications in bio-chemical processing: lab-on-cheap reactors, micromixers, DNA extraction, drug delivery and many others.

The present work considers a two-layer micro/nanoflow of conductive (electrolyte) and non-conductive (dielectric) viscous liquids bounded by two solid walls in an external electric field and pressure gradient (see Fig. 1). The electrolyte–dielectric and the solid–electrolyte interfaces are assumed to be charged, while the solid–dielectric interface is an electrically insulated surface. The charge near the solid is immobile, while the surface charge on the electrolyte–dielectric interface is mobile (Ganchenko *et al* 2015) and references therein. Upon a tangential electric field, these charges produce a Coulomb force and cause a movement of the liquid; experimental evidence for an electroosmotic flow at the liquid–liquid interface and in the liquid bulk is given in (Li *et al* 2012). In spite of almost zero Reynolds numbers
(negligible inertia effects), the electrohydrodynamics of liquid flows at micro- and nanoscales includes complicated instabilities (Demekhin *et al* 2011) and bifurcations (Shelistov *et al* 2011), and even chaotic motion at micro- and nanoscales, which is named as microturbulence.

The problem is described by the Nernst–Planck–Poisson–Stokes (NPPS) system in the liquid–electrolyte phase, the Laplace–Stokes system in the liquid-dielectric phase, and appropriate boundary conditions (BCs) on the solid–electrolyte, the solid–dielectric, and the liquid–liquid interfaces. The problem has 1D steady-state equilibrium solution with a plug-like velocity profile.

Linear stability of the 1D steady-state equilibria in response to sinusoidal perturbations is considered. The stability investigation represents the solution to this problem in terms of a solution to an eigenvalue problem for a system of linear ordinary differential equations; the eigenvalue problem is solved numerically. The results show the coexistence of a long-wave and short-wave instabilities. The short-wave instability occurs for a stronger external field than the long-wave instability, but the growth rate of the short-wave instability is much higher than that of the long-wave instability. For infinitely large Weber numbers (case of a non-deformable liquid–liquid interface), the long-wave instability disappears, while the short-wave instability persists. This is similar to the case of ultrathin gas–liquid films, where the short-wave instability can also reveal itself for an undeformable surface.

Futhermore, the application of pressure gradient results in the destabilization of the one-dimensional flow when the pressure driving force is oppositely directed to the electroosmotic flow. If the pressure driving force is codirected with the electroosmotic flow, then the one-dimensional solution is stabilized. This result is in good agreement with the experiment (Li *et al* 2012) (see Fig. 2).

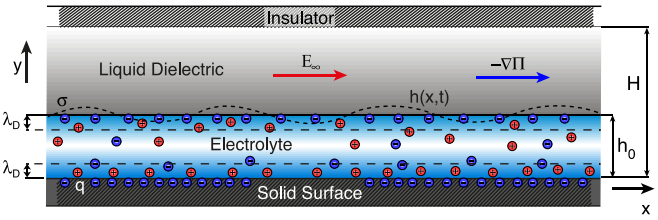


**Figure 1:** Electro-osmotic two-phase electrolyte–dielectric flow under an external tangential electric field and pressure gradient.

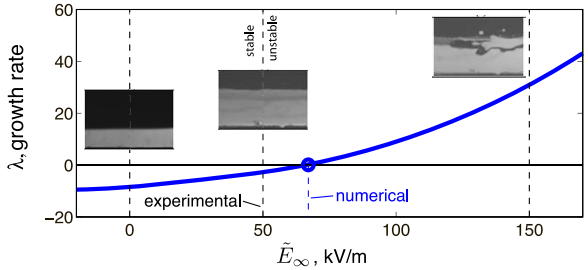


**Figure 2:** Comparison of experimental (Li *et al* 2012) and numerical data of stability flow

**Acknowledgements**
This work was supported, in part, by the Russian Foundation for Basic Research (Projects No. 15-08-02483-a, No. 14-08-01171-a and 15-31-50939-mol_nr)

**References**

E.A. Demekhin, V.S. Shelistov and S.V. Polyanskikh, Linear and nonlinear evolution and diffusion layer selection in electrokinetic instability, Phys. Rev. E, V. 84, 036318 (2011).

G.S. Ganchenko, E.A. Demekhin, M. Mayur and S. Amiroudine, Electrokinetic instability of liquid micro- and nanofilms with a mobile charge, Physics of Fluids, V. 27, 062002 (2015).

H. Li, T.N. Wong and N.-T. Nguyen, Electrohydrodynamic and Shear-Stress Interfacial Instability of Two Streaming Viscous Liquid Inside a Microchannel for Tangential Electric Fields, Micro and Nanosystems, V. 4, 14-24 (2012)

V.S. Shelistov, N.V. Nikitin, G.S. Ganchenko, and E.A. Demekhin, Numerical modeling of electrokinetic instability in semipermeable membranes, Dokl. Phys., V. 56, 538 (2011).

# Two-dimensional numerical simulation of microscale thermoelectrokinetic instability

Nataly Ganchenko[1], Georgy Ganchenko[2], Evgeny Kalaydin[3] and Evgeny Demekhin[2]

[1]Department of mathematical modeling, Kuban State University, 149 Stavropolskay st., Krasnodar, 350040, Russia
[2]Laboratory of Micro- and Nanoscale Electro- and Hydrodynamics for the Krasnodar Branch of Financial University
34 Luzana st., Krasnodar, 350051, Russia
[3]Department of mathematics and informatics, Financial University, 34 Luzana st., Krasnodar, 350051, Russia
Email: ENKalaydin@fa.ru

Problems of electrokinetics have recently captured attention of scientists from different fields of knowledge because of rapid developments in micro- and nanotechnologies. It tends to be very promising for practical issues to use ion-exchange surfaces, permeable only for one type of ions, cation or anion. Among such surfaces are semiselective electric membranes, electrodes and systems of micro- and nanochannels. It is well known that electric current in electrolyte in microgap between semiselective membranes is proportional to voltage ΔV, if the values of ΔV are rather small. With increase of ΔV transition to limited mode takes place (electric current weakly depends on voltage) (Rubinstein and Shtilman 1979). Further magnification of external electric field leads to reappear linear dependence of the electric current from the voltage. Transition from limited to overlimiting mode is caused by appearance of liquid movement owing to instability development, theoretically predicted in (Zaltzman and Rubinstein 2007) and numerically confirmed in (Demekhin *et al* 2013). However, it must be said, that numerical and experimental data used to match only qualitatively, but not quantitatively, e.g. the experimental critical value of potential drop was less than that obtained numerically. As it has been shown in (Demekhin *et al* 2015), neglecting of thermic effects caused by Joule heating may be the reason of such an unpleasant mismatch. A new type of microscale instability, occurring then electric current at the layer is oppositely directed to gravity vector, was found out. The critical potential drop can be smaller than that one for electokinetic instability threshold, if special combination of new introduced parameters is considered.

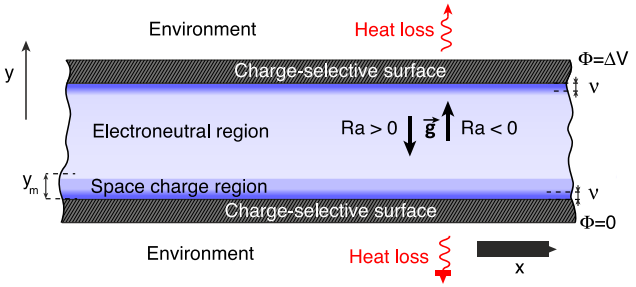


**Figure 1:** Schematics of the system.

In this work we add to Nernst-Planck-Poisson-Stocks system of equation an energy equation with source term caused by Joule heating of the electrolyte owing to electric current in it. Also, an additional term, respected for bouncy force, occurs in the Stocks equation. Membranes are assumed to be partly insulted (see Fig. 1). As have been found during the two-dimensional direct numerical simulation of the problem, the convective motion takes place due to loss of stability by one-dimensional steady state solution. This motion manifested itself in two-dimensional structures (Fig. 2 and Fig. 3), similar to electroconvective rolls (Demekhin *et al* 2013). What fundamentally differs is formation of thin lines connecting the membranes, where the salt concentration reaches its maximum value. Electric charge, obviously, will firstly flow through these lines.

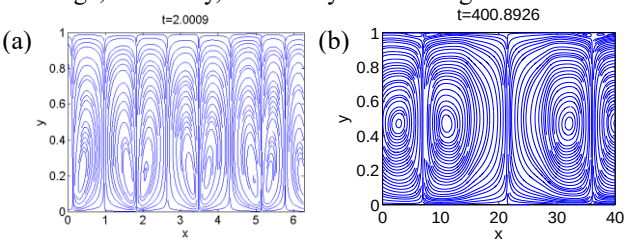


**Figure 1:** Stream lines, (a) $Ra = 0$ (isothermal), $\Delta V = 30$, (b) $Ra = -50, \Delta V = 20$

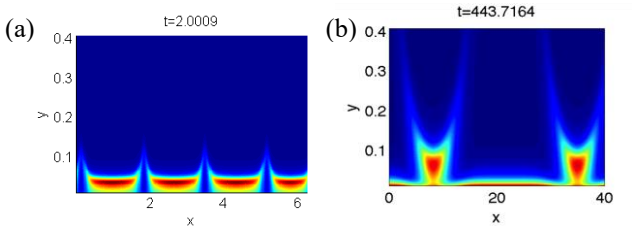


**Figure 2:** Charge density, (a) $Ra = 0$ (isothermal), $\Delta V = 30$, (b) $Ra = -50, \Delta V = 20$

**Acknowledgements**

This work was supported, in part, by the Russian Foundation for Basic Research (Projects No. 14-08-00789-a, No. 15-58-45123-IND_a)

**References**

I. Rubinstein and L. Shtilman, Voltage against current curves of cation exchange membranes, J. Chem. Soc. Faraday Trans. II, V. 75, P. 173-226 (1979)

B. Zaltzman and I. Rubinstein, Electro-osmotic slip and electroconvective instability, J. Fluid Mech., V. 579, P. 173-226 (2007)

E.A. Demekhin, N.V. Nikitin and V.S. Shelistov, Direct numerical simulation of electrokitetic instability and transition chaotic motion, Phys. Fluids, V. 25, 122001 (2013)

E.A. Demekhin, S. Amiroudine, G.S. Ganchenko and N.Yu. Khasmatulina, Thermoelectroconvection near charge-selective surfaces, Phys. Rev. E, V. 91, 063006 (2015)

# Combustion of liquid fuel in rectangular mini and microchannels

V.V. Zamashchikov[1,3], A.A. Korzhavin[1], and E.A. Chinnov[2,3]

[1] Institute of Chemical Kinetics and Combustion SB RAS, 630090 Novosibirsk, Russia
[2]Kutateladze Institute of Thermophysics SB RAS, 630090 Novosibirsk, Russia
[3]Novosibirsk State University, 630090 Novosibirsk, Russia
E-mail: albor@kinetics.nsc.ru

The trend towards a decrease in characteristic sizes of devices in various technical fields determines development of studies on hydrodynamic and heat transfer in mini- and microchannels. At a decrease in the height of flat channels the ratio of surface area to channel volume increases inversely to its minimal transverse size, and this causes high heat transfer intensity in the microsystems. In application to the processes occurring in reacting systems, for instance, burning of combustible liquids in small channels, heat transfer intensification can both improve and deteriorate the situation. Therefore, investigation of combustion processes in such systems is important for development of new applications and improvement of energy efficiency of available technical solutions.

To implement the combustion process, which includes the co-current motion of combustible liquid and gas it is important to get information about the regimes of two-phase flow in the considered channels. For instance, it is necessary to know in advance the conditions suitable for the separate flow, common for combustion.

It is shown in the review on the studies of the two-phase flows Chinnov and Kabov (2006), that the flows in channels of different cross-sections depend significantly on channel transverse dimensions. According to analysis of the maps of air-water flow patterns in horizontal rectangular channels with height 0.4-1 mm Chinnov et al. (2009, 2014), at low liquid and gas velocities, the phases flow separately.

According to Zamashchikov (2009) in the conditions of restricted space flame spreading is impossible without oxdizer supply. The pulsating flame spread regime implementation and mean flame spread rate depend on opposed air flow velocities. Flame spread rates of an order of 0.5 cm/s were obtained. Increase in the flame spread rate oppose the oxidizing flow is possible by enriching the oxidizer with oxygen. Furthermore the flame spread rate depends on the channel height. In this connection the experiments were carried out in a narrow flat channel, the height of which may be varied, and with oxidizing flow that can be enriched with oxygen, n-butanol was used as combustible liquid.

It is significant from practical point of view that these experiments is interesting first of all for fire and explosion safety as they are concerned so important parameter as critical size for flame penetration (quenching size).

The flames, propagating above the surface of n-butanol in mini channels at $h>h_{cr}$, were studied. Here $h_{cr}$ is quenching size for a slot. The channel height could vary, and it was an order less than its width. This was made to achieve the 2D structure of the flows and flame front, as far as possible.

The working section consists of two parallel quartz plates, the distance between which (the channel height) $h$ is set by two metal gaskets with the thickness from 1 to 0.35 mm. The oxidizing gas mixture was fed into the channel. The oxidizing mixture was prepared in the mixer of high pressure by partial pressures. The prepared mixture was fed to the flow controller El-Flow of Bronkhorst production. The accuracy of mixture preparation was 5%. The average velocity of the oxidizer was determined as the ratio of the oxidizer flow rate to the cross-sectional area of the channel. The combustion process was registered from the top in the region between the liquid input and channel outlet by the digital video and photo cameras.

Ignition was performed by the naked flame at the channel outlet. After ignition we recorded the flame front coordinate and obtained the dependence of this coordinate on time. The flame velocity was determined by inclination of this dependence. The accuracy of velocity measurements was 5%.

It is shown that flame spread rate can be high and comparable with velocities of flame propagation in the stoichiometric homogeneous gas mixture. The flame spread rate depends on velocity of oxidizer. It can either increase or decrease with arise of oxidizer velocity, depending on the oxygen content. The flame surface is significantly distorted with increase in average flame spread rate. It is shown that the flame spread rate can be significant and comparable with the laminar burning velocity of the stoichiometric homogeneous gaseous mixture.

This work was supported by the grant of Russian Science Foundation (Agreement No. 15-19-30038).

**References**

Chinnov E. A., Guzanov V. V., Cheverda V. et al., Regimes of Two-phase Flow in Short Rectangular Channel, Microgravity Sci. Technol., Vol. 21, no. 1S, pp. 199-205 (2009).

Chinnov E.A., Kabov O.A., Two phase flow in pipes and capillary channels, High Temperatures, Vol. 44, no. 5, pp. 773-791 (2006).

Chinnov E.A., Ron'shin F.V., Kabov O.A., Study of gas-water flow in horizontal rectangular channels, Thermophysics and Aeromechanics, Vol. 22, no. 5, pp. 645-653 (2015).

Zamashchikov V.V., Flame spread across shallow pools in modulated opposed air flow in narrow tube. Combust. Sci. Technol., Vol. 181, pp. 176–189 (2009).

# The effect of droplets evaporation on flow, turbulence and heat transfer in a two-phase flow in a sudden pipe expansion

Maksim Pakhomov, Viktor Terekhov

Laboratory of Thermal and Gas Dynamics, Kutateladze Institute of Thermophysics,
Siberian Branch of Russian Academy of Sciences,
Novosibirsk, 630090, Russia
E-mails: pakhomov@ngs.ru; terekhov@itp.nsc.ru

Two-phase droplet-laden separated flows are observed in many engineering and natural processes, such as cyclonic separation, flame stabilization in internal combustors, pneumatic transport, and many others. The separated flow is a typical two-dimensional shear flow consisting of several zones: main core flow, shear layer, recirculation, and flow relaxation regions. The interactions between finely dispersed phase and turbulent gas-phase flows are very complex, and many of these interactions remain poorly understood Fessler and Eaton (1999).

The number of papers that have examined two-phase separated flows with evaporating droplets is very limited Hishida et al. (1995) and Pakhomov and Terekhov (2013). These few studies do not provide sufficient information to evaluate all the factors affecting the flow structure, particle dispersion, and turbulence modification in sudden pipe expansion flows with evaporating droplets. The aim of the present short communication is to examine the effect of evaporating droplets on gas turbulence modification and heat transfer enhancement in sudden pipe expansion flow.

Gas–droplet turbulent flow is numerically predicted by the set of steady-state axisymmetrical RANS equations. The Eulerian two-fluid approach for the modeling of dispersed phase is used. The governing mean and fluctuating equations for both phases are described in detail Pakhomov and Terekhov (2013). Gas phase turbulence was modeled with the use of elliptic-blending second-moment closure Fadai-Ghotbi et al. (2008). Two-way coupling is achieved between dispersed and carrier phases in the mean and fluctuating transport. The mean transport equations for both gas and dispersed phases and the turbulence model are solved using a control volumes method on a staggered grid by using QUICK and SIPMLEC procedures.

The diameter of the pipe is $2R_1$ = 20 mm before expansion and $2R_2$ = 60 mm behind the expansion, and the step height is $H$ = 20 mm. The Reynolds number for the gas phase varies within the range $\mathrm{Re}_H = HU_{m1}/\nu = (1.33–4) \times 10^4$. The initial mass fraction changes within the range $M_{L1}$ = 0–0.1.

The largest droplets do not penetrate the recirculation zone, $M_L/M_{L1}$ increases noticeably (see Figure) in the axial region of the pipe (lines *1* and *2*), and an increase in the Stokes number causes an increase in the mass concentration of droplets. Initially, a growth of Stk of the dispersed phase leads to an increase in the droplet concentration in the zone of separation (line *3*). The droplets' concentration decreases considerably with an increase in the Stokes number because they do not get into the area of separated flow. The near-wall region of the pipe (line *4*) is almost free from particles due to their evaporation (for low Stokes numbers) and their absence in the separation zone (for high Stk numbers). Similar trends can also be observed for the non-evaporating particles, but their concentration is significantly higher, especially near the wall.

This work is supported by the Russian Science Foundation (Project No. 14-19-00402).

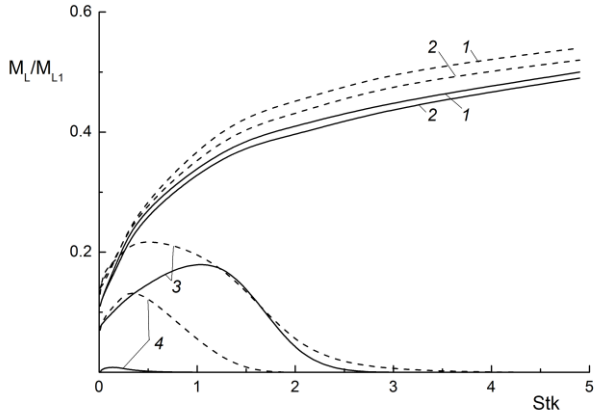


**Figure 1:** The effect of Stokes number in the mean motion on the particles mass fraction at $x/H$ = 6. Solid lines are evaporating droplets, dashed curves are non-evaporating particles. $M_{L1}$ = 0.05. *1* – $r/H$ = 0, *2* – 0.5, *3* – 1, *4* – 1.45.

**References**

Fadai-Ghotbi A., Manceau R., and Boree J., Revisiting URANS computations of the backward-facing step flow using second moment closures. Influence of the numerics, Flow, Turbulence and Combustion, Vol. 81 pp. 395–410 (2008)

Fessler J.R. and Eaton J.K., Turbulence modification by particles in a backward-facing step flow, Journal of Fluid Mechanics, Vol. 314 pp. 97–117 (1999)

Hishida K., Nagayasu T. and Maeda M., Augmentation of convective heat transfer by an effective utilization of droplet inertia, Int. Journal of Heat and Mass Transfer, Vol. 38 pp. 1773–1785 (1995)

Pakhomov M.A. and Terekhov V.I., Second moment closure modelling of flow, turbulence and heat transfer in droplet-laden mist flow in a vertical pipe with sudden expansion, Int. Journal of Heat and Mass Transfer, Vol. 66 pp. 210–222 (2013)

# The effect of temperature and gas Reynolds number on evaporation of a sessile liquid drop in mini-channel

E. Orlik[1], D. Zaitsev[2], E. Orlova[1], E. Bykovskaya[2], O. Kabov[1, 2]

[1] National Research Tomsk Polytechnic University, 634050, Tomsk, Russia
[2] Institute of Thermophysics SB RAS, 1, Lavrentiev Ave, 630090, Novosibirsk, Russia

Email: orlik.evgeniy@gmail.com

Evaporation of sessile liquid droplet is a key point of many processes such as painting, coating, humidification, the agriculture irrigation, etc. and widely studied numerically and experimentally but mostly in motionless air. The influence of air velocity on evaporation of droplet is also known and studied, but all these investigations have been carried out in open ambient air.

In this work we present experimental results on sessile drop evaporation on a heated substrate in mini channel under blowing air laminar flow. Experimental setup with changeable height of channel from 3mm to 20 mm is shown in Fig. 1. The goal is to study the effect of the substrate temperature and Reynolds number of air flow on the evaporation rate of a sessile drop. Distilled deionized nano-filtered water was used as the working liquid. Initial drop volume $V_0$ was slightly varied and was around 100µl. The substrate temperature was maintained at 25, 50 and 70 ±0.5 ºC. Re range was from 0 to 2000. The drop shape is visualized from the top and from the side with the help of the shadow technique with resolution of 6 µm/pix (as shown in Fig. 2). The images from the side are processed in the Drop Shape Analysis software by KRÜSS. We used stainless steel substrate with polished surface; the advancing static contact angle was θ=85±6°.

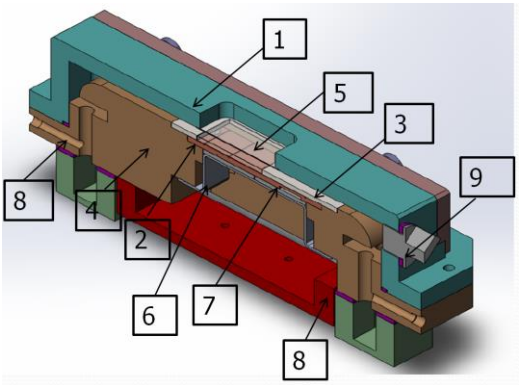


**Figure 1: Setup:** 1 – cover, 2 – copper insert, 3 – stainless steel substrate, 5 – optical window, 6 – heat exchanger, 7 – Peltier element 8 – support, 9 – port for syringe.

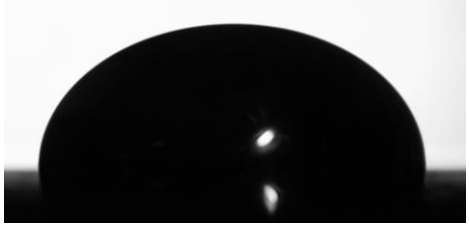

**Figure 2:** Droplet photograph using shadow technique. $V_{droplet}$=100µl, $V_{gas}$= 0 m/s, $T_{substrate}$=50 ºC, θ=88°.

It was found that the evaporation time of liquid droplets strongly depends on Reynolds number without heating as shown in Fig. 3 and dominates by temperature with increase of temperature of substrate (as shown in Fig. 4).

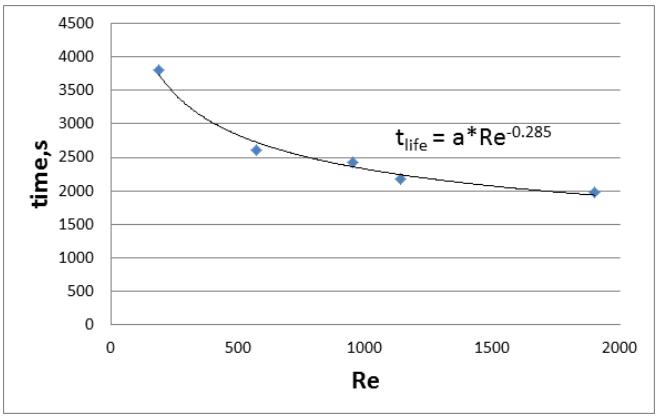


**Figure 3:** Lifetime of water droplet vs. Reynolds number. Temperature of substrate is 25 ºC, height of channel 9mm.

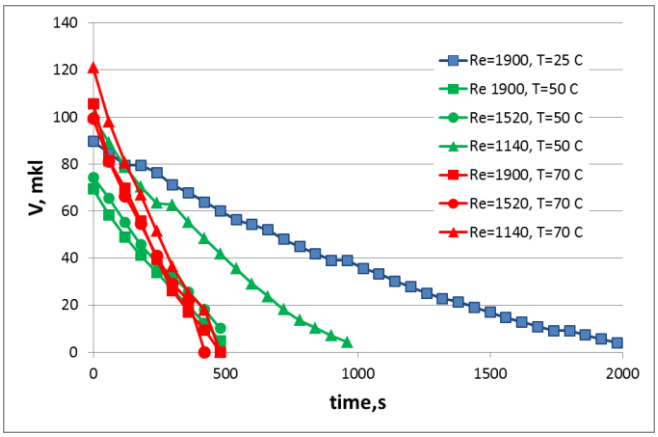


**Figure 4:** Effect of temperature and Reynolds number on evaporation vs. time, height of channel 9mm.

Following conclusion can be drawn from analysis of experimental data, that in the range of Re=1140-1900 the evaporation rate is defined by the substrate temperature as $dV/dt \approx 0.042 + 0.004*(T_{substrate}-T_{25})$.

**Acknowledgements:**
The authors gratefully acknowledge support of this work by Russian Science Foundation (project No. 14–19-01755) and program (project VIU ENIN 94 2014) to improve the competitiveness of the National Research Tomsk Polytechnic University.

# 3D instability of liquid films and rivulets

Sergey Alekseenko, Sergey Aktershev, Aleksey Bobylev,
Vladimir Guzanov, Dmitriy Markovich and Sergey Kharlamov

Kutateladze Institute of Thermophysics, Siberian Branch of the Russian Academy of Science,
Lavrentiev Ave. 1, Novosibirsk 630090, Russia
Novosibirsk State University, Pirogova St. 2, Novosibirsk 630090, Russia

E-mail kharlamov@itp.nsc.ru

Gravity-driven film flow of a viscous liquid down a flat plane is a well known example of convectively unstable free surface flow with instabilities of different kinds leading to the appearance and interaction of surface waves with a great variety of characteristics. Specific type of film flow whereby the fluid flows in the form of many streamlets is typically called rivulet flow, whereas an individual streamlet, bounded by two contact lines, is called a rivulet. Special attention has been paid to rivulet flows because of their practical value when used in a variety of devices in power engineering and chemical technology.

This study presents the results of experimental and theoretical investigations of instabilities in the liquid film and rivulet flows. In the first part of study, the experimental results for transition from two-dimensional (2D) to three-dimensional (3D) waves in falling liquid films are presented. The method of laser induced fluorescence was used to obtain instant shapes of three dimensional waves and to investigate the regularities of formation of 3D wave patterns arising due to transverse instability of 2D waves. The regular 2D waves with prescribed frequency $f$ were forced by harmonic modulation of liquid flow rate. Distilled water, water-glycerine solution (WGS) and water-ethanol solution (WES) were used as working fluids. The obtained results were compared to the results from the published literature on the modeling of 3D wave regimes of film flow.

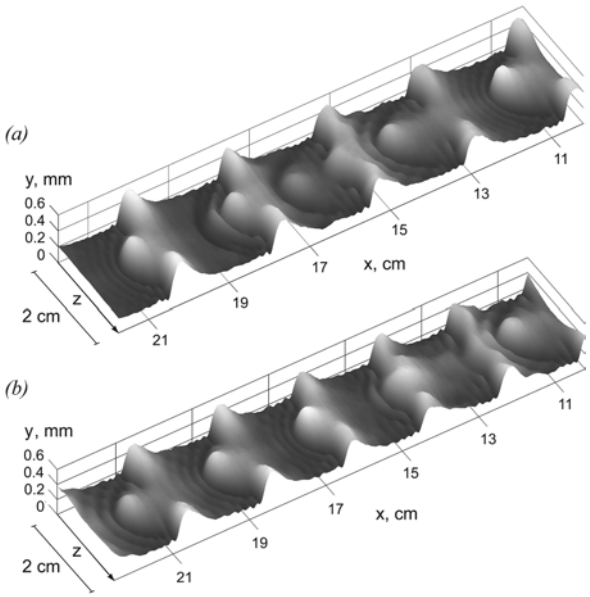


**Figure 1:** Scenarios of 3D wave patterns evolution. $Re$ = 50 and $L$ = 2 cm. (a) $f$ = 17 Hz, oscillatory pattern. (b) $f$ = 20 Hz, passing through pattern.

At moderate Reynolds numbers $Re$, two scenarios of the patterns evolution were observed (see Fig.1). For low frequencies of 2D waves excitation, the leading humps initially run away from the trailing humps. Then their amplitudes and velocities decrease so that the trailing humps which move all the time with approximately constant celerity begin to overtake the leading humps. As the trailing humps approach the leading ones, the latter begin to restore their amplitudes and the pattern structure almost repeats itself through several wave lengths. An example of such oscillatory scenario obtained previously in modeling (Dietze et al. 2014) and observed in experiments (Alekseenko et al. 2012) is shown in Fig. 1(*a*). For high excitation frequencies, the site between trailing humps, which was left by running downstream leading hump, is filled by another leading hump that arrives from above so that the pattern structure also almost repeats itself through several wave lengths as shown in Fig. 1(*b*). We will refer to such scenario as “passing through” one.

The second part of study is devoted to numerical simulation of 3D waves on the surface of a rivulet flowing down a vertical plate are presented. The model (Demekhin, Shkadov 1984) is used for numerical simulation of the forced waves in the rivulet. The results of the simulations are compared with the authors’ previous experimental data (Alekseenko et al. 2010). The calculations are performed only for the conditions implemented in the authors’ previous experiments. The comparison shows that the applied model adequately describes the shape of the wave surface of a rivulet, although the wave propagation velocity and wavelength are underestimated. Figure 2 demonstrates the shape of the developed waves on a WGS rivulet in comparison with experimental data for sufficiently high values of Reynolds number and forcing frequency. As it is

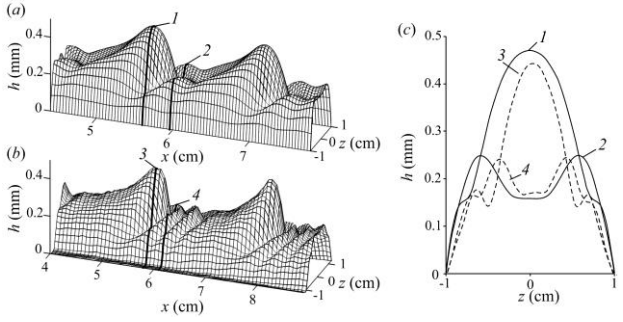


**Figure 2:** : Shape of the wave in the WGS rivulet compared with experimental at $Re$ = 36, $f$ = 23 Hz. (*a*) calculated 3D surface, (*b*) experimental 3D surface, (*c*) rivulet cross sections, (1, 2) calculation, (3, 4) experiment.

clear from the figure, the calculation well describes the shape of the peak with capillary ripples in front of the wave, as well as rivulet profiles in different cross-sections. Significant discrepancy with the experimental data is observed in the wavelength. The calculated distance between peaks is 1.5 cm, while experiment gives 2 cm.

**Conclusions**

We have investigated experimentally the process of transition from 2D to 3D waves in liquid films falling down a vertical plate with a primary goal to examine to which extent the modern modeling approaches (Scheid et al. 2006, Dietze et al. 2014) adequately describe real film flows. The method of laser induced fluorescence is used to obtain instant shapes of three dimensional waves and to investigate the regularities of formation of 3D wave patterns arising due to transverse instability of 2D waves. Although many details of 3D wave patterns correspond well, there are a few significant distinctions between our experiments and modeling. In particular, during 2D-3D wave transition, we observed a strong transverse redistribution of liquid leading to the formation of rivulets on the surface of isothermal liquid film, which is a phenomenon not described previously. Our results show that forming 3D waves always resemble streak-like waves as in (Adomeit, Renz 2000) but not Λ-solitons as in (Demekhin et al. 2010).

A numerical simulation of nonlinear three-dimensional forced waves in a straight rivulet, flowing down a vertical plate, was carried out. The calculations were performed for the two liquids (WES and WGS) with different physical properties, used in experiments (Alekseenko et al. 2010). Compared with the film flow, the waves in rivulets have significant differences. In particular, the wave patterns for the cases of "small" and "large" contact wetting angles are significantly different. The calculations have shown that for WES rivulet ("large" contact wetting angle) the waves are 2D in nature, while in WGS rivulet ("small" contact wetting angle) 3D horseshoe-waves develop. Comparison of experimental data on nonlinear waves with the calculations, made for different values of the Reynolds number within a wide range of the forcing frequency leads to the following conclusions. The applied model (Demekhin, Shkadov 1984) is appropriate to describe in general the shape and amplitude of the waves on the rivulet surface at moderate Reynolds numbers. In particular, for WGS rivulet the model predicts waves of step-wise shape, which were observed in the experiments at low forcing frequencies. For moderate forcing frequencies the model predicts waves with capillary ripples in front of the wave peak. The shape of these waves is in good agreement with the experimental data. For WES rivulet the model predicts well the amplitude of developed waves and the shape of the rivulet wave surface. Besides, for WES rivulet the model predicts no capillary ripple in front of the main peak that is consistent with the experimental data.

**Acknowledgements**

The authors acknowledge the support by the Russian Foundation for Basic Research (projects 15-01-06702 and 15-01-04320.)

**References**

S. V. Alekseenko, V. V. Guzanov, D. M. Markovich, and S. M. Kharlamov, Specific features of a transition from the regular two-dimensional to three-dimensional waves on falling liquid films, Tech. Phys. Lett. Vol. 38, p. 739 (2012)

S. V. Alekseenko, A. V. Bobylev, V. V. Guzanov, D. M. Markovich, S. M. Kharlamov, Regular waves on vertically flowing rivulets at different wetting angles, Thermophys. Aeromech., Vol. 17, pp. 371-384 (2010).

E. A. Demekhin, E. N. Kalaidin, S. Kalliadasis, and S. Yu. Vlaskin, Three-dimensional localized coherent structures of surface turbulence. Model validation with experiments and further computations, Phys. Rev. E, Vol. 82, 036322 (2010).

E. A. Demekhin, E. N. Kalaidin, and A. S. Selin, Three-dimensional localized coherent structures of surface turbulence. III. Experiment and model validation, Phys. Fluids, Vol. 22, 092103 (2010).

E. A. Demekhin, V. Y. Shkadov. Three-dimensional waves in a liquid flowing down a wall, Fluid Dynamics. Vol. 19. p. 689 (1984)

G. F. Dietze, W. Rohlfs, K. Nährich, R. Kneer, and B. Scheid, Three-dimensional flow structures in laminar falling liquid films, J. Fluid Mech. Vol. 743, p. 75 (2014).

B. Scheid, C. Ruyer-Quill, and P. Manneville, Wave patterns in film flows: Modelling and three-dimensional waves, J. Fluid Mech. Vol. 562, p. 183 (2006).

P. Adomeit and U. Renz, Hydrodynamics of three-dimensional waves in laminar falling films, Int. J. Multiphase Flow, Vol. 26, p. 1183 (2000).

# Thin liquid films flowing down heated walls: a review of recent results

Luis Antonio Dávalos O.

Departamento de Polímeros, Instituto de Investigaciones en Materiales, Universidad Nacional Autónoma de México
Ciudad Universitaria, Circuito Exterior S/N, Delegación Coyoacán, 04510 México D. F., ldavalos@unam.mx
ldavalos@unam.mx

Thin liquid films have been the subject of research since many years ago due to their importance in industrial applications. One of them includes the coating of surfaces where it is of interest to have a very smooth solid free surface at the end of the liquid solidification. Another one is the cooling of heat generating systems in order to avoid high temperatures which may produce important or disastrous damages.

Thin liquid films heated from below in the absence of gravity have importance on its own. They have been investigated theoretically under the usual assumption of a very good conducting substrate. The results of this simplification have been relevant to understand in an easy way the behavior of these systems. Even more, the assumption of a flat free surface gives interesting results which might be significant for fluids with very strong surface tension.

In the case of thin films falling down walls the assumption of a very good conducting substrate has been used for years in important papers which have disclosed a number of characteristics of heated films. Among those flow are included meaningful effects as van der Waals forces, disjoining pressure, evaporation, etc.

However, in order to be in agreement with experimental settings it is necessary to include the effects of finite thermal conductivity and geometry of the wall. As a consequence, it is necessary to add two more parameters to the problem.

The geometry of the wall may be characterized by periodic and non periodic deformations which prove to be critical to determine the stability of falling films. Even in this case, the substrate might be a very good conductor in comparison to the fluid.

When the thickness is the only geometric factor of a flat wall, the properties of the wall that affect the stability of the film are the relative thickness and the relative thermal conductivity of the substrate with respect to those of the fluid. The stability changes further when, besides these parameters the geometry of the wall changes in space.

In case the substrate shows deformations, the free surface presents a response which depends on the physical characteristics of the fluid. In case the film is heated from below the surface tension weakens and the response changes accordingly in a nonlinear way. This response corresponds to a spatial perturbation. Time dependent perturbations can be applied superposed to the spatial ones acting on the fluid film. At the end, they will interact nonlinearly. This problem has been investigated in the isothermal case by (Polak and Aksel, 2013, Schorner et al. 2015) and by means of direct numerical analysis by (Trifonov 2014). The effect of topography on drop spreading in the presence of surfactant has been analyzed (Li et al. 2014). The influence of fluid viscoelasticity has been explored in (Dávalos-Orozco 2013, Sadiq 2013). The wavy thick wall might be heated or cooled from below. In that case,new results have been found by (Dávalos-Orozco 2014, 2015). See Fig. 1 and Fig. 2.

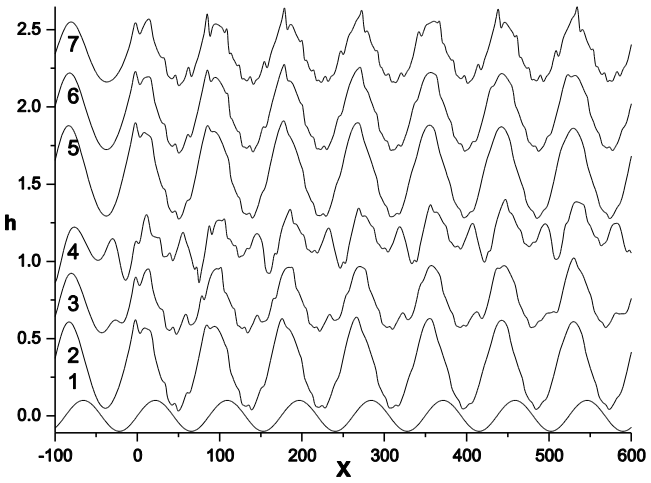


**Fig. 1** With an increase of Marangoni number the amplitude of the response of the free surface to the wall deformation decreases notably. Freq = 0.5, Re = 1.391, L = 5 (resonance). The wall is (1) and for conductivities ratio QC = 0.01: (2) Ma = 10, (3) Ma = 50, (4) Ma = 100. For QC = 0.05: (5) Ma = 10, (6) Ma = 50, (7) Ma = 100. Notice that pure responses are shown from x = –100 to 0. (Pr = 7, S = 1, Bi = 0.1, d = 0.11) IPHT 2 / 1 pp55 - 74 (2014).

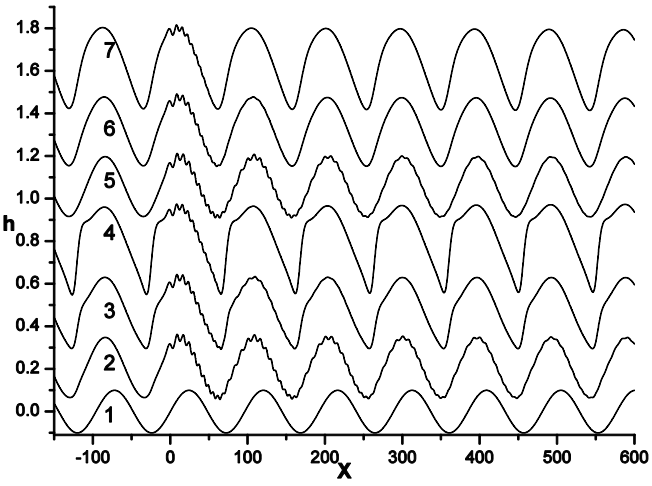


**Fig. 2** With an increase of NEGATIVE Marangoni number the amplitude of the response of the free surface to the wall deformation INCREASES. Freq. = 2, R = 2.783, L = 11. The wall is (1) and for conductivities ratio QC=0.01: 2) Ma=−10, 3) Ma=−50, 4) Ma=−100. For QC=0.05: 5) Ma=−10, 6) Ma=−50, 7) Ma=−100. Notice pure responses from x =−150 to 0. (Pr=7, S=1, Bi=1, d = 0.11). PLA-379, pp962-7 (2015).

In many applications the substrate is cylindrical and it might be horizontal or vertical in the presence of gravity (Moctezuma-Sánchez and Dávalos-Orozco 2015, Weidner 2013, Cheng et al. 2014). The liquid film may have two free surfaces like in liquid sheets. When the sheet is traversed by a temperature gradient it is possible to find a number of different instabilities (Dávalos-Orozco, 1999, Fu et al. 2013, Tong et al. 2014). They may have consequences in other problems like in the thermocapillary instability of a three-layer Poiseuille flow, emulating the flow of a long drop or bubble in a channel (Alvarez and Uguz 2013).

It is the goal of this lecture to review recent research results which appeared in the open literature since the publication of the authors review paper published in 2013 in the international journal **Interfacial Phenomena and Heat Transfer** (Dávalos-Orozco, 2013). Therefore the lecture will review papers published from 2013 to the present. The main topic will be non-isothermal flows, but whenever needed a discussion of isothermal flows will be included to.

**References**

Alvarez, N. J. and Uguz A. K., Impact of deformable interfaces and Poiseuille flow on the themocapillary instability of three immiscible phases confined ina channel, Physics of Fluids Vol. 25/02, 024104 (2013).

Cheng, P.-J., Liu, K.-C. and Wang, C.-C., Nonlinear evolution of the travelling waves in roll coating flows of thin viscoelastic polymer falling films, Applied Mechanics and Materials vol. 479-480 (2014) 45 - 49. Applied Science and precision Engineering Innovation, Parts 1 and 2. Edited by Liu, C. H.

Dávalos-Orozco L. A., Thermocapillary instability of liquid sheets in motion, Colloids and Surfaces A 157, pp 223 – 233 (1999).

Dávalos-Orozco, L. A., Stability of thin liquid films falling down isothermal and non-isothermal walls, Interfacial Phenomena and Heat Transfer, Vol. 1 / 2, pp. 93 - 138 (2013).

Dávalos-Orozco, L. A., Stability of thin viscoelástico films falling down wavy walls, Interfacial Phenomena and Heat Transfer Vol. 1 / 4 pp 301 – 315 (2013).

Dávalos-Orozco, L. A., Nonlinear instability of a thin film falling down a smoothly deformed thick wall of finite thermal conductivity, Interfacial Phenomena and Heat Transfer, Vol. 2 / 1, pp. 55 - 74 (2014).

Dávalos-Orozco, L. A., Nonlinear instability of a thin film falling down cooled wavy thick wall of finite thermal conductivity, Physics Letters A, Vol. 379, pp. 962 - 967 (2015).

Fu Q.-F., Yang L.-J., Tong M.-X. and Wang C., Absolute and convective instability of a liquid sheet with transverse temperature gradient, Int. J. Heat Fluid Flow 44, pp 652 – 661 (2013).

Li, Chunxi, Pei, Jianjun and Ye, Xuemin, Spreading of droplet with insoluble surfactant on corrugated topography, Physics of Fluids 26-092103 (2014).

Moctezuma-Sánchez, M. and Dávalos-Orozco, L. A., Azimuthal instability modes in a viscoelastic liquid layer flowing down a heated cylinder, Int. J. Heat Mass Transfer 90, pp 15 – 25 (2015)

Pollak, T. and Aksel, N., Crucial flow stabilization and multiple instability branches of gravity-driven films over topography, Phys. Fluids 25, 024103 (2013).

Sadiq M. R., Influence of temperature gradient on the stability of a viscoelastic film with gradually fading memory over a topography with ridges and furrows, Chinese J. of Eng., paper 751909 (2013) Hindawi, Open Access.

Schorner, M., Reck, D. And Aksel, N., Does the topography specific shape matter in general for stability of film flows, Physics of Fluids 27, 042103 (2015).

Tong, M.-X., Yang L.-J. and Fu Q.-F., Thermocapillar instability of a two-dimensional viscoelastic planar liquid sheet in surrounding gas Physics of fluids 26, 033105 (2014) pp 1 - 14.

Trifonov, Y., Stability of a film flowing down an inclined corrugated plate: The direct Navier-Stokes computations and Floquet theory, Physics of Fluids 26-114101 (2014).

Weidner, D. E., Suppression and reversal of drop formation on horizontal cylinders due to surfactant convection, Physics of Fluids 25/08 082110 (2013).

# Modern view on the nanofluids viscosity and thermal conductivity

Valery Rudyak[1], Andrey Minakov[1,2,3], Sergey Krasnolutskii[1], Maxim Pryagnikov[1,2]

[1]Novosibirsk University of Architecture and Civil Engineering, Novosibirsk, Leningradskaya, 113, 630063, Russia,
[2]Siberian Federal University, Krasnojarsk, Svobodny, 79, Russia
[3]Kutateladze Institute of Thermophysics, SB RAS, Novosibirsk, Lavrentiev str., 1, Russia
valery.rudyak@ mail.ru

Nanofluids are a new class of dispersed fluids consist on the carrier fluid and dispersed nanoparticles. The nanofluids research has both fundamental and application motivation. On the one hand the transport properties of nanofluids are not described as a rule by classical theories (Einstein, Batchelor, Maxwell, etc.). On the other hand the nanofluids may be utilized in several applications, for example, engine cooling, refrigeration, thermal storage, drilling, lubrications, solar water heating, in different biomedical technologies, and so forth. In all cases the viscosity and thermal conductivity of nanofluids play the key role. The studying of the nanofluids thermophysical properties begun twenty years ago has included great number of the papers. However the obtained results are very contradictory (see for example reviews Hosseini et al 2011, Mahbubul 2012, Rudyak, 2013, Kumar, 2013 and references cited therein). The last results obtained by the authors permit to make the defined conclusions about dependence of the viscosity and thermal conductivity on different parameters. These data are systematically discussed in present paper. The experimental and molecular dynamics simulation data are considered. To molecular dynamics simulate the special molecule-nanoparticle and nanoparticle-nanoparticle interaction potentials were used (Rudyak and Krasnolutskii, 1999, 2002, Rudyak et al, 2012).

We analyzed more than fifty different nanofluids. In particular, it was shown that in all cases the viscosity coefficient of nanofluids is much more than corresponding value of the coarse dispersed fluids. In addition, the viscosity coefficient of nanofluids essentially depend on the size of the dispersed nanoparticles, it increases with decreasing nanoparticle size. For the first time it was shown by the molecular dynamics method that viscosity coefficient depends on the material of nanoparticles. This conclusion also is confirmed in experiments with nanofluids based on the water with the particles $Al_2O_3$, $TiO_2$ and $SiO_2$ with the size 100 and 150 nm.

Usually in papers connected with the study of the thermal conductivity of the nanofluids it is noticed that it is much more than predicted by the Maxwell's theory. Our molecular dynamics simulation carried out with model nanofluids (argon as based fluid with the Al and Zn nanoparticles) have shown that nanofluids can have the thermal conductivity less than the Maxell's one. Simultaneously the similar results were obtained experimentally for the nanofluids water+$SiO_2$. Here nanofluid with small nanoparticles had the thermal conductivity less than the Maxell's one. Further it was established that thermal conductivity coefficient increases if the particle size grows. However in all cases the dependence of the thermal conductivity on the volume concentration of the particles increases and then monotonously aspires to some limiting value.

Finally the enhancement of the thermal conductivity does not depend on thermal conductivity of the nanoparticles material. On the other hand this enhancement is determined by the density of the nanoparticles material. The enhancement of the thermal conductivity is increased with growing of the nanoparticles density.

The molecular dynamics simulation obtained parallel with the experiments permit to analyze the different mechanisms determining the considered transport coefficients. It was shown that these mechanisms are differed from the discussed ones early.

This work was supported by Russian Science Foundation (grant No. 14-19-00312).

**References**

Hosseini S. Sh., Shahrjerdi A. and Vazifeshenas Y. A review of relations for physical properties of nanofluids, Aust. J. Basic Applied Sci., Vol. 5(10) pp. 417-435 (2011).

Kumar1 P.M., Kumar J., Tamilarasan R., Sendhilnathan1 S. and Suresh S., Review on nanofluids theoretical thermal conductivity models, Engineering Journal, Vol. 19(1) pp. 67-83 (2015).

Mahbubul I.M, Saidur R. and Amalina M.A. Latest developments on the viscosity of nanofluids, Int. J. Heat Mass Transf., Vol. 55 pp. 874-885 (2012).

Rudyak V.Ya. Viscosity of nanofluids. Why it is not described by the classical theories, Adv. Nanopart. Vol. 2 pp. 266-279 (2013).

Rudyak V.Ya. and Krasnolutskii S.L. The interaction potential of dispersed particles with carrier gas molecules, in: Proc. 21st Int. Symp. on RGD, Gépadués-Éditions, Toulouse, Vol. 1 pp. 263-270 (1999).

Rudyak V.Ya, and Krasnolutskii S.L. Diffusion of nanoparticles in a rarefied gas, Tech. Phys., Vol. 47(7) pp. 807-813 (2002).

Rudyak V.Ya., Krasnolutskii S.L. and Ivanov D.A., The interaction potential of nanoparticles, Dokl. Phys. Vol. 57(1) pp. 33-35 (2012).

# Thermal and fluid issues in proton exchange membrane fuel cells

Hang GUO[1,2,*], Jiaxing LIU[1], Fang YE[1] and Chongfang MA[1]

1. MOE Key Laboratory of Enhanced Heat Transfer and Energy Conservation, and Beijing Key Laboratory of Heat Transfer and Energy Conversion, College of Environmental and Energy Engineering, Beijing University of Technology, Beijing 100124, China
2. Collaborative Innovation Center of Electric Vehicles in Beijing, Beijing 100081
*Corresponding author, E-mail: hangguo@sohu.com

As is known to all, hydrogen and oxygen are supplied to proton exchange membrane fuel cells (PEMFCs) for the electrochemical reaction, and water and heat are produced. As a result, various fluids, i.e. hydrogen, oxygen, liquid water, and water vapor, transport in the fuel cell. The fluids couples with heat, which introduces complicated thermal and fluid issues. The Thermal and fluid issues broadly exist in the PEMFC. Examples of thermal and fluid issues show as follows: Droplet behavior and movement in fuel cells; gas-liquid two-phase flow in the fuel cell components; heat transfer between fluids and components of the fuel cells; interaction between water and heat; heat flux across the fuel cell components and so on. All these phenomena affect the performance of PEMFCs. Besides, the safe and stable operation of the fuel cell highly relies on these phenomena. Investigation of these phenomena helps to understand the related mechanism in PEMFCs.

Water, one of the various fluids, plays a vital role in the PEMFC. As a product of electrochemical reaction, water involves diverse phenomena in PEMFC, such as droplet behavior in the porous layer (Liu and Pan (2012)), two-phase flow in the gas channel (Guo et al. 2014). Droplet behavior and two-phase flow are important phenomena in PEMFC, which are related to interfacial phenomena.

Interfacial phenomena are difficult to be investigated in PEMFC because of its structure. It is well known that the PEMFC consists of several components. The main components are gas channel, gas diffusion layer, catalyst layer, and membrane. Interfacial phenomena occur inside the fuel cell, which is difficult to be directly investigated. For example, the contact angle is difficult to be measured, especially for droplet in the gas diffusion layer of an operating fuel cell. In consequence, transparent window installed in end plate of fuel cell has been developed to visually observe the two-phase flow in the gas channel. The gas-liquid phase boundary may be identified in the visualization images. However, merely observation is not enough. Although two-phase images can be obtained by high speed camera or other instruments, interfacial phenomena related parameters e.g. contact angle cannot be reflected in these images. In other words, interfacial phenomena are rarely investigated in the two-phase flow visualization. Even though the two-phase flow can be visualization, difficulties remain from the fluid point of view. The interfacial phenomena such as two-phase flow coupled with electrochemical reaction, heat transfer, and mass transport is a complex transient process, which is rather intractable. Electrochemical reaction produces water and heat, which introduces interfacial phenomena and heat transfer in the fuel cell. In turn, interfacial phenomena and heat transfer affect electrochemical reaction by influencing mass transport and other factors. These phenomena affect and interact with each other, which complicates any single issue.

Heat generation and transfer is another important issue in PEMFC. Better thermal management makes the fuel cell operate more safe and steady. To monitor parameters related to heat is helpful for reasonable thermal management. However, parameters measurement in fuel cell is a huge challenge because of the limitation of its structure. Temperature, heat flux, and other parameters related to thermal issue are desired to be obtained to better understand the heat transfer inside the fuel cell. Although temperature measurements using thermocouple (Mench et al. 2003) and infrared thermal imaging (Guo et al. 2015) in PEMFC have been conducted, difficulties still remain. Thermocouple is easy to be damaged, and it needs to be inserted into fuel cell, which deteriorates the performance of fuel cell. Fuel cells need to be reconstructed by using infrared thermal imaging method. Little work has been conducted on the measurement of heat flux and thermal conductivity of components. Similar to the temperature measurement, problem exists to measure the heat flux inside fuel cells. The effect of measurement methods on the performance of fuel cells and the safety and reliability of the measurement tool are needed to be considered. More works are still wanted in this area.

**Keywords**
flow field, heat and mass transfer, phase change, proton exchange membrane fuel cells, two-phase flow

**Acknowledgement**
The authors are grateful to the National Natural Science Foundation of China (Grant No.: 51476003) for the financial support.

**References**

Guo H., Liu X., Zhao J. F., Ye, F., and Ma, C. F., Experimental study of two-phase flow in a proton exchange membrane fuel cell in short-term microgravity condition, Appl. Energy, Vol. 136 pp. 509-518 (2014)

Guo H., Wang, M. H., Liu, J. X., Nie, Z. H., Ye, F., and Ma C. F., Temperature distribution on anodic surface of membrane electrode assembly in proton exchange membrane fuel cell with interdigitated flow bed, J. Power Sources, vol. 273 pp. 775-783 (2015)

Liu T. L., and Pan C., Visualization and back pressure analysis of water transport through gas diffusion layers of proton exchange membrane fuel cell, J. Power Sources, vol. 207, pp. 60-69. (2012)

Mench M. M., Burford D. J., and Davis T. W., In situ temperature distribution measurement in an operating polymer electrolyte fuel cell, Proceedings of ASME International Mechanical Engineering Congress & Exposition, Washington D.C., pp. 415-428 (2003)

# Investigating the 3D conservative equations for a vertically flowing wavy liquid film

Dmitriy Arkhipov and Oleg Tsvelodub

Institute of Thermophysics SB RAS
1 Lavrentyev Ave., Novosibirsk, 630090, Russia
Novosibirsk State University
2 Pirogova Street, Novosibirsk, 630090, Russia

To date, many technologies for simulating flows with moving boundaries have been developed. Most popular have become methods of continuous calculation, in which the computational domain is fixed and covers not only the liquid flow area but also the surrounding space with different physical characteristics. Such methods do not distinguish an interface by, for example, refining the adaptive mesh or modifying the model equations, but assume that the medium drastically changes in the vicinity of the interfacial boundaries. One of the most developed alternative approaches is based on reducing the original statement to the problem with a pre-defined flow region.

Alekseenko et al. (2011) using the tensor transformation of coordinates derived the system of equations for simulating the two-dimensional wave regimes of thin viscous liquid film flowing over a vertical surface. In the present study a similar approach is applied to generalize the system for the three-dimensional case. As a result the following system has been obtained:

$$\frac{\partial(uh)}{\partial t}+\frac{\partial\left(u^2h\right)}{\partial x}+\frac{\partial(uvh)}{\partial \eta}+\frac{\partial(uwh)}{\partial z}=$$
$$=gh+\frac{\partial}{\partial \eta}\left(\frac{\mu}{\rho h}\frac{\partial u}{\partial \eta}\right)+\frac{\sigma}{\rho}h\frac{\partial}{\partial x}\left(\frac{\partial^2 h}{\partial x^2}+\frac{\partial^2 h}{\partial z^2}\right)$$
$$\frac{\partial(wh)}{\partial t}+\frac{\partial(uwh)}{\partial x}+\frac{\partial(wvh)}{\partial \eta}+\frac{\partial\left(w^2h\right)}{\partial z}= \qquad (1)$$
$$=\frac{\partial}{\partial \eta}\left(\frac{\mu}{\rho h}\frac{\partial w}{\partial \eta}\right)+\frac{\sigma}{\rho}h\frac{\partial}{\partial z}\left(\frac{\partial^2 h}{\partial x^2}+\frac{\partial^2 h}{\partial z^2}\right)$$
$$\frac{\partial h}{\partial t}+\frac{\partial(uh)}{\partial x}+\frac{\partial(wh)}{\partial z}+\frac{\partial(vh)}{\partial \eta}=0$$
$$u(x,0,z,t)=0,\quad w(x,0,z,t)=0,$$
$$v(x,0,z,t)=v(x,1,z,t)=0,\quad \frac{\partial u}{\partial \eta}(x,1,z,t)=0,\ \frac{\partial w}{\partial \eta}(x,1,z,t)=0$$

Here $h$ is the film thickness, the $xz$-plane at $\eta=y/h=0$ corresponds to a solid wall, $\eta=1$ is the free surface equation, $u$, $v$, w are the longitudinal, cross and transversal contravariant components of velocity, respectively, σ is the surface tension, ρ is the density, μ is the dynamic viscosity of fluid, and $g$ is the gravity acceleration.

After the shift over the cross coordinate $\eta'=\eta-1$ the equations of the system are invariant under the parity transformation:

$$\eta'\to-\eta'$$
$$u(x,\eta',z,t)\to u(x,-\eta',z,t),$$
$$w(x,\eta',z,t)\to w(x,-\eta',z,t),$$
$$v(x,\eta',z,t)\to -v(x,-\eta',z,t)$$

In the two-dimensional case this significantly simplifies the search of steady-state traveling solutions by spectral methods of Galerkin type. An example of an implicit use of the detected symmetry may be the well-known articles by Ruyer-Quil and Manneville (1998), in fact, selecting only symmetric basis functions, as it was proved in (Arkhipov et al. 2015).

The main advantage of the obtained system is the possibility to consider the problem in the region with pre-determined boundaries. In other words, the free-surface problem turns out to be, in a certain sense, solved. Meanwhile, this problem has been already solved by using a simple change of variables in the hydrodynamic equations. Here, the obtained system is shown to agree with the equations, derived by such a method for a two-dimensional case by Geshev and Ezdin (1985). However, the system (1) has the above mentioned symmetry and a conservative form, being perfect for designing numerical efficient conservative difference schemes.

Under the assumption of self-similar profile of longitudinal velocity the equations with boundary conditions are proved to coincide with the well-known Demekhin-Shkadov's model for the case of moderate Reynolds numbers. It is also shown that at small Reynolds numbers the system is reduced to a three-dimensional Nepomnyaschii evolution equation for the film thickness.

The study was financed by the Russian Science Foundation (grant No. 14-22-00174).

**References**

Alekseenko S. V., Arkhipov D. G., and Tsvelodub O. Yu. Divergent system of equations for a fluid film flowing down a vertical wall, Dokl. Physics, Vol. 56 pp. 22-25 (2011)

Arkhipov D., Vozhakov I., Tsvelodub O. On the topological structure of steady-state traveling solutions to the problem of wavy flowing down liquid films, Bifurcations and Instabilities in Fluid Dynamics, Paris ESPCI, p. 105. (2015)

Ruyer-Quil C., Manneville P. Modeling film flows down inclined planes, The Europ. Phys. J. B-Condensed Matter and Complex Systems, Vol. 6 pp. 277-292 (1998)

Geshev P. I., Ezdin B. S. Calculation of velocity profile and wave shape on the falling liquid film, Hydrodynamics and Heat and Mass Transfer of Liquid Flows with Free Surface, pp. 49-58 (1985)

# Vapor condensation on curvilinear fins with condensate suction from the interfin space

Igor Marchuk[1], Ella Barakhovskaya[1], Yuriy Lyulin[2] and Oleg Kabov[2]

[1]Novosibirsk State University, Pirogova Str. 2, Novosiborsk, 630090, Russia
[2]Institute of Thermophysics, Russian Academy of Sciences, Prosp. Lavrentyev 1, Novosibirsk, 630090, Russia
marchuk@itp.nsc.ru

Vapor condensation on finned surfaces is widely used in technique applications. The flooding of the interfin space in condenser leads to decreasing of intensive condensation area and reduces significantly the intensity of condensation. The problem of removing condensate from the interfin space is particularly important at microgravity conditions. One solution to this problem would be to use suction of the condensate from the interfin grooves. The idea of the condenser with condensate suction is depicted in Fig. 1.

The numerical study of film condensation on the curvilinear fins with the suction of condensate from the interfin space has been performed. The approach presented by Marchuk and Kabov (2015, 2016) is used for the modelling. The results of calculations of condensation of ethanol on the fins of a round and optimized shapes have been obtained for different slopes of the fins with respect to the direction of the gravity vector, Fig. 2. The heat transfer coefficients for the optimized fins are much greater than for the fins with round shape. The value of the flooding level of the interfin grooves significantly affects the intensity of condensation as a whole, however, it does not affect the process of condensation on the convex part of the fins. For the calculation of operational parameters of the condenser it is possible to take into account the total condensate flow only from the convex part of the condenser fins to determine its average performance. It was found that for a fixed rate of condensing liquid suction from interfin groove there is a certain interval for the temperature difference. This interval corresponds to the interval of stationary flooding depth of the groove when a stable equilibrium between suction outflow of condensate and condensed liquid flow rate takes place, Fig 3.

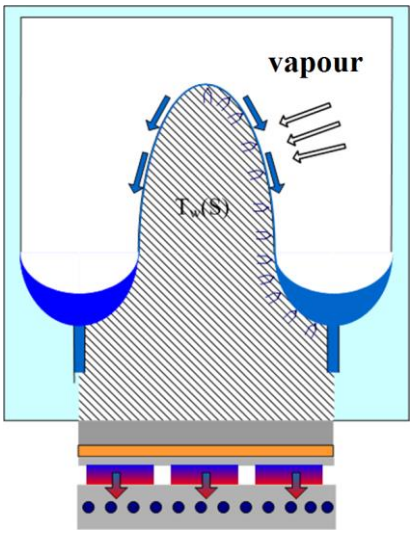


**Figure 1:** Condenser with the suction of the condensate.

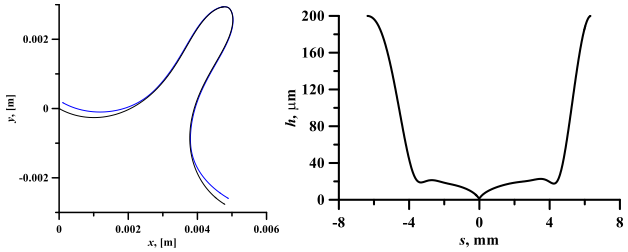


**Figure 2:** Calculated **c**ondensate film thickness along the inclined fin surface.

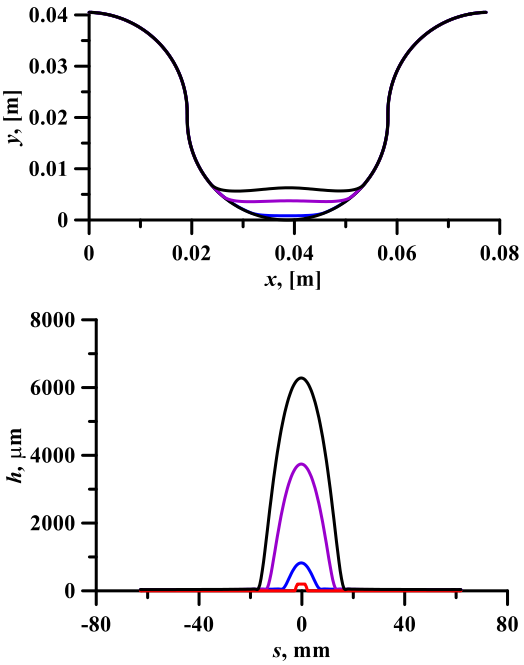


**Figure 3:** Condensate film thickness at different ΔT. Blue curve ΔT=1.0 K, purple ΔT=1.25 K, black ΔT=2.0 K, red curve is the condensate suction velocity 0.2 mm/s.

**Acknowledgements** This study was supported by the Ministry of Education and Science of the Russian Federation, project no. RFMEFI61614X0016**.**

## References

Marchuk I.V. and Kabov O.A., Film Wise Vapor Condensation on Curvilinear Surfaces, Encyclopedia of Two-Phase Heat Transfer and Flow II: Special Topics and Applications, Volume 3: Special Topics in Condensation, Editors: J.R. Thome and J. Kim, World Scientific Publishing Company, Singapore, Chapter 5, pp. 133-176, (2015).

Marchuk I.V. and Kabov O.A., Model of Filmwise Vapor Condensation on Curved Surfaces, Doklady Physics, 61 (1), pp. 19-23, (2016).

# Investigation of coalescence-induced droplet jumping for dropwise condensation

Yongpan Cheng, Bo Zhang, Yanfang Fan, Jinliang Xu*
Beijing Key Loboratory of Multiphase Flow and Heat Transfer for Low Grade Energy,
North China Electric Power University, Beijing, 102206, China
E-mail: xjl@ncepu.edu.cn

Condensation heat transfer is widely used in power generation, refrigeration, waste heat recovery etc. , and it has great significance in improving the energy utilization and relieving pollution problems. The condensation can be classified into dropwise and filmwise condensations. In the filmwise condensation the condensate will spread into a thin film on the cooling surface, thus prevent the direct contact between the condensing vapor and sub-cooled surface, so the heat transfer will be deteriorated. On the contrary, in the dropwise condensation the condensate will not wet the sub-cooled surfaces, its heat transfer efficiency can be one order higher than that of the filmwise condensation. However, in order to maintain the stable and efficient dropwise condensation, the condensate should be removed quickly from the sub-cooled surfaces.

Boreyko and Chen [1, 2] found that the condensate of 30 times smaller than the capillary length could jump from the superhydrophobic surfaces spontaneously without any external forces, and the resulting departure speed could be as high as 1 m/s. They also found that the kinetic energy for jumping came from the released surface energy, the jumping velocity followed the capillary-inertial law, which was proved on chilled superhydrophobic surface, as well as the heated Leidenfrost surface. So far there have been quite a few studies on the coalescence-induced droplet jumping through both numerical simulation and experiment, but the effect of contact angle as well as its hysteresis was seldom studied. The energy conversions among surface energy, kinetic energy, gravitational energy and viscous dissipation also had not been investigated in details. Our work would focus on such points.

Figure 1 shows the schematic diagram of dropwise condensation in the condenser, with vapor flowing inside and the coolant flowing outside. When the vapor released heat to the cooling wall, it would be condensed into the droplets. When the two adjacent droplets coalesced, the excess surface energy would be released due to reduction of surface area. Due to the counter action of the substrate upon impingement of liquid bridge for coalescing droplets, the droplet would jump up from the substrate. In our simulation, the diffuse interface model was adopted to study the coalescence-induced jumping process of droplets.

Our study [3] showed that contact angle had negative effect on the jumping velocity, with the decreasing contact angle, both peak jumping velocities and radius range for droplet jumping would be reduced. For the capillary-inertial process the normalized droplet jumping velocity was at the order of 0.2. Although more than half of the released surface energy could be converted into the kinetic energy, only less than 10% of the released surface energy could be converted into the translational kinetic energy for droplet jumping. The contact angle hysteresis had significant effect on the droplet jumping, the larger advancing contact angle could help improve the droplet jumping velocity, while the lower receding contact angle could reduce the droplet jumping velocity. Our results might provide useful guideline for design of efficient dropwise condensation heat transfer through coalescence-induced droplet jumping on superhydrophobic surfaces.

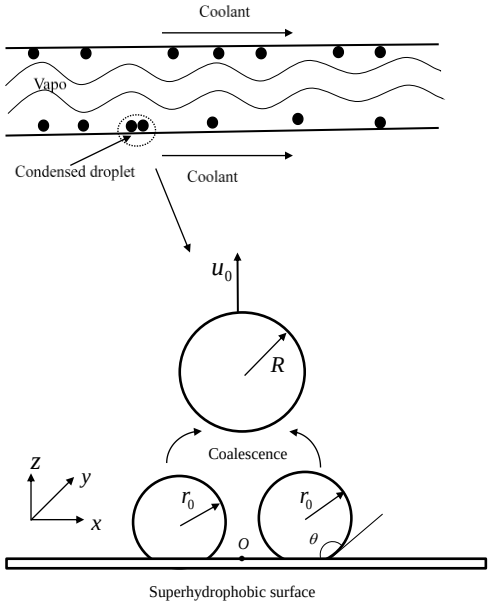


**Figure 1:** Schematic of coalescence-induced jumping on superhydrophobic surfaces

## References

[1] J. B. Boreyko, C. H. Chen, Self-propelled dropwise condensate on superhydrophbic surfaces, Phys. Rev. Lett., 103 (2009) 184501.

[2] J. B. Boreyko, C. H. Chen. Self-propelled jumping drops on superhydrophobic surfaces, Phys. Fluids, 22 (2010) 091110.

[3] Y. P. Cheng, J. L. Xu, Y. Sui. Numerical investigation of coalescence-induced droplet jumping on superhydrophobic surfaces for efficient dropwise condensation heat transfer. Int. J. Heat and Mass Transfer, in press, (2016).

# Unsteady Heat Transfer In a Gas Mixture

Alexey Polikarpov[1,2], Minh Tuan Ho[3], Irina Graur[4]

[1]Ural Federal University, Physics Department, Lenina str. 51, 620000, Ekaterinburg, Russia
[2]Kutateladze Institute of Thermophysics SB RAS, Lavrentyev Ave., 1, Novosibirsk, 630090, Russia
[3]James Weir Fluids Laboratory, Department of Mechanical and Aerospace Engineering, University of Strathclyde, Glasgow G1 1XJ, UK
[4]Aix-Marseille University, rue Enrico Fermi 5, 13013, Marseille, France
E-mail:Alexey.polikarpov@urfu.ru

Heat and mass transfer phenomena in a gas near a heated surface play a key role in large number of technological processes, particularly, in electronic cooling. In addition, in most of these devices the transport phenomena are essentially time-dependent. Actual tendency of the technical devices miniaturization leads to increase of a ratio between the molecular mean free path and the characteristic scale of a device (so called Knudsen number). If the Knudsen number becomes larger than one a gas inside this device must be considered as rarefied and its behavior must be simulated on the basis of the Boltzmann equation.

Here the fundamental problem of the transient heat transfer through a gas mixture between two parallel plates, induced by the instantaneous temperature rise of one of two plates, is simulated on the basis of the McCormack kinetic model [1].

Initially a gas mixture between two parallel plates is in an equilibrium state. Then, the temperature of one plate increases instantaneously and the relaxation of this system to its new equilibrium state is observed. The time evolution of the heat flux is investigated in a wide range of governing parameters: Knudsen number, gas mixture composition and species concentration. The cases of the mixtures with similar (Ne-Ar) and different (He-Xe) molecular masses are considered. The time-dependent linearized kinetic equation for a binary gas mixture is solved numerically

$$\frac{\partial h_\alpha}{\partial t} + v_y \frac{\partial h_\alpha}{\partial y} = \sum_{\beta=1,2} L_{\alpha\beta} h_\beta, \qquad \alpha = 1,2$$

where $L_{\alpha\beta} h$ is the linearized collision term. The McCormack model is used here for the calculations of the collision term.

The discrete-velocity method is used to solve numerically the McCormack model equation. The second order spatial discretization with explicit time integration is used. The governing parameters for this task are:

The molar concentration of the mixture, which is defined as

$$C = \frac{n_1}{n_1 + n_2}$$

$n_\alpha$ ($\alpha = 1,2$) is the number density of specie $\alpha$.

The rarefaction parameter which is defined as

$$\delta = \frac{pH}{\mu v_0}$$

Here p is the gas mixture pressure, $v_0$ is the most probable molecular speed, $\mu$ is the gas mixture viscosity.

The time needed to reach the steady-state conditions is calculated. Figures 1 and 2 show the time evolution of heat flux in the center of the gap between the plates for three values of concentration C and δ=10 (near continuum regime).

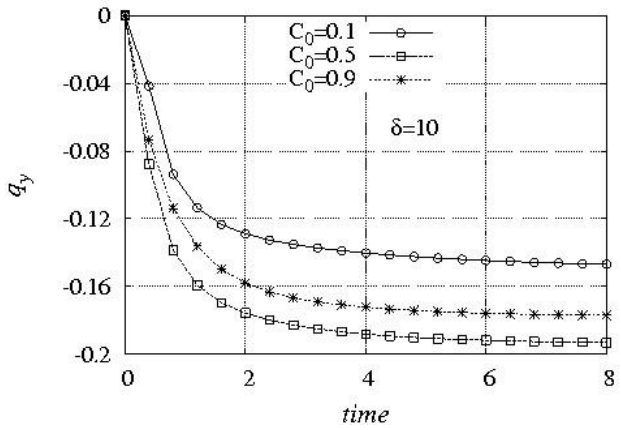


**Figure 1:** Time evolution of normal heat flux in the center of the gap for mixture Ne-Ar. Time unit on abscissa axis corresponds to one thousand discrete time steps Δt.

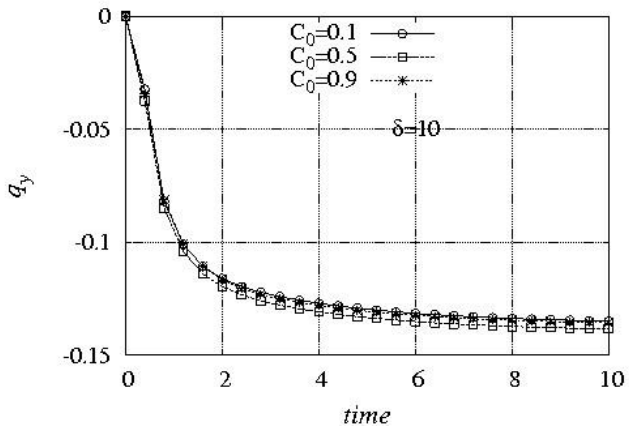


**Figure 2:** Time evolution of normal heat flux in the center of the gap for mixture He-Ar. Time unit on abscissa axis corresponds to one thousand discrete time steps Δt.

**Acknowledgment**

The study was supported by the Ministry of Education and Science of Russia (project identifier RFMEFI61614X0016)

**References**

McCormack F. J. Construction of linearized kinetic models for gaseous mixtures and molecular gases. Phys. Fluids 16, 12. 1973.

# Temperature profile at liquid-gas interface with phase transition

Elizaveta Gatapova[1], Vladimir Aniskin[1,2] and Maxim Filipenko[1]

[1]Kutateladze Institute of Thermophysics SB RAS, Lavrentyev Ave., 1, Novosibirsk, 630090, Russia
[2]Khristianovich Institute of Theoretical and Applied Mechanics SB RAS, Institutskay Str., 4/1, Novosibirsk, 630090, Russia
E-mail gatapova@itp.nsc.ru

The processes with phase change at liquid–vapor/gas interface are still not fully understood, especially for microsystems, where the interface itself is difficult to determine as well as the effects in the Knudsen-layer-sized domain near this interface become important. An approach to the description of heat and mass transfer in the two-phase system, based on the full Navier–Stokes equations with the temperature and pressure jumps boundary conditions, was suggested in (Gatapova et al. 2015a). The analysis showed good agreement between the proposed solutions and temperature and pressure profiles obtained from the solution of the Boltzmann equations. However, there is a lack of the experimental data on the pressure and temperature jumps at the gas-liquid interface (Gatapova et al. 2015b).

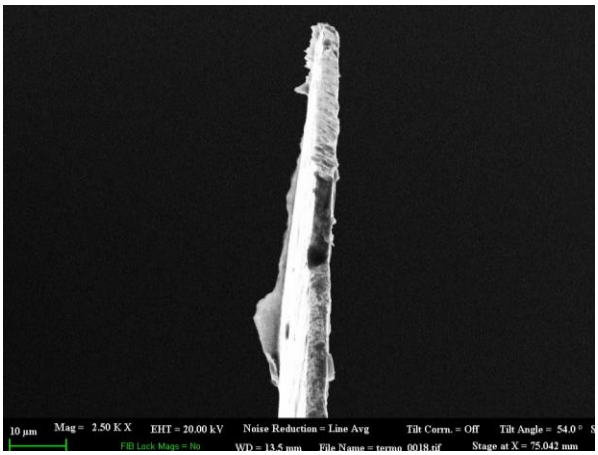


**Figure 1:** Photo of microthermocouple on FIB Crossbeam 1540 XB.

In the present study the temperature field across the liquid-gas two-layers system is investigated experimentally. The liquid layer is locally heated from the bottom substrate and the intensive liquid evaporation is observed. Ultrapur Water (Merck Millipore) is used as working fluid for experiments. To measure the temperature profile across the both liquid and gas layers the unique microthermocouple is displaced with small step of 0.5 – 20 µm through two layers. The thickness of the microthermocouple sensor is less than 4 µm, Fig. 1. Calibration of the manufactured unique microthermocouple is carried in the range of temperature 5 – 100 °C. Indications are tested using two reference thermometers ETS-100, for which the error of the test range is 0.05 K. The styles of position of the thermocouples, which measure the temperature in gas and liquid phases, are in such a way to avoid the influence of the thermal conduction along the wires. Data collection is carried out by means of temperature control and measurement system consisting of a system of data collection (NI 9214) and software. Precise miniature motorized linear stage is used as micropositioner displaces the microthermocouple and determines the position. The range of movement of the micropositioner is 25.4 mm in 0.05 µm. The micropositioner is connected to a personal computer and controlled by special software. A special software have been developed to automate experiments.

The measurements allowed obtaining the detailed information on the temperature profile. The temperature jump on the liquid-gas interface is measured (Fig. 2) and it is found that its value increases with increasing temperature.

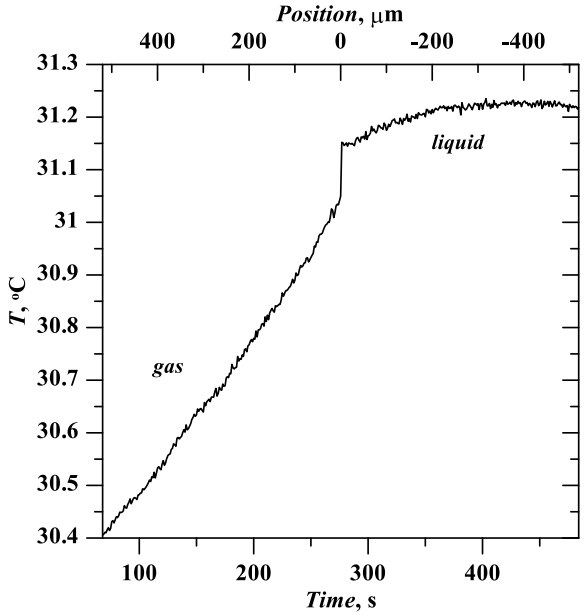


**Figure 2:** Temperature profile at water – air interface. Speed of microthermocouple displacement 5 µm/s, 2 reads per seconds, humidity 62%, air pressure 0.99 kPa., heating power 0.14 W.

The work is supported by the Ministry of Education and Science of Russia (project identifier RFMEFI61614X0016).

## References

Gatapova E.Ya., Graur I.A., Sharipov F., Kabov O.A. The temperature and pressure jumps at the vapor-liquid interface: Application to a two-phase cooling system // *Int. J. Heat Mass Transfer* 83. P. 235 – 243 (2015a)

Gatapova E.Ya., Filipenko R.A., Lyulin Yu.V., Graur I.A., Marchuk I.V., Kabov O.A., Experimental investigation of the temperature field in the gas-liquid two-layer system, Thermophysics and Aeromechanics 22, (6), P. 729-734 (2015b)

# Numerical investigation of heat and mass transfer processes in a spherical layer of viscous incompressible liquid with free boundaries

Alla Zakurdaeva and Ekaterina Rezanova

Altai State University, Faculty of Mathematics and Information Technologies
61 Lenina avenue, Barnaul, 656049, Russia
and Institute of Thermophysics SB RAS, Laboratory of Enhancement of Heat Transfer
1 Lavrentyeva avenue, Novosibirsk, 630090, Russia
alla2300@bk.ru

The problem of flows of a mixture of the viscous incompressible liquid and gas, filling a spherical layer with free boundaries, and containing a gas bubble within itself (Goncharova 1987), is investigated numerically. The mathematical model includes the Navier-Stokes equations, the equations of the heat transfer and diffusion of the gas considering as a passive admixture. It is assumed that all the transfer coefficients depend on temperature. On free boundaries the following conditions are fulfilled: the kinematic and dynamic conditions; the Henry law that links the gas concentration at the boundaries with pressure outside this area; the equation that determines the energy balance and the condition of temperature continuity on the internal free surface. Pressure, density and absolute temperature of the gas inside the bubble satisfy the ideal gas law. On the external free boundary the heat exchange with the atmosphere is prescribed.

The parametric analysis of the problem is performed. The algorithm for the numerical solution of the problem is constructed. It consists of the following steps:

1. Determination of the velocity of changing of the spherical shell's volume, the density of the gas in the bubble and the internal radius by solving the Cauchy problem for a system of the ordinary differential equations. The numerical solution is carried out with the help of the fourth-order Runge–Kutta method.
2. Calculation of the external radius of the fluid layer according to the conservation law of shell's volume.
3. Transition from the domain with moving boundaries to the fixed region (to the Lagrangian coordinates).
4. Computation of the temperature distribution inside the fluid layer. It includes a tridiagonal matrix algorithm (Thomas algorithm) with a parameter, which is the unknown value of temperature at the internal free boundary (Rezanova and Zakurdaeva 2015).
5. Computation of the gas concentration in the fluid shell with the help of a finite-difference scheme of the second approximation order.

The impact of the external thermal regime and external pressure, the level of gas saturation in the fluid layer and the amount of gas in the bubble on the dynamics of spherical shells has been investigated. Herewith the Dirichlet, Neumann and Newton boundary conditions for temperature at external surface of the sphere are considered.

Numerical experiments on the formation of the liquid glass shells, which contain the carbon dioxide gas within themselves, have been performed. Also the comparison of calculation results for the full and simplified thermal problem statement, when the diffusion process of the gas is not taken into account, has been carried out. It is determined that besides the external thermal regime a significant influence on the size of the spherical layer and the heat and mass transfer processes inside it, is provided by the process of gas diffusion (Figure 1). The external thermal regime is set as:

$$\begin{cases} T_{ex} = T_{ex1} + \dfrac{(T_{ex2} - T_{ex1})}{t_2 - t_1}(t - t_1), t_1 \le t \le t_2, \\ T_{ex} = T_{ex2}, t > t_2. \end{cases}$$

Here $T_{ex}$ is the external temperature, $t$ is the time, $T_{ex1}$ = 1171.1K, $T_{ex2}$ = 1673 K, $t_1$ = 0 s, $t_2$ = 0.3 s.

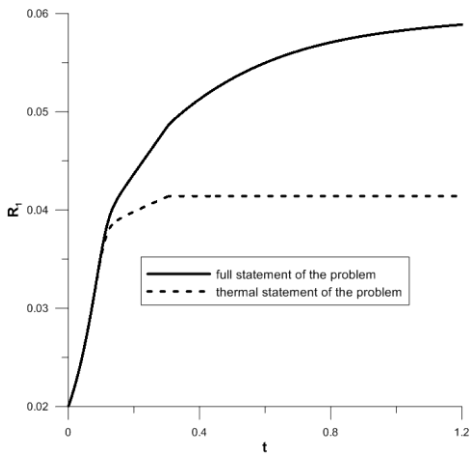


**Figure 1:** Comparison of variation of internal radius $R_1$ of the spherical layer in time t in the case of investigations for the full (solid line) and simplified, thermal problem statement (dashed line).

The results of investigations show that for the full problem statement a more intense extension of the shell is observed and a stationary regime is achieved later than in the case of the thermal statement without consideration of the gas diffusion (see Figure 1).

**Acknowledgments.** The study was supported by the Russian Ministry of Education and Science (project indicator RFMEFI61314X0011).

**References**

Goncharova O.N., Mathematical model of spherical shells in a short-term weightlessness, Dinamika sploshnoy sredi, N. 82 pp. 66-79 (1987) (in Russian)

Rezanova E.V., Zakurdaeva A.V., Numerical investigation of influence of external atmosphere's pressure on dynamics of a spherical fluid layer, Omskiy nauchniy vestnik, (2015) (accepted for publication) (in Russian)

# Two-dimensional liquid bridge between horizontal cylinders

Pavel Geshev and Nurzia Safarova

Novosibirsk State University, Physical Department, Pirogova Str. 2
Institute of Thermophysics SB RAS, Lavrentev Ave. 1
Novosibirsk, 630090, Russia
Geshev@itp.nsc.ru

Various equilibrium shapes of two-dimensional liquid bridges formed between two horizontal cylinders of identical radius $R'$ are calculated. Cylinders are located vertically (1) or horizontally (2). Parameters in the problem: liquid density $\rho$, gravity $g$, radius of cylinder $R'$, distance between the cylinders $d'$, and surface tension $\sigma$ create two criteria: the Bond number $Bo = \rho g R'^2/\sigma$ and the ratio of two sizes $d = d'/R'$. A contact angle $\theta_c$ is the third dimensionless parameter of the problem. Our goals are the calculations of shapes of bridges with minimum and maximum areas of cross section and evaluation of the capillary forces acting between the cylinders and estimation of the evaporation time for liquid in the bridge.

The equations for the free surfaces, obtained from the hydrostatics, look for vertical (1) or horizontal (2) cases as

$$y - y_0 = \int_{x_0}^{x} \frac{A(x)dx}{\sqrt{1-A(x)^2}} \qquad (1)$$

$$y_k - y_{k0} = \int_{0}^{\varphi} \frac{\delta(\varphi)\cos\varphi\, d\varphi}{K_{k0} \pm Bo\ \delta(\varphi)} \qquad (2)$$

where subscript $k$ =1, 2 (for a horizontal case there is two free surfaces – upper and lower), $A(x) = \sin\varphi$ and $\delta(\varphi)$ are known functions from the angle $\varphi$ (an inclination angle of a free surface to the axis *x*), $K_{k0}$ are the curvatures of free surfaces at the bottom points of meniscuses. The solutions of the problem are found by iterations (by Newton's method).

In Fig.1 for contact angle $\theta_c = 20^0$ and $Bo$ =1 the examples of calculated bridges for vertical arrangement of cylinders are shown for several increasing distances $d$. Bridge's neck becomes zero at maximal distance $d = 1.8$ between cylinders. For larger distances a stable bridge can not exist.

In Fig.2 for the same contact angle and for two distances $d = 0$, 1 and two values of the Bond criterion $Bo$ =1, 4 the examples of calculated bridges of maximal area are shown. Horizontal forces between two cylinders can be repulsive for small Bond numbers and small *d*, but usually these forces are attractive.

The boundaries of existence for nonlinear solutions of system of integral equations (2) in three-dimensional parametric space were defined. The steady-state solution of the problem for temperature profile is found by method of integral boundary equations and used for estimations of evaporation time for liquid in the bridge.

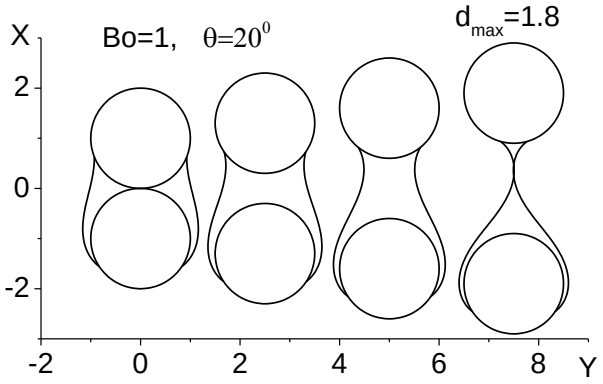


**Figure 1:** Example of bridges calculated for four distances *d* for vertical arrangement of cylinders.

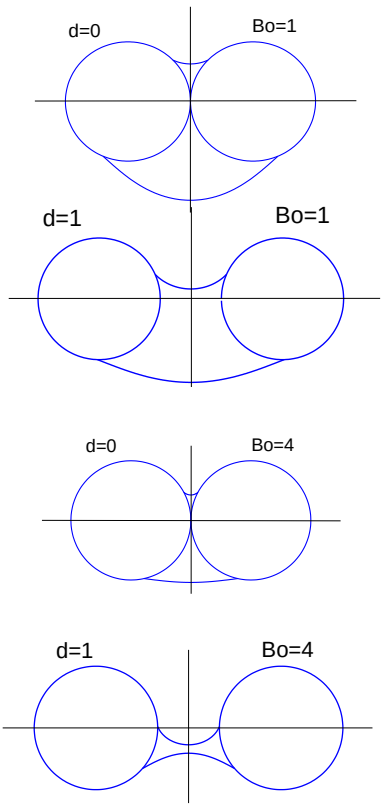


**Figure 2:** Maximal bridges for horizontal arrangement.

# Experimental investigation of transient characteristics of a liquid film, formed from an impinging gas-droplet multi-jet pulsed spray

P.N. Karpov[1], A.D. Nazarov[1,3], A.F. Serov[1,2], and V.I. Terekhov[1,2]

[1] Kutateladze Institute of Thermophysics SB RAS, Novosibirsk, Russia
[2] Novosibirsk State Technical University, Novosibirsk, Russia
[3] Novosibirsk State University
E-mail: terekhov@itp.nsc.ru

The paper presents investigation results on characteristics of the film flow on a vertical surface of the heat exchanger in a wide range of specific coolant flow rate. Measurement results on the parameters of integral and local heat transfer are presented for the regime of the pulsed coolant supply with considerable variation of the ratio of pulse duration to the time between the pulses, which leads to the regimes with partially wetted surface and formation of an ultrathin cooling film. It is determined that the heat transfer regime depends on the time-integrated mass flow and on-off time ratio of the liquid phase flow.

For the spray at evaporative cooling ($T_w$ = $70^0$C), the temperature gradient at the liquid - solid interface plays a major role in heat transfer due to the Marangoni effect. A significant contribution to heat transfer intensification is made by thermocapillary convection due to evaporative cooling on a moving film-dry surface interface. In the regime of island film cooling, when the tangential forces and local gradient of surface tension are generated at insufficient wetting, the shear film flows, dry spots, local film areas, rivulets and droplets are formed. The regimes of forming a thin evaporating film allow high heat transfer rate, and they can be used for cooling the microelectronic equipment with high heat release.

The experimental section [1] is a multifunctional setup consisting of the following units: programmable multi-jet source of a pulsed gas-droplet flow (pulse injector), automated calorimeter with a removable heat exchanger, and automated system for registration of the gas-droplet flow parameters with the original capacitive sensors for the liquid film thickness and wave velocity and gradient sensors for the local heat flux.

According to analysis of effectiveness of cooling by the pulse flow, when the short pulses with a high on-off time ratio are formed, heat transfer per a unit of specific flow rate increases by 2-3 times due to intensive evaporation of a thin film. Data of the gradient sensor of the heat flux make it possible to analyze the behavior of the liquid film formed on the heat exchanger surface and the heat flux at maximal and minimal thicknesses for the given regime of pulse spray.

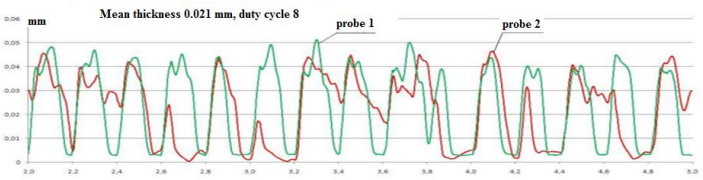


**Figure 1**. Local thickness of a “thin” film.

Efficiency of heat transfer to the pulse gas-droplet flow is characterized by the ratio of frequency to duration of liquid nozzle opening (on-off time ratio).

At low on-off time ratio, corresponding to the specific flow rate of above 0.06 kg/m$^2$s and higher, cooling efficiency decreases (Fig. 1). A stable liquid film of about ~ 300 μm is formed on the surface; at that, the value of heat transfer coefficient tends to the value of heat transfer coefficient at film cooling. The regime of droplet irrigation with a high on-off time ratio and specific flow rate of below 0.012 kg/m$^2$s forms the spots of thin liquid and droplets on the heat exchanger surface. This regime increases specific heat transfer more than twice in comparison with film cooling.

The work was financially supported by the Russian Foundation for Basic Research (project 16-38-00853).

**References**

1. Nazarov A.D., Serov A.F., Bodrov M.V. “Intensification of cooling by a pulsed gas-droplet flow: Equipment, parameters, and results”. - JTP. – 2010. – T.80, №5. – c.132-135.
2. .Nazarov A.D., Serov A.F., Terekhov V.I., Sharov K.A. “Experimental investigation of evaporative pulse-spray impingement cooling”. Journal of Engineering Physics and Thermophysics – 2009. – T.82, №6. – c.1160-1166.
3. Chinov E.A., Kharlamov S.M., Nazarov A.D., Sokolov E.E., Markovich D.M., Serov A.F., Kabov O.A. “Integrated measurement of the wave characteristics of heated film of liquid by the capacitance and fluorescence methods”. High Temperature. 2008. T. 46. № 5. C. 709-716.

# Characteristics of layered gels formation by additive technologies

Boris Pokusaev, Sergey Karlov, Andrey Vyazmin, Kseniya Okhotnikova

Moscow State University of Mechanical Engineering, Environmental and Chemical Engineering Institute
ul. Staraya Basmannaya 21/4, Moscow, 105066, Russia
pokusaev2005@yandex.ru, av1958@list.ru

Gels is a dispersive system with liquid dispersing medium, and the dispersion phase makes up a spatial structured mesh due to intermolecular interaction in the contact sites.

The promising application of gels is the use in regenerative medicine for growth of biological issues, including the problem of culturing stem cells in vitro (Westrin and Axelsson, 1991). This capillary network is intended for the delivery of nutrients to individual cells, and to remove products from the metabolism. One of the solutions to this problem is to create a synthetic gel matrix with ordered spatial system of nano-channels. It seems promising the idea that gels can used as a carrier during the formation of ordered bio-structured elements (based on the 3D printing) for additive medical technology. However, there are a number of factors that influence diffusion transport in gels and change mass-transfer laws. For example, the selective interaction of the diffusible component with structural elements of gel was found (Pokusaev et al., 2013).

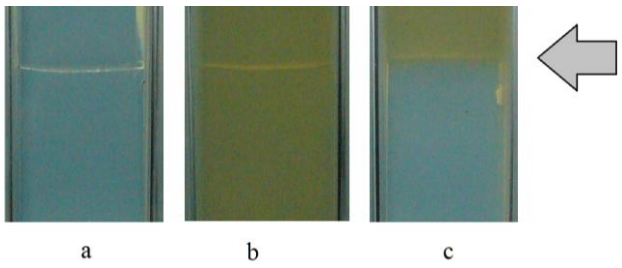


**Figure 1:** Photos of silica gel two-layer systems of different densities: a – both layers with density of 1.04 g/cm$^3$, b- both layers with 1.08 g/cm$^3$, c – the upper layer has the density of 1.08 g/cm$^3$; the lower has the density 1.04 g/cm$^3$. The arrow indicated the separation surface between these two layers.

Gels are very promising for use in additive technologies, since they are easily form matrixes of different shapes and densities (figure 1). Moreover it is possible to apply a denser layer of gel on the less dense without any mixing corresponding to liquid media. Additive technologies can form within the matrix a microchannels network which provides a convective transport inside the bioreactor.

The formation of silica gel from liquid media requires a few minutes and it is associated with chemical changes and the process of the poly-condensation. As a result a structured phase is occurred; gel has significantly different rheological properties from original liquids. It is found that on the surface of thin layers of silica gel there are convective structures (figure 2). These structures make more complicated to depose the upper layers of the gel at bioprinting.

**Figure 2:** Photo of the convective structures appearing on the surface of a thin layer of silica gel during its formation.

Another factor complicating the use of additive technologies to gels is their spontaneous densification (the compressibility of the medium). As a result of the pressure of the upper layers of the liquid is squeezed out of the lower layers forming the system drops on the perimeter of the upper layer (figure 3). Such a drop will obstruct the uniform application of the subsequent layers of the gel.

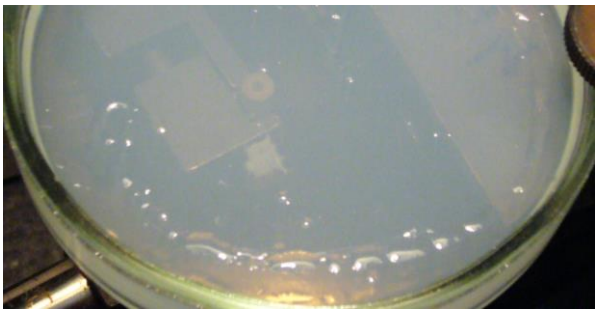

**Figure 3:** Photo of liquid drops formed along the perimeter during the formation silica gel thin two-layer matrix.

.

Hence, for the effective use of gel matrix in additive technology formation of bioreactors for growing biological tissues from stem cell it is essential to solve fundamental problems of heat and mass transfer with chemical transformations in the rheological complex media.

This work was supported by the Russian Science Foundation (project no. 15-19-00177).

## References

Pokusaev B.G., Karlov S.P., Vyazmin A.V. and Nekrasov D.A. Peculiarities of diffusion in gels, Thermophysics and Aeromechanics, Vol. 20, pp. 749-756 (2013).

Westrin B.A. and Axelsson A. Diffusion in gels containing immobilized cells: a critical review, Biotechnology and Bioengineering, Vol. 38, pp. 439-446 (1991).

# Cavitating flow control through continuous tangential mass injection

Mikhail V. Timoshevskiy, Ivan I. Zapryagaev, Konstantin S. Pervunin, Dmitriy M. Markovich

Kutateladze Institute of Thermophysics, Siberian Branch of the Russian Academy of Sciences
1, Lavrentyev Ave., Novosibirsk, 630090, Russia
Department of Scientific Research, Novosibirsk State University
2, Pirogov Str., Novosibirsk, 630090, Russia
timoshevskiy.mv@gmail.com

Unsteady cavitation phenomena in hydropower systems are known to be one of the major sources of instabilities and mechanical damage. Cavitation causes flow instabilities, pulsations and other forms of local and bulk unsteadiness, which disrupt the system operation and diminish the energy conversion efficiency. The flow unsteadiness inevitably leads to structural instabilities, load imbalance, noise and vibration of the equipment elements, their fatigue and eventual permanent damage. The consequences can be the machine failure or, in the worst cases, emergency situations. Thus, preventing or at least diminishing and controlling cavitation in an effective way is still an issue. In the paper, we applied continuous mass injection along a hydrofoil surface to manipulate a cavitating flow dynamics.

The experiments were carried out in the Cavitation tunnel in Kutateladze Institute of Thermophysics SB RAS. Its description as well as details on the measurement techniques applied can be found in (Kravtsova et al. 2014). The test foil of $C$ = 100 mm chord length was a scaled-down model of a Francis turbine guide vanes (GV). High-speed imaging was used to analyze spatial patterns and time dynamics of the gas-vapor cavities, as well as for evaluating the characteristic integral parameters. A hydroacoustic pressure transducer was employed to register time-spectra of pressure fluctuations behind the hydrofoil and, thereby, determine specific frequencies of unsteady regimes. A PIV technique was applied to measure the velocity fields and its fluctuations, which were compared for the free and forced flow conditions. The active flow control was implemented by means of a continuous liquid supply with different flow rates through a slot channel located in the GV surface at the distance of 0.6$C$ from the foil leading edge.

It was found that the active mass injection does not influence the primary flow upstream of the slot channel position absolutely. At small angles of incidence, the injection flow at velocities in the range between zero to 0.76 of the mean bulk velocity was observed not to practically influence the distributions of turbulent characteristics so that the global difference is only between the free and forced flow conditions. For cavitation-free and cavitation inception cases, the active mass injection was shown to make the flow turbulence structure more developed and the wake past the GV section more intense. However, the active flow control system considered also allows a favorable and efficient flow manipulation, especially at the regimes with developed gas-vapor cavities (see Figure 1). Moreover, the active flow management makes it possible to reduce substantially the amplitude or totally suppress the periodic cavity length oscillations and pressure pulsations associated with them.

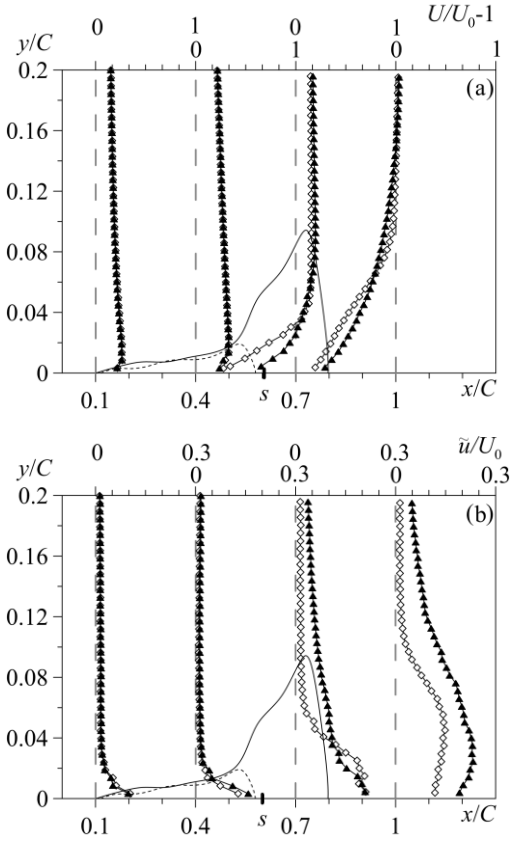


**Figure 1:** Downstream evolution of (a) the streamwise component of the mean velocity and (b) the streamwise turbulence intensity (rms-values) over the suction side of the GV model for unsteady cavity/transitional cavitation at $\sigma$ = 0.89, $U_{in}/U_0$ = 0.74. $\alpha$ = 3°. ▲ – w/o injection, ◇ – with injection. Solid and dashed lines represent interfaces (extracted from visual data) of the attached cavities of maximum size on the GV section for the free and forced flow conditions. $s$ denotes the position of the slot channel in the foil surface. The flow direction is from the left.

**Acknowledgements**

The research was funded by a grant from the Russian Foundation for Basic Research (project no. 16-38-00814-mol_a) and a grant of the President of the Russian Federation for the state support of leading scientific schools (project no. NSh-0179.2016.8).

**References**

Kravtsova A. Yu., Markovich D. M., Pervunin K. S., Timoshevskiy M. V. and Hanjalić K. High-speed visualization and PIV measurements of cavitating flows around a semi-circular leading-edge flat plate and NACA0015 hydrofoil. International Journal of Multiphase Flow, 60: 119–134 (2014)

# Rayleigh – Taylor instability of viscous liquid – vapor interface with heat and mass transfer

Vladimir Konovalov and Tatyana Lyubimova

Institute of Continuous Media Mechanics of the Ural Branch of Russian Academy of Science
1, Ak. Koroleva, Perm, 614013, Russia
konovalov@icmm.ru, lubimova@psu.ru

Two-layer system consisting of the viscous heat-conducting liquid and its vapor and bounded from below and from above by perfectly conductive rigid boundaries is considered. It is assumed that the temperature of lower boundary is higher than the saturation temperature and the saturation temperature is higher than the temperature of upper boundary. There exists a basic state of this system with the balanced heat flux at the interface and less dense vapor phase located below the layer of more dense liquid phase. In this case, phase transition, which is defined through the deviation of interphase boundary temperature from the saturation temperature and heat flux disbalance, is absent. We study linear stability of this basic state in the gravity field with the acceleration vector directed downwards.

The configuration described above was studied earlier in the framework of the lubrication approximation in (Kanatani 2010), the suppression of the Rayleigh - Taylor instability by the phase transition was found. This phenomenon was already described in the literature for the situation where a heat transfer in a liquid occurs as a result of natural convection and obeys the Newton - Richman law with the constant heat transfer coefficient (Panzarella et al. 2000).

The study of the system under consideration using the lubrication approximation and the quasi-equilibrium approximation, in which the rate of the phase transition is determined from the solution of the problem of thermal equilibrium (Hsieh 1978) did not allow to reveal some features of the effect of thermal properties of liquid and its vapor on the stabilization of vapor film surface.

In the framework of rigorous linear theory we found that the intensity of the phase transition in the limit case of large heat flux passing through the system is limited by the convective heat transfer in two media as a result of flows induced by the phase transition. Because of that there exists the maximum thickness of the vapor film, which can be stable in the gravity field due to the effect of the phase transition.

As one can see from Figure 1, which corresponds to the system water - aqueous vapor, the threshold thickness of the vapor film depends on the thickness of the liquid layer, and on the presence of the developed convective flows in the liquid caused by the density inhomogeneities of the medium.

Another phenomenon that can not be studied within the quasi-equilibrium approximation is the enhancement of the growth of long-wave perturbations due to the effect of pressure on the local saturation temperature. This factor limits below the critical heat flux required for the suppression of the Rayleigh - Taylor instability by phase transition, as it is seen from Figure 2.

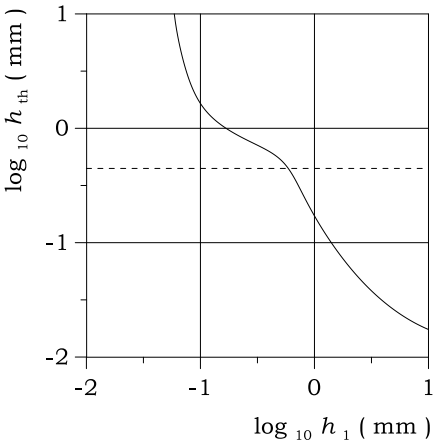


**Figure 1:** Threshold thickness of vapour film *versus* liquid layer thickness. Dashed line shows the result for the case of natural convection in a liquid at fixed value of Nusselt number Nu = 30.

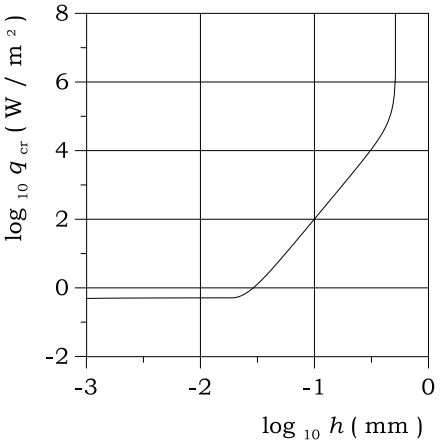


**Figure 2:** Critical heat flux *versus* vapour film thickness for the case of equal thicknesses of layers of two media.

The work was carried out under financial support of Russian Science Foundation (grant 14-21-00090).

**References**

Kanatani K., Interfacial instability induced by lateral vapor pressure fluctuation in bounded thin liquid-vapor layers, Phys. Fluids, Vol. 22 pp. 012101 (1-13) (2010)

Panzarella C.H., Davis S.H. and Bankoff S.G., Nonlinear dynamics in horizontal film boiling, J. Fluid Mech., Vol. 402 pp. 163-194 (2000)

Hsieh D.Y., Interfacial stability with mass and heat transfer, Phys. Fluids, Vol. 21 pp. 745-748 (1978)

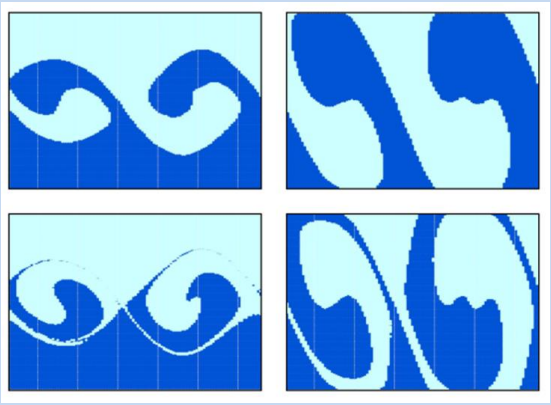

**Vinogradova**

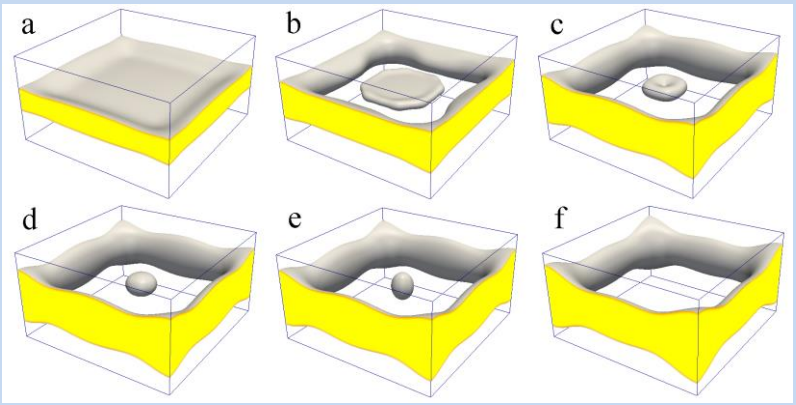


**Kupershtokh**

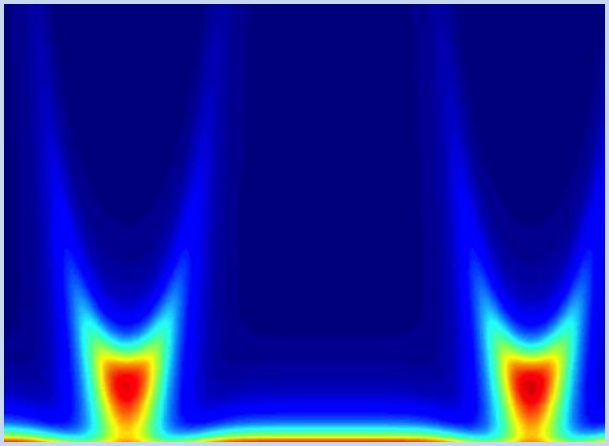

**Ganchenko et al.**

**Ronshin et al.**

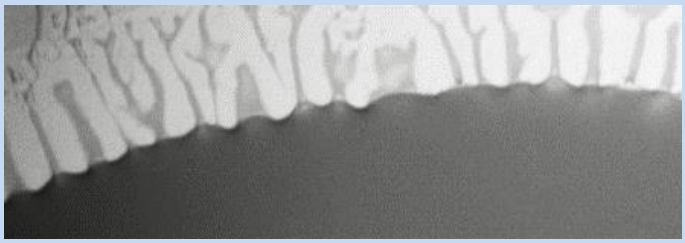

**Gatapova and Kabov**

**Machrafi and Dauby**

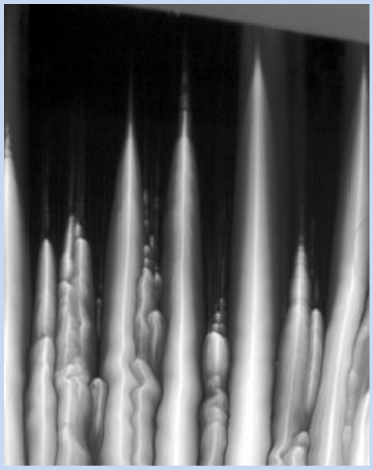

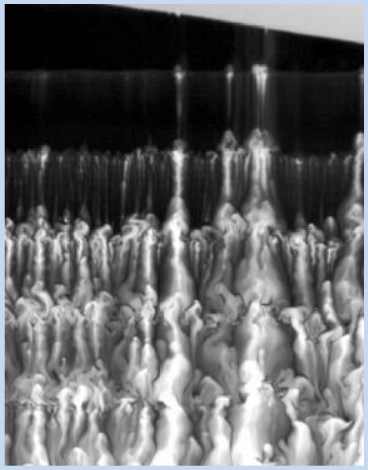

**Charogiannis et al.**

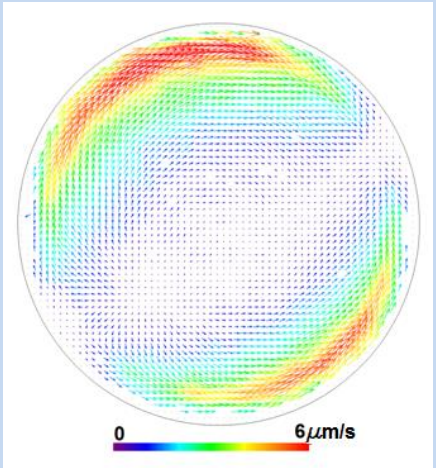


**Yagodnitsyna et al.**